

Mannose-functionalized PAMAM dendrimers : their synthesis, characterization and use in refining the model of protein-carbohydrate interactions
by Eric Kevin Woller

A dissertation submitted in partial fulfillment of the requirements for the degree of Doctor of Philosophy in Chemistry
Montana State University
© Copyright by Eric Kevin Woller (2003)

Abstract:
The interaction between proteins and carbohydrates is an important first step for many biological processes. For example, viral and bacterial infections, antibody-antigen interactions, fertilization and other cell-cell interactions all rely on protein-carbohydrate interactions as a first step in recognition. It is known, however, that the affinity between a lectin and a single sugar is quite weak. The increase in binding affinity in most biological systems is a result of what is often generically referred to as multivalent binding.

A number of carbohydrate-containing synthetic organic molecules have been synthesized to study multivalent protein carbohydrate interactions. Examples include small molecules that typically contain fewer than 10 sugars, medium sized molecules that contain between 10 and 100 sugars, and large polymeric systems that can contain thousands of sugars.

While most carbohydrate-containing systems have provided valuable insight into the mechanism of multivalent interactions, no class of carbohydrate containing system existed prior to this work in which the number of sugars and the size of the ligand could be varied independently. Such a system should provide specific information on the optimal geometric arrangement of ligands toward various receptors.

We have homogeneously and heterogeneously functionalized polyamidoamine (PAMAM) dendrimers up to generation six with mannose using a thiourea linkage by the reaction of an isothiocyanate on the carbohydrate with the terminal amines on the dendrimer. The result is water-soluble carbohydrate-containing dendritic molecules. Methods to characterize these dendritic macromolecules by nuclear magnetic resonance spectroscopy and matrix-assisted laser desorption ionization time-of-flight mass spectrometry were developed.

The effectiveness of the dendrimers as ligands for the lectin Concanavalin A has been demonstrated by means of a hemagglutination assay, a precipitation assay and a turbidity assay. Results indicate that the size of the dendrimer has a great effect, with the larger dendrimers being most active with Concanavalin A. In addition, the degree of functionalization has a profound effect, with the optimum degree of functionalization for binding being below full functionalization. Results also suggest mannose-functionalized PAMAM dendrimers effectively recruit and cluster lectins.

MANNOSE-FUNCTIONALIZED PAMAM DENDRIMERS: THEIR SYNTHESIS, CHARACTERIZATION AND USE IN REFINING THE MODEL OF PROTEIN-CARBOHYDRATE INTERACTIONS.

by

Eric Kevin Woller

A dissertation submitted in partial fulfillment
of the requirements for the degree

of

Doctor of Philosophy

in

Chemistry

MONTANA STATE UNIVERSITY-BOZEMAN
Bozeman, Montana

April 2003

D378
W835

APPROVAL

of a dissertation submitted by

Eric Kevin Woller

This dissertation has been read by each member of the dissertation committee and has been found to be satisfactory regarding content, English usage, format, citations, bibliographic style, and consistency, and is ready for submission to the College of Graduate Studies.

Dr. Mary J. Cloninger Mary Cloninger 4/2/03
(Signature) Date

Approved for the Department of Chemistry

Dr. Paul A. Grieco _____ 4-2-03
(Signature) Date

Approved for the College of Graduate Studies

Dr. Bruce R. McLeod Bruce R. McLeod 4-17-03
(Signature) Date

STATEMENT OF PERMISSION TO USE

In presenting this dissertation in partial fulfillment of the requirements for a doctoral degree at Montana State University, I agree that the Library shall make it available to borrowers under rules of the Library. I further agree that copying of this dissertation is allowable only for scholarly purposes, consistent with "fair use" as prescribed in the U.S. Copyright Law. Requests for extensive copying or reproduction of this dissertation should be referred to Bell & Howell Information and Learning, 300 North Zeeb Road, Ann Arbor, Michigan 48106, to whom I have granted "the exclusive right to reproduce and distribute my dissertation in and from microform along with the non-exclusive right to reproduce and distribute my abstract in any format in whole or in part."

Signature 

Date 4-10-03

To Denice

ACKNOWLEDGEMENTS

First and foremost, I must thank my wife Denice for tolerating me and everything associated with grad school. Thanks for putting up with my perpetual absence, busy schedule and all around lack of attention to you. It will soon all be over and we can get back to a 'normal' life, whatever that may be. To my unborn baby, keep growing. I'll see you soon. A big thank you to my advisor, Mary Cloninger. Thank you for your guidance, advice, direction, funding and friendship. The amount of things I learned during my work with you is extensive and certainly not just limited to this project. To the Cloninger research group. Thanks to Joel, Nick, Lynn, Mary Smart, Mark, and all the others that have been part of the group. Your camaraderie has been of great value. A HUGE thank you for reading my dissertation and providing suggestions and insight. That's the nicest thing you've ever done for me. To Jake, we've been through a lot, and it has all been fun. I'm glad I got to know you. You've been a good friend and an all around bad influence. Thanks. Eric WaL-ker, I have greatly enjoyed our most cerebral conversations. Always remember, happy hour is indeed the happiest hour of the day. I must thank Bethany Lutheran College for allowing me the time to leave my position and get my degree. As well as allowing me back. A final and most gracious thank you to C, H, N, O, and even S for being such great elements to work with. Thanks to my PowerBook, coffee, the 24 hours in each day, National Geo. Adventure, Spectators, and Bob, the best custodian in the world.

TABLE OF CONTENTS

1. INTRODUCTION, BACKGROUND AND RATIONALE 1

Protein-Carbohydrate Interactions 1
Multivalent Interactions and Glycoside Clustering 2
Design of Synthetic Multivalent Ligands 5
Various Modes of Multivalent Binding 7
Monovalent Interactions 7
Multivalent Interactions 8
Glycoside Cluster Effect 8
Cross-linking 9
Complications in Multivalent Ligand Design 10
Ligand Design 12
Dendrimers 18
PAMAM Dendrimers 20
Concanavalin A 24
PAMAM Dendrimer Functionalization Strategy 28
Methods of PAMAM Functionalization 29
Goals 33
Summary 34
Organization 35

2. SYNTHESIS OF PHENYL MANNOSIDE DENDRIMERS 37

Background 37
Phenyl Mannoside Approach 38
NMR Characterization 40
MALDI-TOF MS Characterization 43
Development of MALDI-TOF MS Procedure for PAMAM Dendrimers 45
MALDI-TOF Results and Discussion 48
MALDI-TOF Analysis of Dendrimer Functionalization Reaction 57
Solubility Issues 60
Summary 61
Experimental Procedures 62
General methods 62
MALDI 62
Synthetic procedures 63

3. SYNTHESIS OF POLYETHYLENE GLYCOL MANNOSIDE DENDRIMERS 68

Background 68
Synthesis of Carbohydrates 69

TABLE OF CONTENTS-CONTINUED

Attempted Synthesis of 1-*O*-(8-isothiocyanato-3,6-dioxaoctyl) -α-D-mannopyranoside....71
Synthesis of 1-*O*-(5-isothiocyanato-3-oxapentyl)- α-D-mannopyranoside....77
Dendrimer Functionalization Using 1-*O*-(5-isothiocyanato-3-oxapentyl)-2,3,4,6-tetra-*O*-acetyl-α-D-mannopyranoside....80
NMR Characterization....81
MALDI-TOF MS Characterization....86
Comparison of MALDI-TOF MS and NMR Data....90
Hemagglutination Inhibition Assay Introduction....92
Hemagglutination Inhibition Assay Results Using Mannose-Functionalized PAMAM Dendrimers....95
Glycoside Clustering and the Effect of Sugar Density....97
Cross-Linking and Aggregates....99
Turbidity Study....100
Summary....105
Experimental Procedures....106
General methods....106
MALDI-TOF MS....106
Dynamic Light Scattering....107
Synthetic procedures....108
General hemagglutination assay procedure....120
Turbidity Assays....123
Additional synthetic procedures (unoptimized)....124

4. HETEROGENEOUS PAMAM FUNCTIONALIZATION....131

Introduction....131
Heterogeneous Dendrimer Functionalization....133
Initial Attempt to Heterogeneously Functionalize a PAMAM Dendrimer....135
Characterization of Heterogeneously Functionalized Generation 4.0 PAMAM-Based Thiourea-Linked Phenyl Ethanol and Phenyl-α-D-mannopyranoside Dendrimers....136
Heterogeneous Functionalization of G(6)-PAMAM Using *p*-Isothiocyanatophenyl-α-D-mannopyranoside (**7**) and 2-(4-Isothiocyanatophenyl) Ethanol (**43**)....140
Summary of Heterogeneous PAMAM Functionalization Using *p*-Isothiocyanatophenyl-α-D-mannopyranoside (**7**) and 2-(4-Isothiocyanatophenyl) Ethanol (**43**)....143

TABLE OF CONTENTS-CONTINUED

Heterogeneous PAMAM Functionalization Using 2-(2-Isothiocyanatoethoxy)ethanol (**28**) and 1-*O*-(5-isothiocyanato-3-oxapentyl)-2,3,4,6-tetra-*O*-acetyl-α-D-mannopyranoside (**29**) 144
Characterization of Heterogeneous Functionalized Dendrimers 147
Hemagglutination Assay of Heterogeneously Functionalized Dendrimers 157
Precipitation Assay 164
Summary 171
Experimental Procedures 173
General methods 173
MALDI-TOF MS 173
Hemagglutination assay 173
Computer Modeling 173
General quantitative precipitation assay procedure 174
Synthetic procedures 175

5. SUMMARY AND CONCLUSIONS 212

The Benefits of Using Isothiocyanates 212
Characterization 213
Activity Determination 214

APPENDICES 216

Appendix A: Methods of MALDI-TOF MS data analysis 217
General Formulas 218
Data Transfer and Analysis Using the PerSeptive System 218
Data Analysis Using the Bruker System 220
Appendix B: Application of MALDI-TOF MS to Additional Dendrimer Examples 223
Background 224
Spin-Labeled PAMAM Dendrimers 224
Novel Iodinated Dendritic Nanoparticles 226
Appendix C: Attempts Using Isothermal Microcalorimetry 230
Background 231
General ITC Experiment Considerations 232
Attempted ITC Measurements 233
Experimental Procedures 236
Appendix D: Studies Toward alpha-D-Galactose Functionalized Dendrimers 238
Introduction 239
Approaches to an Isothiocyanato Galactose 240
Sulfonylcarbamate Method of Activating Galactose 245

TABLE OF CONTENTS-CONTINUED

Single Attempt to Functionalize a PAMAM Dendrimer with Benzylated Galactose....246
Experimental Procedures....248
REFERENCES CITED....251

LIST OF TABLES

Table Page

1.1 Theoretical properties of PAMAM dendrimers. 23

2.1 Mass (g/mol) and polydispersity data for **8-10** and G(4)-, G(5)-, and G(6)-PAMAMs 48

3.1 MALDI-TOF MS determination of mannose-functionalization of G(1)- to G(6)-PAMAMs 90

3.2 Hemagglutination inhibition assay results for **36-41** with Con A 95

4.1 Data for heterogeneously functionalized PAMAM dendrimers shown in Scheme 4.2. 137

4.2 Data for heterogeneously functionalized PAMAM dendrimers shown in Scheme 4.3 141

4.3 Molecular weight data from MALDI-TOF MS for heterogeneously functionalized dendrimers. 154

4.4 Summary of results for hemagglutination inhibition assay and precipitation assay 159

4.5 Quantities of reactants used to synthesize **44a-e**. 176

4.6 Quantities of reactants used to synthesize **45a-e**. 179

4.7 Quantities of reactants used to synthesize **54a-f**. 182

4.8 Quantities of reactants used to synthesize **55a-p**. 187

4.9 Quantities of reactants used to synthesize **56a-h**. 196

4.10 Quantities of reactants used to synthesize **57a-m**. 202

LIST OF FIGURES

Figure Page

1.1 Various biological interactions that rely on protein-carbohydrate interactions. 1

1.2 Mono-, di-, and tri-valent galactose ligands designed and used by Lee and co-workers to observe the *glycoside cluster effect.* 3

1.3 Interaction of a macrophage and bacteria mediated by antibodies. 4

1.4 Various modes of protein-carbohydrate interactions 10

1.5 Small, trivalent molecule synthesized by Kiessling and co-workers 13

1.6 Polyacrylamide synthesized by Whitesides containing 20% sialic acid residues. 14

1.7 Ring-opening metathesis polymerization reaction as demonstrated by Grubbs. 15

1.8 *C*-mannoside neoglycopolymer synthesized using ROMP by Kiessling 16

1.9 STARFISH inhibitor designed to interact with Shiga-like toxins. 17

1.10 Schematic depicting divergent dendrimer synthesis 19

1.11 Schematic depicting divergent dendrimer synthesis. 19

1.12 Structure of a generation four PAMAM dendrimer 22

1.13 Two views of the crystal structure of Concanavalin A. 26

1.14 The binding site of Con A, showing the participating amino acids and metal ions required for binding. 27

2.1 ^{1}H NMR spectrum of **8** in d_6-DMSO. 42

2.2 ^{1}H NMR spectrum of **9** in d_6-DMSO. 42

2.3. ^{1}H NMR spectrum of **10** in d_6-DMSO. 43

2.4 MALDI-TOF MS spectra of (a) G(4)-PAMAM, (b) **8**. 49

2.5 MALDI-TOF MS spectra of (a) G(5)-PAMAM, (b) **9**. 50

2.6 MALDI-TOF MS spectra of (a) G(6)-PAMAM, (b) **10**. 51

2.7 MALDI-TOF MS spectra of G(4)-PAMAM with horse heart myoglobin, and G(6)-PAMAM with bovine serum albumin. 56

2.8 Graph showing the relationship between equivalents of **7** added and molecular mass of **8**. 58

LIST OF FIGURES-CONTINUED

Figure Page

2.9 Graph of mass of **8** versus time of reaction between G(4)-PAMAM and **7**. 59

3.1 Molecules **11** and **12** were targeted to increase the water solubility of the subsequent functionalized PAMAM dendrimer. 68

3.2 The anomeric effect and neighboring group participation 70

3.3 ^{1}H NMR spectra (500 MHz) of (a) **31** (b) **37** in d_6-DMSO. 83

3.4 ^{1}H NMR spectra (500 MHz) of (a) **33** (b) **41** in d_6-DMSO. 84

3.5 ^{1}H NMR spectra (500 MHz) of (a) **33** (b) **39** in d_6-DMSO. 85

3.6 MALDI-TOF MS spectra of (a) G(2)-PAMAM, (b) **37**, (c) **31**. 87

3.7 MALDI-TOF MS spectra of (a) G(4)-PAMAM, (b) **39**, (c) **33**. 88

3.8 MALDI-TOF MS spectra of (a) G(6)-PAMAM, (b) **41**, (c) **35**. 89

3.9 General description of a hemagglutination inhibition assay. 93

3.10 Graphs from turbidity assay for G(4) dendrimer **39**. 102

3.11 Graphs from turbidity assay for (a) **36** (G(1)) and (b) **38** (G(3)) 103

3.12 Graph from turbidity assay of **39** with varying concentrations of Con A. 104

4.1 Systems that demonstrate the effect of epitope density. 132

4.2 Heterogeneous dendrimer functionalization by including the various epitopes with each dendron. 134

4.3 Heterogeneous dendrimer functionalization by adding the epitopes directly to an existing dendrimer. 135

4.4 ^{1}H NMR spectrum of **44c**. 138

4.5 ^{1}H NMR spectrum of **45a**.. 142

4.6 ^{1}H NMR (500 MHz) spectra of peracetylated and deprotected **55l**. 149

4.7 MALDI-TOF MS spectra of: (a) **47j**, (b) **51j**, (c) **55j**. 151

4.8 MALDI-TOF MS spectra of: (a) **49i**, (b) **53i**, (c) **57i**. 152

4.9 Graphs of activity toward Con A. 163

4.10 Precipitation assay data for G(3) series. 165

4.11 Precipitation assay data for G(4) series.. 166

LIST OF FIGURES-CONTINUED

Figure Page

4.12 Precipitation assay data for G(6) series. 167

4.13 Precipitation assay data for G(5) series. 168

4.14 Graph showing the calculated and the experimentally determined maximum number of Con A lectins that can be complexed by the dendrimers. 169

4.15 Reference numbers for assignment of peaks in the ^{1}H NMR of **44a-e** and **45a-e**. 176

4.16 Reference numbers for assignment of peaks in the ^{1}H NMR of **50a-f**. 183

4.17 Reference numbers for assignment of peaks in the ^{1}H NMR of **51a-p**. 188

4.18 Reference numbers for assignment of peaks in the ^{1}H NMR of **52a-h**. 197

4.19 Reference numbers for assignment of peaks in the ^{1}H NMR of **53a-m** 203

A.1 Method for continuous polymer data processing. 220

B.1 MALDI spectrum of **66**. 228

C.1 ITC profiles for the titration of Con A with methyl mannose, and for the titration of RNase A with 2'-CMP 234

C.2 ITC Isotherms for **38** and buffer 236

D.1 Inverse HETCOR NMR spectra of **68** 241

D.2 Neighboring group participation by the ester protecting group. 242

D.3 Inverse HETCOR NMR spectra of **71** 244

D.4 Proposed reaction of the glycosyl sulfonylcarbamate with a Lewis acid to form an oxonium ion. 245

LIST OF SCHEMES

Scheme Page

1.1 Synthesis of PAMAM dendrimers. 21

1.2 Various methods of PAMAM dendrimer functionalization. 31

2.1 General reaction scheme utilizing an isothiocyanate functionalized carbohydrate to react with a primary amine. 37

2.2 Synthesis of isothiocyanate **7**....38

2.3 Synthesis of phenyl mannose-functionalized PAMAM using **7**. 39

2.4 Various errors leading to imperfect PAMAM dendrimers 53

3.1 General reaction for the coupling of alcohols with mannose....69

3.2 Synthesis of acetyl protected α-D-mannosyl trichloroacetimidate....71

3.3 Formation of various alcohols for the attempted synthesis of **12**. 73

3.4 Reactions in an attempt to form **12**. 75

3.5 Synthesis of the short PEG isothiocyanato alcohol....77

3.6 Successful attempt of coupling an alcohol to **13** in the presence of an isothiocyanate group....78

3.7 Application of successful coupling conditions of an alcohol to **13** in the presence of an isothiocyanate group....79

3.8 Functionalization of first- through sixth-generation PAMAM dendrimers. 80

4.1 Synthesis of **43** to be used as a spacer in heterogeneous dendrimer functionalization....135

4.2 Initial effort for heterogeneous functionalization of G(4)-PAMAM using **7** and **43**. 136

4.3 Heterogeneous functionalization of G(6)-PAMAM using **7** and **43**....141

4.4 Heterogeneous functionalization of PAMAM dendrimers using **28** and **29**....145

4.5 Complete functionalization of G(3)- to G(6)-PAMAM dendrimer with just **28**. 147

B.1 Functionalization of a G(6)-PAMAM dendrimer with TEMPO. 225

B.2 The reoxidation of TEMPOL-H to TEMPOL by the use of **63** or **64**. 226

LIST OF SCHEMES-CONTINUED

Scheme Page

B.3 Synthesis of iodinated nanoparticle **66**, by the partial functionalization of a G(4)-PAMAM with **65**. 227

D.1 Synthesis of trichloroacetimidate of galactose....240

D.2 Coupling of **28** with **67**....241

D.3 Synthesis of benzyl protected trichloroacetimidate....243

D.4 Coupling of **28** with activated galactose residue....243

D.5 General reaction for the formation and reaction of a sulfonylcarbamate of galactose....245

D.6 Coupling of isothiocyanate **28** with sulfonylcarbamate **72**....246

D.7 Functionalization of a G(4)-PAMAM dendrimer with benzylated galactose and unsuccessful attempts to perform a global deprotection....247

ABSTRACT

The interaction between proteins and carbohydrates is an important first step for many biological processes. For example, viral and bacterial infections, antibody-antigen interactions, fertilization and other cell-cell interactions all rely on protein-carbohydrate interactions as a first step in recognition. It is known, however, that the affinity between a lectin and a single sugar is quite weak. The increase in binding affinity in most biological systems is a result of what is often generically referred to as multivalent binding.

A number of carbohydrate-containing synthetic organic molecules have been synthesized to study multivalent protein carbohydrate interactions. Examples include small molecules that typically contain fewer than 10 sugars, medium sized molecules that contain between 10 and 100 sugars, and large polymeric systems that can contain thousands of sugars.

While most carbohydrate-containing systems have provided valuable insight into the mechanism of multivalent interactions, no class of carbohydrate containing system existed prior to this work in which the number of sugars and the size of the ligand could be varied independently. Such a system should provide specific information on the optimal geometric arrangement of ligands toward various receptors.

We have homogeneously and heterogeneously functionalized polyamidoamine (PAMAM) dendrimers up to generation six with mannose using a thiourea linkage by the reaction of an isothiocyanate on the carbohydrate with the terminal amines on the dendrimer. The result is water-soluble carbohydrate-containing dendritic molecules. Methods to characterize these dendritic macromolecules by nuclear magnetic resonance spectroscopy and matrix-assisted laser desorption ionization time-of-flight mass spectrometry were developed.

The effectiveness of the dendrimers as ligands for the lectin Concanavalin A has been demonstrated by means of a hemagglutination assay, a precipitation assay and a turbidity assay. Results indicate that the size of the dendrimer has a great effect, with the larger dendrimers being most active with Concanavalin A. In addition, the degree of functionalization has a profound effect, with the optimum degree of functionalization for binding being below full functionalization. Results also suggest mannose-functionalized PAMAM dendrimers effectively recruit and cluster lectins.

CHAPTER 1

INTRODUCTION, BACKGROUND AND RATIONALE

Protein-Carbohydrate Interactions

The interaction between proteins and carbohydrates is an important first step for many biological processes. For example, viral and bacterial infections, antibody-antigen interactions, fertilization and other cell-cell interactions all rely on protein-carbohydrate interactions as a first step in recognition (Figure 1.1).[1-8]

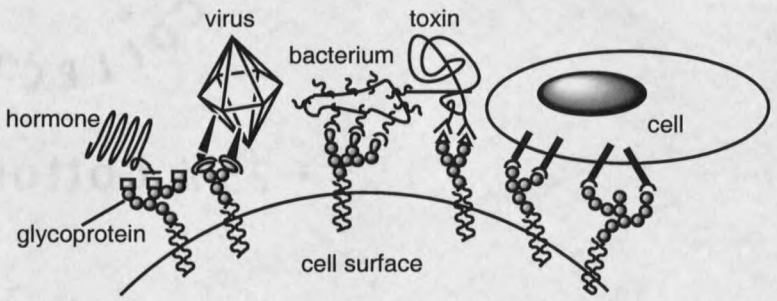


Figure 1.1 Various biological interactions that rely on protein-carbohydrate interactions. Adapted from reference 4.

A well studied case is the infection of human cells by influenza virus.[2, 9-21] In the first step of infection, hemagglutinin on the surface of the virus interacts with sialic acid (a sugar that is present on many glycoproteins) located on the surface of a bronchial epithelial cell. Once the interaction has occurred, barring an adequate immune response, viral infection will proceed.

It is known, however, that the affinity between a carbohydrate receptor, such as a lectin, and a single sugar is quite weak. In the case of binding between hemagglutinin and monomeric α-sialosides, the association constant has been determined to be about 10^3 M^{-1}.[17] However, the interaction between influenza virus and the cell surface is strong enough to lead to an eventual infection.

Other studies of the affinity of lectins for saccharide units have also shown that, typically, a single sugar is only weakly bound.[22, 23] The increase in binding affinity in most biological systems is apparently a result of what is often generically referred to as multivalent binding.

Multivalent Interactions and Glycoside Clustering

Yuan C. Lee at Johns Hopkins University performed pioneering work on the study of multivalent interactions. Lee and co-workers found tremendous enhancements in affinity between small clusters of galactose residues and mammalian hepatic carbohydrate receptors.[24] They found that the binding affinity for monovalent, divalent and trivalent ligands (Figure 1.2) increased roughly from 1 to 1000 then to 1 million, respectively! To describe this general observation, Lee first coined the term "glycoside cluster effect." The glycoside cluster effect is defined by Lee as "affinity enhancement achieved by multivalent ligands over

monovalent ones that is greater than would be expected from a simple effect of concentration increase."[25]

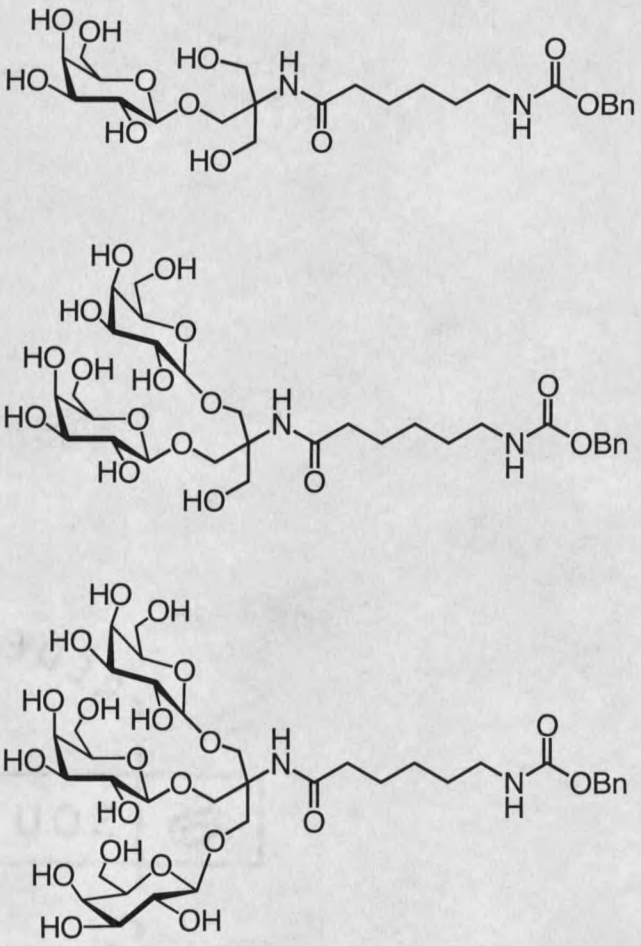


Figure 1.2 Mono-, di-, and tri-valent galactose ligands designed and used by Lee and co-workers to observe the *glycoside cluster effect*.

The term "multivalent interaction" refers to a more specific interaction, that being when a ligand presents multiple epitopes (carbohydrate residues) and binds to two or more distant binding sites on a receptor (protein). What is remarkable is that multivalent interactions are often stronger than the sum of

each individual interaction. In fact, they may be orders of magnitude better. Building synthetic systems that can provide answers for why and how multivalent interactions occur is the focus of the research project presented here.

An excellent example in which multivalent interactions are critical is during an immune response. During an immune response, not only do multivalent interactions increase the affinity between molecules, but they are also necessary to induce the appropriate response.[2]

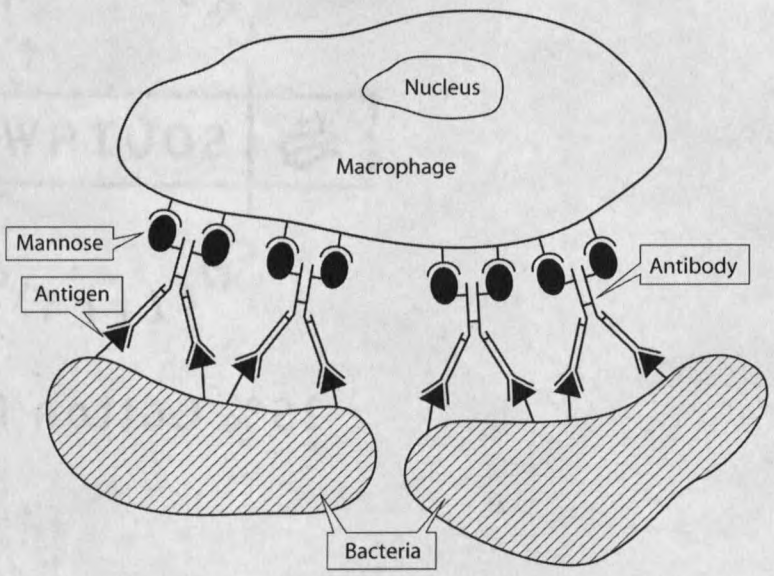


Figure 1.3 Interaction of a macrophage and bacteria mediated by antibodies. The macrophage will not recognize the bacteria without the antibodies. In addition, the macrophage will not digest the bacteria until enough antibodies have attached to the bacteria and the macrophage. This is an example in which multivalent interactions are required for a biological response. (Adapted from reference 2)

Antibodies have multiple equivalent binding receptor sites. Depending on the antibody, it may have two, four, six, or ten sites. The antibodies recognize and bind to a specific, repeating epitope (antigen) on the surface of a pathogen.

Multivalent binding is necessary to ensure a strong enough interaction between the antibody and pathogen (Figure 1.3).

After the antibodies have attached multivalently to the surface of the pathogen, mannose residues on the tail of the antibody interact with mannose receptors on the surface of a macrophage. Once enough antibodies are bound to the macrophage, then and only then does the macrophage proceed to ingest and destroy the pathogen. If only one antibody (free or bound to a pathogen) interacts with the macrophage, a response by the macrophage is not induced. Interaction with multiple antibodies is critical.

Indeed, the effect that multivalent binding has on biological systems has long been recognized. However, what causes the observed increase in affinity is still unclear, and there is no consensus among the scientific community as to its cause.[26] It is clear that more studies of multivalent interactions must be done in order to uncover the underlying principles and mechanisms of multivalent interactions. By doing so, it may one day be possible to rationally design multivalent therapeutic drugs that can treat or prevent disease.

Design of Synthetic Multivalent Ligands

Given the prevalence of protein-carbohydrate interactions in biological systems, it is no surprise that a great deal of research has dealt with the design

of synthetic ligands that mimic native ligands in order to act as inhibitors or effectors.

In the case of inhibitors, a synthetic ligand would be required to interact with an invading pathogen more favorably than a native ligand. For example, in the case of the influenza virus described above, a synthetic ligand that presents copies of sialic acid on its surface would, if designed correctly, bind preferentially with the virus and prevent interaction with the sialic acid on the epithelial cells. The net effect would be inhibition of the virus.[9, 12, 16, 27] A number of multivalent ligands have been synthesized that show inhibiting abilities in a variety of systems.[28-33]

In contrast to inhibitors, are the effectors. An effector is a moiety that causes a biological signaling process to occur. There are a number of examples in which the dimerization (or higher aggregation) of cell surface receptors is necessary for signal transduction to occur.[21, 34-38] For example, protein tyrosine kinases (PTKs), which catalyze the phosphorylation of tyrosine in various proteins, consist of an intracellular binding domain, a transmembrane domain and the cytoplasmic catalytic site. As a monomer, PTKs are inactive. However, when a divalent ligand binds with the extracellular binding domain, it causes the PTKs to be in close enough proximity that ATP binding is possible which then leads to transphosphorylation of tyrosine. Effectors are ligands that in some

cases could cause or enhance a biological response by clustering receptors on a cell surface resulting in signal transduction for some process.

Various Modes of Multivalent Binding

When considering the design of multivalent ligands, it is necessary to consider the various modes of binding that could lead to enhanced interactions. It must be recognized, however, that in any given system, synthetic or natural, more than one mode may be involved. It is this complexity that makes multivalent ligand systems difficult to study and understand. In fact, the activity observed for a multivalent interaction may be a result of a combination of binding modes. A variety of reviews have previously described the various modes of multivalent interactions, and only a brief description of the most common and important modes is given here.[39, 40]

Monovalent Interactions

Monovalent binding (Figure 1.4a) is the simplest scenario. During a monovalent interaction, one sugar binds with one binding site. As already mentioned, this interaction is quite weak and typically does not induce a biological response.

Multivalent Interactions

A multivalent interaction is also referred to as the chelate effect.[41-43] For multivalent interactions to take place, a given ligand must be capable of binding to multiple binding sites (Figure 1.4b). Multivalent binding is favorable because after the initial interaction (which is analogous to a monovalent interaction) a second interaction is essentially intramolecular. The initial interaction costs one translational entropic unit, which does not have to be paid by the second interaction.[41, 44] However, depending on the system, the cost of losing conformational flexibility after the second interaction may be too great. As the binding sites get farther and farther apart, the linker connecting the binding epitope becomes critical. The conformational entropy penalty becomes greater as the linker becomes longer.[2, 22, 45, 46]

Glycoside Cluster Effect

The glycoside cluster effect is also referred to as a statistical effect or a local concentration effect (Figure 1.4c). Many times in the literature, the term "glycoside cluster effect" and "multivalent binding" are used to refer to the same effect.[22, 47-50] For the discussion of our work, we adopt the definition of glycoside clustering given in the literature, but apply it in a narrower context than is sometimes used. We define glycoside clustering and monovalent binding as related but distinct terms. Glycoside cluster effect is the result of local

concentration around one given receptor. If a binding epitope dissociates from a receptor, a ligand with a high concentration of epitopes has a higher chance of rebinding due to the number of epitopes immediately available to the receptor. This contrasts with the definition given for multivalent interactions, namely, that multivalent interactions involve multiple binding sites on the same receptor. Typically, glycoside clustering shows small to moderate enhancements in binding, while multivalent interactions can show large and dramatic enhancements in binding.

Cross-linking

Another mode that must be considered in the context of this work is cross-linking (Figure 1.4e). In this case, a ligand binds with multiple receptors. If the cross-linking is extensive enough, large aggregates can form. If the aggregates become large enough, they typically precipitate out of solution.

It should be noted that the definitions given above are meant to be examples and are not all-inclusive. Other aggregate motifs may well be important in protein-carbohydrate interactions. For example, many lectins may be bound in a multivalent manner to each dendrimer (see discussion starting on page 18 for a full description of dendrimers).

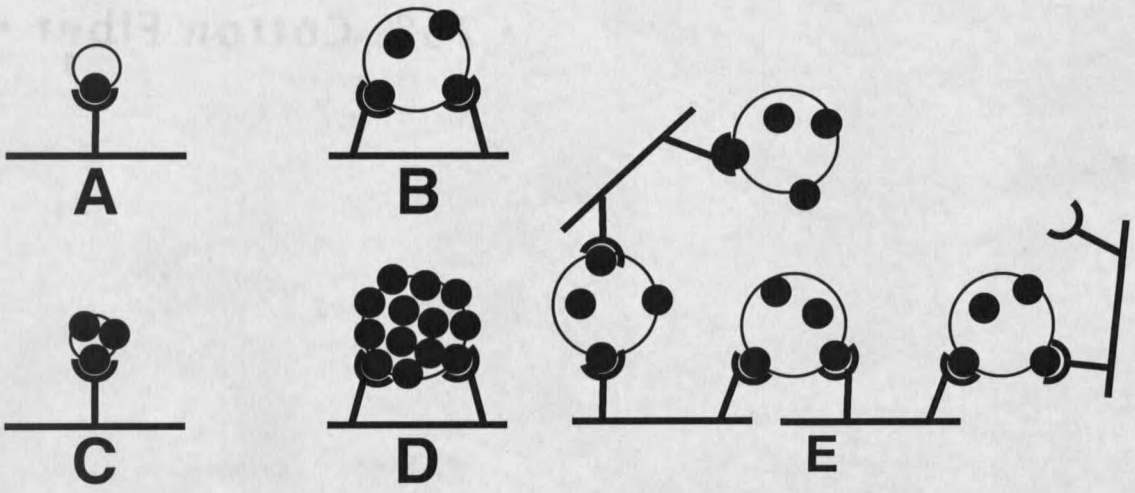


Figure 1.4 Various modes of interactions: a) monovalent, b) multivalent, c) glycoside clustering, d) both multivalent interactions and glycoside clustering, e) cross-linking.

Complications in Multivalent Ligand Design

With all of the possible modes of binding available for protein-carbohydrate interactions, it becomes evident that in a real system, one mode may not be the exclusive type of interaction. In a given system any combination of the binding modes described here (as well as those not described here) may be involved. Therefore, the observed activity is the activity of the whole system, rather than the activity of various types of interactions. Figure 1.4d shows a case in which both multivalent interactions and glycoside clustering are occurring. To what extent each contributes to the observed affinity of ligand for receptor is difficult to determine.

In the simple monovalent case, the association constant (K_a) thermodynamically describes the relationship between the two states of ligand and receptor (free or bound). In a more complicated case, any measurement would not be able to distinguish between the various modes present in that system. For example, if a system can chelate and crosslink, any measurement would give a net effect and the unique contributions of each mode would be lost. To explore the various modes of binding requires a variety of ligand systems and assays. Understanding what contributions each interaction makes would be extremely useful in guiding the design of highly effective therapeutic polyvalent ligands.

Currently, the design of multivalent ligands is largely a trial and error endeavor. The state of the art is such that a molecule is designed and synthesized to present a number of binding epitopes (a small sampling of approaches is given in the following section). This molecule is then tested using a variety of assays to determine its performance as a multivalent ligand, after which, the design can be optimized and the process repeated.

Another concern in the study of multivalent interactions is the assays used. There are a number of assays available to measure the effectiveness of the designed multivalent ligands (a number of assays pertinent to this work will be described when appropriate), however, if a variety of ligands are tested by a

given assay, the comparison of results can only be valid if all the ligands tested participate in the same modes of binding.

A second concern is that the assays used are by necessity exceedingly simplified relative to actual biological systems. While they present a very good starting point for the analysis of multivalent ligands, ultimately, the viability of a ligand will be determined in the actual (and more complex) biological system.

The basic challenge in designing a multivalent ligand is to optimize the presentation of a binding epitope to a specific receptor. We propose that carefully designed ligands may be used to systematically study the various interactions independently, thus providing insight into how to optimize multivalent ligand displays.

Ligand Design

In order to achieve the goal of understanding how multivalent interactions work and how they can be exploited, many artificial carbohydrate-containing systems have been developed to act as inhibitors or effectors. Currently, one of the major hurdles to the design of synthetic ligands is the lack of understanding of the underlying mechanism of multivalent interactions. Nonetheless, carbohydrate-containing systems have provided a great deal of insight into the problem of understanding how multivalent interactions work. Most synthetic ligands can be roughly classified into three main types based primarily on size:

small, medium (such as dendritic glycosides), and large molecules (such as polymeric ligands).[22, 40, 46, 51]

The simplest ligands to synthesize and test are small molecules containing clusters of carbohydrates.[18, 19, 47, 52-57] Many carbohydrate-containing small molecule ligands show enhanced binding affinities. In most cases, the enhancement is more than additive. In 2000, Kiessling and co-workers reported placing mannose on a rigid macrocyclic scaffold (Figure 1.5).[52]

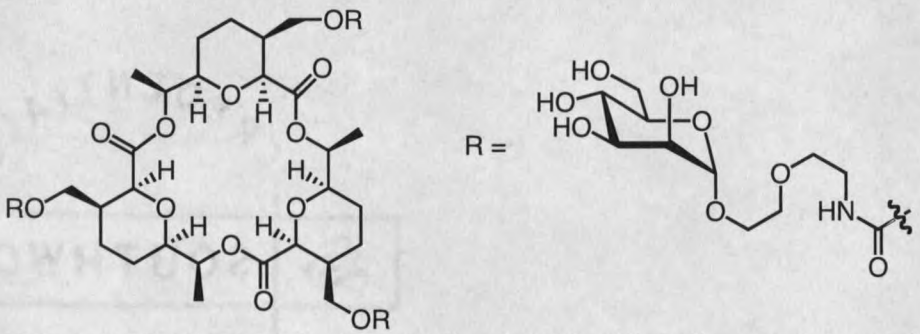


Figure 1.5 Small, trivalent molecule synthesized by Kiessling and co-workers to study the glycoside cluster effect.

This trivalent ligand was found to be more potent than the corresponding monovalent ligand due to its ability to cluster the receptor (Concanavalin A) in solution. Multivalent binding is not expected to occur as the small molecules are typically too small to span multiple binding sites. So, the enhanced binding that is occurring is a result of glycoside clustering (Figure 1.4c) and crosslinking (Figure 1.4e). Small molecules typically are more potent because they precipitate the

lectin.[33, 47, 57, 58] The Kiessling example is the first documented case of soluble aggregation.

In contrast to the small molecules, the large carbohydrate-containing molecules can present many sugar residues. Polymeric glycoside clusters, for example, typically contain about 1000 sugars per polymer. A common technique for the formation of glycopolymers is by the free-radical polymerization of acrylamides.

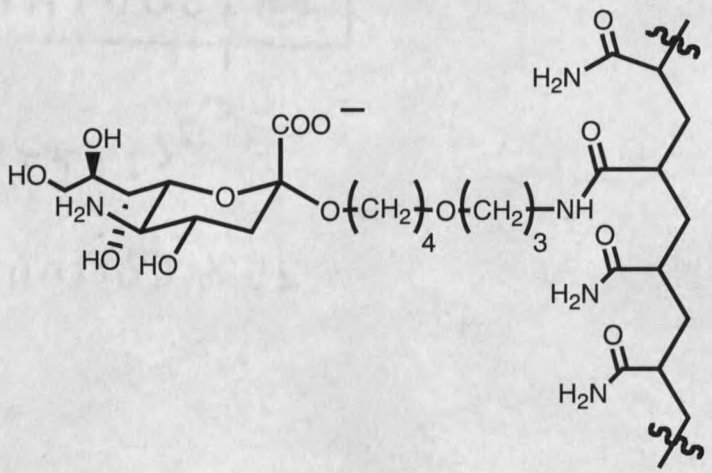


Figure 1.6 Polyacrylamide synthesized by Whitesides containing 20% sialic acid residues. This example had a molecular weight of 10,000 and an activity 100,000 greater than monomeric sialic acid.

Studies using glycopolymers have shown that binding is much more favorable with very large multivalent systems than the binding of proteins with single sugars.[14, 59-64] For example, in 1991, Whitesides and co-workers showed that polyacrylamides with MW of 10,000 and at least 20 mol% sialic acid as a side chain were up to 100,000 times more effective at inhibiting hemagglutination

(hemagglutination inhibition will be discussed in detail in the section starting on page 92) than monomeric methyl α-sialoside (Figure 1.6).[11]

One major drawback of many of glycopolymers formed by free radical or cationic mechanisms is that the size of the polymer chain is very difficult to control or predict, thus making it difficult to control the presentation of the carbohydrates. Therefore, a more controlled and systematic study of the relationship between size, number of sugars and ligand activity proved nearly impossible using large glycopolymers.

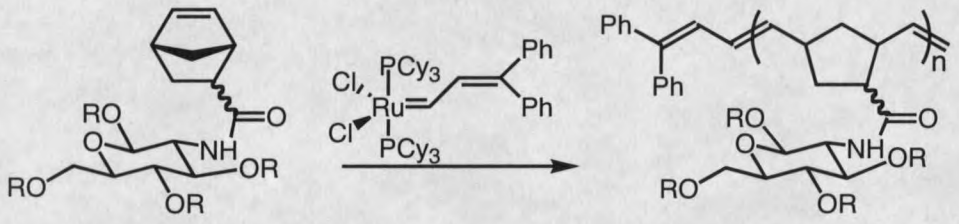


Figure 1.7 Ring-opening metathesis polymerization reaction demonstrated by Grubbs as an effect means for the controlled formation of carbohydrate-containing polymers.

A significant advance in the field came when Grubbs and co-workers showed that it was possible to control the size of glycoside containing polymers using the ring-opening metathesis polymerization (ROMP) technique.[65] In this reaction, a ruthenium catalyst is used to polymerize carbohydrate-containing norbornene molecules (Figure 1.7).[66-68] This method has been exploited by a number of groups. Kiessling and co-workers have contributed extensively to the development of this method.[1, 21, 62, 69-74] In one example, they observed a

50,000-fold enhancement in inhibitory activity for the *C*-mannoside neoglycopolymer relative to the monovalent derivative (Figure 1.8).[75]



Figure 1.8 *C*-mannoside neoglycopolymer synthesized using ROMP by Kiessling that showed 50,000-fold enhancement in inhibitory activity.

The third general class of molecules, the medium sized ligands, is of special interest to the work described herein. While the most common types are dendritic in nature (more attention will be given to dendritic ligands in a later section), there are a number of other examples that are of interest.

One example that bears mention is the so-called "STARFISH" ligand developed by Kitov *et. al.*.[43] The inhibitor shown in Figure 1.9 displayed *in vitro* inhibitory activity 1 million to 10 million times higher towards Shiga-like toxins I and II than that of the monovalent ligand. Shiga-like toxins are produced by *Escherichia coli* and are responsible for the deleterious effects of *E. coli* infection. The Shiga-like toxin I (SLT-I) is a doughnut-shaped pentamer with three saccharide-binding sites per monomer. All 15 binding sites are on one face of the toxin. The STARFISH inhibitor was designed to interact with the ten most active binding sites on the toxin (known as sites 1 and 2). What they found was that instead of one inhibitor interacting with one toxin, two toxins were interacting with each inhibitor to form a sandwich-like complex.

While this provides an excellent example of a very potent inhibitor, the development of this ligand required extensive experimentation. In addition, while this ligand and its development are certainly not without merit for the field as a whole, it must be recognized that the results described are for a very specific case.

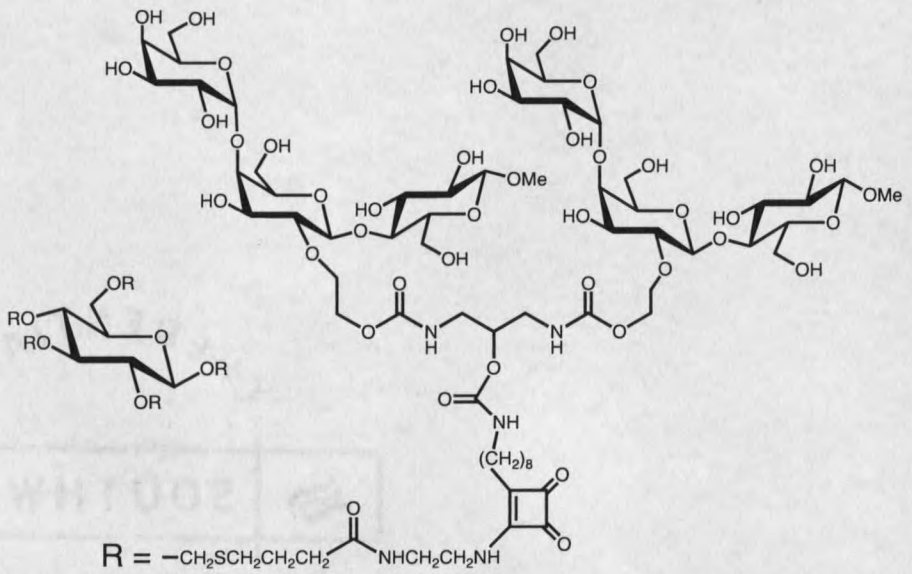


Figure 1.9 STARFISH inhibitor designed to interact with Shiga-like toxins. This example showed activity up to 10 million times greater than the trisaccharide unit.

The basic challenge still remains: explain what is happening on a molecular level to give multivalent ligands enhanced activity and (more importantly) apply this explanation to the development of other multivalent ligands in order to optimize therapeutic capabilities.

In the polymeric ligand systems, it seems clear that both multivalent binding and glycoside clustering are responsible for enhanced binding. Yet, it is not clear to what extent each is responsible. In the case of linear polymers, the

size of the molecule and number of sugars are intrinsically linked (i.e. the size cannot be changed without changing the number of sugars and vise versa). Currently, there has been no system designed that can delineate between the two effects. A desirable system would be one in which the size, number of sugars and how the sugars are displayed can be varied independently. In addition, a wide range of sizes must be readily available. Dendrimers are a class of molecules that fit these criteria.

Dendrimers

Dendrimer chemistry has received a great deal of attention in recent years.[76-87] Dendrimers are spherical polymers that branch out from an inner core. There are two main synthetic methods that can be used to synthesize dendrimers, convergent or divergent.

In a divergent synthesis, a central core molecule is functionalized to create a new layer or generation (Figure 1.10). The surface of the newest generation is then functionalized to create another generation. This continues until the desired size is reached. As the dendrimer grows, the number of surface groups doubles with each generation.

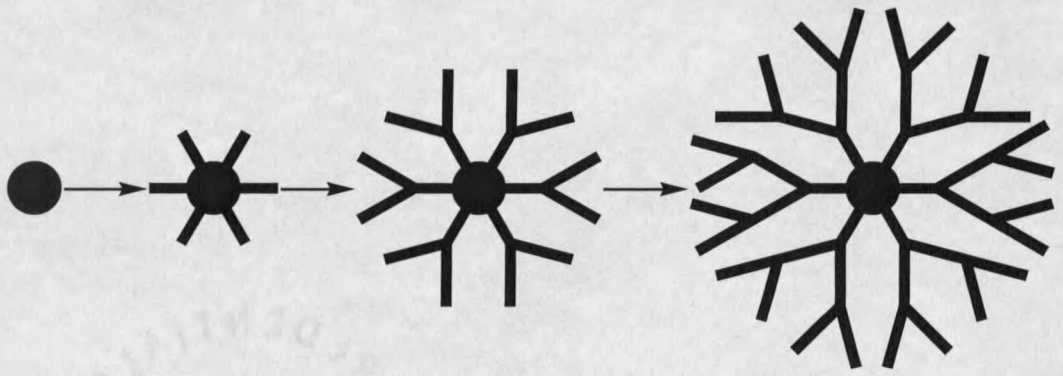


Figure 1.10 Schematic depicting divergent dendrimer synthesis

In a convergent synthesis, "pieces" of the dendrimer are synthesized (Figure 1.11). One of the final steps is the combination of the pieces to form the final dendrimer. While this method is more labor intensive, one of the main benefits is that specific regions of the dendrimer can be functionalized differently.

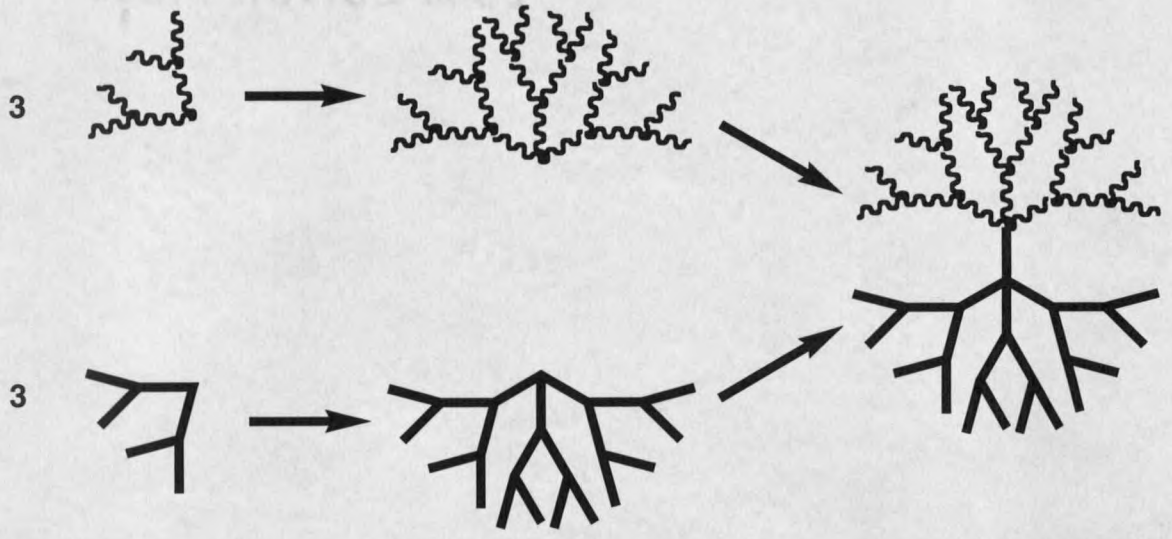


Figure 1.11 Schematic depicting divergent dendrimer synthesis.

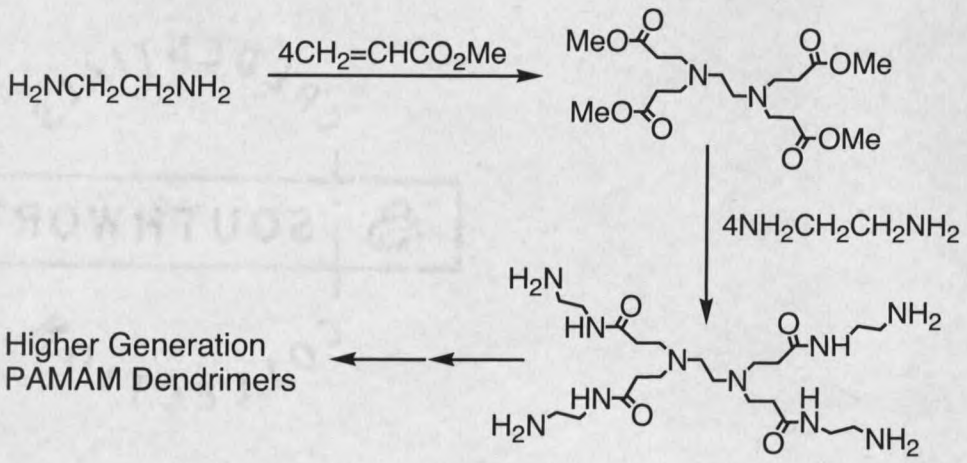
PAMAM Dendrimers

The dendrimers of interest in this research project are poly(amidoamine) dendrimers (PAMAM). PAMAM dendrimers were first described by Tomalia in 1985 and are often referred to as "starburst" dendrimers due to their star shape.[88] They are commercially available in a number of sizes, and terminally functionalized with amines or carboxylates. PAMAM dendrimers are easy to handle and are moderately robust. They are soluble in a number of organic solvents and water. Because of their ready availability and ease of handling, many uses of PAMAMs are described in the literature.[79, 87, 89-95]

PAMAM dendrimers are divergently synthesized by the Michael addition of ethylene diamine to four molecules of methyl acrylate to form a tetraester. This is followed by reaction with four molecules of ethylene diamine to form a tetraamide (Scheme 1.1).[91] The result is a generation zero PAMAM dendrimer that contains four terminal amines. Higher generations are obtained by the reiteration of the Michael addition and the amide formation steps. After each sequence of steps, the number of terminal amines doubles.

It should be noted that the terminology of other divergently synthesized dendrimers, such as DAB dendrimers (poly(propylene imine) dendrimers), varies. For DAB dendrimers, after the first iteration the dendrimer is labeled a generation

one dendrimer rather than generation zero as is done for PAMAM even though both macromolecules contain four terminal amines.



Scheme 1.1 Synthesis of PAMAM dendrimers.

A two-dimensional representation of a generation four PAMAM dendrimer is seen in Figure 1.12. This necessarily distorted drawing depicts what would be, in three dimensions, a nearly spherical macromolecule.

The three dimensional structure of PAMAM dendrimers varies from generation to generation. By using computer simulations along with physical measurements, Tomalia *et. al.,* as well as others, determined that generations 1-3 are highly asymmetric and ellipsoidal in nature. Generations 5-7 are nearly spherical while generation 4 has a spheroid shape somewhere in between.[89, 96] A functionalized G(4)-PAMAM would be expected to be more spherical than the G(4)-PAMAM starting material.[90]

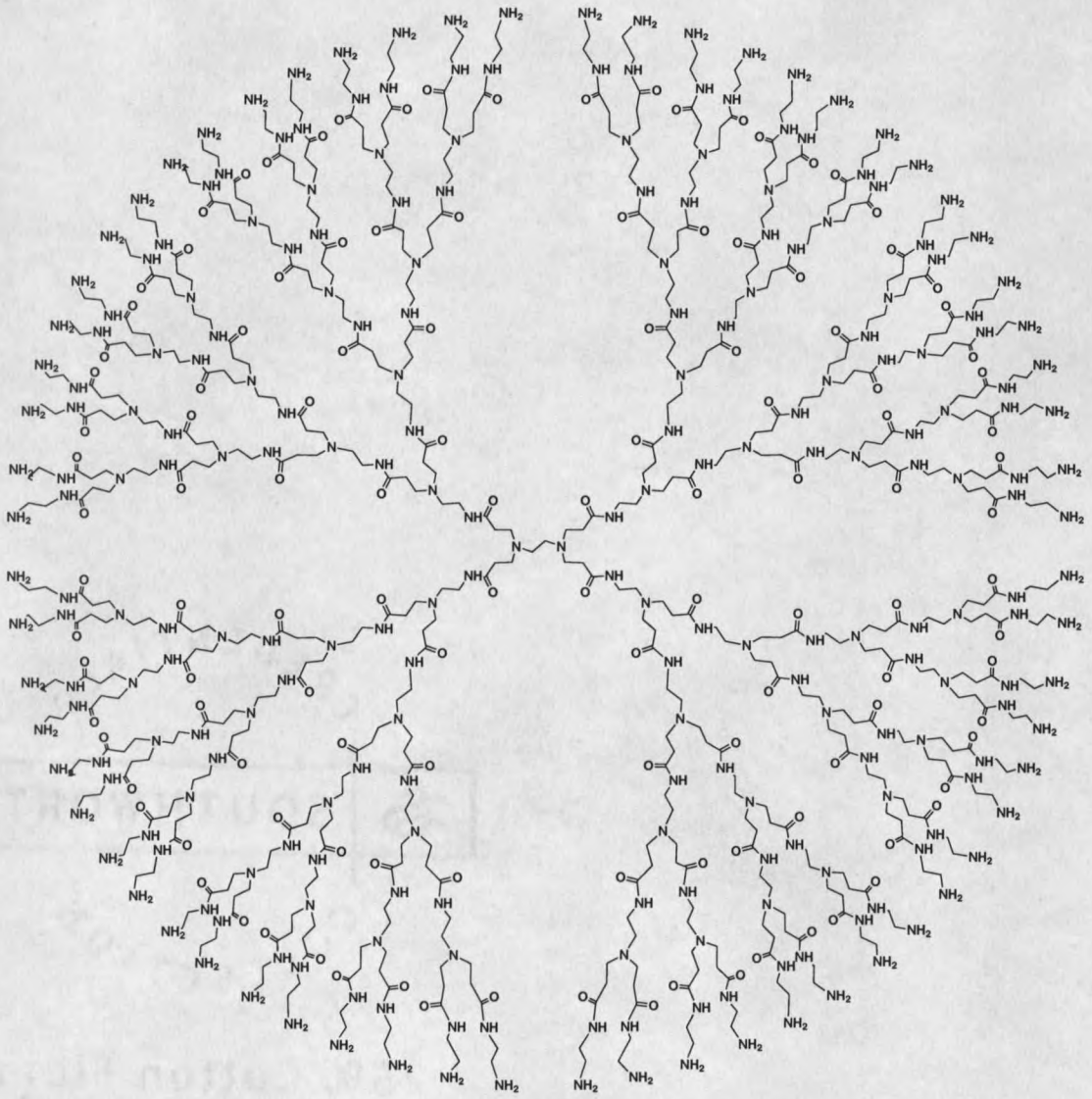


Figure 1.12 Structure of a generation four PAMAM dendrimer

Unlike most polymers, dendrimers tend to have polydispersities[97] very close to one. In other words, dendrimers tend to be more homogeneous than other polymers that are often mixtures of large molecules with a wide variety of molecular weights. What this means for the purpose of this work is that dendrimers are excellent scaffolds for the presentation of carbohydrates.

Table 1.1 Theoretical properties of PAMAM dendrimers taken directly from the Dendritech, Inc website.

Generation	Molecular weight	Measured diameter (Å)	Surface groups
0	517	15	4
1	1,430	22	8
2	3,256	29	16
3	6,909	36	32
4	14,215	45	64
5	28,826	54	128
6	58,048	67	256
7	116,493	81	512
8	233,383	97	1024
9	467,162	114	2048
10	934,720	135	4096

Shown in Table 1.1 is data for PAMAM dendrimers up to generation 10.[98] The values shown are theoretical values, and as will be seen later, do not completely describe PAMAM dendrimers. Specifically, as the generation increases, the actual molecular weight values become increasingly less than predicted, while the diameters become greater than predicted. This will be addressed in further detail later.

Despite this inconsistency between theoretical and actual values, PAMAM dendrimers are still an attractive scaffold for the formation of medium sized ligands for probing protein-carbohydrate interactions. By the controlled functionalization of PAMAM dendrimers with carbohydrates, it should be possible to control the number of carbohydrates on the surface. At the same time, by using different generations, it should be possible to alter the size of the ligand in

a controlled manner. By varying the size and degree of functionalization independently, it should be possible to measure the effect of multivalent binding and glycoside clustering independently (Figure 1.4b and c). As a result we will gain valuable insight into the mechanism of multivalent binding.

In addition to the structural stability of PAMAM dendrimers, studies have shown that *in vitro* and *in vivo* toxicity and immunogenicity were well within safe limits.[99] This suggests that PAMAM dendrimers may safely serve as a part of a drug delivery system or in other biomedical applications.[79]

Concanavalin A

For our studies, the lectin we chose was Concanavalin A (Con A). Con A is a plant lectin isolated from the jackbean. While its function in the jackbean is unknown (the function of most lectins is unknown), it has been widely studied and a great deal is known about Con A.[3, 100-104] Lectins such as Con A bind with carbohydrates in a non-covalent manner, but are devoid of any catalytic activity. Most lectins have two or more active binding sites.

Each Con A monomer is comprised of 137 amino acids and has a molecular weight of 26,000 g/mol. In the pH range of 5.0-5.6, Con A exists as a dimer, while at pH above 7.0 it exists as a tetramer. Con A is a C-type lectin,

which means it requires the presence of calcium (as Ca^{2+}) to be active. In addition, for Con A to be active, it must also incorporate a Mn^{2+} ion.[105-110]

Numerous high-resolution crystallographic structures of Con A both in native and saccharide-bound forms have been reported (Figure 1.13).[101, 108, 111-115] In the tetramer form, the sugar-binding sites are 65 Å apart. The overall shape of Con A is similar to that of a tetrahedral molecule. The result is that for a large multivalent dendrimer, two binding sites are readily available, while the other two are not. In contrast, large linear glycopolymers can wrap around Con A and interact with all four binding sites.

Since erythrocytes have a number of sugars on the surface, lectins can bind with them. If extensive cross-linking occurs between the lectins and cells, a process known as cell agglutination occurs. This process is also known as hemagglutination. Hemagglutination can be inhibited by the use of an appropriate ligand, typically using a sugar that the lectin binds with specifically. The concentration of ligand at which hemagglutination stops is considered the inhibiting dosage. This is the basis for an assay known as the hemagglutination inhibition assay, which will be described in more detail later (hemagglutination inhibition will be discussed in detail in the section starting on page 92).

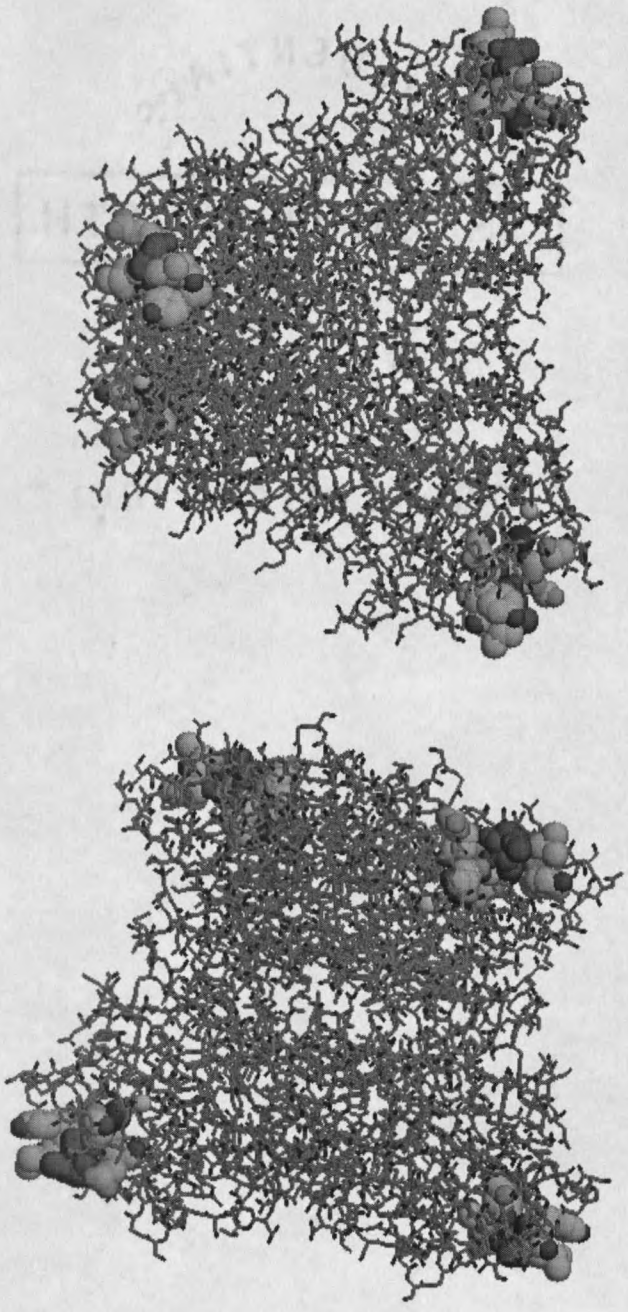


Figure 1.13 Two views of the crystal structure of Concanavalin A. Con A is a tetramer with each monomer in a tetrahedral arrangement. The space-filling portions of the structure are the binding sites. In this case, methyl mannose is shown in the binding site as the dark space filling atoms.

Each Con A monomer has one sugar-binding site that binds specifically with the α-pyranose forms of D-mannose and D-glucose. Con A does not bind appreciably with galactose or fucose. The strength of binding is sensitive to structure. Methyl-α-D-mannopyranoside has an association constant around 7700 M^{-1} while α-D-mannose has a value of 1700 M^{-1}. The trend is similar for glucose. Methyl-α-D-glucopyranoside has an association constant around 2400 M^{-1} while α-D-glucose is even lower at around 500 M^{-1}. The interaction is stronger with branched oligosaccharides.[23, 42, 116-118] For example, a trimannoside has an association constant of around 10^6 M^{-1}.[42, 117]

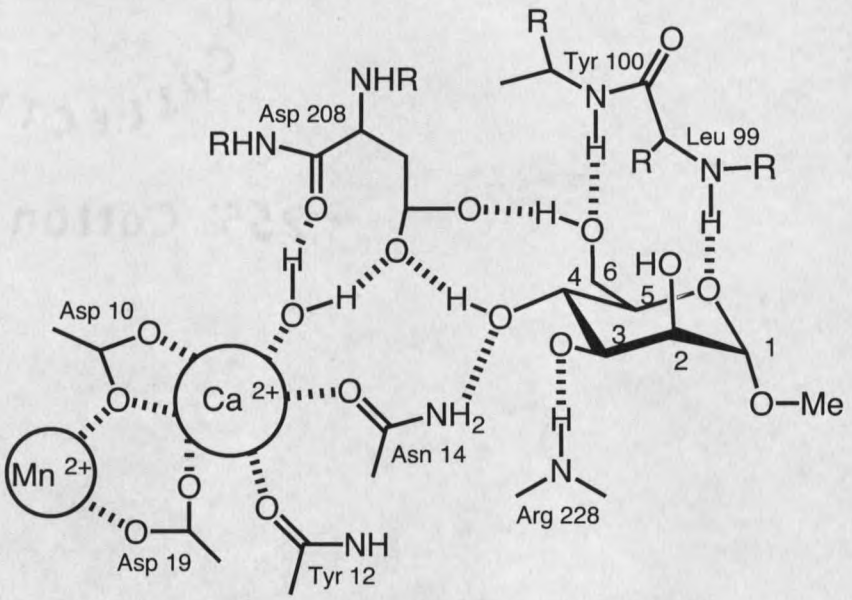


Figure 1.14 The binding site of Con A, showing the participating amino acids. Also shown are the metal ions required for binding.

Figure 1.14 shows the binding cleft and the amino acid residues involved in the interaction.[119] From this diagram, a qualitative assessment can be made about the observed selectivity. Since Con A binds with both glucose and mannose, the stereochemistry at C-2 on the sugar has only a small affect on the strength of binding. While it is clear that hydrogen bonding of the hydrophilic regions of the sugar is the key interaction, the observed fact that glucose is bound more weakly than mannose indicates that hydrophobic interactions are important as well. When the C-2 hydroxyl group is axial (as it is in mannose), a larger portion of the hydrocarbon ring of the sugar is exposed to a hydrophobic region of the binding site. Putting the hydroxyl group in the equatorial position (as it is in glucose), places a polar group directly in the vicinity of the same hydrophobic region, thus weakening the interaction, albeit slightly. Changing the stereochemistry at C-4 yields a much more dramatic effect. Placing the hydroxyl group in an axial position (as it is in galactose) essentially eliminates all ability to bind, indicating the critical involvement of hydrogen bonding between this hydroxyl group and the carboxylate of aspartic acid-208 and amide nitrogen of asparagine-14.

PAMAM Dendrimer Functionalization Strategy

Because of the specificity of Con A for D-mannose, the carbohydrate of interest in our initial studies has been D-mannose. A carbohydrate-functionalized

generation six PAMAM dendrimer (G(6)-PAMAM) is expected to be large enough to span the 65 Å between binding sites (Figure 1.4b and d). Whereas, a carbohydrate-functionalized G(3)-PAMAM is too small to be able to span multiple binding sites (Figure 1.4c). In this way, by using different generations of dendrimers, multivalent interactions can be avoided or expected.

In addition to controlling the size of the molecule, PAMAM dendrimers should be amenable to heterogeneous functionalization. Through heterogeneous functionalization it should be possible to vary the number of sugars on the surface of the dendrimers and to observe the effect of sugar density. Specifically, it should be possible to functionalize G(6)-PAMAM and G(3)-PAMAM with a similar density of carbohydrates on the surface. By doing so, the effects associated with glycoside clustering and multivalent interactions can be delineated (Figure 1.4 b and c).

Methods of PAMAM Functionalization

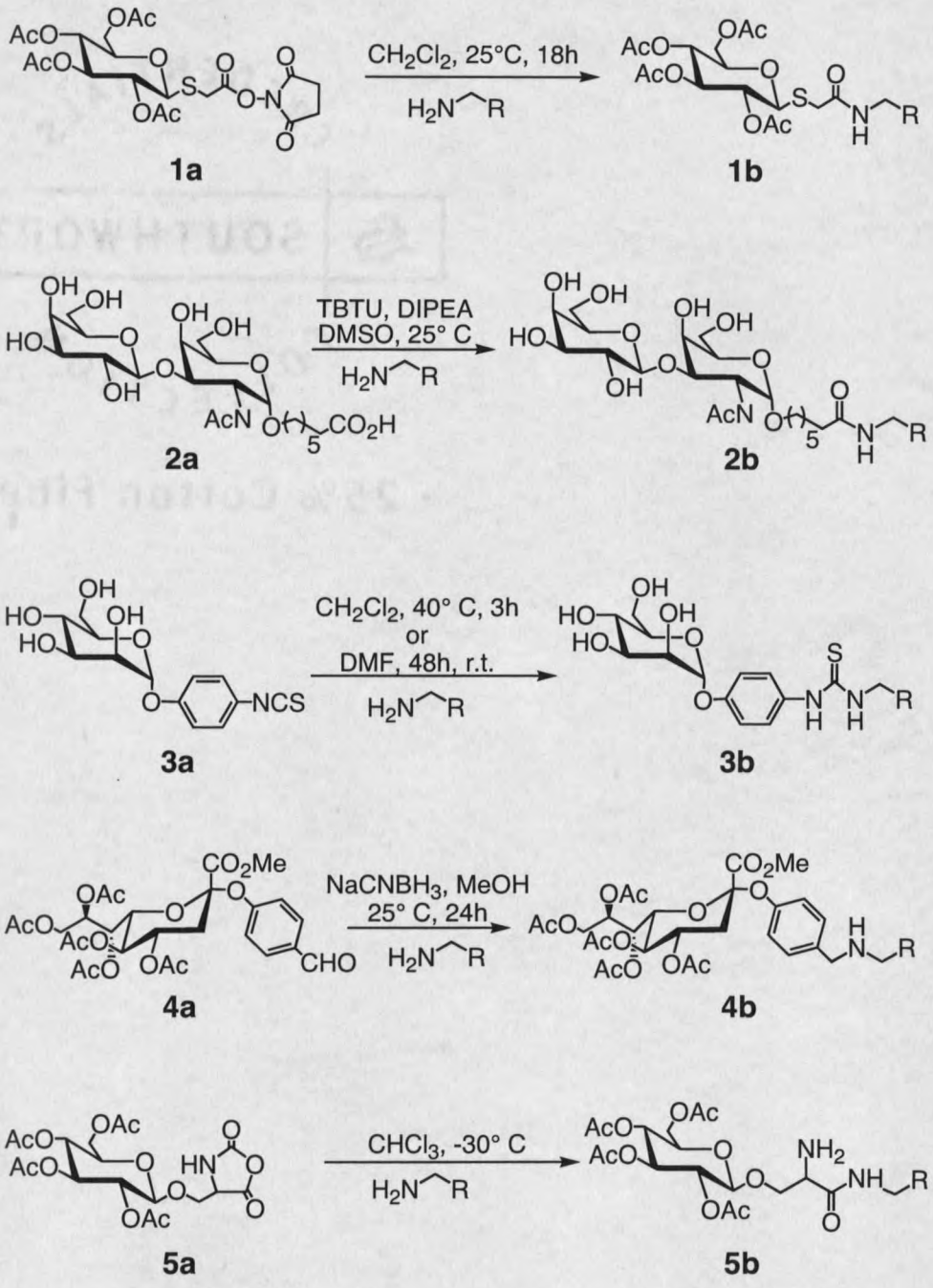
The carbohydrate functionalization of dendrimers has been reported extensively. Therefore, it is of interest for the purpose of putting this work in context to *briefly* review the various methods used to functionalize dendrimers and the results observed. Specifically, a number of methods to functionalize amine terminated PAMAM dendrimers with carbohydrates are described.[120]

Scheme 1.2 shows a variety of methods used to functionalize amine-terminated PAMAM dendrimers.

Meijer, Stoddart and co-workers have used an *N*-succinimidyl activated ester (**1a**) to functionalize amine terminated dendrimers with 64 end groups. The coupling reaction, common to peptide chemistry, is mild and effective. In this case the yield of **1b** was 95%.[121]

René Roy from the University of Ottawa has worked extensively with PAMAM dendrimers. He has described a number of methods to functionalize PAMAM dendrimers with carbohydrates. Recently, Roy also borrowed from peptide chemistry to couple T-antigen, β-Gal-(1-3)-α-GalNAc (**2a**), to a G(3)-PAMAM (32 terminal amines) using 2-(1H-benzotriazole-1-yl)-1,1,3,3-tetramethyluronium tetra-fluoroborate (TBTU) and *N,N*-diisopropylethylamine (DIPEA) to form **2b** in 73% yield.[122]

PAMAM dendrimers have also been successfully functionalized using isothiocyanates. An example is the addition of **3a** to a PAMAM dendrimer to form **3b**.[123] This example, taken from the work of Roy and Pagé, was done in refluxing CH_2Cl_2 for 3h to functionalize generations zero through two (4-mer through 16-mer) and in DMF for 48h to functionalize the less soluble generation three (32-mer).



Scheme 1.2 Various methods of PAMAM dendrimer functionalization.

Isothiocyanate chemistry, as will be seen later, is the cornerstone method for dendrimer functionalization used in the work described herein. It is

advantageous in that isothiocyanates react selectively with amines. The observed selectivity avoids the necessity of protecting the sugar hydroxyl groups, which can be burdensome and problematic when attempting global deprotection of over 200 sugars on a dendrimer.

A fourth method is the reductive amination using $NaCNBH_3$. Sashiwa and co-workers have used this reaction to attach sialic acid to dendrimers.[124, 125] In the example given, *p*-formylphenyl-α-sialoside **4a** is attached by reductive amination with $NaCNBH_3$ to form **4b**. While yields were not given for the step shown, the authors did indicate that in the presence of excess **4a** resulted in unavoidable *N,N*-disubstituted product as well.

A unique method that has been used to functionalize PAMAM dendrimers is by the use of sugar-substituted α-amino acid *N*-carboxyanhydrides (glycoNCAs). An example from the work of Okada is the reaction of PAMAM dendrimer with *O*-(tetra-*O*-acetyl)-β-D-glucopyranosyl)-L-serine *N*-carboxyanhydride **5a** to form glucose substituted product **5b**.[126] While the use of glycoNCAs is not widespread, one reason for performing such a reaction in this case is the formation of a new primary amine, which can be further functionalized under appropriate conditions.

Goals

The first goal of this project was to develop a method for the carbohydrate functionalization and purification of PAMAM dendrimers up to generation six (extension beyond generation six PAMAMs is unattractive due to the increased cost and complexity of the starting materials). While there are a number of references to the functionalization of PAMAM dendrimers up to generation three, there are very few for the functionalization of generation four. There are even fewer for generation five and six. In fact, to the best of our knowledge, there are only two references to carbohydrate functionalization of generations five and six.

Roy *et. al.* reported the functionalization of a generation five PAMAM dendrimer with lactose to study how the topology of binding site presentation and ligand display affects binding selectivity.[127] Okada and co-workers report the galactose and *N*-acetylglucose functionalization of PAMAM generations six, seven and eight to study the effect sugar density had on the ability of the dendrimer to recognize and encapsulate a naphthalenesulfonate salt. In addition, they measured the ability of the galactose functionalized dendrimers to inhibit wheat germ agglutinin lectin.[128]

A second goal was to develop methodology to heterogeneously functionalize PAMAM dendrimers up to generation six. This will allow us to control the number of sugars present on the surface of the dendrimer.

With the success of the synthetic portion, the development of methods to characterize the synthesized carbohydrate-functionalized dendrimers was critical. One of the biggest hurdles in the dendrimer field is the difficulty of characterizing macromolecules. While proton and carbon NMR are well-established techniques, the use of mass spectrometry is less prevalent. The use of a reliable mass spectrometry technique would provide valuable information such as an accurate percent loading of carbohydrates on the surface based on the molecular weight data. Therefore, we desired to work out a method to analyze macromolecules (specifically the glycodendrimers described here) by matrix assisted laser desorption ionization time-of-flight mass spectrometry (MALDI-TOF MS). This was no trivial task, but we have presented a general MALDI method for functionalized PAMAM dendrimers.

Finally, it was necessary to measure the biological activity of mannose-functionalized PAMAM dendrimers toward Con A. A number of assays were employed. Details of the biological assays will be given when appropriate, but the mannose-functionalized dendrimers we synthesized were studied extensively with a hemagglutination assay, precipitation assay, and turbidity assay.

Summary

Studies of the mannose-functionalized PAMAM dendrimers have revealed that they are much more active towards Con A than monomeric α-methyl

mannoside with the largest dendrimers showing the greatest activity.[129, 130] The assays have also shown that the degree of functionalization of the dendrimer has a profound effect on the activity.

From the results described in the following chapters, some clear differences in the contributions of multivalent interactions and glycoside clustering can be made. Future development of this project based on the foundations presented in this work should contribute greatly to the understanding of the underlying causes of enhanced binding in multivalent interactions. The developments described here may ultimately contribute significantly to the design of multivalent therapeutic agents.

Organization

The work presented here will be organized into three main phases. The first phase is the synthesis of α-phenyl mannoside and the functionalization of PAMAM dendrimers with this sugar. Along with this is the development of methods of characterization, specifically matrix assisted laser desorption ionization (MALDI) mass spectrometry and NMR techniques.

The second phase is the development of a polyethylene glycol substituted mannoside and subsequent PAMAM dendrimer functionalization. This sugar was necessary because the phenyl mannoside functionalized dendrimers were not

appreciably soluble in water. With water-soluble dendrimers in hand, a number of assays to determine their biological activity were performed.

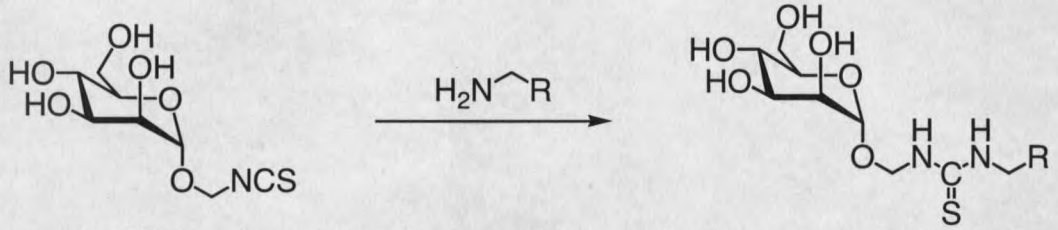
The third phase dealt with the heterogeneous functionalization of PAMAM dendrimers to measure the effect that varying the density of sugars had on the dendrimers activity.

CHAPTER 2

SYNTHESIS OF PHENYL MANNOSIDE DENDRIMERS

Background

Of all the methods for the functionalization of PAMAM dendrimers described in Chapter 1 the method chosen for this work involved the reaction of isothiocyanates with the terminal amines of the dendrimer. The attachment of a carbohydrate to a dendrimer via a thiourea linkage for the formation of glycodendrimers is well known in the field.[33, 123, 131-135] A general reaction is shown in Scheme 2.1.



Scheme 2.1 General reaction scheme utilizing an isothiocyanate functionalized carbohydrate to react with a primary amine.

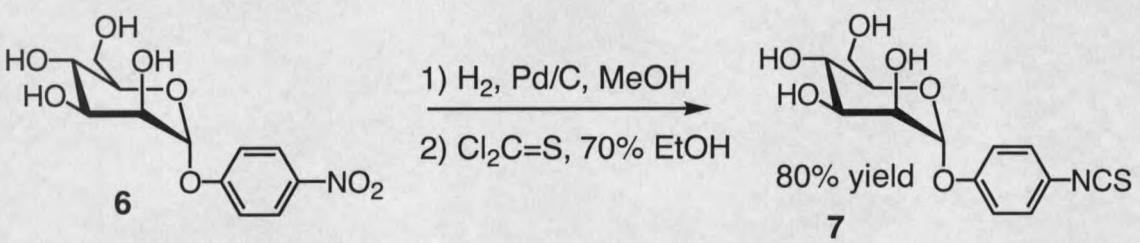
One of the main benefits to using the isothiocyanate methodology is that isothiocyanates react specifically with amines. This makes the protection of the carbohydrate hydroxyl groups unnecessary. In addition to the specificity, the reaction between amines and isothiocyanates is favorable and typically proceeds in high yield without the requirement of forcing conditions such as high

temperature or excess reagents. Finally, the isothiocyanates described in this work tend to be quite robust and stable. No noticeable deterioration of the isothiocyanates is observed even after a year in storage at −4° C.

Phenyl Mannoside Approach

[Portions of the work described in the following sections has been published in: Woller, E.K., and Cloninger, M.J. (2001). Mannose Functionalization of a Sixth Generation Dendrimer. Biomacromolecules, *2*, 1052-1054.]

As a point of departure, **7** was chosen as the desired molecule for the functionalization of PAMAM dendrimers. This choice was not made arbitrarily. It has been known for several decades that placing an aromatic ring at the alpha position of a carbohydrate increases the inhibitory potency towards Con A (as well as other lectins) relative to the methyl glycoside.[136-140] Apparently, the binding pocket in Con A is more accommodating towards a larger hydrophobic group at the alpha position of the glycoside (see Figure 1.14).

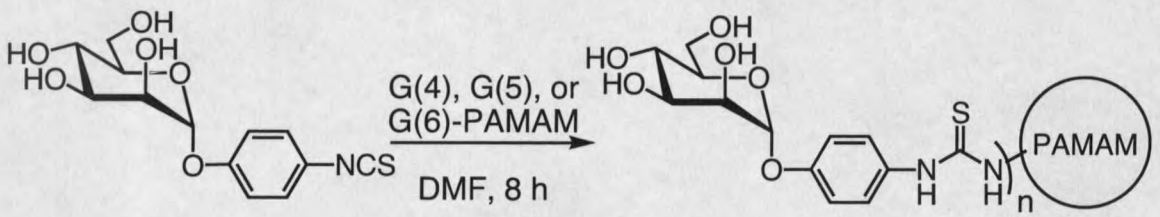


Scheme 2.2 Synthesis of isothiocyanate **7**.

The synthesis of **7** was straightforward. As shown in Scheme 2.2, nitro phenyl **6** was reduced quantitatively by hydrogen in the presence of palladium on

carbon.[141] Following a procedure by Goldstein *et. al.*, the amine was converted to the isothiocyanate in 80% yield.[142]

The synthesis of mannose-functionalized fourth, fifth and sixth generation dendrimers is shown in Scheme 2.3. Reaction of **7** with amino-terminated G(4), G(5), and G(6)-PAMAMs afforded mannosylated dendrimers **8-10.** Only a slight excess of **7** (≤1.1 equiv/amine) was used. As mentioned previously, protection of the mannose hydroxyl groups was not necessary as isothiocyanates react selectively with primary amines.



7

8 G(4); n = 64 (92%)
9 G(5); n = 128 (77% unoptimized)
10 G(6); n = 256 (85%, DMSO)

Scheme 2.3 Synthesis of phenyl mannose-functionalized PAMAM using **7**.

The functionalized dendrimers were purified by dialysis against a water/DMSO mixture using a cellulose tube (MW cutoff of 1000 g/mol). The majority of water was removed *in vacuo*, and the remaining solvent was removed by lyophilization.

Yields, which were determined using the experimentally determined molecular weights (vide infra), are quite good. Dendrimers **8, 9,** and **10** were isolated in 92%, 77% (unoptimized), and 85% yield, respectively.

NMR Characterization

Although characterization of macromolecular compounds can be quite difficult, dendrimers **8-10** proved amenable to characterization by ^{1}H NMR spectroscopy. The ^{1}H NMR (500 MHz) spectra of mannose-functionalized dendrimers **8-10** in d_6-DMSO are shown in Figure 2.1, Figure 2.2, and Figure 2.3, respectively. For improved peak resolution and accuracy of peak integration during the NMR experiment, a 15 s relaxation delay was used.[143]

For dendrimer **8** (Figure 2.1), the aromatic peaks of **7** shifted upfield about 0.2 ppm upon reaction with the dendrimer, and no remaining **7** is detectable in the spectrum of the product. Integration of the aromatic peaks and the thiourea NH peaks shows (as expected) a 2:1 ratio of aromatic to NH signals (δ 9.4, s, CSN*H*Ar, 1H; δ 8.0, s, CSN*H*R, 1H; δ 7.2, d, Ar, 2H; δ 7.0, d, Ar, 2H). Integration of the amide proton signals from the interior of **8** (δ 7.8 and δ 7.6, 2 s, 1H each) reveals a 1:1 ratio of thiourea NH signals to amide NH signals. For fully functionalized **8**, 124 amide protons and 128 thiourea protons are expected.

In addition to ^{1}H NMR, ^{13}C was used to characterize the mannose-functionalized dendrimers. The ^{13}C spectrum of the G(4)-, G(5)- and G(6)-PAMAM dendrimers in DMSO shows a peak at 42.0 ppm and at 41.2 ppm which corresponds to the α- and β-methylene carbons of the terminal amino groups, respectively. After functionalization, there is no evidence of peaks at 42.0 ppm or

41.2 ppm in the ^{13}C.[144] Presumably, after functionalization the methylene peaks become equivalent to other PAMAM methylene carbons. Thus, based on the proton and carbon NMR spectra, we conclude that within detections limits of NMR, all surface amino groups on the G(4)-PAMAM dendrimer have been functionalized with mannose residues.

For dendrimers **9** and **10** the ratio of amide protons to thiourea protons is again 1:1 (see Figure 2.2, and Figure 2.3). Theoretical values for **9** are 252 amide and 256 thiourea protons. Theoretical values for **10** are 508 amide and 512 thiourea protons. Although the spectral broadening observed for dendrimer **10** reduces the accuracy of the integration, the NMR spectra of **9** and **10** also indicate that the degree of mannose functionalization is high.

For dendrimer **10**, averaging the integrations for the 10 protons with signals between 10.0 and 4.3 ppm indicates that one proton from the dendrimer surface integrates to 1.2. Thus, a value of 3.6 for the integration of the two signals from amide protons and one signal from a thiourea proton (δ 8.2-7.4) suggests a 1:1 ratio of surface thiourea to interior amide protons.

While the NMR data is useful for the characterization of dendrimers, due to potential defects in the dendrimer structure, NMR does not indicate the number of sugars on the surface of the dendrimer. To determine the actual number of sugars on the surface and to determine any defects in the dendrimer structure mass spectroscopy data (specifically MALDI-TOF MS) must be used.

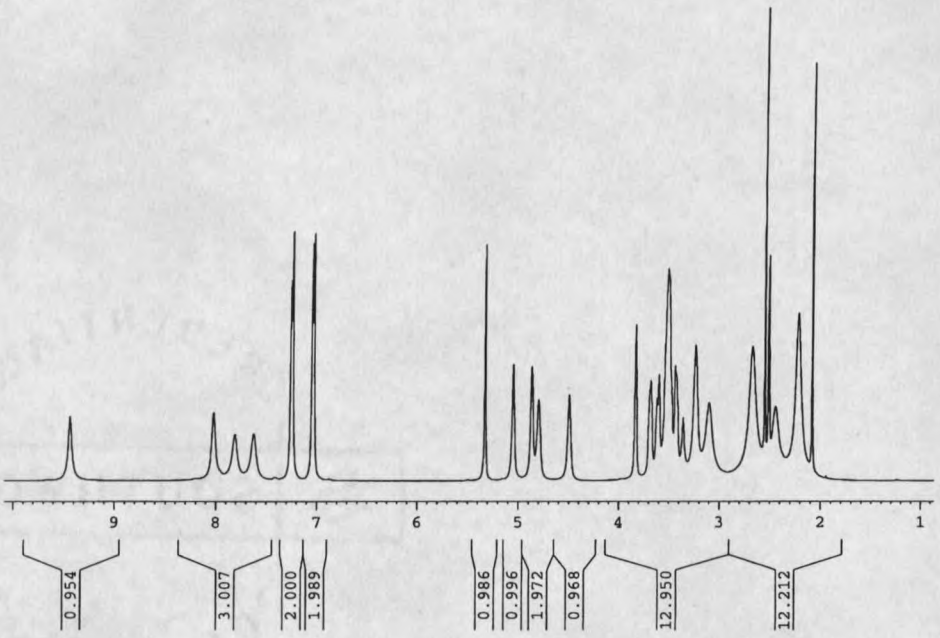


Figure 2.1 ^{1}H NMR spectrum of **8** in d_6-DMSO.

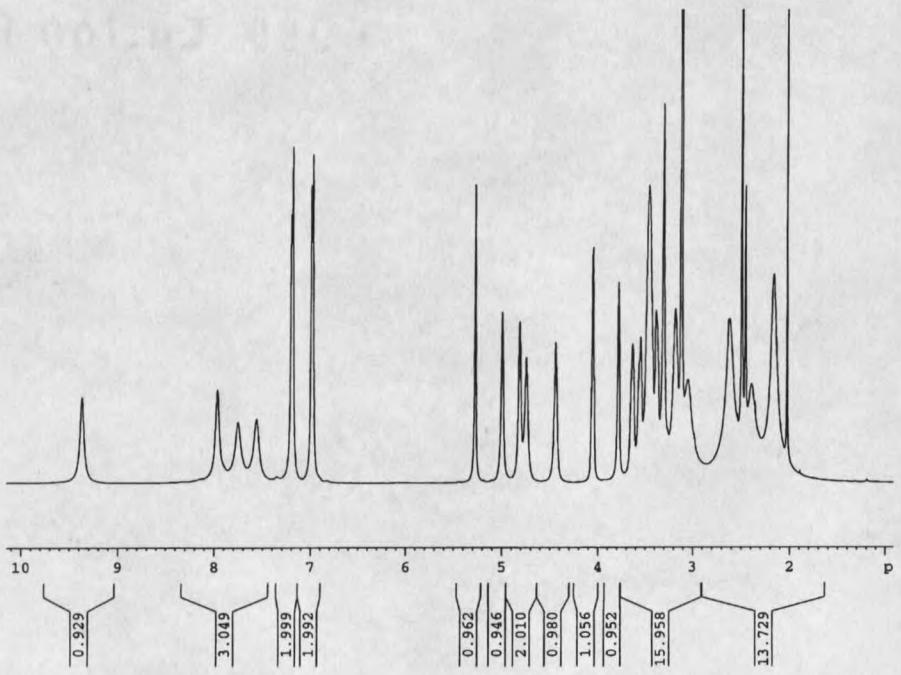


Figure 2.2 ^{1}H NMR spectrum of **9** in d_6-DMSO.

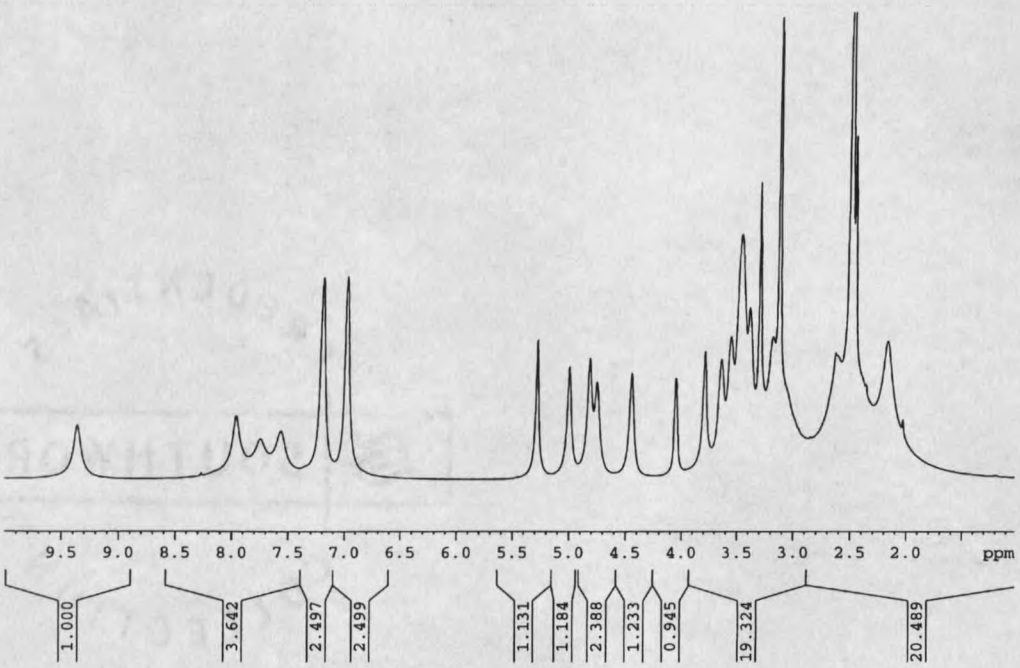


Figure 2.3. ^{1}H NMR spectrum of **10** in d_6-DMSO.

MALDI-TOF MS Characterization

Matrix-assisted laser desorption ionization time-of-flight (MALDI-TOF) mass spectrometry has proven to be a very powerful technique for the characterization of the functionalized dendrimers described in this work. The use of MALDI-TOF is a relatively new mass spectrometry technique for polymer analysis as it has been utilized for under 15 years. The first description of MALDI-TOF being used to analyze biopolymers with molecular weights over 10,000 g/mol was done in 1988 by Karas and Hillenkamp.[145] Karas and Hillenkamp obtained a spectrum of bovine albumin, which has an approximate molecular weight of 67,000 g/mol.

Later, in 1992, the same researchers successfully applied MALDI-TOF to the analysis of synthetic polymers in which they obtained a spectrum of polystyrene with a molecular weight of 70,000 g/mol.[146] This was a significant achievement, as synthetic polymers tend to be polydisperse, which results in broad peaks. Another hurdle that had to be overcome was the fact that synthetic polymers are typically not soluble in aqueous solutions and thus, had to be prepared and treated differently than biopolymers.

Since the early descriptions, the technique of MALDI-TOF MS has matured rapidly. This developing area of analytical chemistry has far reaching applications in several areas including biochemistry and polymer science. There are a number of reviews that cover the development of MALDI MS.[147-154] For the sake of this work, a brief description of the technique and its uses in the field of dendrimer chemistry are given.[77]

The distinguishing feature of MALDI is the method of analyte ionization. The analyte is mixed with a matrix with a matrix to analyte molar ratio that can range from 500:1 to 10^6:1. The entire system is under high vacuum with pressures as low as 10^{-9} torr. The dry, solid mixture is pulsed with a laser (typically a nitrogen laser at 337 nm). The matrix absorbs the laser energy and transfers the energy to the analyte. This results in the formation of a gaseous ion of the analyte. Choosing an appropriate matrix for a given analyte is often a trial

and error endeavor. There is no certain way to determine what matrix will work with what analyte.

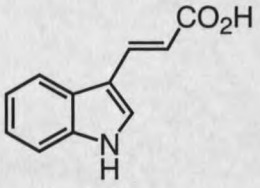
Because of the nature of the pulsed ion formation, MALDI is most often teamed with a time-of-flight detector. Time-of-flight detectors have high sensitivity and in principle no maximum mass range. In general, a detector is placed at the end of a tube about one meter in length. The ions formed as a result of the laser pulse are propelled down the tube by an electric field on the order of 30 kV. Since the time it takes for the ions to reach the detector depends on the mass and charge of the analyte, the mass is determined by measuring the time it takes to reach the detector.

Development of MALDI-TOF MS Procedure for PAMAM Dendrimers

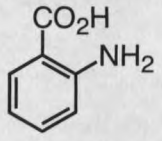
Working out the conditions for analysis of carbohydrate-functionalized described using MALDI-TOF MS involved a significant amount of effort. However, once appropriate conditions were determined and optimized, MALDI-TOF MS has become of paramount importance to the success of this project. The biggest hurdle was sample preparation, specifically the determination of an appropriate matrix.

As mentioned earlier, finding an appropriate matrix is a trial and error endeavor. Not only was the matrix required to transfer energy to the dendrimers, but since the dendrimers originally synthesized were not soluble in water, the

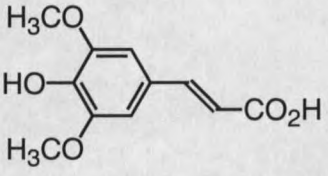
matrix had to be soluble in organic solvents. In addition, the number of organic solvents that could be used to dissolve the functionalized dendrimers was limited. The only solvents that were found to solvate the original dendrimers (**8-10**) were *N,N*-dimethylacetamide (DMA), DMF, and DMSO. Since DMSO and DMA are not appreciably volatile, the only practical choice for MALDI sample preparation was DMF.



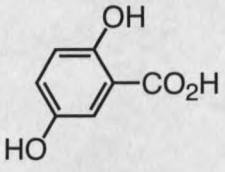
trans-3-indoleacrylic acid



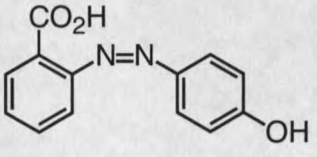
anthranilic acid



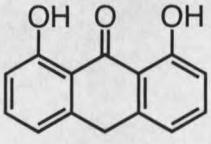
sinapinic acid



2,5-dihydroxybenzoic acid (DHB)



2-(4-hydroxyphenylazo)-benzoic acid (HABA)



Dithranol

Chart 2.1Structures of organic acids that were surveyed for use as MALDI MS matrices.

To find a matrix that worked for mannose-functionalized PAMAM dendrimers, a number of standard matrices were surveyed. The matrices

surveyed included sinapinic acid, 2,5-dihydroxybenzoic acid (DHB), 2-(4-hydroxyphenylazo)-benzoic acid (HABA), anthranilic acid, dithranol, and *trans*-3-indoleacrylic acid (see Chart 2.1 for structures). All of the prospective matrices were tested using various ratios of matrix to analyte.

In some cases (DHB for example), the matrix was not appreciably soluble in DMF, which limited the range of matrix to analyte ratios possible. After significant experimentation, it was found that the best matrix (in fact, the only matrix of the ones tested) for mannose-functionalized PAMAM dendrimers was *trans*-3-indoleacrylic acid (IAA).

While specific details are given in the experimental procedures section, a brief description of the procedure is as follows. A DMF solution of the dendrimer and a DMF solution of IAA were mixed so that the ratio of IAA to dendrimer was between 3000:1 and 1000:1. An aliquot of this solution corresponding to 12-15 pmol of analyte was deposited on the MALDI target plate. The sample was allowed to dry over the course of an hour. With most matrices, the crystals formed have a definite shape and structure. The IAA typically did not form what one would consider "good" crystals. After drying, the results resembled a film more than crystals. Despite this, good signals were obtained. In fact, it seemed that the best results came when the matrix appeared more amorphous than crystalline. This is not typical for MALDI-TOF analysis.

MALDI-TOF Results and Discussion

The MALDI-TOF MS of mannose-functionalized dendrimers **8-10** are shown in Figure 2.4, Figure 2.5, and Figure 2.6 respectively. In each of these three figures, the top spectra is of the starting material G(4)-, G(5)-, and G(6)-PAMAMs.

Upon investigation of the MALDI spectra, two features are immediately apparent. First of all, the peaks are quite broad. In the case of **10**, the peak spans a range of 40 kDa (Figure 2.6). This large range suggests a potentially polydisperse molecule. Secondly, the peaks are centered at molecular weights that are lower than the theoretical values. Table 2.1 shows the theoretical values and measured number-average (M_N) and weight-average (M_W) molecular weights for the starting materials and products as well as the polydispersities (See Appendix A for formulas used to calculate M_N, M_W and polydispersities). In all cases, the measured value was lower than the theoretical values.

Table 2.1 Mass (g/mol) and polydispersity data for **8-10** and G(4)-, G(5)-, and G(6)-PAMAMs

Compound	Mol Wt (theory)	M_N	M_W	polydispersity
G(4)-PAMAM	14,215	13,135	13,170	1.0026
8	34,247	27,787	28,269	1.0174
G(5)-PAMAM	28,826	25,893	25,997	1.0040
9	68,890	57,562	58,270	1.0123
G(6)-PAMAM	58,048	52,882	53,035	1.0029
10	138,176	106,204	109,268	1.0290

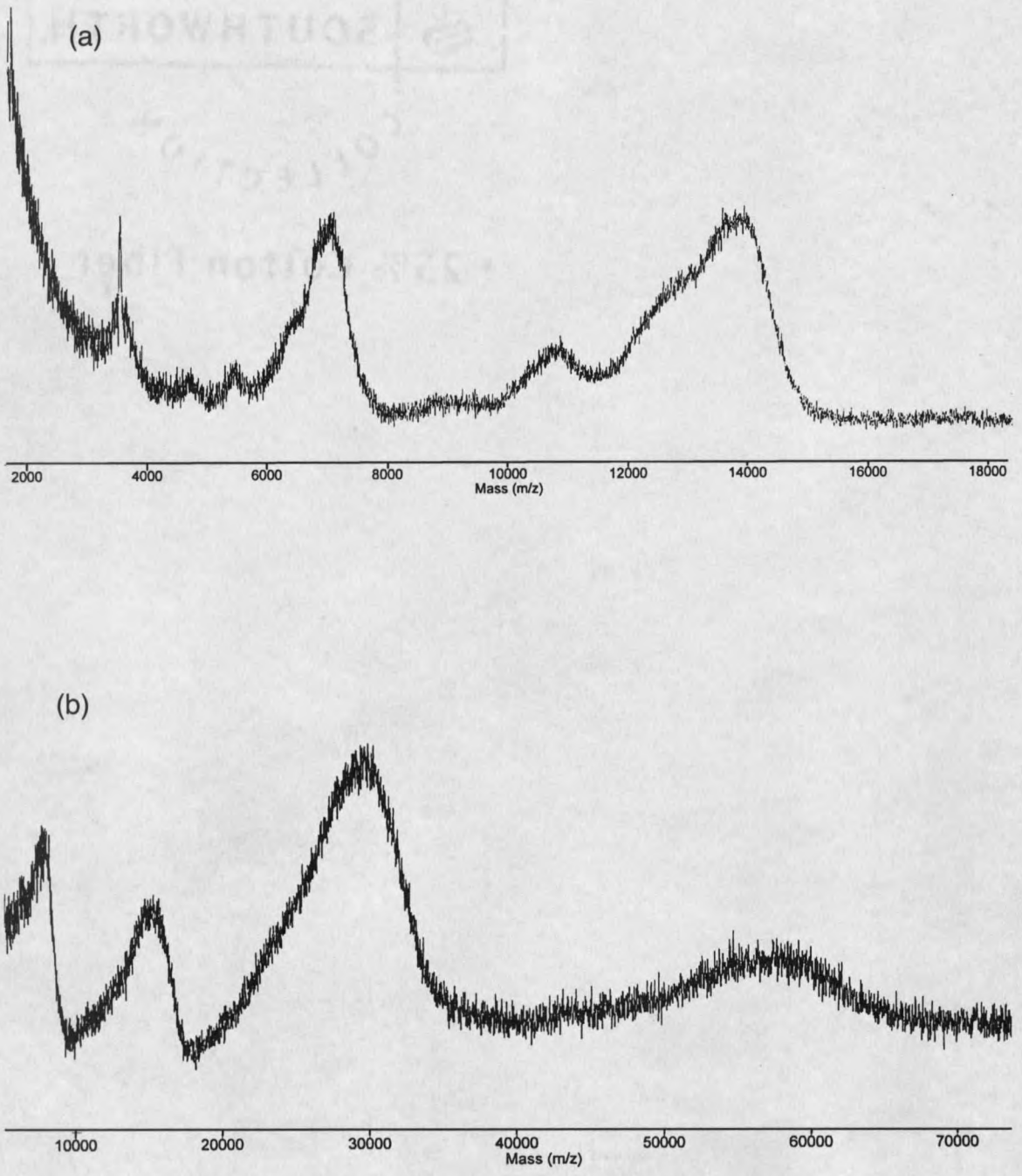


Figure 2.4 MALDI-TOF MS spectra of (a) G(4)-PAMAM, (b) **8**.

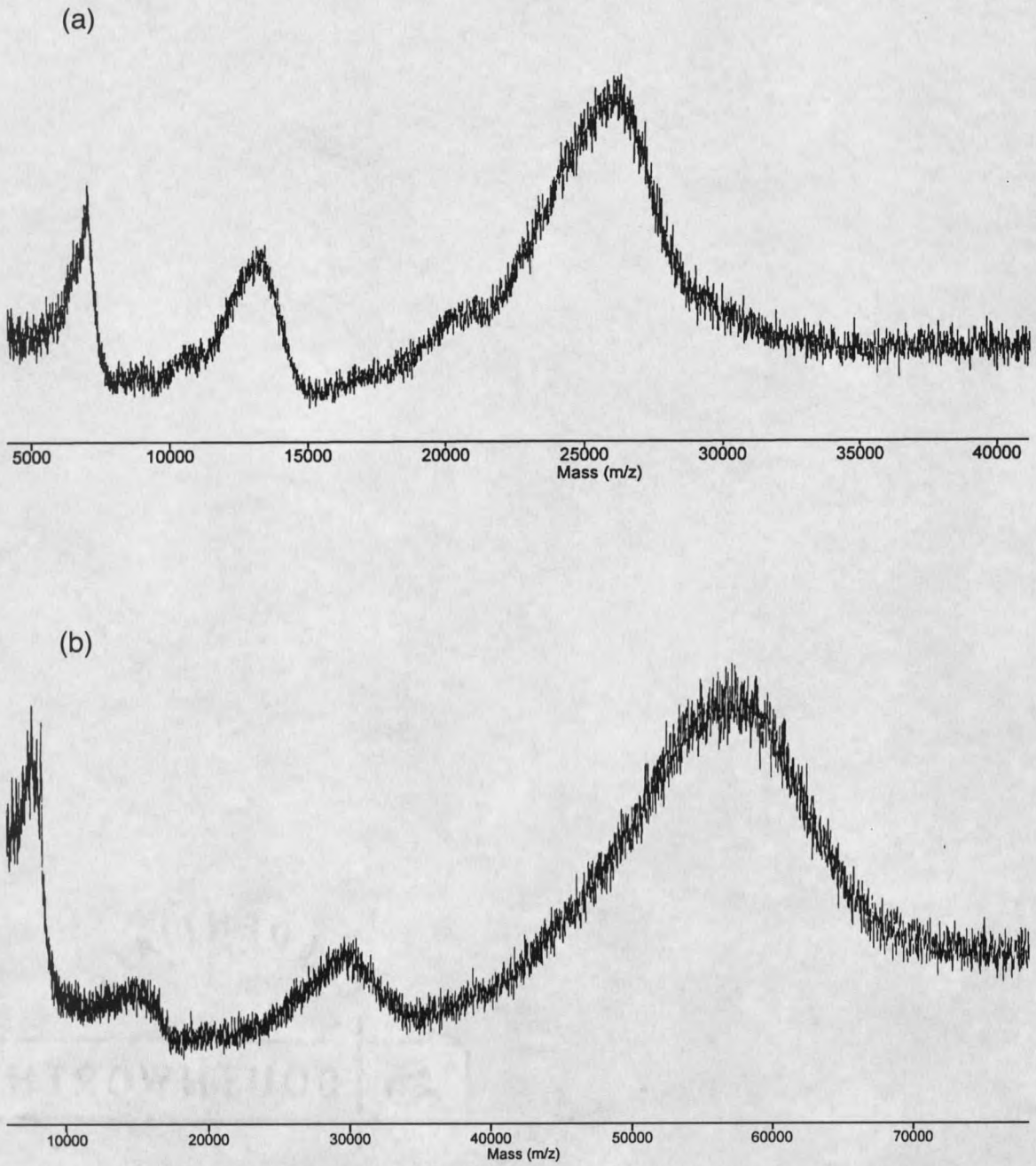


Figure 2.5 MALDI-TOF MS spectra of (a) G(5)-PAMAM, (b) **9**.

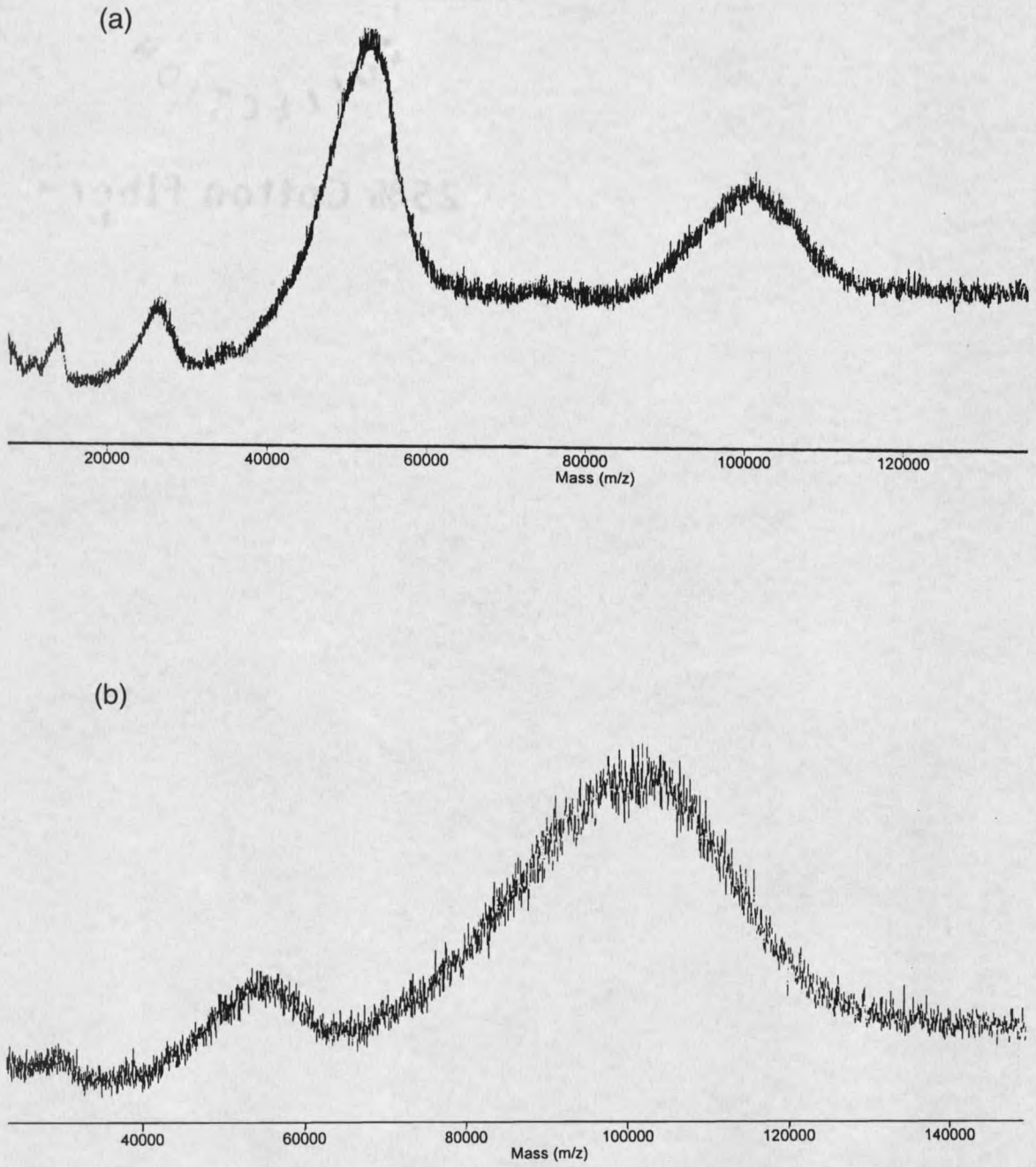
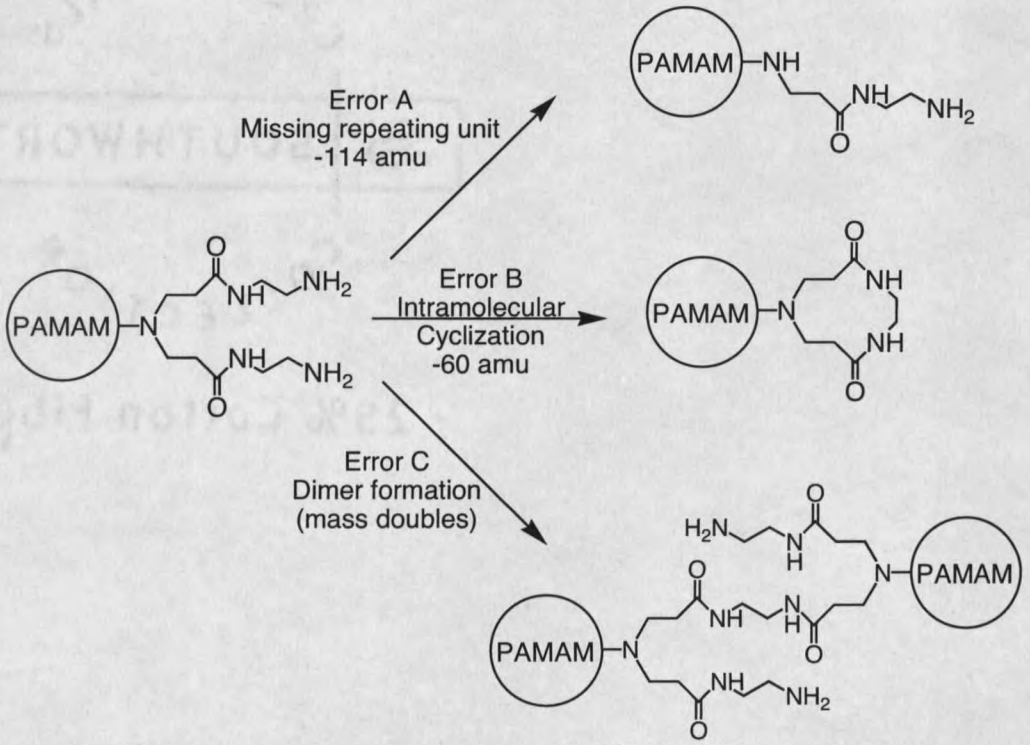


Figure 2.6 MALDI-TOF MS spectra of (a) G(6)-PAMAM, the peak centered around 100,000 g/mol is dimer formed during the MALDI-TOF experiment, (b) **10**.

The "missing" mass can be traced back to defects in the synthesis of the PAMAM starting materials (Scheme 2.4). There are three main errors that can occur in the synthesis of a PAMAM dendrimer. Error A shows the omission of what amounts to a methyl acrylate and an ethylene diamine (see Scheme 2.4) or a $CH_2CH_2CONHCH_2CH_2NH_2$ repeating unit. This is the most common error and would account for a loss of 114 mass units.[155] Both error B and C involve the formation of an amide either inter- or intra-molecularly. This would account for a loss of 60 mass units, though in the case of dimer formation, the resulting molecule would be twice as large as expected making the loss of 60 mass units imperceptible upon analysis. In addition, since the dimer would be so large, it should have been removed during the commercial synthesis of the starting material.

If we consider the PAMAM starting materials and simplify the situation by assuming that all errors occur in the outer generation, subtraction of M_W from the theoretical molecular weight of the starting materials and division by 114 indicates that on average 9, 26, and 44 terminal amino groups are missing from G(4)-, G(5)-, and G(6)-PAMAM respectively. The iterative synthesis of PAMAMs (see Scheme 1.1) supports the assumption that the majority, if not all, of the missing groups are in the outer layer. Using electrospray, Tomalia et al. have reported that the average molecular weights of the PAMAMs are actually smaller

than the theoretical molecular weights; our MALDI results are consistent with Tomalia's electrospray MS result.[155]



Scheme 2.4 Various errors leading to imperfect PAMAM dendrimers

To determine the percent mannose functionalization of the dendrimers, M_W of the dendrimer starting materials was subtracted from the M_W of the product dendrimers **8-10**. Division of the remaining masses by 313 (the molecular weight of mannose residue **7**) suggest that an average of 48, 87, and 176 mannose units are incorporated into **8-10**. On the basis of the number of amino groups determined above, this corresponds to a percent incorporation of 87% for **8**, 87% for **9**, and 83% for **10**.

Although our initial ^{1}H NMR studies indicated that complete functionalization of the dendrimer surface was achieved, MALDI suggests a considerably lower (83-87%) value. We propose that MALDI-TOF can account for deletions in the dendrimer that would lead to lower functionalization more accurately than NMR can. The repetitive (and dynamic) nature of dendrimer structure likely makes detection of dendrimer defects difficult by NMR. We moreover propose that NMR alone is unable to adequately characterize surface-functionalized dendrimer products.

Many literature examples report only NMR characterization of dendrimers. For example, Okada and co-workers use ^{13}C NMR to determine whether any primary amine groups on the dendrimer surface remain after functionalization.[126, 128, 144, 156] Support for complete functionalization is made by the absence of peaks in the ^{13}C NMR spectra ascribed to the α- and β-carbons of the unreacted primary amino groups.

While we do not dispute the results or quality of their work, we suggest that NMR provides information only about the percent functionalization of available endgroups. It does not indicate how many available endgroups are present on the dendrimer, and thus, does not provide information about how many residues have been placed on the dendrimer.

Although the MALDI signals are broad, the polydispersities are quite good; no value is above 1.03, see (Table 2.1).Tomalia *et. al.* have also reported

polydispersities for PAMAM dendrimers that differ slightly from the values given here.[155] This difference may simply be reflective of the less precise nature of the MALDI-TOF data. That the shape of the product peak is a nearly perfect overlay of the substrate peak indicates that most (if not all) of the peak broadening in the product is caused by the peak broadening in the reactant (see Figure 2.4).

An internal standard of horse heart myoglobin gives a much sharper signal than G(4)-PAMAM (Figure 2.7a), indicating that the peak broadening is due to the dispersity in the dendrimers rather than to errors in attenuation of the instrument (an external standard of horse heart myoglobin gave an even sharper signal since no other peak is under the standard in this case). Also shown in Figure 2.7b is G(6)-PAMAM with bovine serum albumin (BSA) as an internal standard. Again, Tomalia's electrospray MS results predicted that the MALDI-TOF signals would be broad because they are created by a number of compounds of similar molecular weights.[155]

A feature of MALDI that is worth noting is evident in Figure 2.7. That is the formation of doubly charged molecules. Looking at both spectra in Figure 2.7, the peak farthest to the right is the parent ion (M^+) of the reference (16,952.58 g/mol for myoglobin in Figure 2.7a or 66,821 g/mol for BSA in Figure 2.7b). The next peak from the right is the parent peak of the G(4)-PAMAM (14,378.93 g/mol) in Figure 2.7a and G(6)-PAMAM (51,500 g/mol) in Figure 2.7b. This is the singly charged ion. The next peak from the right is a doubly charged ion of the

reference molecule (M^{2+}) (8476.78 g/mol for myoglobin and 33301 g/mol for BSA), while the peak farthest to the left is the doubly charged ion of G(4)-PAMAM (7345.95 g/mol) or G(6)-PAMAM (26,300 g/mol).

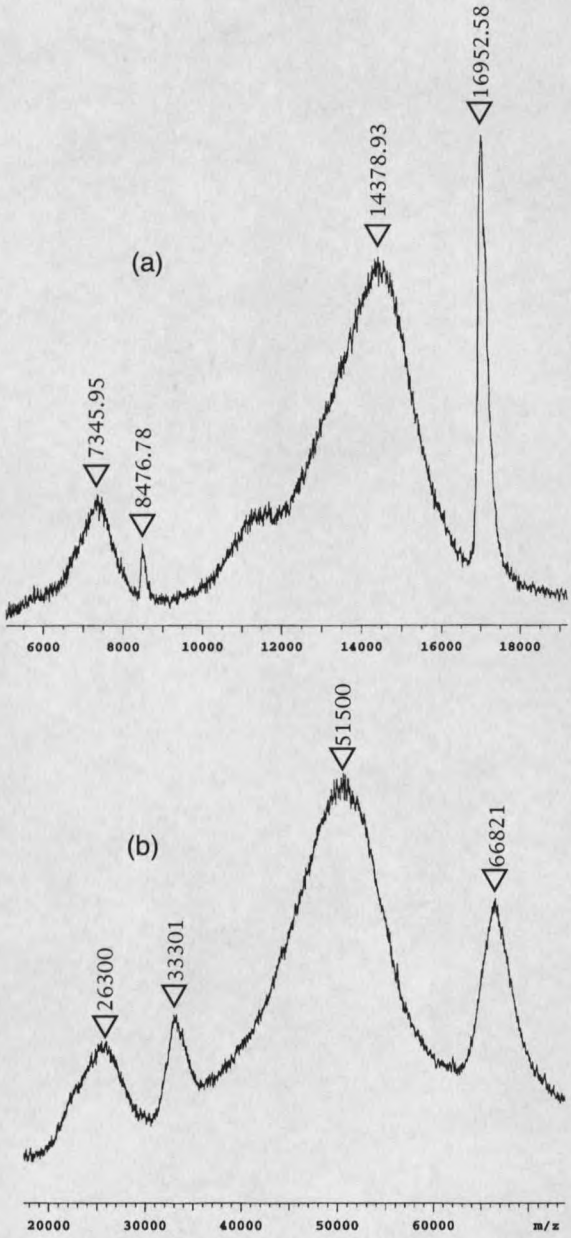


Figure 2.7 MALDI-TOF MS spectra of (a) G(4)-PAMAM with horse heart myoglobin, (b) G(6)-PAMAM with bovine serum albumin.

The formation of multiply charged ions of molecules in MALDI is common, especially with macromolecules. In fact, it is common when using MALDI to see dendrimers that form ions with five or six charges on them. Figure 2.4, Figure 2.5, and Figure 2.6 show the formation of multiply charged ions.

The formation of dimers during the MALDI-TOF MS experiment is also very common. If the sample is concentrated enough and the laser power is high enough, dimers will form in the mass spectrometer. Figure 2.6a shows a broad peak centered at about 100,000. This is a dimer of the G(6)-PAMAM being analyzed. When a dimer is detected in the spectrum, it is necessary to determine whether the dimer is present in the sample or whether it is merely forming during the MALDI experiment. To do so, the concentration of the sample and the laser power are varied. If the intensity relative to the other peaks changes, this indicates the dimer is being formed during the MALDI experiment and is not present in the sample.

MALDI-TOF Analysis of Dendrimer Functionalization Reaction

During this phase of the project, it was found that amino terminated PAMAM dendrimers could be easily functionalized using isothiocyanates. However, more information regarding the actual reaction was desired. In order to determine how long it took for the reaction to reach completion, and whether an

excess amount of isothiocyanate was beneficial or necessary, a pair of experiments were run in which the results were followed by MALDI-TOF.

In the first experiment, the formation of **8** (Scheme 2.3) was monitored by MALDI-TOF as **7** was added. An aliquot of the reaction was removed after each addition of 10 equivalents of **7**. The aliquot was prepared for MALDI-TOF as described in the experimental procedures. Removing an aliquot after the addition of 10 equivalents of **7** was continued until a 2.5-fold excess of **7** (160 equivalents) had been added. A graph of the results is seen in Figure 2.8.

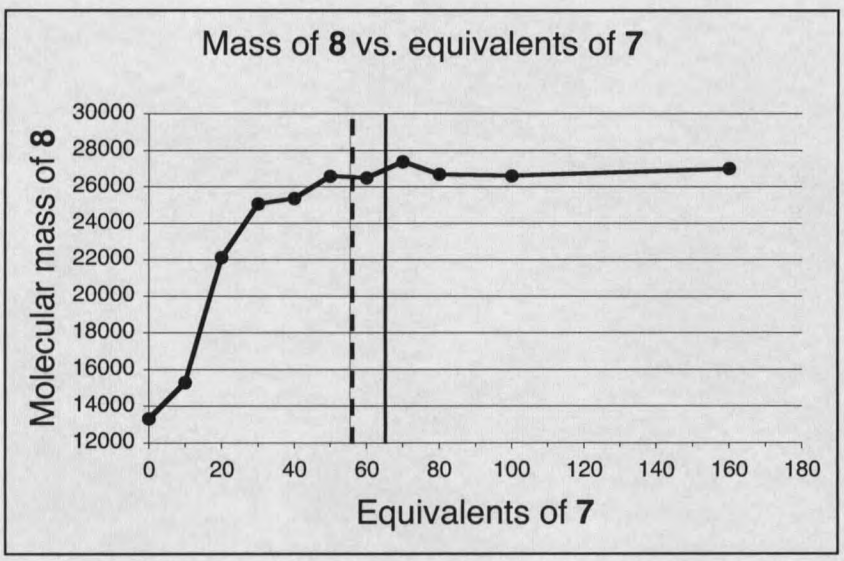


Figure 2.8 Graph showing the relationship between equivalents of **7** added and molecular mass of **8**. The solid vertical line marks the theoretical maximum of number of amines on the surface. The dashed line marks the experimentally determined maximum number of amines that are actually on the surface (the lines connecting the dots are included to show the relative relationships between dots; A curve fit is not implied).

A couple conclusions can be made from this data. First, the addition of an excess of isothiocyanate is not necessary. The reaction between the amines and

the isothiocyanate works so well that the dendrimer is fully functionalized even after the minimum number of equivalents of isothiocyanate has been added.

Another interesting observation is that the maximum mass is reached before the theoretical maximum number of equivalents (64) of **7** has been added. The solid vertical line on the graph shows the theoretical number of equivalents necessary. The dashed line shows the experimentally determined maximum number of amines on the surface and thus the actual maximum number of equivalents (55) of **7** needed. The maximum mass is reached just before 55 equivalents of **7** have been added, indicating that there are not 64 amines available on the surface as expected, which is consistent with our earlier mass spectrometry results.

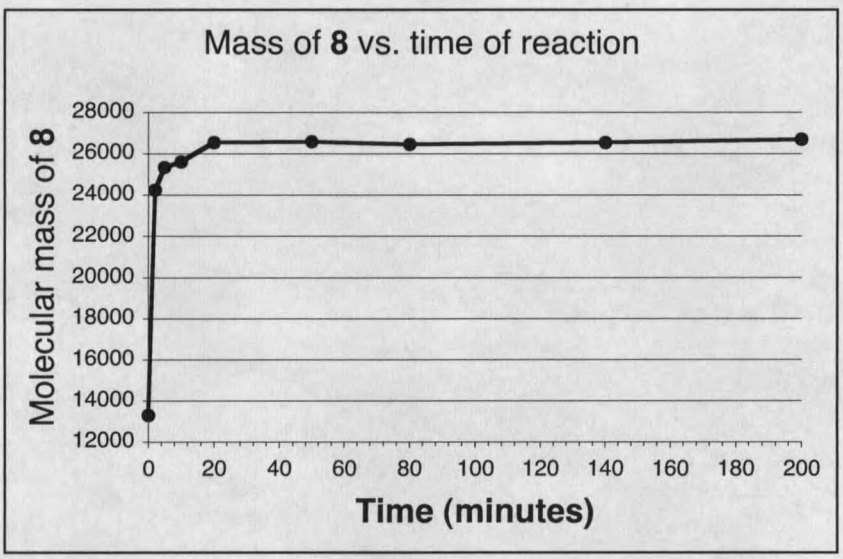


Figure 2.9 Graph of mass of **8** versus time of reaction between G(4)-PAMAM and **7**.

The second experiment was performed to qualitatively measure the rate of reaction, in order to determine whether lengthy reaction times were necessary. To do this experiment, 70 equivalents of **7** were added to G(4)-PAMAM in DMF. At various time intervals, a 1 μL aliquot was removed and immediately prepared for MALDI-TOF analysis. The masses were then determined for each time interval. The results are shown in Figure 2.9. From this graph it is obvious that the reaction is complete rather quickly. In fact, after only about 20 minutes the mass of **8** has reached a maximum. Extended reaction times are not necessary.

Solubility Issues

Although the synthesis and characterization methods described here will likely prove quite valuable to us and other researchers synthesizing biomacromolecules, compounds **8-10** are not soluble in aqueous solutions. The only readily available solvents that could dissolve **8-10** were DMA, DMF and DMSO. Because of the solubility problems, studies of the activity of **8-10** with lectins could be performed only under forcing conditions. Hemagglutination assays performed in 1:1 DMSO:aqueous buffer indicate that both **8** and **10** are roughly 2 orders of magnitude more active with Concanavalin A (Con A) than methyl mannose (details of the hemagglutination assay will be given later in the context of successful results). While results were obtained, reproducibility was difficult as the high levels of DMSO interfered with the assay.

The solubility problems encountered were surprising, considering the number of hydroxyl groups on the surface but not unprecedented. Roy *et. al.* have synthesized similar molecules and experienced similar solubility issues.[123, 157] The aqueous insolubility may be a result of the presence of the hydrophobic phenyl ring in combination with the amphiphilic nature of the carbohydrates, though the former is the more likely culprit. The obvious solution (as will be seen later) was to replace the phenyl ring with a linker that would enhance rather than detract from the solubility.

Summary

Even though this first approach produced dendrimers that were not water-soluble, the results and knowledge gained were critical to the success of this project. To our knowledge, this was the first report of the synthesis of a mannose-functionalized dendrimer larger than the fifth generation. The mannose functionalization of G(4)-, G(5)-, and G(6)-PAMAM dendrimers using a thiourea linkage was found to occur in high yield (77-92%) with good percent incorporation of sugar residues (~85%). We suggest that isothiocyanates, which are readily prepared, are excellent reagents for reactions with amino-terminated dendrimers.

Moreover, our research indicates that MALDI-TOF MS is an excellent method of characterization for macromolecular systems including dendrimers.

Although the results are less precise than those of sophisticated methods such as the previously described electrospray ionization Fourier transform ion cyclotron resonance mass spectrometric methods,[155] even large compounds (MW ≥ 100,000 g/mol) can be evaluated using MALDI-TOF. We propose that MALDI-TOF MS may be the simplest, most practical means of accurately characterizing dendrimers.

Experimental Procedures

General methods

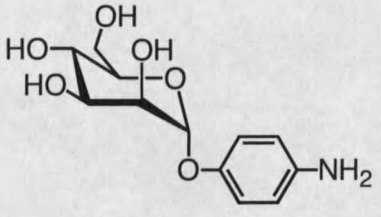
General reagents were purchased from Aldrich, Sigma, and Acros. Generation 4 PAMAM dendrimers were purchased from Aldrich. Generations 5 and 6 PAMAM dendrimers were purchased from Dendritech. All solvents and reagents were used as supplied. All melting points are uncorrected.

MALDI

Matrix assisted laser desorption ionization (MALDI) mass spectra were acquired using a PerSeptive Biosystems Voyager RP time-of-flight mass spectrometer time-of-flight mass spectrometer. Positive ion mass spectra were acquired in linear mode, and the ions were generated by using a nitrogen laser (337 nm) pulsed at 3 Hz with a pulse width of 3 nanoseconds. Ions were accelerated at 25,000 volts and amplified using a multichannel plate. Spectra (45 to 200) were acquired and downloaded to a computer for data processing. Data

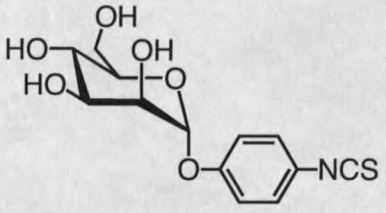
processing was performed using GRAMS (Gallactic Industries–Salem, NH). Spectra of all dendrimers were obtained using a *trans*-3-indoleacrylic acid matrix with a matrix-analyte ratio of 8500:1. Horse heart myoglobin (MW 16,969 g/mol or bovine serum albumin (MW 66,431 g/mol)) was used as an external standard. An aliquot corresponding to 13.8 pmol of the analyte was deposited on the laser target. Values of M_N, M_W, and polydispersity were obtained by selecting the theoretical molecular weight of the compound as one endpoint and a point of comparable intensity on the other side of the peak as the second endpoint (to account for a slightly uneven baseline). Although values are obviously not accurate to a single amu, full values are reported and carried through calculations of sugar incorporation (or amino residue deletion) and the final value is rounded to the nearest whole number of sugars (or amine residues).

Synthetic procedures



p-Aminophenyl-α-D-mannopyranoside.[141] A solution of *p*-nitrophenyl-α-D-mannopyranoside (4.90 g, 16.3 mmol) in methanol (500 mL) was hydrogenated with Pd/C (700 mg, 5%). After 4 hours, the catalyst was removed by filtration, and the methanol was evaporated *in vacuo* to give 4.40 g (98%) of product as white fluffy crystals. An analytical sample was crystallized from ethanol: m.p.

165-166 °C (lit. 164 °C[141]) ^{1}H NMR (500 MHz, CD_3SOCD_3) δ 6.78 (d, 2H, J = 8.7 Hz, PhH), 6.48 (d, 2H, J = 8.7 Hz, PhH), 5.06 (s, 1H, H-1), 4.89 (d, 1H, C-2 OH), 4.78 (d, 1H, C-4 OH), 4.67 (d, 1H, C-3 OH), 4.44 (t, 1H, C-6 OH), 3.77 (s, 1H, H-2), 3.55-3.65 (m, 2H, H-3, H-6), 3.49-3.50 (m, 3H, H-4, H-5, H-6) ppm; ^{13}C NMR (75 MHz, CD_3OD) δ 151.0, 143.4, 119.2, 117.8, 101.3, 75.1, 72.4, 72.2, 68.4, 62.7 ppm.



p-Isothiocyanatophenyl-α-D-mannopyranoside (**7**). *p*-Aminophenyl-α-D-mannopyranoside (4.00g, 14.8 mmol) dissolved in 95% EtOH (350 mL) was stirred while thiophosgene (2.55 g, 1.7 mL, 22.2 mmol) was added via syringe. After 10 min, the solvent was removed *in vacuo* to produce a brown solid. The product was crystallized from 70% aqueous EtOH to yield 3.72 g (81%) of **7** as white fluffy crystals: m.p. 180-181 °C; ^{1}H NMR (300 MHz, CD_3SOCD_3) δ 7.37 (d, 2H, J = 8.8 Hz, PhH), 7.12 (d, 2H, J = 8.8 Hz, PhH), 5.39 (s, 1H, H-1), 5.04 (d, 1H, C-2 OH), 4.84 (t, 1H, C-6 OH), 4.76 (d, 1H, C-3 OH), 4.44 (d, 1H, C-4 OH), 3.80 (s, 1H, H-2), 3.25-3.70 (m, 5H, H-3, H-4, H-6 (2H), H-5) ppm; ^{13}C NMR (75 MHz, CD_3SOCD_3) δ 156.0, 126.9, 125.4, 117.9, 99.3, 74.6, 71.3, 70.8, 67.2, 61.6 ppm; IR (KBr) 3500, 2094 cm^{-1}.

Generation 4.0 PAMAM-based thiourea-linked phenyl-α-D-mannopyranoside dendrimer (**8**). A methanolic solution of amine-terminated G(4)-PAMAM dendrimer (1.5 g of a 10% (w/w) solution in MeOH, 11.6 μmol of dendrimer based on the M_W of 13,170 g/mol as determined by MALDI-TOF) was evaporated under reduced pressure. The resulting residue was dissolved in DMF (15 mL) followed by the addition of **7** (254 mg, 0.82 mmol, 71 equiv). After 8 hours, the solvent was removed under reduced pressure. The resulting off-white solid was dissolved in DMSO (2 mL) and dialyzed against 2:1 DMSO:H_2O (MW cutoff 1 kDa). The solution was lyophilized to give 301 mg (92% based on the M_W of 28,260 g/mol as determined by MALDI-TOF) of **8** as an off -white solid. ^{1}H NMR (500 MHz, CD_3SOCD_3) δ 9.38 (bs, 1H, NHC(S)N*H*Ph), 7.98 (bs, 1H, N*H*C(S)NHPh), 7.50-7.85 (2bs, amide NH's), 7.20 (d, J= 8.2 Hz, 2H, ArH), 6.99 (d, J= 8.2 Hz, 2H, ArH) 5.28 (s, 1H, H-1), 5.00 (bs, C-2 OH), 4.81 (bs, C-6 OH) 4.75 (bs, C-3 OH), 4.45 (bs, C-4 OH), 3.78 (bs, 1H, H-2), 3.25-3.70 (m, 5H, H-3, H-4, H-6 (2H), H-5), 2.90-3.25 (m, 4H, CH_2), 2.05-2.75 (m, 8H, CH_2) ppm; ^{13}C NMR (125 MHz, CD_3SOCD_3) δ 180.7, 171.8, 171.4, 153.6, 133.0, 125.5, 118.1, 116.9, 99.2, 74.8, 70.7, 70.1, 66.7, 61.1, 52.2, 49.5, 43.6, 38.0, 36.9, 33.1 ppm; MALDI-TOF MS (pos) *m/z* 28,024 (calcd 34,247 for $C_{1454}H_{2208}N_{314}O_{508}S_{64}$)

Generation 5.0 PAMAM-based thiourea-linked phenyl-α-D-mannopyranoside dendrimer (**9**) unoptimized conditions. A methanolic solution of amine-terminated G(5)-PAMAM dendrimer (0.79 g of a 28% (w/w) solution in

MeOH, 221 mg, 8.5 μmol of dendrimer based on the M_W of 25,990 g/mol as determined by MALDI-TOF) was evaporated under reduced pressure. The resulting residue was dissolved in DMF (15 mL) followed by the addition of **7** (486 mg, 1.55 mmol, 180 equiv). After 8 hours, the solvent was removed under reduced pressure. The resulting off-white solid was dissolved in DMSO (2 mL) and dialyzed against 2:1 DMSO:H_2O (MW cutoff 1 kDa). The solution was lyophilized to give 380 mg (77% based on the M_W of 58,270 g/mol as determined by MALDI-TOF) of **9** as an off -white solid. ^{1}H NMR (500 MHz, CD_3SOCD_3) δ 9.37 (bs, 1H, NHC(S)N*H*Ph), 7.97 (bs, 1H, N*HC*(S)NHPh), 7.45-7.85 (2bs, amide NH's), 7.20 (d, J= 8.2 Hz, 2H, ArH), 6.98 (d, J= 8.2 Hz, 2H, ArH) 5.28 (s, 1H, H-1), 5.00 (bs, C-2 OH), 4.81 (bs, C-6 OH) 4.75 (bs, C-3 OH), 4.45 (bs, C-4 OH), 3.78 (bs, 1H, H-2), 3.25-3.70 (m, 5H, H-3, H-4, H-6 (2H), H-5), 2.90-3.25 (m, 4H, CH_2), 2.05-2.75 (m, 8H, CH_2) ppm; ^{13}C NMR (125 MHz, CD_3SOCD_3) δ 180.7, 171.9, 171.4, 153.6, 132.9, 125.5, 116.9, 99.2, 74.8, 70.6, 70.1, 66.7, 61.0, 49.5, 48.6, 43.6, 38.0, 33.1 ppm; MALDI-TOF MS (pos) *m/z* 57,952 (calcd 68,890 for $C_{2926}H_{4448}N_{634}O_{1020}S_{128}$).

Generation 6.0 PAMAM-based thiourea-linked phenyl-α-D-mannopyranoside dendrimer (**10**). A methanolic solution of amine-terminated G(6)-PAMAM dendrimer (2.4 g of a 11% (w/w) solution in MeOH, 5.1 μmol of dendrimer based on the M_W of 53,000 g/mol as determined by MALDI-TOF) was evaporated under reduced pressure. The resulting residue was dissolved in

DMSO (15 mL) followed by the addition of **7** (415 mg, 1.33 mmol, 261 equiv). After 8 hours, the reaction mixture was dialyzed against DMSO (MW cutoff 1 kDa). The solution was lyophilized to give 473 mg (85% based on the M_W of 109,268 g/mol as determined by MALDI-TOF) of **10** as an off-white solid. ^{1}H NMR (500 MHz, CD_3SOCD_3) δ 9.36 (bs, 1H, NHC(S)N*H*Ph), 7.96 (bs, 1H, N*H*C(S)NHPh), 7.40-7.85 (2bs, amide NH's), 7.20 (d, J= 8.2 Hz, 2H, ArH), 6.98 (d, J= 8.2 Hz, 2H, ArH) 5.28 (s, 1H, H-1), 5.00 (bs, C-2 OH), 4.81 (bs, C-6 OH) 4.75 (bs, C-3 OH), 4.45 (bs, C-4 OH), 3.78 (bs, 1H, H-2), 2.90-3.70 (m, 9H, H-3, H-4, H-6, H-5, CH_2), 2.00-2.75 (bm, 8H, CH_2) ppm; ^{13}C NMR (125 MHz, CD_3SOCD_3) δ 180.7, 171.9, 171.5, 153.6, 132.9, 125.5, 117.0, 99.2, 74.8, 70.6, 70.1, 66.7, 61.0, 52.1, 49.5, 48.6, 43.6, 38.0, 36.9, 33.1 ppm; MALDI-TOF MS (pos) *m/z* 107,677 (calcd 138,176 for $C_{5870}H_{8929}N_{1274}O_{2044}S_{256}$).

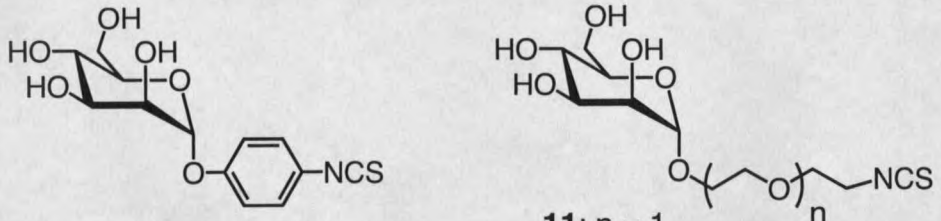
CHAPTER 3

SYNTHESIS OF POLYETHYLENE GLYCOL MANNOSIDE DENDRIMERS

[Portions of the work described in the following sections has been published in: Woller, E. K., and Cloninger, M. J. (2002). The Lectin Binding Properties of Six Generations of Mannose-Functionalized Dendrimers. Organic Letters, *4*, 7-10.]

Background

After having successfully synthesized and characterized mannose-functionalized PAMAM dendrimers **8-10**, we focused our attention on the synthesis of water-soluble analogs. To this end, it became obvious that the most straightforward change would be to replace the phenyl ring of **7** with some linker that could improve the solubility in water. Upon consultation with colleagues and perusal of the literature, we decided our best approach would be to use a polyethylene glycol (PEG) linker in place of the phenyl ring (Figure 3.1).[158-161]



7

11; n = 1

12; n = 2

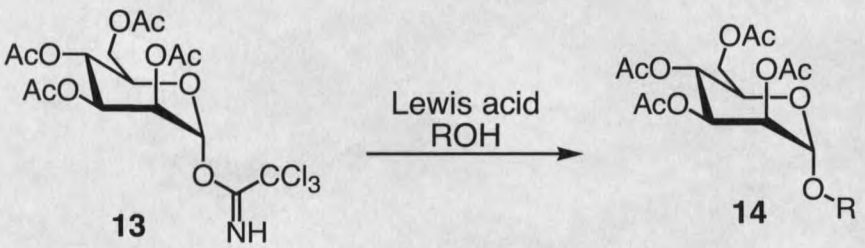
Figure 3.1 Molecules **11** and **12** were targeted to increase the water solubility of the subsequent functionalized PAMAM dendrimer.

At the outset, it was not clear whether 1-*O*-(5-isothiocyanato-3-oxapentyl)-α-D-mannopyranoside (**11**) or 1-*O*-(8-isothiocyanato-3,6-dioxaoctyl)-α-D-

mannopyranoside (**12**) would be better. The only difference between the two is the length of the PEG linker. The solubility of the functionalized dendrimers would have to be evaluated, but it was hoped that the shorter PEG linker (as in **11**) would be sufficiently soluble. This is mainly due to the desire to maintain as much rigidity in the linker as possible so that the spatial orientation of the carbohydrate can more easily be ascertained.

Synthesis of Carbohydrates

The general procedure for the formation of **11** or **12** was to couple an appropriate alcohol in the presence of a Lewis acid with a carbohydrate possessing an activated anomeric position. The desired method for the activation of the anomeric position was the use of a trichloroacetimidate. The coupling procedure between α-D-mannosyl trichloroacetimidate **13** and a generic alcohol is shown in Scheme 3.1.



Scheme 3.1 General reaction for the coupling of alcohols with mannose.

This method is attractive because a wide range of alcohols can be used, but more importantly, the product is predominantly the α anomer. In the case of

mannose, as will be seen later, the β anomer is undetectable by NMR. This is due in part to the anomeric effect.

The anomeric effect, illustrated in Figure 3.2a, involves the overlap of the axial nonbonded electrons of the cyclic oxygen with the antibonding sigma orbital of the exocyclic carbon-oxygen bond. This overlap is favorable enough to overcome the steric cost of having a group in the axial position. Another result of the anomeric effect is that the cyclic C—O is shortened and the exocyclic C—O bond is lengthened. The anomeric effect is general for most sugars and other pyranose type molecules.

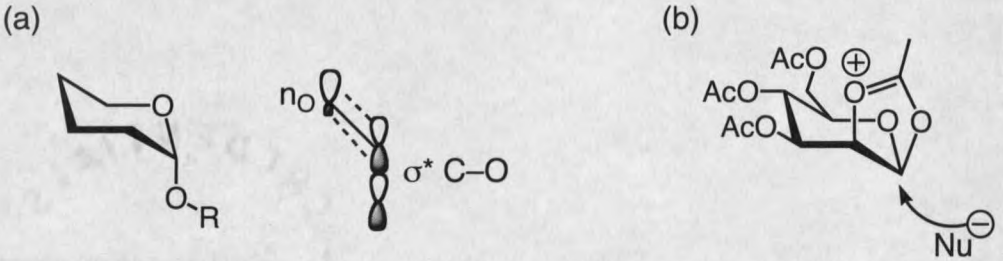
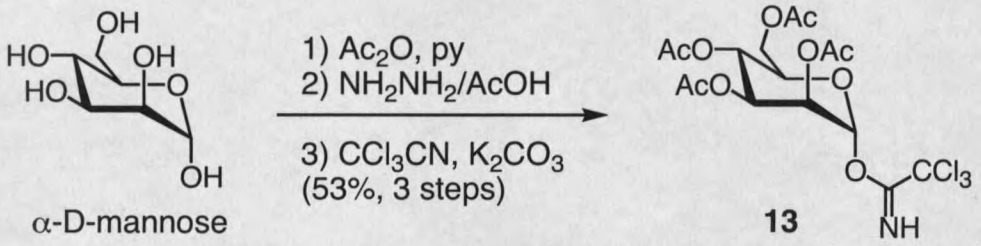


Figure 3.2 (a) The anomeric effect involves overlap of the nonbonded electrons on the cyclic oxygen with the σ* orbital of the exocyclic C—O bond. (b) Neighboring group participation of the acetyl group with the anomeric position.

In the case of mannose, in which the 2-OH group is in the axial position, there is an even more biasing feature. When the hydroxyl groups are protected with some type of ester (typically acetate or benzoate) the protecting group on the 2-OH group can participate with the anomeric group. This neighboring group participation results in formation of an intermediate shown in Figure 3.2b. The carbonyl oxygen forms a bond with the anomeric carbon to form the oxocarbenium ion shown. Because the group is in the axial position, it effectively

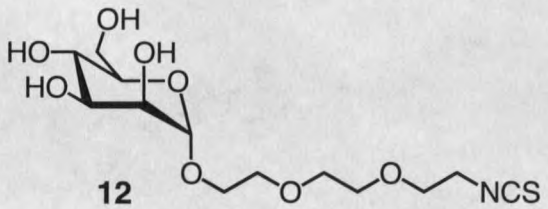
blocks the nucleophile from attacking from the equatorial position, which in the absence of the neighboring group participation would be less hindered. The combination of the neighboring group participation and the anomeric effect results in the exclusive formation of the α anomer.

The synthesis of **13** is shown in Scheme 3.2.[162-164] Peracetylation of D-mannose was achieved using acetic anhydride in pyridine. The anomeric position was selectively deprotected using hydrazine acetate in DMF at 55° C. The formation of the trichloroacetimidate **13** was achieved by reaction with trichloroacetonitrile in CH_2Cl_2 in the presence of K_2CO_3. The use of diazabicyclo[5.4.0]undec-7-ene (DBU) as base to form **13** was also explored, but product purification was much easier when K_2CO_3 was used.



Scheme 3.2 Synthesis of acetyl protected α-D-mannosyl trichloroacetimidate.

Attempted Synthesis of 1-*O*-(8-isothiocyanato-3,6-dioxaoctyl)-α-D-mannopyranoside

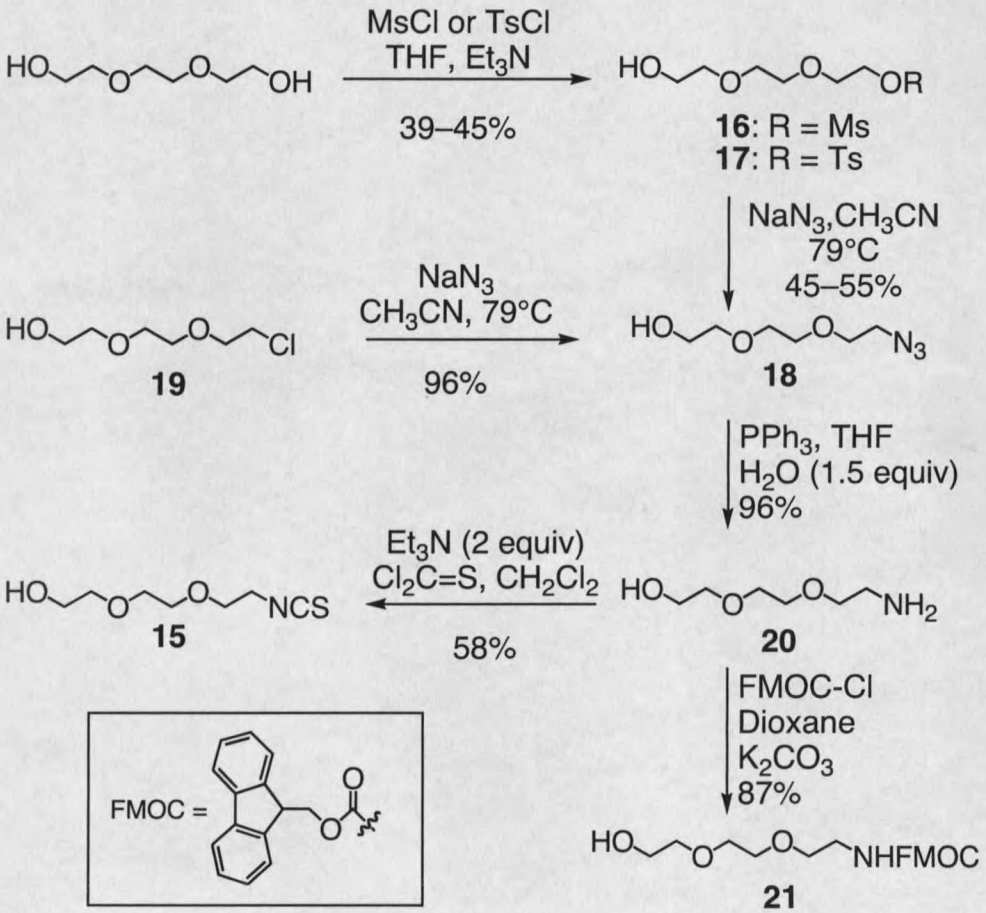


A number of approaches were taken to synthesize **12**. As will be seen later, the subsequent success in the formation of gram quantities of **11** made the pursuit of **12** unnecessary at this time. However, during the attempt to form **12** a significant amount of information was learned about molecules such as **11** and **12**. Also, one could envision a future evaluation of the effect of tether length on the lectin binding properties of Con A. In such a study **12** would be essential.

The first step towards forming **12** required the synthesis of an alcohol that could be coupled with **13** to form either **12** or a precursor that could easily be converted to **12**. The most obvious alcohol to use would be **15** (shown in Scheme 3.3), however, whether the isothiocyanate would survive the acid catalyzed coupling reaction or not was a serious question. Under the Lewis acid catalyzed reaction conditions, the alcohol and isothiocyanate might react to form a thiocarbamate (among other deleterious side reactions). As will be seen later, this fear was unfounded, though at this stage a cautious approach was explored.

A variety of alcohols are shown in Scheme 3.3. Mono-mesylation or mono-tosylation of triethylene glycol was accomplished according to published procedures by reaction with methanesulfonyl chloride or *p*-toluenesulfonyl chloride in the presence of triethylamine to form **16** or **17**, respectively.[159] The mesylate or tosylate was displaced by azide in refluxing acetonitrile to form **18** in moderate yield.

Since the overall yield for formation of **18** was rather poor (including the guaranteed loss of desired product due to formation of dimesylate or ditosylate during formation of **16** or **17**), another method for the formation of **18** was explored. The reaction of NaN_3 with 2-(2-(2-chloroethoxy)ethoxy)ethanol (**19**) proved to be a much better approach. The conversion of **19** to **18** occurred in 96% yield, which offset additional cost of purchasing **19** rather than the cheaper triethylene glycol.



Scheme 3.3 Formation of various alcohols for the attempted synthesis of **12**.

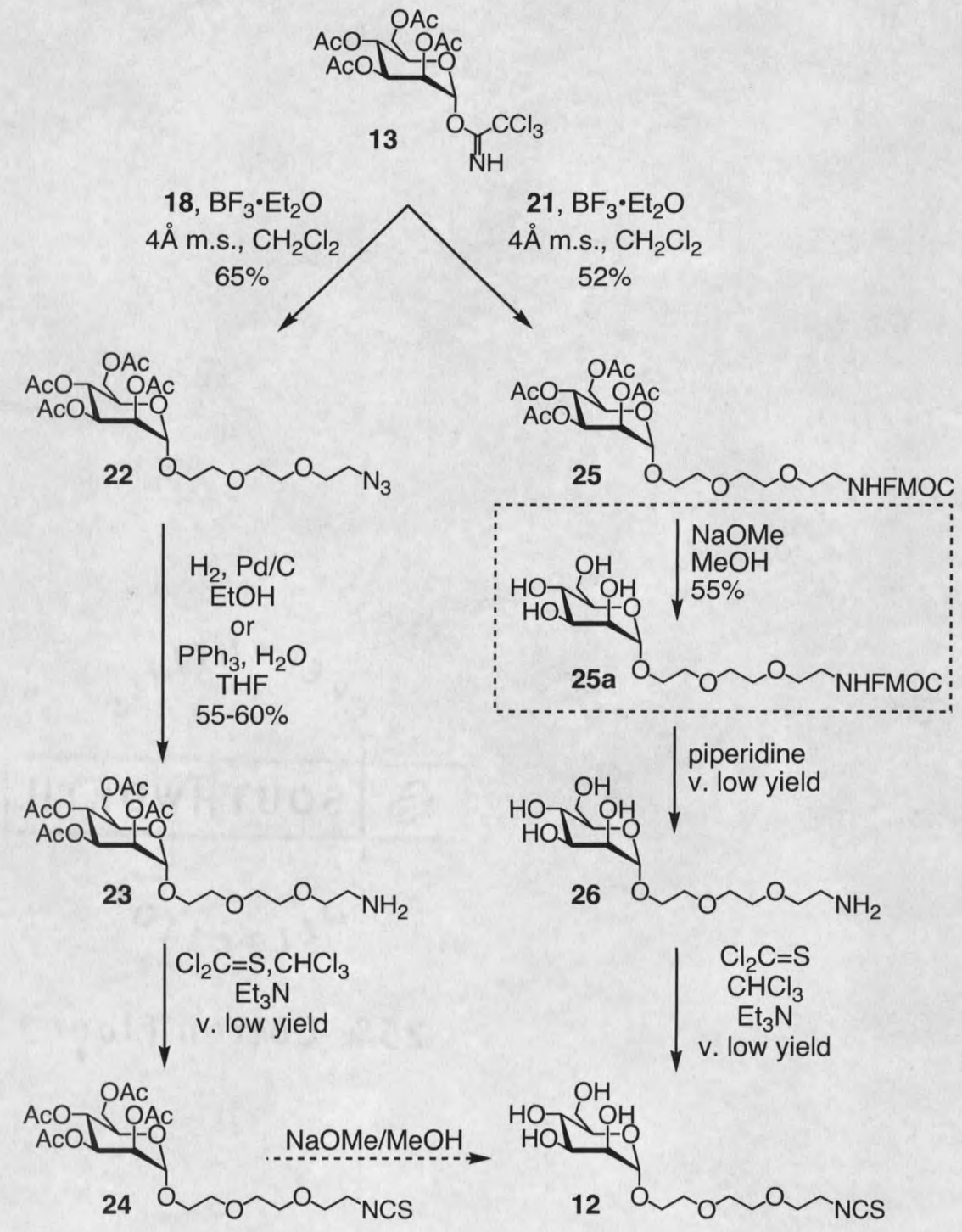
Reduction of the azide to the amine **20** occurred smoothly in the presence of PPh_3 in wet THF. The conversion of **20** to the isothiocyanate **15** occurred in modest yield. The isothiocyanato alcohol **15** was formed with the intent of using it to heterogeneously functionalize the PAMAM dendrimer rather than to directly couple it to the activated sugar **13** for reasons previously described.

The amine was protected with a 9-fluorenylmethoxycarbonyl (FMOC) protecting group. The FMOC protected **21** was formed in 87% yield using FMOC chloride in the presence of K_2CO_3 in dioxane.

Several approaches were attempted to form **12**, two of which are shown in Scheme 3.4. The first attempt started with the coupling of **18** to **13**. This was done by using one equivalent of $BF_3 \cdot Et_2O$ in the presence of 4Å molecular sieves in dry CH_2Cl_2. Literature references on similar systems report the use of TMSOTf, however in our hands, the $BF_3 \cdot Et_2O$ mediated reaction proceeded in much higher yield.

The azide **22** was reduced either using hydrogen in the presence of palladium on carbon or by the use of PPh_3 in wet THF. Both methods gave similar results, though the hydrogenation reaction was easier to purify.

With the amine in hand, attempts to form the isothiocyanate were less than successful. Very low yields of the product were obtained, and it became evident that this procedure was not going to be adequately productive.



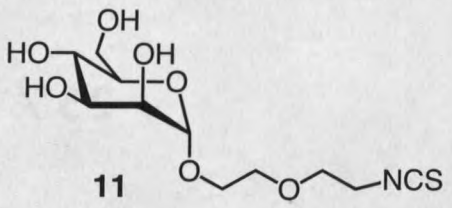
Scheme 3.4 Reactions in an attempt to form **12**.

Similar results were achieved using the second method shown in Scheme 3.4. In this reaction sequence, the same conditions were used to couple **21** to **13**. Deprotection of the amine in neat pipieridine[165] resulted in the removal of the FMOC protecting group, in addition to the acetyl groups to form **26**. Incidentally, the acetyl groups of **25** could be removed to form **25a** using NaOMe:MeOH without removing the FMOC group. The reaction of **26** with thiophosgene in $CHCl_3$ showed that **12** could be formed albeit in very low yield.

Since the yield in the isothiocyanate-forming step was so low, few of the other reaction conditions in Scheme 3.4 were optimized. However, it was during this time that ongoing work to synthesize **11** revealed that **11** could easily be formed and that the use of **12** may be unnecessary at this time. Therefore, work to develop a route to **12** was abandoned.

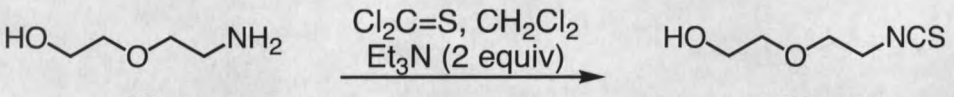
Although none of the compounds shown in Scheme 3.4 were used in dendrimer functionalization, they did suggest important improvements in tether solubility. For example, compound **23** was not very soluble in water while **26** (which lacked the acetyl protecting groups) was very soluble in water. While this was certainly no proof that the dendrimer functionalized with **11** or **12** would be soluble, we anticipated that similar solubility properties would manifest themselves in the macromolecule.

Synthesis of 1-*O*-(5-isothiocyanato-3-oxapentyl)-α-D-mannopyranoside



11

As in the development of **12**, the synthesis of a suitable alcohol to couple to **13** to form **11** was necessary. However, in this case it was much more straightforward. Originally, the various manipulations required for the formation of **12** were planned in an analogous manner to the formation of **11**. However, due to the difficulties in making **12**, direct coupling of the isothiocyanato alcohol to the activated sugar was explored. To that end, readily available amino alcohol **27** was converted to the isothiocyanate **28** using thiophosgene in the presence of Et_3N in 68% yield (Scheme 3.5).



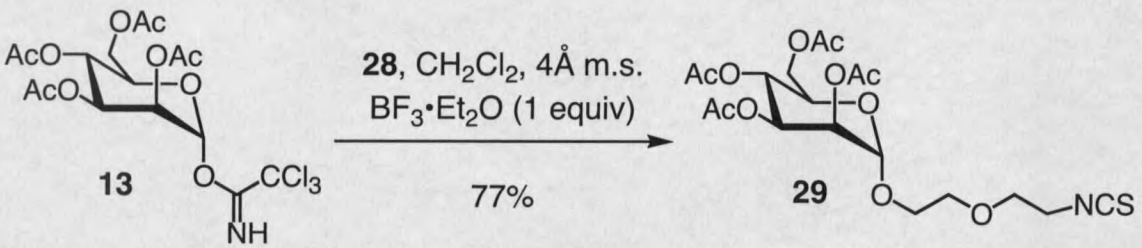
27 **28**

Scheme 3.5 Synthesis of the short PEG isothiocyanato alcohol.

The coupling of **28** to **13** turned out to be relatively straightforward. In the presence of one equivalent of $BF_3 \cdot Et_2O$ and 4Å molecular sieves, the reaction proceeded quite smoothly in 77%. As before, other Lewis acids were surveyed, including TMSOTf, however, $BF_3 \cdot Et_2O$ was the best. The $BF_3 \cdot Et_2O$ catalyzed

reaction proceeded so well that it could be scaled up to multi-gram quantities without appreciable loss of yield.

To form **29**, the acetyl protecting groups are required. Manipulations to form **7**, on the other hand, did not require hydroxyl protection. For reasons that will be discussed later in context of characterization of the functionalized dendrimers, deprotection of the hydroxyl groups was not performed on **29** until after it was attached to the dendrimer.



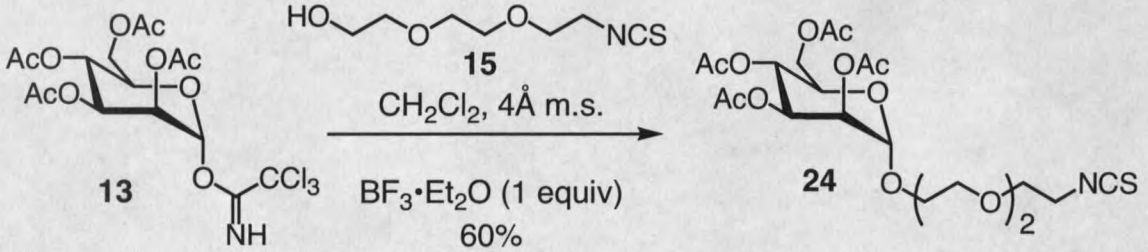
Scheme 3.6 Successful attempt of coupling an alcohol to **13** in the presence of an isothiocyanate group.

As expected, only one anomer was formed during the coupling reaction (Scheme 3.6). Due to neighboring group participation of the C-2 acetyl group, the exclusive product was most likely the α anomer, although proof was needed. Typically, ^{1}H NMR is sufficient to determine the stereochemistry at C-1 by observing the strength of coupling between the anomeric proton and the proton on C-2. For example, in the case of glucose, the coupling constant for the anomeric proton is around 3 to 4 Hz for the α anomer (i.e. the proton is in the equatorial position and the coupling with the axial H-2 is weak) while it is around

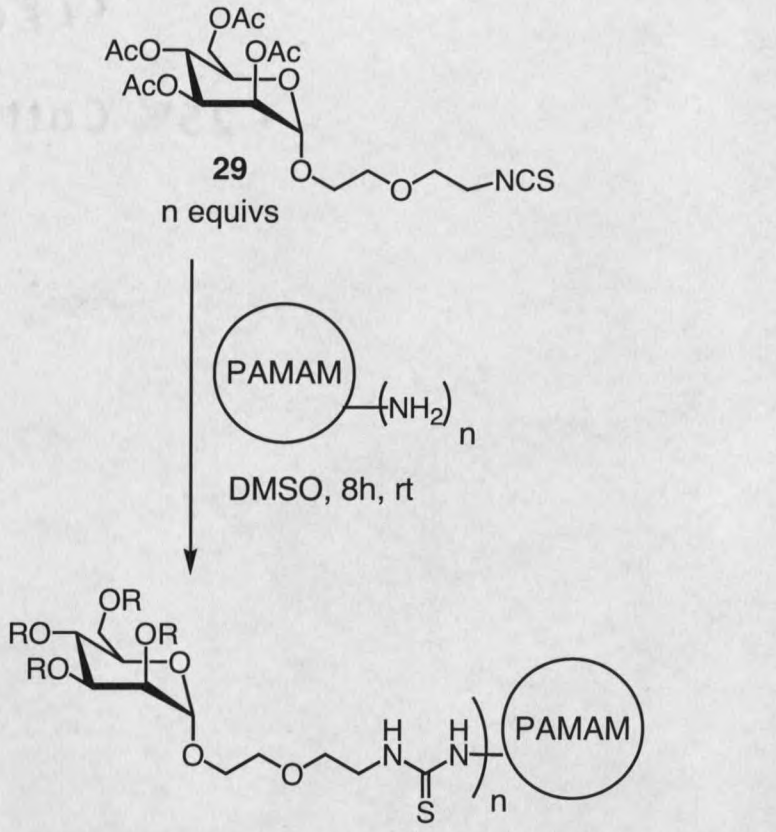
10 to 14 Hz for the β anomer (i.e. the proton is in the axial position and the coupling with the axial H-2 is much stronger).

However, in mannose because the proton on C-2 is in the equatorial position, the coupling between the H-1 and H-2 for both anomers is weak, and the coupling constant is small, around 3 to 4 Hz, for both anomers. In order to determine the stereochemistry, the H-^{13}C coupling constant must be used. For the α anomer the coupling constant is around $^{1}J_{CH}$ 171 Hz and for the β anomer it is around $^{1}J_{CH}$ 154 Hz.[166-168] The constant for **29** was determined to be $^{1}J_{CH}$ 172 Hz, which indicates **29** is indeed the α anomer as expected.

With the knowledge that the reaction in Scheme 3.6 works so well, the same strategy was applied to the formation of **24** (the protected form of **12**) directly from **13** and the isothiocyanato alcohol **15** (see Scheme 3.7). The yield was lower, but the reaction worked well. However, based on results from dendrimers functionalized with **29**, the formation of **12** or **24** was no longer necessary at this time.



Scheme 3.7 Application of successful coupling conditions of an alcohol to **13** in the presence of an isothiocyanate group.



30 G(1); R = Ac, n = 8		**36** G(1); R = H, n = 8
31 G(2); R = Ac, n = 16		**37** G(2); R = H, n = 16
32 G(3); R = Ac, n = 32	NaOMe →	**38** G(3); R = H, n = 32
33 G(4); R = Ac, n = 64	MeOH	**39** G(4); R = H, n = 64
34 G(5); R = Ac, n = 128		**40** G(5); R = H, n = 128
35 G(6); R = Ac, n = 256		**41** G(6); R = H, n = 256

Scheme 3.8 Functionalization of first- through sixth-generation PAMAM dendrimers.

Dendrimer Functionalization Using 1-*O*-(5-isothiocyanato-3-oxapentyl)-2,3,4,6-tetra-*O*-acetyl-α-D-mannopyranoside

The functionalization of G(1)-, through G(6)-PAMAM dendrimers is shown in Scheme 3.8. Addition of **29** to the dendrimer gave acetylated dendrimers **30-35**. Excess **29** was removed by dialysis against DMSO (cellulose tube, MW cutoff

1000 g/mol). Lyophilization of the DMSO left a sticky, off-white solid. At this stage (i.e. acetylated) the dendrimers **30-35** were not soluble in water.

Global deacetylation of **30-35** was accomplished using Zemplén conditions (NaOMe in MeOH:H_2O 1:1)[169, 170] to form dendrimers **36-41**. Acetylated dendrimers **30-35** were not appreciably soluble in the methanol:water mix. Therefore, a suspension of **30-35** was stirred vigorously until all reactants had dissolved. The products, **36-41**, were soluble in the methanol:water mixture, but more importantly, they were soluble in just water. The products were purified by dialysis against methanol:water 1:1 which was eventually converted to water. Lyophilization of the water resulted in **36-41** in purified form as fluffy white solids.

Although the acetyl protecting groups are not required during thiourea formation, we have chosen to deprotect the sugars after addition to the dendrimer. This is because the acetyl groups give diagnostic signals in the ^{1}H NMR spectra and because the molecular weight (MALDI-TOF MS) of the products both before and after deacetylation can be compared to determine the number of sugars present (vide supra).

NMR Characterization

The ^{1}H NMR (500 MHz) spectra of acetyl-protected mannose-functionalized dendrimer **31** and deacetylated form **37** in d_6-DMSO are shown in Figure 3.3. The spectra of acetyl-protected mannose-functionalized dendrimer **33**

and deacetylated form **39** in d_6-DMSO are shown in Figure 3.4, and the spectra of acetyl-protected mannose-functionalized dendrimer **35** and deacetylated form **41** in d_6-DMSO are shown in Figure 3.5.

For acetylated dendrimers **30-35**, the amide protons from the interior of the dendrimer are the peaks that are farthest downfield (7.7 ppm and 8.0 ppm). The peak at 7.5 ppm is the thiourea NH signals. The peaks between 3.7 and 5.2 ppm are from the sugar proton signals. The peaks between 2.1 and 3.7 ppm are a combination of signals from the dendrimer and the PEG linker. The acetyl methyl group signals are clearly seen between 1.8 and 2.1 ppm.

The relative integrations of the peaks from the amide signals suggest that a high degree of surface functionalization has been achieved. For example, in **31** there are 12 amide and 16 thiourea protons, so a 1:1.33 ratio of peaks is expected. Since the observed ratio is 1:1.25, this suggests that 96% of the possible functionalization occurred. In all cases, NMR indicates ≥90% functionalization. Unfortunately, the MALDI-TOF MS results suggest a lower degree of surface loading.

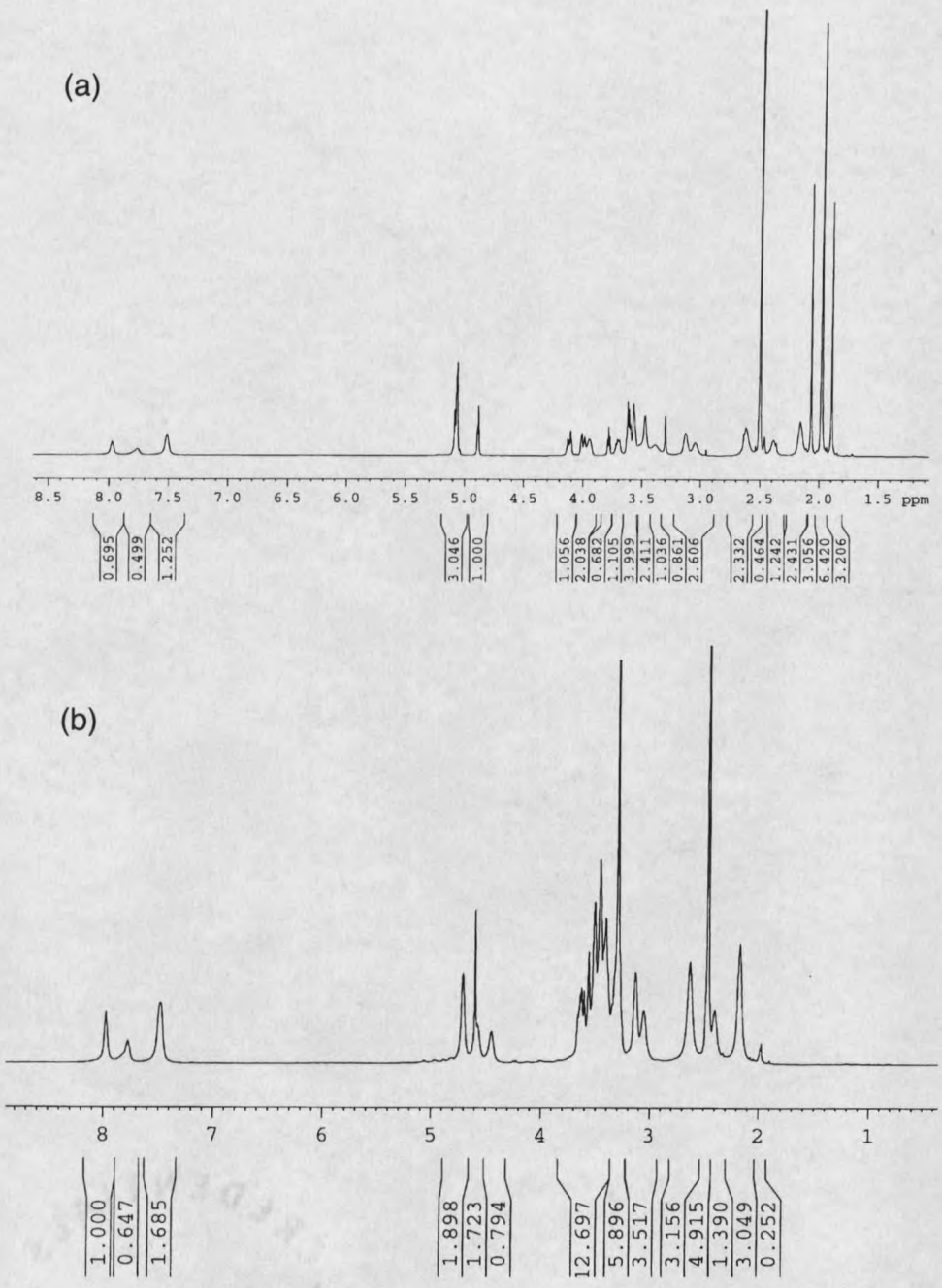


Figure 3.3 ^{1}H NMR spectra (500 MHz) of (a) **31** (b) **37** in d_6-DMSO.

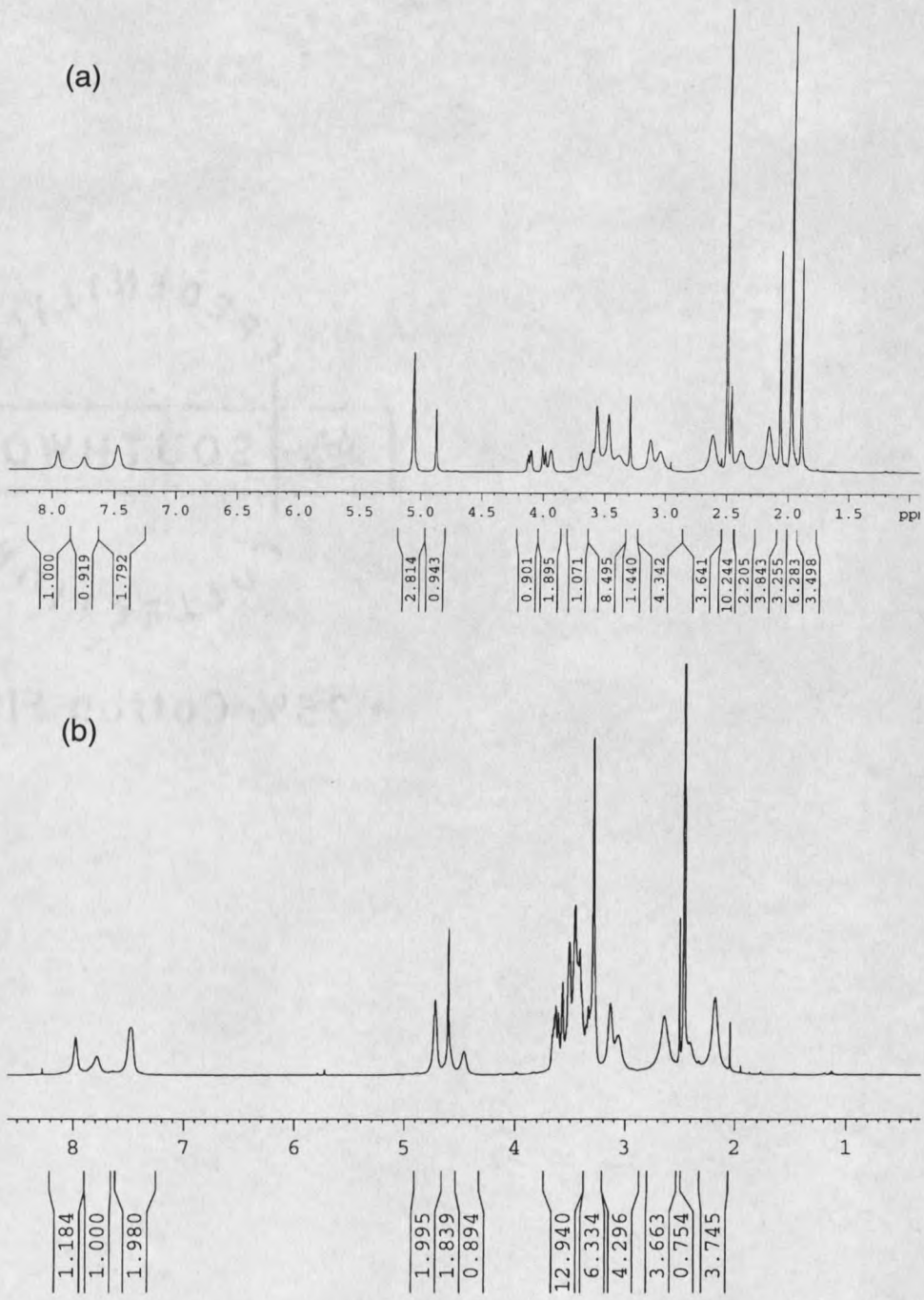


Figure 3.4 ^{1}H NMR spectra (500 MHz) of (a) **33** (b) **41** in d_6-DMSO.

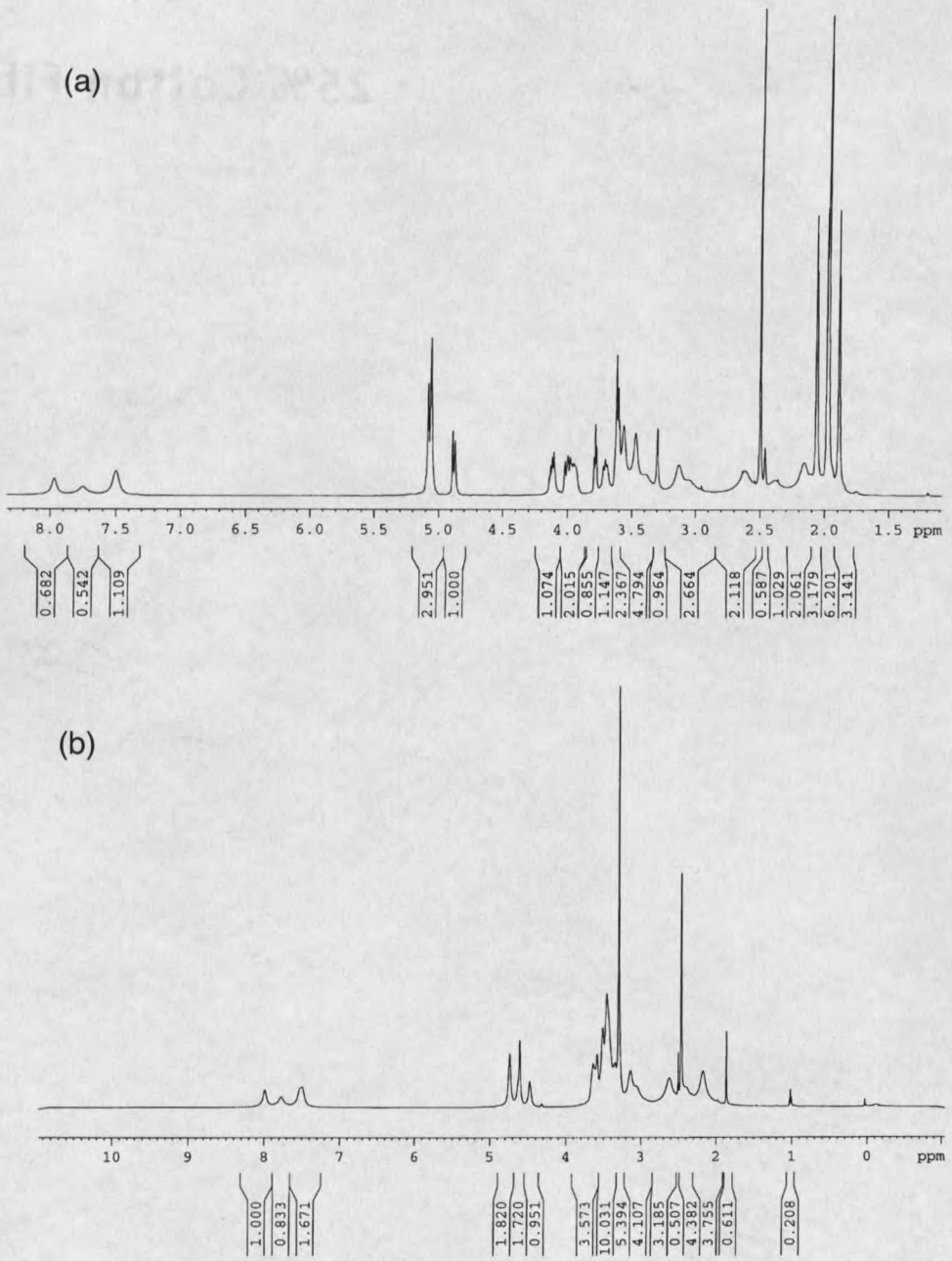


Figure 3.5 ^{1}H NMR spectra (500 MHz) of (a) **33** (b) **39** in d_6-DMSO.

MALDI-TOF MS Characterization

The MALDI-TOF MS spectra of generation two PAMAM-based mannose-functionalized dendrimers **31**, **37**, and the G(2)-PAMAM starting material are shown in Figure 3.6. The spectra for generation four dendrimers **33**, **39**, and the G(4)-PAMAM starting material are shown in Figure 3.7. The spectra for generation six dendrimers **35**, **41**, and the G(6)-PAMAM starting material are shown in Figure 3.8. For G(4)- to G(6)-PAMAMs, the measured molecular weights of the dendrimers were lower than the theoretical values (see Chapter 2 for a discussion on the lower than expected molecular weights).[155] In all spectra, the parent peak is the largest peak on the right of the spectra. The smaller peaks to the left of the parent peak are multiply charged molecules.

Subtraction of the experimentally determined molecular weight of the PAMAM starting materials from the molecular weight of **30-41** and division by 477 (molecular weight of **29**) or 309 (molecular weight of deacetylated **29**) indicates that the percent incorporation of mannose residues is 100% for G(1)- and G(2)-PAMAMs, 92% for G(3)-PAMAM, and 84%, 73%, and 63% for G(4)-, G(5)-, and G(6)-PAMAM, respectively (Table 3.1).

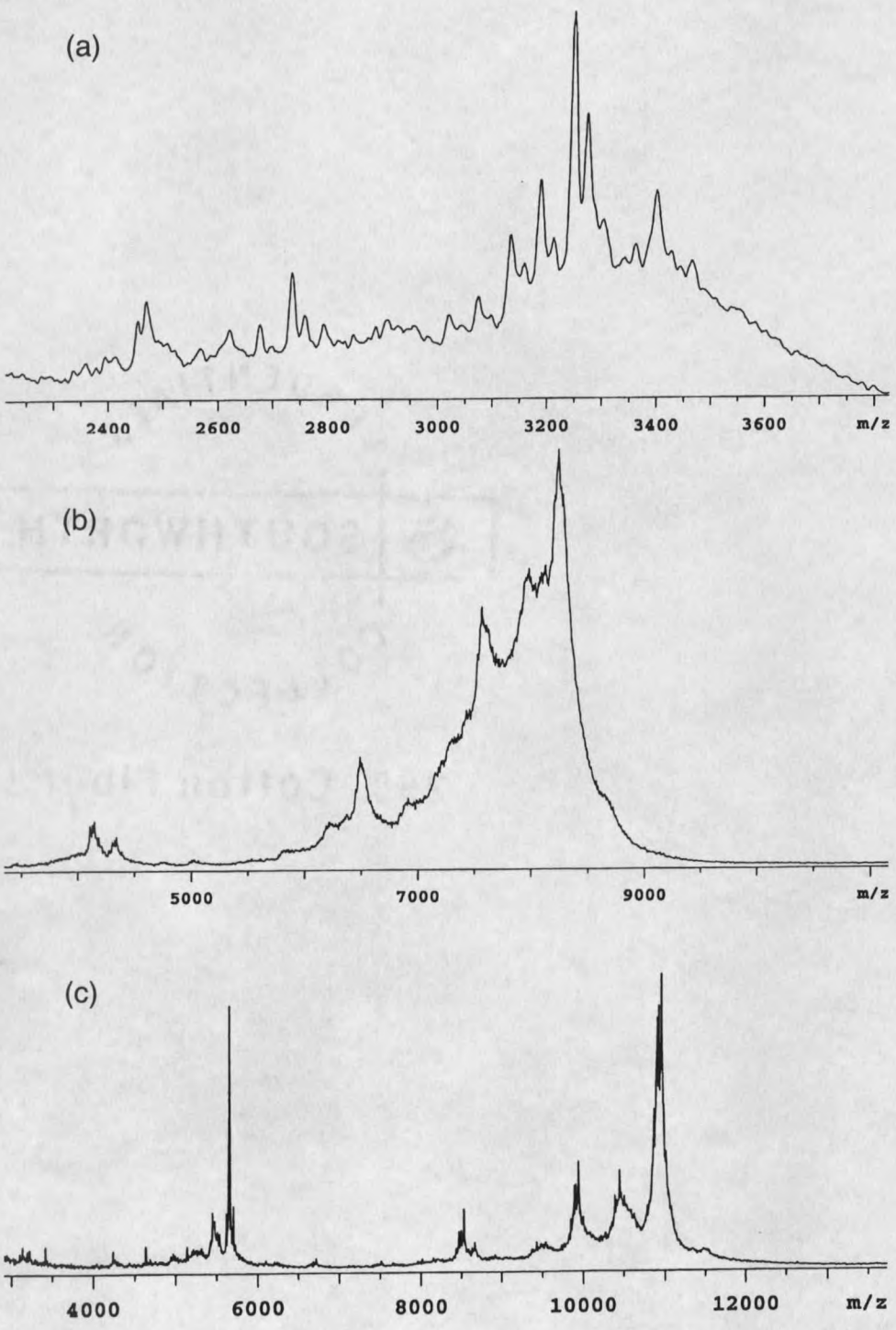


Figure 3.6 MALDI-TOF MS spectra of (a) G(2)-PAMAM, (b) **37**, (c) **31**.

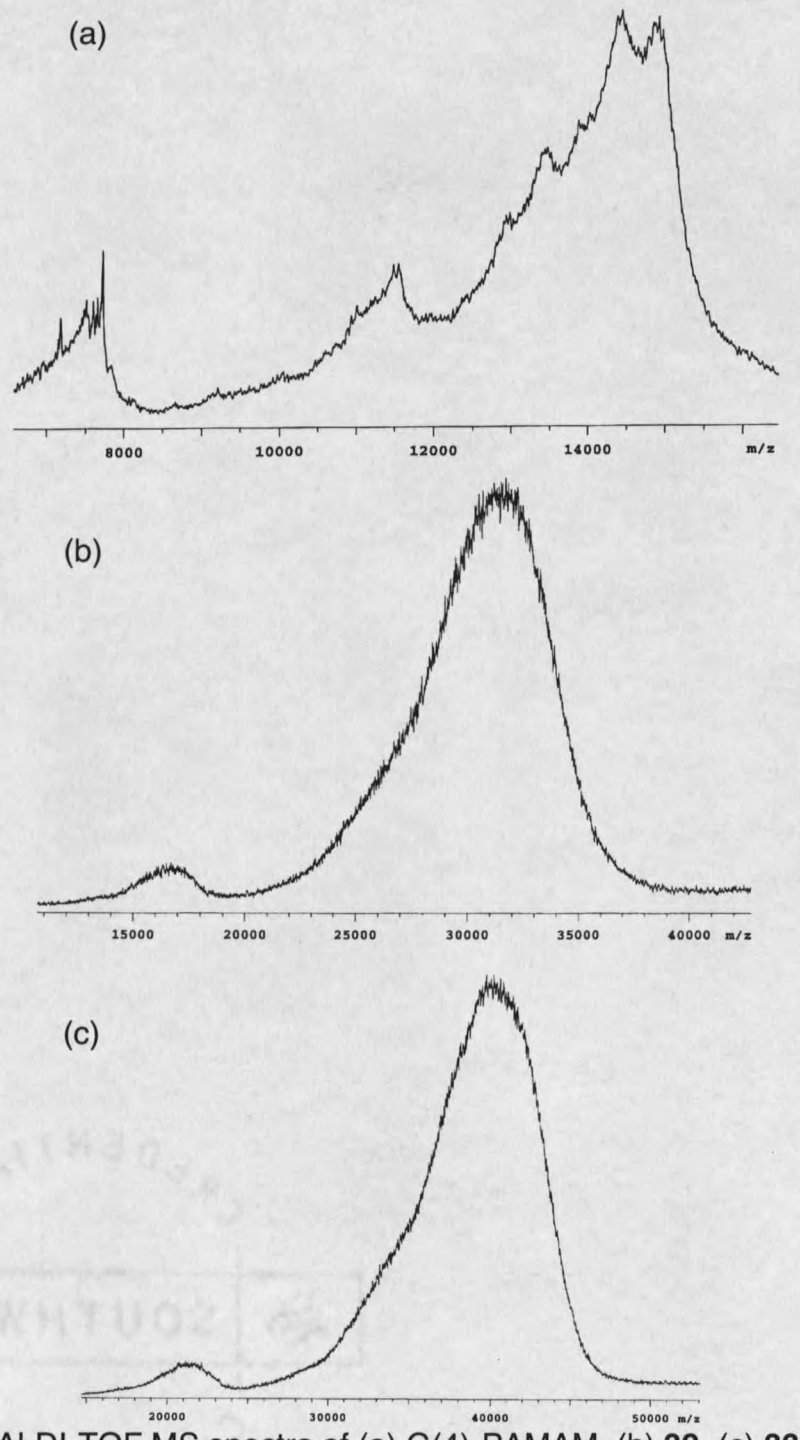


Figure 3.7 MALDI-TOF MS spectra of (a) G(4)-PAMAM, (b) **39**, (c) **33**.

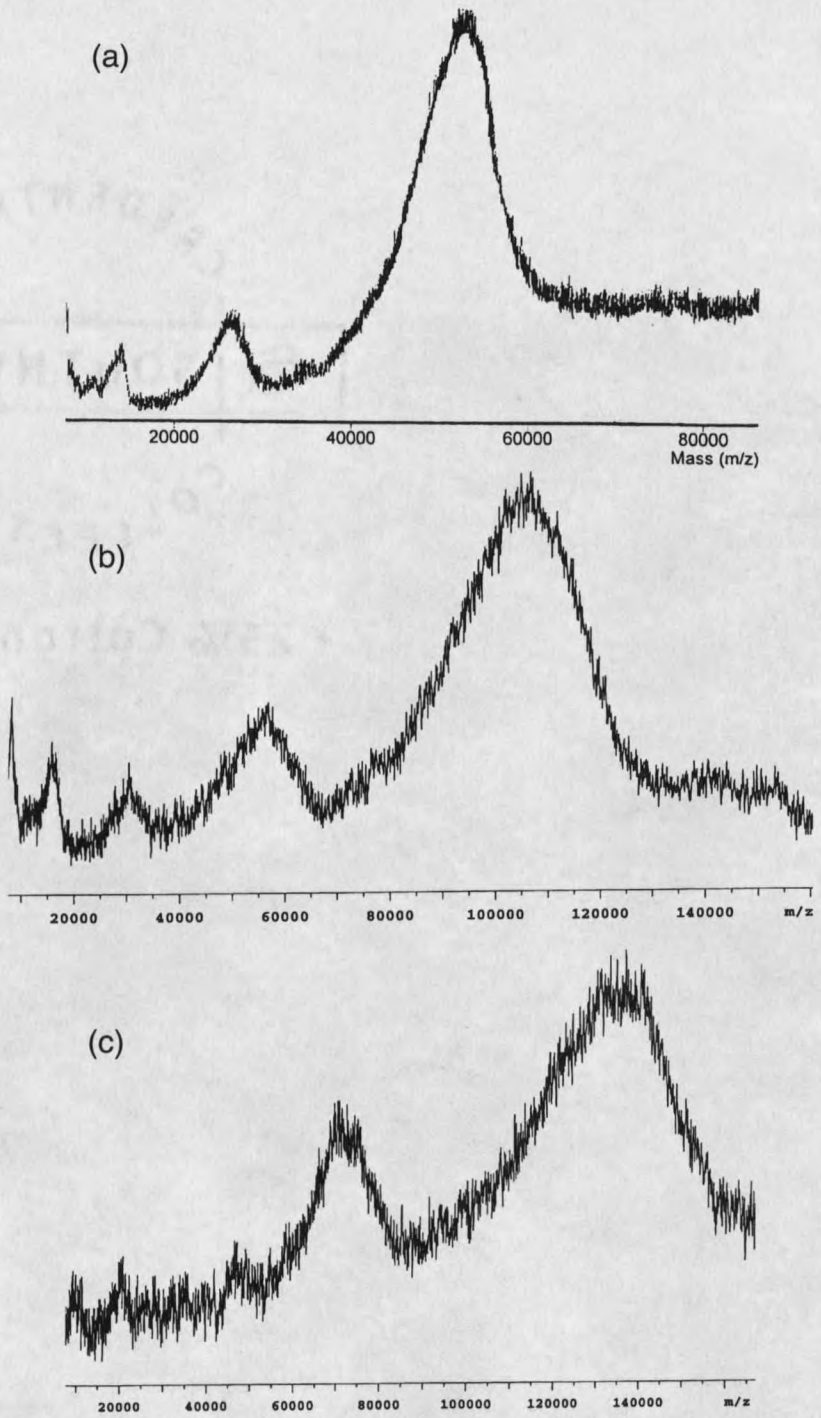


Figure 3.8 MALDI-TOF MS spectra of (a) G(6)-PAMAM, (b) **41**, (c) **35**.

Table 3.1 MALDI-TOF MS determination of mannose-functionalization of G(1)- to G(6)-PAMAMs.

Dendrimer	M_W from MALDI (g/mol)	Calculated no. of Sugars[a]	Average % loading[b]
G(1)-PAMAM	1430	–	
30	5280	8	100
36	3877	8	
G(2)-PAMAM	3260	–	
31	10960	16	100
37	8250	16	
G(3)-PAMAM	6910	–	
32	21000	30	92
38	15930	29	
G(4)-PAMAM	13500	–	
33	39300	54	84
39	30620	55	
G(5)-PAMAM	25500	–	
34	69600	92	73
40	55000	95	
G(6)-PAMAM	50800	–	
35	133500	173	67
41	103800	172	

[a] For 30-35: # sugars = $(MW_{30\text{-}35} - MW_{G(1)-G(6)\text{-}PAMAM})/477$. For 36-41: # sugars = $(MW_{36-41} - MW_{G(1)-G(6)\text{-}PAMAM})/309$.

[b] Average % loading based on theoretical number of endgroups.

Comparison of MALDI-TOF MS and NMR Data

The simplest explanation for the discrepancy between the NMR and the MALDI-TOF MS determinations of percent loading is that, because of the high degree of symmetry present in PAMAMs, NMR does not identify structural defects as well as MALDI-TOF MS. If we assume the loss of terminal

$CH_2CH_2CONHCH_2CH_2NH_2$ units (which corresponds to 114 mass units) as the predominant defects present in the starting materials, then our results indicate that at least 90% of the amines are functionalized.

In other words, there are not as many amines on the surface of the dendrimers to functionalize as thought according to theoretical calculations. For example, the difference between the theoretical mass of a G(4)-PAMAM (14,215 g/mol; see Table 1.1) and the MALDI-TOF value (13,500 g/mol; see Table 3.1) is 715. If this is attributed to the loss of units of 114 g/mol, that indicates six amines are missing on the surface. Theoretically, there are 64 amines on the surface, with the absence of six, there are only 58 left to functionalize. From Table 3.1 the actual number of sugars on the surface of **39** is 55, which corresponds to 95% functionalization.

If the above calculations are repeated for G(5) and G(6) the same trend is observed. G(5)-PAMAM is missing 29 amines, which leaves the dendrimer with 99 surface amines, and, the degree of functionalization of **40** is 95%. G(6)-PAMAM is missing 64 amines, which leaves the dendrimer with 192 surface amines, and if an average of 173 sugars have been added, the degree of functionalization of **41** is 90%. It must be noted, however, that the calculations used to determine the number of missing amines rely on the assumption that the main source of error in the PAMAM dendrimer is the loss of $CH_2CH_2CONHCH_2CH_2NH_2$ units on the outer shell. This assumption is made to

simplify a potentially extremely complex problem (see Scheme 2.4 and discussion on page 52).

In essence, we suggest that both the NMR and MALDI-TOF results indicate a high degree of surface functionalization is occurring, but that defects in the PAMAMs preclude higher sugar loading (see Chapter 2 for details).

Hemagglutination Inhibition Assay Introduction

One of the most straightforward assays for the determination of ligand activity is a hemagglutination inhibition assay (HIA). One of the first descriptions of the HIA procedure was presented by Osawa and Matsumoto in 1972.[171] Since then, the HIA has been used extensively as a first test for various ligands with a number of lectins.

Although HIA does not provide direct information regarding binding affinity,[22, 47] The use of the HIA to measure inhibition of protein-carbohydrate interactions is well documented and provides an essential entry-level comparison of the glycodendrimers reported here with other glycopolymers.[13, 20, 54, 55, 75] In an article discussing activity vs. affinity and the use of the HIA, Toone and coworkers note that "in many respects hemagglutination assays are a far more relevant measure of activity than are assays designed exclusively to evaluate protein-carbohydrate binding."[47]

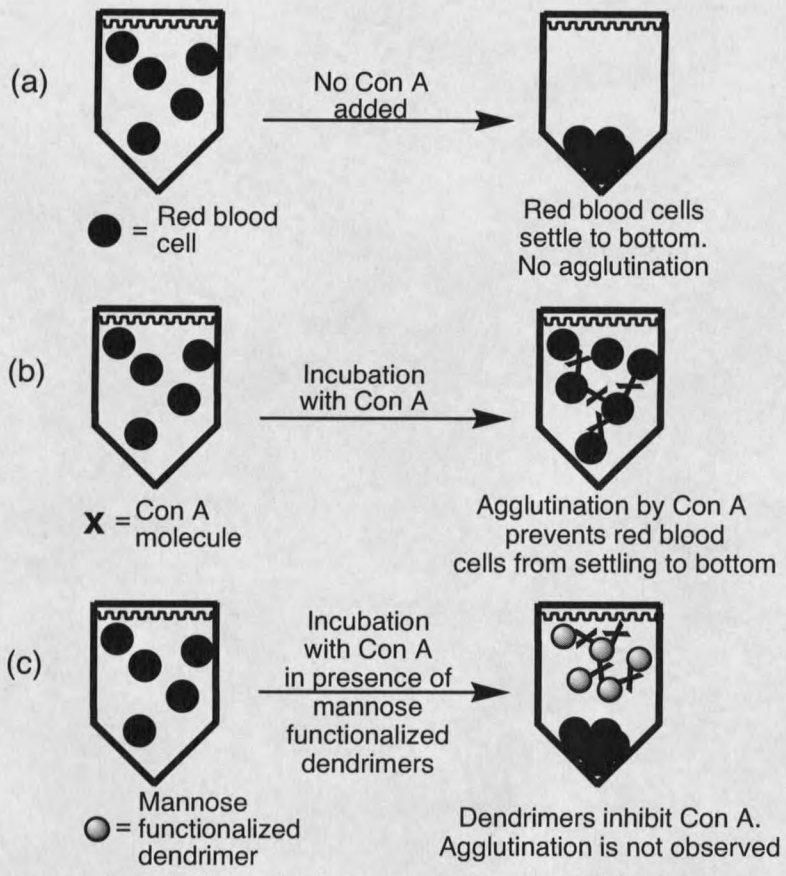


Figure 3.9 General description of a hemagglutination inhibition assay. (a) Red blood cells in buffer with no Con A result in no hemagglutination, (b) Red blood cells and Con A result in hemagglutination, (c) Red blood cells and Con A with a mannose containing ligand result in inhibition of hemagglutination.

The general scheme of HIA is given in Figure 3.9. The HIA is typically done in a microtiter plate with V-shaped wells. Figure 3.9a shows the result of placing just red blood cells in buffer. After about an hour, the red blood cells settle to the bottom and form a red "button" in the well. When Con A is present in the solution (Figure 3.9b) the lectin binds with mannose-containing glycoproteins expressed on the surface of the cells, thus creating a large crosslinking lattice. This is hemagglutination, and the red blood cells do not settle out of solution.

Figure 3.9c shows the inhibition of the Con A by a mannose-functionalized dendrimer (or other mannose containing ligand as well as methyl mannose). When Con A is incubated with the ligand, if the ligand concentration is high enough (depending on its activity towards Con A), it will bind with the Con A and prevent the interaction between Con A and the red blood cells. The result is that hemagglutination is inhibited and the red blood cells settle to the bottom of the well as in Figure 3.9a.

While a detailed procedure is included in the experimental section, a brief description is given here. Erythrocytes (rabbit) were added to preincubated solution of Con A and varying concentrations of dendrimer. The lowest amount of dendrimer that caused inhibition of hemagglutination was determined. This was the inhibiting dose and was compared to the inhibiting dose of methyl mannose.

While the HIA is easy to perform and interpret, the results must be taken with some caution. As mentioned already, the results derived from this assay cannot be interpreted as binding affinities. A binding affinity is a specific value that describes the strength of binding between a sugar and a lectin (see Figure 1.4a). In the HIA, a number of modes of binding are possible and all are observed in terms of the whole rather than of the parts (Figure 1.4).

Another potential downfall of this assay is in the increased potential for human error or bias. First, the dilution in the wells is a two-fold serial dilution. Therefore, the error possible in this case is ±1 well, or in other words a factor of

two. Related to this is the fact that two observers may interpret the endpoint differently. The success of the HIA relies on the use of a strict protocol and the use of consistent parameters. To ensure the maximum accuracy and consistency is achieved, each HIA is repeated *at least* three times (often more), and the same person performs the determination of the endpoint each time using the same criteria for each trial.

Hemagglutination Inhibition Assay Results Using Mannose-Functionalized PAMAM Dendrimers

The results for mannose-functionalized dendrimers **36-41** are shown in Table 3.2. Each value represents at least three assays. The large standard deviations occur because, while the trends are always the same, different blood sources (different rabbits on different days) give different numbers.

Table 3.2 Hemagglutination inhibition assay results for **36-41** with Con A

Compound	Number of Sugars	Relative activity/sugar
Methyl mannoside	1	1
36	8	1
37	16	1.5 ± 0.1
38	29	21 ± 5
39	55	275 ± 90
40	95	510 ± 295
41	172	660 ± 230

When compared to the control monomer methyl mannose, dendrimers **36** and **37** did not show any increase in activity towards Con A. Thus, we surmise that **36** and **37** bind monovalently (Figure 1.4a). Either clustering (Figure 1.4c) or

monovalent binding (Figure 1.4a) was expected, since the lower generation dendrimers are too small to span multiple binding sites (i.e., to bind multivalently).

In addition, our findings indicate that **38** (G(3)-PAMAM core) binds roughly one order of magnitude better than **36**, **37** or methyl mannoside. This is suggestive of a glycoside clustering motif (Figure 1.4c). As with **36** and **37**, **38** is too small for multivalent binding to occur.

Roy and Pagé reported similar results using an enzyme-linked lectin assay (ELLA) on the generations one through three versions of **8-10** described earlier.[123] They contained the phenyl ring between the mannose unit and the PAMAM dendrimer (see Scheme 2.3), but were of similar size and valency to **36-38**. While the absolute values of activity differ (most likely due to the different assay utilized), the results using ELLA on the dendrimers described by Roy and Pagé are of the same order of magnitude relative to methyl mannose as **36-38**.

Dendrimers **39-41** all show increases in activity (relative to methyl mannose) of 2 orders of magnitude. This indicates that multivalent binding is occurring (Figure 1.4d). Since **39-41** are all large enough to span multiple binding sites of Con A, this seems like a reasonable explanation for the desired increase in activity with Con A (relative to methyl mannose). However, more subtle factors may also be involved.

As previously mentioned, for the various binding motifs described in Figure 1.4, any observed enhancement in activity may be a result of a combination of modes. In the case of **39-41** it is clear that along with multivalent binding, glycoside clustering as depicted in Figure 1.4c could also be contributing to the enhancement (the work described in Chapter 4 will attempt to delineate between the two contributing factors).

Glycoside Clustering and the Effect of Sugar Density

Molecular mechanics calculations (Macromodel V. 6.5, MM2*) suggest that reaction of **29** with the dendrimer will add a maximum of about 13 Å to the radius of the molecule. Thus, using published radii for the original PAMAM's (G(4)-PAMAM radius ~22.5 Å, G(5)-PAMAM radius ~27 Å, G(6)-PAMAM radius ~ 33.5 Å),[172, 173] we can calculate the expected approximate area that each endgroup would occupy on the dendrimer surface. Assuming **39-41** are spherical,[89, 96] the area available to the endgroups on **41** is considerably smaller than the area available to endgroups on **39**. We postulate that, although all the larger dendrimers apparently bind multivalently, some may be better at glycoside clustering than others

The use of the published dendrimer diameter data and the calculated length of **29** is appropriate for the qualitative comparison of glycoside clustering and the effect of sugar density. However, spin-labeled studies have indicated that

the actual sizes of functionalized PAMAM dendrimers are different. The section starting on page 157 describes the spin-labeled studies in more detail.

The phenomenon that some multivalent ligands may be better at glycoside clustering than others has also been observed by Kiessling and coworkers.[69] When testing a variety of their glycopolymers, they found a dramatic increase in activity towards Con A when the polymers became long enough to span multiple binding sites. However they observed an increase potency of the longest polymers even when additional multivalent interactions were not possible. This was presumably due to the increased local concentration of mannose residues.

In effect, the increase in concentration (or density) of mannose residues displayed by dendrimers **39-41**, affects the rate of dissociation. Increasing the number of sugars available to the Con A binding site slows dissociation and favors reassociation more and more, which results in greater activity.

It seems logical to attribute the large increase in activity to the ability of the ligands to bind multivalently. The continued increase in binding is attributable to glycoside clustering, which is essentially a statistical effect. However, there is also the possibility of cross-linking as shown in Figure 1.4(e) that could be a contributor.

Cross-Linking and Aggregates

Cross-linking is an intermolecular mode of binding that leads to large aggregates and even precipitation of lectin and ligand if the aggregates become large enough. A number of researchers in this field are of the opinion that the increase in activity or affinity of multivalent ligands is predominantly a result of the favorable formation of aggregates or precipitate.[22]

The work of Brewer *et. al.* has shown that in some systems, cross-linking is occurring and can even enhance the specificity of the glycopolymers for the lectin.[174-178] There are also a number of biological systems that require carbohydrate mediated aggregation in order to function.[179-181]

One example involves the apoptosis of T-cell by galectin-1. Galectin-1 is a member of the β-galactoside binding proteins and possesses growth regulatory and immunomodulatory activities. Dose-response analysis of the amount of galectin-1 required to induce T-cell apoptosis indicated that the dimeric form was necessary to induce apoptosis.[180] Clearly, cross-linking is another realistic mode for the observed increase in activity, especially for small ligands that cannot bind to multiple site. However, to what extent crosslinking occurs is difficult to determine.

In the carbohydrate-functionalized dendrimer systems described here, if aggregation is responsible for the increased activity observed in the hemagglutination assay, it should be possible to observe a precipitate or colloidal suspension. This is expected due to the size of the molecules involved and the valency of the dendrimers (i.e. each dendrimer can conceivably attach to multiple tetramers of Con A). To be able to observe at what concentration ranges precipitation occurred, the following turbidity study was done.

It should be noted that attempts to perform dynamic light scattering experiments to measure the size of molecules in solution in the same concentration ranges as the hemagglutination assay failed. The failure was most likely due to the fact that particle size was below the detection limits of the instrument, suggesting that if cross-linking is occurring, it is not extensive enough to form large aggregates.

Turbidity Study

To address whether the formation of aggregates was occurring in the hemagglutination assay, a turbidity study was performed. In brief, a solution of Con A and dendrimer were mixed together in a UV cuvet. As a precipitate formed (if it formed) the absorbance at 500 nm was measured over time. Neither the Con A nor the dendrimers absorb at 500 nm, so any increased absorbance (which is more accurately described as decreased transmittance) would be a result of the

precipitate blocking the light. The data for the turbidity study of **36**, **38**, and **39** is shown in Figure 3.10 and Figure 3.11. The concentration of Con A in Figure 3.10a and both graphs in Figure 3.11 was 0.2 mg/mL and in Figure 3.10b it was 0.4 mg/mL. After the Con A and dendrimer were mixed, a precipitate formed quickly as evidenced by the sharp increase in absorbance at 500 nm. After about 8 hours, the precipitate had nearly reached a maximum. The amount of precipitate formed (as determined by the absorbance at 500 nm) was related to the amount of dendrimer present.

The formation of a precipitate between Con A at concentrations of 0.2 mg/mL and 0.4 mg/mL and the dendrimers at concentrations ranging from 0.98 μg/mL to 2500 μg/mL indicates they can and do form large aggregates. However, when the same test was used for solutions in the same concentration range used in the HIA (Con A 0.025-0.050 mg/mL), there was no increase in absorbance at 500 nm (i.e. no precipitation) (see Figure 3.12).

In each of the turbidity tests, after about 25 hours, a solution of methyl mannose equal to the moles of mannose present based on dendrimer concentration was added to each sample. In each case, the precipitate cleared up completely indicating the aggregates had completely dissolved. The fact that methyl mannose was able to displace the dendrimers shows that the interaction between the Con A and mannose-functionalized dendrimer is both specific and reversible.

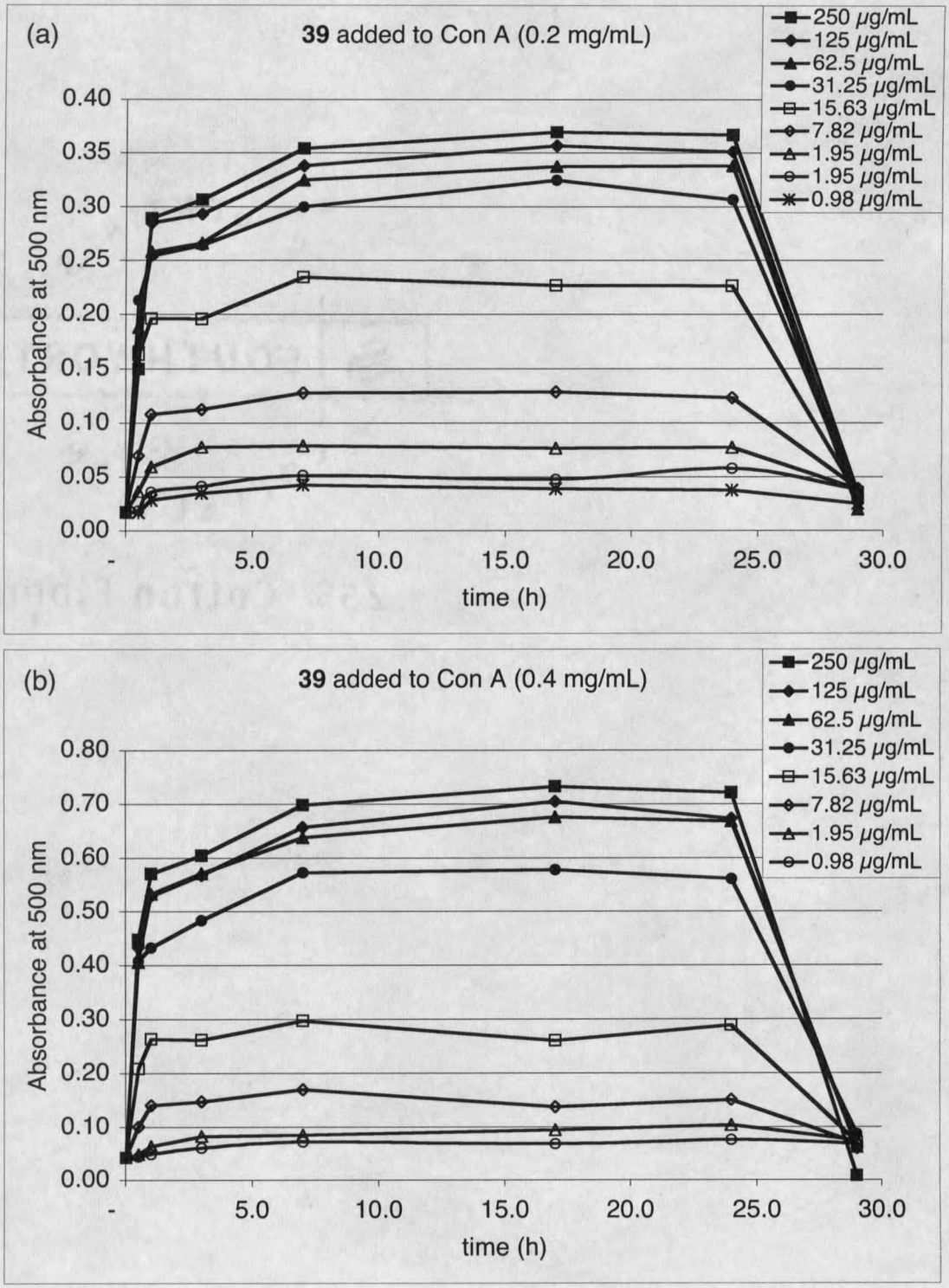


Figure 3.10 Graphs from turbidity assay for G(4) dendrimer **39** at (a) 0.2 mg/mL Con A and (b) 0.4 mg/mL Con A.

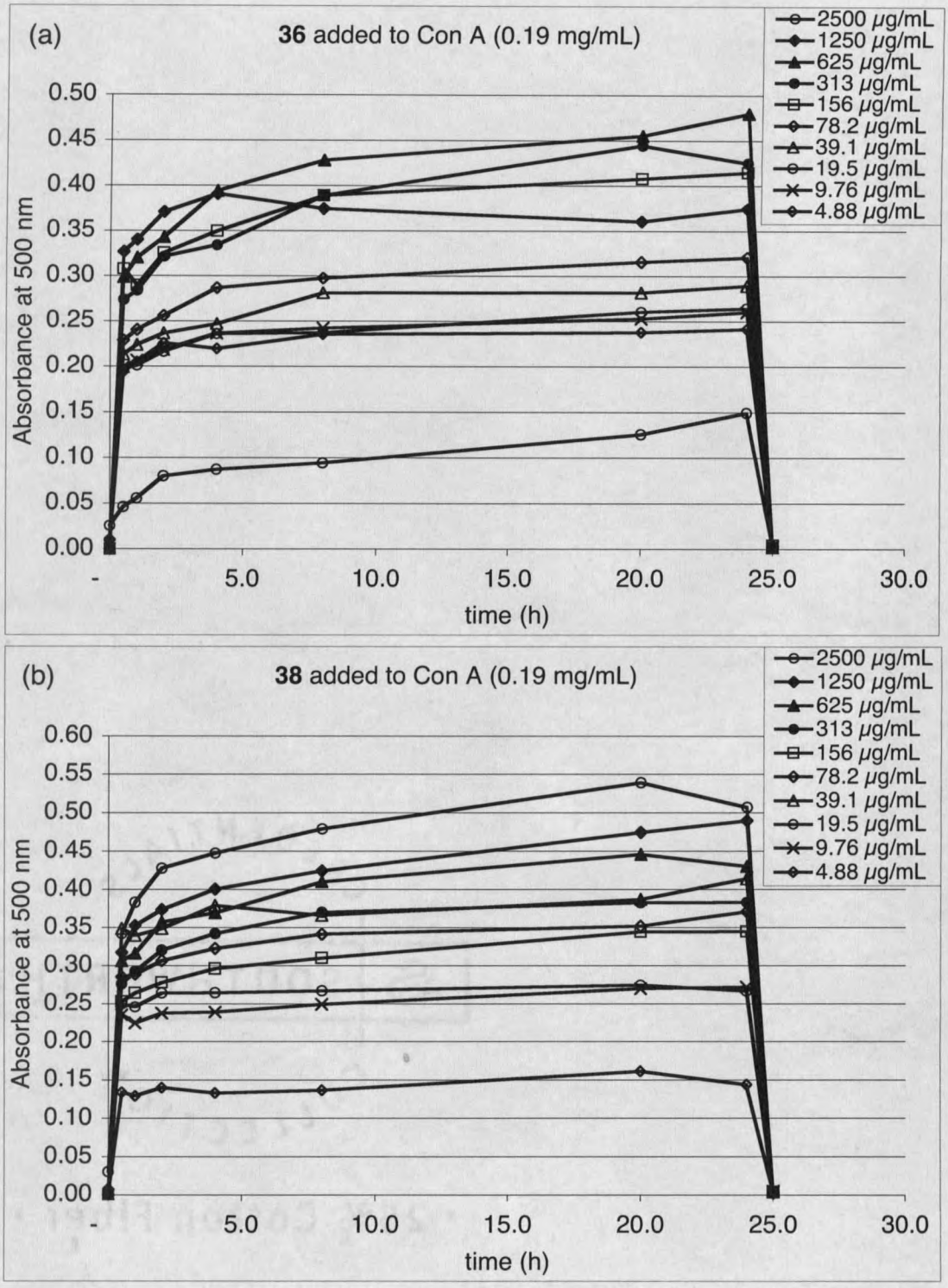


Figure 3.11 Graphs from turbidity assay for (a) **36** (G(1)) and (b) **38** (G(3))

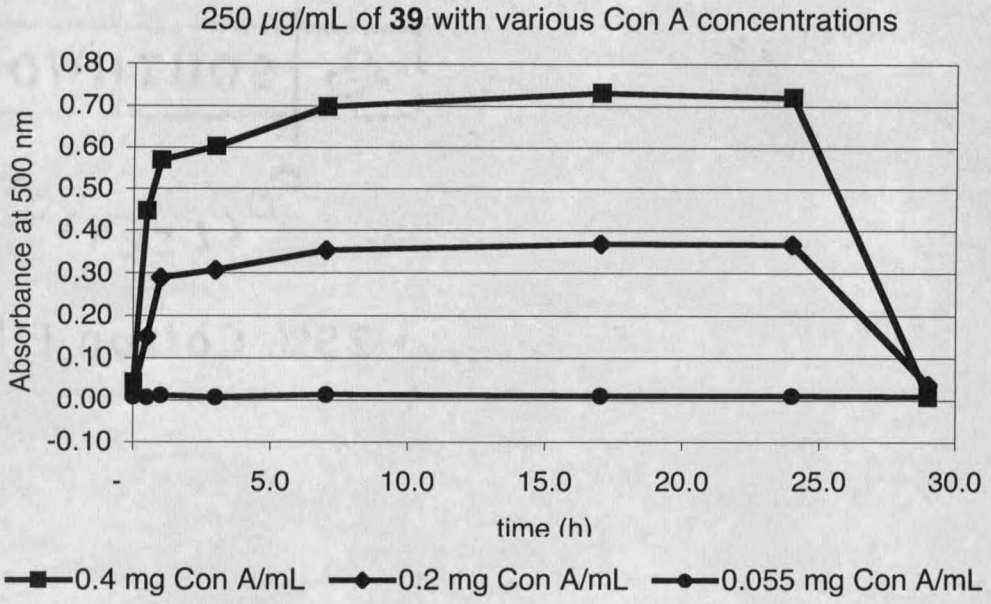


Figure 3.12 Graph from turbidity assay of **39** with varying concentrations of Con A. Closed circles are at Con A concentration of the hemagglutination assay. No precipitation is observed at this concentration of Con A.

What can be concluded from the turbidity tests is that under appropriate conditions, aggregation of Con A and the mannose-functionalized dendrimers can occur, however aggregation does not seem to be a major contributor in the HIA in which the Con A concentration is nearly 10-fold lower. The fact that **36** (generation one dendrimer) does not show increased activity relative to methyl mannose, yet can be forced to form aggregates at high concentrations of Con A supports the claim that cross-linking and aggregate formation is not a significant mode of interaction in the HIA. If cross-linking were significant, **36** would be expected to have a higher activity, since it (like the other mannose-functionalized dendrimers) is a prime candidate for cross-linking Con A molecules together.

Summary

In this phase of the project, a number of significant goals were achieved. First and foremost, a water-soluble mannose-functionalized dendrimer was synthesized. By the use of a polyethylene glycol linker, it has become possible to attach a sugar to a dendrimer and maintain water-solubility. In the pursuit of water-soluble dendrimers, it was discovered that the coupling of an isothiocyanato alcohol to a trichloroacetimidate could be accomplished using $BF_3 \cdot Et_2O$ in high yield on a large scale.

Most importantly, it is apparent, based on hemagglutination inhibition assays, that the size of the dendrimer makes a critical difference. The interaction of a mannose-functionalized PAMAM dendrimer with Con A is similar to that of a mannose monomer if the PAMAM dendrimer is generation one or two. Generation three exhibits enhanced activity with Con A due to glycoside clustering, which could be due to the shape of the dendrimer and thus, the proximity of the mannose units. The larger generations (four, five and six) demonstrate the ability of glycodendrimers to multivalently interact with the lectin. Since they are large enough, they span multiple binding sites, and the results are dramatic.

While we would like to be able to use the results from our HIA and turbidity assay as well as the results in the literature for other glycodendrimers to predict with certainty how to design therapeutic multivalent ligands, we obviously cannot.

The next step, as described in the following chapter, is to vary the number of sugars on the surface of the dendrimer. This provides more information on the details of multivalent interactions.

Experimental Procedures

General methods

General reagents were purchased from Aldrich, Sigma, and Acros. Generations 1 to 4 PAMAM dendrimers were purchased from Aldrich or Dendritech. Generations 5 and 6 PAMAM dendrimers were purchased from Dendritech. Methylene chloride was purified on basic alumina. $BF_3 \cdot Et_2O$ was freshly distilled from CaH_2 before use (62° C at 33 mm Hg). *trans*-3-Indoleacrylic acid was crystallized from absolute ethanol. Concanavalin A was purchased from Calbiochem. All other solvents and reagents were used as supplied. All MALDI-TOF MS reference standards were purchased from Sigma and used as supplied.

MALDI-TOF MS

Matrix assisted laser desorption ionization (MALDI) mass spectra were acquired using a Bruker Biflex-III time-of-flight mass spectrometer. Spectra of all functionalized dendrimers were obtained using a *trans*-3-indoleacrylic acid matrix with a matrix-analyte ratio of 3000:1 or 1000:1. Horse heart myoglobin (MW 16,952 g/mol), bovine serum albumin (MW 66,431 g/mol), Bradykinin (MW 1061 g/mol),Cytochrome C (MW 12,361 g/mol), and Trypsinogen (MW 23,982 g/mol)

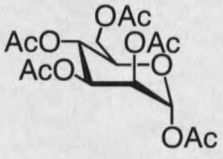
were used as external standards. An aliquot corresponding to 12-15 pmol of the analyte was deposited on the laser target. Positive ion mass spectra were acquired in linear mode, and the ions were generated by using a nitrogen laser (337 nm) pulsed at 3 Hz with a pulse width of 3 nanoseconds. Ions were accelerated at 19-20,000 volts and amplified using a discrete dynode multiplier. Spectra (100 to 200) were summed into a LeCroy LSA1000 high-speed signal digitizer. All data processing was performed using Bruker XMass/XTOF V 5.0.2. Molecular mass data and polydispersities of the broad peaks were calculated by using the Polymer Module included in the software package. The peaks were analyzed using the *continuous* mode. Delta values were set at minimum levels.

Dynamic Light Scattering

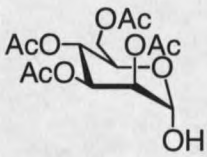
Dynamic light scattering (DLS) experiments were performed using a Brookhaven Instruments Corporation 90Plus dynamic light scattering instrument. All data was collected and analyzed using the dynamic light scattering software from Brookhaven Instruments. The sample cuvet was rinsed with saline that had been filtered using a 0.1 μm nonpyrogenic Pall syringe filter. The light source was a 661 nm diode laser at 15 mW of power. A photomultiplier detector at 90 degrees from the sample was used to observe scattered light. A correlation function was determined by a BI-9000AT autocorrelator. The autocorrelator is an exponential decay or sum of decays from the scattered light. The correlation function was fit using a non-negatively least squares fit to yield a particle size

histogram. All samples were prepared in filtered (0.1 μm Pall syringe filter) PBS. At the concentrations of Con A and glycodendrimers used for the assay, no signal was observed. This indicates that any aggregates that are forming are below the detection limits of the DLS instrument.

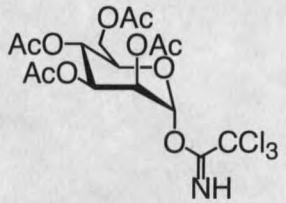
Synthetic procedures



1,2,3,4,6-penta-*O*-acetyl-α-D-mannopyranoside. A solution of α-D-mannose (26.6 g, 148 mmol) and pyridine (150 mL) was cooled to 0 °C. While stirring, acetic anhydride (82.8 g, 811 mmol) was added, followed by a catalytic amount of DMAP. The reaction was allowed to warm to room temperature. After 4 hours, the majority of the pyridine was removed *in vacuo*. Ether (75 mL) was added to the concentrated solution, and the product was washed with 20% HOAc (2 x 75 mL). The aqueous layers were combined and extracted with Et_2O (75 mL). The organic layers were combined and washed with water (4 x 75 mL). The ether was dried over $MgSO_4$ and evaporated *in vacuo* to leave 45.5 g (80%) of the acetylated sugar as a foamy soap-like residue. The product was used without further purification.

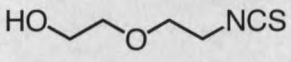


2,3,4,6-tetra-*O*-acetyl-α-D-mannopyranoside.[162] A solution of 1,2,3,4,6-penta-*O*-acetyl-α-D-mannopyranoside (19.0 g, 48.7 mmol), hydrazine acetate (5.83 g, 63.3 mmol) and DMF (50 mL) were stirred at 55 °C for 30 min. EtOAc (50 mL) was added and the organic layer was washed with water (50 mL). The aqueous layer was extracted with EtOAc (50 mL). The organic layers were combined and washed with water (3 x 50 mL), sat. aqueous $NaHCO_3$ (3 x 50 mL), and brine (3 x 50 mL). The ether was dried over $MgSO_4$ and concentrated under reduced pressure to leave 11.92 g (70%) of product as a highly viscous oil. This product was used without further purification. ^{1}H NMR (300 MHz, $CDCl_3$) δ 5.37 (ap dd, 1H, J = 10.1, 3.3 Hz, H-1), 5.18-5.28 (m, 3H), 4.18-4.23 (m, 2H), 4.09-4.12 (m, 1H), 3.80 (bs, 1H, OH), 2.12 (s, 3H, $COCH_3$), 2.07 (s, 3H, $COCH_3$), 2.01 (s, 3H, $COCH_3$), 1.96 (s, 3H, $COCH_3$) ppm.



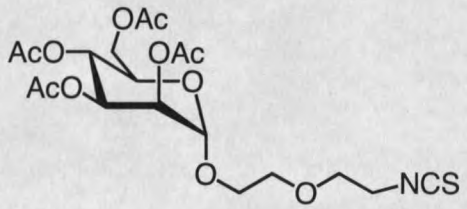
2,3,4,6-tetra-*O*-acetyl-α-D-mannosyl trichloroacetimidate (**13**).[162] *DBU method:* DBU (0.50 g, 0.5 mL, 3.3 mmol) was added drop wise to a solution of 2,3,4,6-tetra-*O*-acetyl-α-D-mannopyranoside (25.4 g, 72.9 mmol) and trichloroacetonitrile (36 g, 25 mL, 250 mmol) in CH_2Cl_2 (200 mL) at 0 °C. After 3 hours, the solvent was removed *in vacuo* and the residue was filtered through a plug of silica (60:40 hexanes:ethyl acetate). The solution was concentrated to

leave a yellow oil which was purified on silica gel (60:40 hexanes:ethyl acetate) to yield 30 g (84%) of **13**. *Potassium carbonate method*: Solid K_2CO_3 (13g, ~7 equiv) and 2,3,4,6-tetra-*O*-acetyl-α-D-mannopyranoside (4.84 g, 13.8 mmol) were stirred in 65 mL of CH_2Cl_2 while trichloroacetonitrile (2.98 g, 2 mL, 20.7 mmol) was added via syringe. The reaction was stirred for 5 hours. The reaction mixture was filtered over celite. The solvents were removed *in vacuo* and the crude product was purified as before to yield 5.08 g (75%) of **13**. ^{1}H NMR (300 MHz, $CDCl_3$) δ 8.75 (s, 1H, NH), 6.14 (d, 1H, J = 1.7 Hz, H-1), 5.32 (m, 1H), 5.22-5.30 (m, 2H), 3.96-4.17 (m, 3H), 2.06 (s, 3H), 1.95 (s, 3H), 1.93 (s, 3H), 1.87 (s, 3H) ppm; ^{13}C NMR (125 MHz, $CDCl_3$) δ 170.5, 169.7, 169.6, 169.5, 169.4, 159.7, 90.5, 71.2, 68.7, 67.8, 65.3, 62.0, 20.8, 20.7, 20.6, 20.6 ppm.



2-(2-Isothiocyanatoethoxy)ethanol (**28**). A solution of 2-(2-aminoethoxy)ethanol (7.35 g, 7.0 mL, 70 mmol) and triethylamine (14.2 g, 20 mL, 140 mmol) in $CHCl_3$ (100 mL) was added via syringe over the course of an hour (syringe pump) to a stirred solution of thiophosgene (8.04 g, 5.4 mL, 70 mmol) in $CHCl_3$ (400 mL). Upon completion of the addition of the amino alcohol, the solvent was removed *in vacuo*. The residue was dissolved in water (100 mL) and extracted with CH_2Cl_2 (2 x 100 mL). The organic layers were combined and washed with water (2 x 50 mL), dried over $MgSO_4$, and removed *in vacuo*.

Column chromatography on silica gel (1:1 ethyl acetate/hexanes) yielded 7.18 g of a yellowish oil. This product was further purified by Kugelrohr distillation (100 °C , 0.1 mm Hg) to give 6.97 g (68%) of a clear oil. ^{1}H NMR (300 MHz, $CDCl_3$) δ 3.72 (t, 2H, J = 4.9 Hz, HOCH_2), 3.62-3.68 (m, 4H, CH_2OCH_2), 3.58 (t, 2H, J = 4.2 Hz, SCNCH_2), 2.34 (s, 1H, OH); ^{13}C NMR (75 MHz, $CDCl_3$, a signal for N*C*S was not observed) δ 72.8, 69.6, 62.1, 45.8 ppm; HRMS (CI) *m/z* 148.0428 (M + H, calcd 148.0432 for $C_5H_{10}NO_2S$), found; IR (film) 1337, 1437, 2108, 2872, 2932, 3412 cm^{-1}.



1-*O*-(5-isothiocyanato-3-oxapentyl)-2,3,4,6-tetra-*O*-acetyl-α-D-mannopyranoside (**29**). The trichloroacetimidate **13** (8.0 g, 16.3 mmol) was dissolved in CH_2Cl_2 (200 mL) with **28** (2.39 g, 16.3 mmol) and 4 Å molecular sieves (0.8 g). Under an N_2 atmosphere, $BF_3{\cdot}Et_2O$ (2.31 g, 2.0 mL, 16.3 mmol) was added slowly and the reaction was stirred at room temperature for 7 h. Solid $NaHCO_3$ (1 g) was added to the reaction. The mixture was filtered over Celite, concentrated *in vacuo*, and purified by silica gel chromatography (1:1 hexanes:ethyl acetate) to give a yellow oil. This oil was crystallized from 3:1 (ethyl ether:petroleum ether) to yield **29** (5.7 g, 73%). M.p. = 51—52° C; ^{1}H NMR (300 MHz, $CDCl_3$) δ 5.13-5.35 (m, 3H), 4.82 (s, 1H), 4.15-4.30 (m, 1H), 3.94-4.10

(m, 3H), 3.70-3.83 (m, 1H), 3.63 (bs, 6H), 2.09 (s, 3H), 2.04 (s, 3H), 1.98 (s, 3H), 1.92 (s, 3H) ppm; ^{13}C NMR (125 MHz, $CDCl_3$) δ 170.4, 169.8, 169.7, 169.6, 132.8, 97.6 ($^1J_{CH}$ = 172 Hz, C-1), 70.1, 69.4, 69.3, 69.0, 68.4, 67.2, 66.0, 62.4, 45.3, 20.7, 20.6, 20.6, 20.5 ppm; H-C coupled ^{13}C NMR (125 MHz); HRMS (CI) *m/z* 495.1632 (M + NH_4, calcd 495.1648 for $C_{19}H_{31}N_2O_{11}S$); IR (film) 1366, 1748, 2108, 3048 cm^{-1}.

Generation 1.0 PAMAM-based thiourea-linked 1-*O*-(5-thiourea-3-oxapentyl)-2,3,4,6-tetra-*O*-acetyl-α-D-mannopyranoside dendrimer (**30**): A methanolic solution of amine-terminated Starburst PAMAM dendrimer (generation 1.0) (0.554 g of a 22% (w/w) solution, 85.2 μmol of dendrimer based on the M_W of 1430 g/mol as determined by MALDI-TOF) was evaporated under reduced pressure. The resulting residue was dissolved in DMSO (3 mL) followed by the addition of **29** (487 mg, 1.02 mmol). After 8 hours, the reaction mixture was dialysed against DMSO (MW cutoff 1 kDa). The solution was lyophilized to give **30** as an oily solid. This product was used without further purification. ^1H NMR (500 MHz, CD_3SOCD_3) δ 7.98 (bs, 2H, amide NH's), 7.79 (bs, 1H, amide NH's), 7.52 (bs, 4H, $CH_2NHC(S)NHCH_2$), 5.07 (m, 6H), 4.88 (d 2H), 4.12 (dd, 2H), 3.90-4.05 (m, 4H), 3.79 (t, 2H), 3.71 (m, 2H), 3.25-3.63 (m, 18H), 3.13 (bs, 3H), 3.05 (bs, 2H), 2.64 (bs, 4H), 2.47 (s, 2H), 2.38 (bs, 2H), 2.20 (t, 4H), 2.07 (s, 6H), 1.98 (s, 12H), 1.90 (s, 6H) ppm; MALDI-TOF-MS (pos) 5280.

Generation 1.0 PAMAM-based thiourea 1-*O*-(5-thiourea-3-oxapentyl)-α-D-mannopyranoside dendrimer (**36**): A suspension of **30** in MeOH:H_2O (1:1, 20 mL) and 1 M methanolic NaOMe (140 μL) was stirred overnight until all of the solid had dissolved. The solution was neutralized with Amberlite IR-120 (acidic) and filtered. The methanol was evaporated under reduced pressure, and the resulting aqueous dendrimer solution was purified by dialysis against H_2O (MW cutoff 1 kDa). The solution was lyophilized to give 150 mg (33% for two steps. Percent yield based on the M_W of 3877 g/mol as determined by MALDI-TOF) of **36** as a fluffy, white solid. ^{1}H NMR (500 MHz, CD_3SOCD_3) δ 8.01 (bs, 2H, amide NH's), 7.85 (bs, 1H, amide NH's), 7.52 (bs, 4H, $CH_2NHC(S)NHCH_2$), 4.73 (bs, 4H), 4.63 (bs 2H), 4.60 (bs, 2H), 4.47 (bs, 2H), 3.20-3.80 (m, 40H), 3.00-3.18 (m, 8H), 2.00-2.80 (m, 18H) ppm; ^{13}C NMR (125 MHz, CD_3SOCD_3) δ 182.6, 171.7, 170.8, 100.4, 74.4, 71.4, 70.7, 69.8, 67.4, 67.0, 66.1, 61.7, 52.1, 49.5, 43.5, 43.2, 38.2, 36.9, 33.0, 20.7 ppm; MALDI-TOF-MS (pos) 3877.

Generation 2.0 PAMAM-based thiourea-linked 1-*O*-(5-thiourea-3-oxapentyl)-2,3,4,6-tetra-*O*-acetyl-α-D-mannopyranoside dendrimer (**31**): A methanolic solution of amine-terminated Starburst PAMAM dendrimer (generation 2.0) (0.506 g of a 20% (w/w) solution, 31.0 μmol of dendrimer based on the M_W of 3260 g/mol as determined by MALDI-TOF) was evaporated under reduced pressure. The resulting residue was dissolved in DMSO (3 mL) followed by the addition of **29** (296 mg, 0.621 mmol). After 8 hours, the reaction mixture

was dialysed against DMSO (MW cutoff 1 kDa). The solution was lyophilized to give **31** as an oily solid. This product was used without further purification. ^{1}H NMR (500 MHz, CD_3SOCD_3) δ 7.97 (bs, 4H, amide NH's), 7.76 (bs, 3H, amide NH's), 7.51 (bs, 8H, $CH_2NHC(S)NHCH_2$), 5.06 (m, 12H), 4.88 (d 4H), 4.12 (m, 4H), 3.90-4.05 (m, 8H), 3.79 (t, 4H), 3.71 (m, 4H), 3.25-3.63 (m, 36H), 3.00-3.13 (bs, 12H), 2.64 (bs, 12H), 2.38 (bs, 8H), 2.16 (bs, 12H), 2.07 (s, 12H), 1.98 (s, 24H), 1.90 (s, 12H) ppm; MALDI-TOF-MS (pos) 10,950.

Generation 2.0 PAMAM-based thiourea 1-*O*-(5-thiourea-3-oxapentyl)-α-D-mannopyranoside dendrimer (**37**): A suspension of **31** in MeOH:H_2O (1:1, 20 mL) and 1 M methanolic NaOMe (100 μL) was stirred overnight until all of the solid had dissolved. The solution was neutralized with Amberlite IR-120 (acidic) and filtered. The methanol was evaporated under reduced pressure, and the resulting aqueous dendrimer solution was purified by dialysis against H_2O (MW cutoff 1 kDa). The solution was lyophilized to give 174 mg (69% for two steps. Percent yield based on the M_W of 8250 as determined by MALDI-TOF) of **37** as a fluffy, white solid.^{1}H NMR (500 MHz, CD_3SOCD_3) δ 7.98 (bs, 2H, amide NH's), 7.78 (bs, 1H, amide NH's), 7.48 (bs, 4H, $CH_2NHC(S)NHCH_2$), 4.70 (bs, 4H), 4.50-4.62 (m 4H), 4.44 (bs, 2H), 3.20-3.80 (m, 36H), 3.00-3.18 (m, 8H), 2.00-2.80 (m, 16H) ppm; ^{13}C NMR (125 MHz, CD_3SOCD_3) δ 172.3, 100.4, 74.4, 71.4, 70.7, 69.8, 69.3, 67.4, 66.1, 61.7, 52.7, 50.0, 44.0, 33.6, 21.0 ppm; MALDI-TOF-MS (pos) 8250.

Generation 3.0 PAMAM-based thiourea-linked 1-*O*-(5-thiourea-3-oxapentyl)-2,3,4,6-tetra-*O*-acetyl-α-D-mannopyranoside dendrimer (**32**): A methanolic solution of amine-terminated Starburst PAMAM dendrimer (generation 3.0) (0.771 g of a 15% (w/w) solution, 16.7 μmol of dendrimer based on the M_W of 6910 g/mol as determined by MALDI-TOF) was evaporated under reduced pressure. The resulting residue was dissolved in DMSO (5 mL) followed by the addition of **29** (319 mg, 0.669 mmol). After 8 hours, the reaction mixture was dialysed against DMSO (MW cutoff 1 kDa). The solution was lyophilized to give **32** as an oily solid. This product was used without further purification. ^{1}H NMR (500 MHz, CD_3SOCD_3) δ 7.98 (bs, 1H, amide NH's), 7.75 (bs, 1H, amide NH's), 7.50 (bs, 2H, $CH_2NHC(S)NHCH_2$), 5.07 (m, 6H), 4.88 (d 2H), 4.12 (m, 2H), 3.90-4.05 (m, 4H), 3.79 (t, 2H), 3.71 (m, 2H), 3.25-3.63 (m, 20H), 2.95-3.18 (m, 6H), 2.64 (bs, 4H), 2.38 (bs, 4H), 2.16 (bs, 6H), 2.07 (s, 6H), 1.98 (s, 12H), 1.90 (s, 6H) ppm; MALDI-TOF-MS (pos) 21,000.

Generation 3.0 PAMAM-based thiourea 1-*O*-(5-thiourea-3-oxapentyl)-α-D-mannopyranoside dendrimer (**38**): A suspension of **32** in MeOH:H_2O (1:1, 20 mL) and 1 M methanolic NaOMe (106 μL) was stirred overnight until all of the solid had dissolved. The solution was neutralized with Amberlite IR-120 (acidic) and filtered. The methanol was evaporated under reduced pressure, and the resulting aqueous dendrimer solution was purified by dialysis against H_2O (MW cutoff 1 kDa). The solution was lyophilized to give 165 mg (62% for two steps. Percent

yield based on the M_W of 15,900 as determined by MALDI-TOF) of **38** as a fluffy, white solid.^{1}H NMR (500 MHz, CD_3SOCD_3) δ 7.97 (bs, 1H, amide NH's), 7.77 (bs, 1H, amide NH's), 7.47 (bs, 2H, $CH_2NHC(S)NHCH_2$), 4.71 (bs, 2H), 4.52-4.62 (m 2H), 4.45 (bs, 1H), 3.20-3.80 (m, 17H), 2.95-3.18 (m, 4H), 2.00-2.80 (m, 8H) ppm; ^{13}C NMR (125 MHz, CD_3SOCD_3) δ 172.3, 171.9, 100.4, 74.4, 71.4, 70.7, 69.8, 69.3, 67.4, 66.1, 61.7, 52.6, 50.0, 43.8, 38.6, 37.3, 33.6, 20.8 ppm; MALDI-TOF-MS (pos) 15,900.

Generation 4.0 PAMAM-based thiourea-linked 1-*O*-(5-thiourea-3-oxapentyl)-2,3,4,6-tetra-*O*-acetyl-α-D-mannopyranoside dendrimer (**33**): A methanolic solution of amine-terminated Starburst PAMAM dendrimer (generation 4.0) (1.146 g of a 10% (w/w) solution, 8.48 μmol of dendrimer based on the M_W of 13500 g/mol as determined by MALDI-TOF) was evaporated under reduced pressure. The resulting residue was dissolved in DMSO (5 mL) followed by the addition of **29** (283 mg, 0.594 mmol). After 8 hours, the reaction mixture was dialysed against DMSO (MW cutoff 1 kDa). The solution was lyophilized to give **33** as an oily solid. This product was used without further purification. ^{1}H NMR (500 MHz, CD_3SOCD_3) δ 7.96 (bs, 1H, amide NH's), 7.74 (bs, 1H, amide NH's), 7.48 (bs, 2H, $CH_2NHC(S)NHCH_2$), 5.06 (bs, 3H), 4.88 (s 1H), 4.12 (m, 1H), 3.90-4.05 (m, 2H), 3.70 (m, 1H), 3.25-3.63 (m, 9H), 2.95-3.20 (m, 4H), 2.62 (bs, 4H), 2.38 (bs, 2H), 2.16 (bs, 4H), 2.07 (s, 3H), 1.98 (s, 6H), 1.90 (s, 3H) ppm; MALDI-TOF-MS (pos) 39,300.

Generation 4.0 PAMAM-based thiourea 1-*O*-(5-thiourea-3-oxapentyl)-α-D-mannopyranoside dendrimer (**39**): A suspension of **33** in MeOH:H_2O (1:1, 20 mL) and 1 M methanolic NaOMe (108 μL) was stirred overnight until all of the solid had dissolved. The solution was neutralized with Amberlite IR-120 (acidic) and filtered. The methanol was evaporated under reduced pressure, and the resulting aqueous dendrimer solution was purified by dialysis against H_2O (MW cutoff 1 kDa). The solution was lyophilized to give 216 mg (83% for two steps. Percent yield based on the M_W of 30,600 as determined by MALDI-TOF) of **39** as a fluffy, white solid.^{1}H NMR (500 MHz, CD_3SOCD_3) δ 7.98 (bs, 1H, amide NH's), 7.79 (bs, 1H, amide NH's), 7.48 (bs, 2H, $CH_2NHC(S)NHCH_2$), 4.72 (bs, 2H), 4.60 (bs 2H), 4.46 (bs, 1H), 3.20-3.80 (m, 19H), 2.95-3.18 (m, 4H), 2.00-2.80 (m, 8H) ppm; ^{13}C NMR (125 MHz, CD_3SOCD_3) δ 172.2, 171.8, 100.4, 74.3, 71.4, 70.7, 69.8, 69.3, 67.4, 66.1, 61.7, 52.6, 50.0, 43.9, 38.7, 37.2, 33.4, 21.0 ppm; MALDI-TOF-MS (pos) 30,600.

Generation 5.0 PAMAM-based thiourea-linked 1-*O*-(5-thiourea-3-oxapentyl)-2,3,4,6-tetra-*O*-acetyl-α-D-mannopyranoside dendrimer (**34**): A methanolic solution of amine-terminated Starburst PAMAM dendrimer (generation 5.0) (0.495 g of a 21% (w/w) solution, 4.07 μmol of dendrimer based on the M_W of 25,500 g/mol as determined by MALDI-TOF) was evaporated under reduced pressure. The resulting residue was dissolved in DMSO (5 mL) followed by the addition of **29** (232 mg, 0.487 mmol). After 8 hours, the reaction mixture

was dialysed against DMSO (MW cutoff 1 kDa). The solution was lyophilized to give **34** as an oily solid. This product was used without further purification. ^{1}H NMR (500 MHz, CD_3SOCD_3) δ 7.97 (bs, 1H, amide NH's), 7.75 (bs, 1H, amide NH's), 7.50 (bs, 2H, $CH_2NHC(S)NHCH_2$), 5.06 (m, 3H), 4.88 (m 1H), 4.12 (m, 1H), 3.90-4.05 (m, 2H), 3.70 (m, 1H), 3.25-3.63 (m, 9H), 2.95-3.20 (m, 4H), 2.62 (bs, 3H), 2.38 (bs, 2H), 2.16 (bs, 3H), 2.07 (s, 3H), 1.98 (s, 6H), 1.90 (s, 3H) ppm; MALDI-TOF-MS (pos) 69,600.

Generation 5.0 PAMAM-based thiourea 1-*O*-(5-thiourea-3-oxapentyl)-α-D-mannopyranoside dendrimer (**40**): A suspension of **34** in MeOH:H_2O (1:1, 20 mL) and 1 M methanolic NaOMe (92 μL) was stirred overnight until all of the solid had dissolved. The solution was neutralized with Amberlite IR-120 (acidic) and filtered. The methanol was evaporated under reduced pressure, and the resulting aqueous dendrimer solution was purified by dialysis against H_2O (MW cutoff 1 kDa). The solution was lyophilized to give 159 mg (72% for two steps. Percent yield based on the M_W of 55,000 as determined by MALDI-TOF) of **40** as a fluffy, off-white solid. ^{1}H NMR (500 MHz, CD_3SOCD_3) δ 7.98 (bs, 1H, amide NH's), 7.78 (bs, 1H, amide NH's), 7.48 (bs, 2H, $CH_2NHC(S)NHCH_2$), 4.73 (bs, 2H), 4.60 (bs 2H), 4.70 (bs, 1H), 3.20-3.80 (m, 21H), 2.95-3.18 (m, 4H), 2.64 (bs, 4H), 2.18 (bs, 4H) ppm; ^{13}C NMR (125 MHz, CD_3SOCD_3) δ 172.4, 171.9, 100.4, 74.3, 71.3, 70.7, 69.8, 69.3, 67.4, 66.2, 61.7, 52.6, 49.9, 43.9, 38.7, 37.3, 33.5, 20.7 ppm; MALDI-TOF-MS (pos) 55,000.

Generation 6.0 PAMAM-based thiourea-linked 1-*O*-(5-thiourea-3-oxapentyl)-2,3,4,6-tetra-*O*-acetyl-α-D-mannopyranoside dendrimer (**35**): A methanolic solution of amine-terminated Starburst PAMAM dendrimer (generation 6.0) (0.88 g of a 11% (w/w) solution, 1.9 μmol of dendrimer based on the M_W of 51,000 g/mol as determined by MALDI-TOF) was evaporated under reduced pressure. The resulting residue was dissolved in DMSO (5 mL) followed by the addition of **29** (212 mg, 0.45 mmol). After 8 hours, the reaction mixture was dialysed against DMSO (MW cutoff 1 kDa). The solution was lyophilized to give **35** as an oily solid. This product was used without further purification. ^{1}H NMR (500 MHz, CD_3SOCD_3) δ 7.97 (bs, 1H, amide NH's), 7.75 (bs, 1H, amide NH's), 7.50 (bs, 2H, $CH_2NHC(S)NHCH_2$), 5.07 (m, 3H), 4.88 (m 1H), 4.12 (m, 1H), 3.90-4.05 (m, 2H), 3.71 (m, 1H), 3.25-3.63 (m, 9H), 2.95-3.20 (m, 3H), 2.62 (bs, 2H), 2.38 (bs, 2H), 2.16 (bs, 2H), 2.07 (s, 3H), 1.98 (s, 6H), 1.90 (s, 3H) ppm; MALDI-TOF-MS (pos) 133500.

Generation 6.0 PAMAM-based thiourea 1-*O*-(5-thiourea-3-oxapentyl)-α-D-mannopyranoside dendrimer (**41**): A suspension of **35** in MeOH:H_2O (1:1, 20 mL) and 1 M methanolic NaOMe (180 μL) was stirred overnight until all of the solid had dissolved. The solution was neutralized with Amberlite IR-120 (acidic) and filtered. The methanol was evaporated under reduced pressure, and the resulting aqueous dendrimer solution was purified by dialysis against H_2O (MW cutoff 1 kDa). The solution was lyophilized to give 138 mg (70% for two steps. Percent

yield based on the M_W of 103,800 as determined by MALDI-TOF) of **41** as a fluffy, off-white solid.^{1}H NMR (500 MHz, CD_3SOCD_3) δ 7.99 (bs, 1H, amide NH's), 7.77 (bs, 1H, amide NH's), 7.50 (bs, 2H, $CH_2NHC(S)NHCH_2$), 4.74 (bs, 2H), 4.61 (bs 2H), 4.48 (bs, 1H), 3.20-3.80 (m, 19H), 2.95-3.20 (m, 4H), 2.62 (bs, 4H), 2.17 (bs, 4H) ppm; ^{13}C NMR (125 MHz, CD_3SOCD_3) δ 182.8, 172.1, 171.4, 100.0, 73.9, 70.9, 70.3, 70.2, 69.4, 68.9, 67.0, 65.7, 61.3, 52.2, 49.5, 43.4, 38.2, 36.8, 33.1, 21.1 ppm; MALDI-TOF-MS (pos) 103,800.

General hemagglutination assay procedure

Concanavalin A preparation: In a 10 mL centrifuge tube, approximately 5 mg of concanavalin A (Con A) was dissolved without agitation in 10 mL of HEPES buffer with 100 μM $CaCl_2$ (pH = 8.5). The tube was stored at 4 °C for 8 hours to allow the Con A to dissolve. Afterwards, the solution was placed in a dialysis tube and dialyzed against 1 L of tris-buffered saline (TBS) for 4 hours. This was repeated with fresh TBS solution, followed by dialysis against 1 L of phosphate-buffered saline (PBS) for 8 hours. The dialysis was done to remove any excess Ca^{2+} from the lectin solution. The Con A solution was removed from the tube and stored at 4 °C until needed (the Con A solution can be stored at temperatures below 0 °C for longer periods of time).

Blood Preparation: Fresh whole rabbit blood was obtained from the MSU animal care center. It was drawn into a tube containing EDTA. Alsever's solution was added to the blood to make a 60% v/v solution of blood in Alsever's solution.

The blood solution was separated into 2 mL aliquots in 15 mL centrifuge tubes. Care was taken to avoid hemolysis of the red blood cells. The red blood cells were diluted to 12 mL with Alsever's solution. The cells were pelleted by centrifugation (1100 rpm x 10 min.). The layer of white blood cells and plasma proteins was removed by pipet. This process was repeated 2 more times using PBS instead of Alsever's solution. Finally, the volume of the red blood cells was estimated (usually about 0.3 mL) and a 2% v/v suspension was made using the assay buffer (0.5% w/v BSA in PBS).

Con A titration: Decreasing amounts of Con A were incubated with red blood cells to determine the lectin concentration required to agglutinate the cells. Serial two-fold dilutions were made in the wells of a 96-well V-bottomed microtiter plate. The two-fold dilutions were made by adding 50 μL of Con A solution in the first well. In all of the other wells (typically, a total of 24 wells is used), 50 μL of assay buffer was added. In the second well, 50 μL of the Con A solution was mixed with the assay buffer. After mixing, 50 μL of this solution was added to the third well. After mixing, 50 μL of the solution in the third well was added to the fourth well etc. . . This was repeated until the Con A was diluted through all of the wells of interest. In the end, there should be 50 μL of solution in each well. To each of the wells, 50 μL of the red blood cell suspension was added (the suspension was frequently agitated gently to ensure consistent mixing of the red blood cells). Once the blood has been added, the wells were incubated for 1.5

hours at 22 °C (ideally 1 h @ 25 °C). After this time, the wells were examined. The minimum concentration required to fully agglutinate the 2% cell suspension was determined. This was considered 1 Unit.

The wells in which hemagglutination occurred were differentiated from those in which hemagglutination did not occur. When hemagglutination did NOT occur, the red blood cells settled to the bottom to form a red "button." This was best demonstrated with a control that does not contain Con A. When hemagglutination occurred, the solution in the well stayed as a cloudy suspension. Often, there was an intermediate well that was borderline.

For the assay with inhibitor, 8 times the minimum concentration (8 Units) was used. To determine this concentration, the corresponding well was found, and based on the serial two-fold dilution, the necessary dilution of the stock Con A was calculated. About 15 mL of the 8 Unit concentration Con A was made.

The concentration of this Con A solution was determined spectrophotometrically at 280 nm using $A^{1\%,\,1\,cm} = 13.7$ @ pH = 7.2 and expressed in terms of the monomer (26,500). Example: for A = 0.616, then 0.616 x 10 mg/mL ÷ 13.7 = 0.45 mg/mL. Since, the FW = 26,500, then 0.45 mg/mL ÷ 26,500 mg/mmol = 0.000017 M or 17 μM.

Inhibiting dose determination: Starting with a concentration of about 10 mg/mL, serial two-fold dilutions of various inhibitors were made in the same fashion as the two-fold dilutions of the Con A described above. The inhibitor

solutions (50 μL) were incubated with the 8 Unit Con A solution (50 μL for 3 hours at 22 °C (ideally 2 h @ 25°C). After which, 50 μL of the red blood cell suspension was added. The wells were mixed and incubated for 1 h at 22 °C. The minimum concentration causing inhibition of the Con A was determined from the inspection of the wells. This is the inhibiting dose.

Buffers:

Alsever's solution, pH 6.0 (quantities for 1L), contained NaCl (4.2 g), sodium citrate (8.0 g, 2.72 mmol), and glucose (20.5 g).

Phosphate buffered saline (PBS), pH 7.2 (quantities for 4L), consisted of 0.15 M NaCl (35 g), 0.007 M NaH_2PO_4 (3.86 g of dihydrate), 0.018 M Na_2HPO_4 (10.22 g of anhydrous or 19.3 g of heptahydrate).

HEPES buffer, pH 8.5 (quantities for 1L), consisted of 100 μM $CaCl_2$ (14.7 mg) and 10 mM HEPES (2.38 g HEPES, N-[2-hydroxyethyl]piperazine-N-[2-ethanesulfonic acid]). The pH was adjusted to 8.5 using NaOH.

Tris buffered saline (TBS), pH 7.4 (quantities for 4L), consisted of 0.15 M NaCl (35 g), 0.042 M Trizma HCl (26.44 g), 0.008 M Trizma base (3.88 g). The pH was adjusted to 7.4 using HCl if necessary.

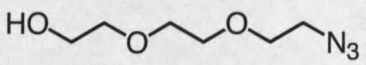
Turbidity Assays

Concanavalin A was prepared as for the hemagglutination assays. Following the method of Okada,[144, 182] turbidity was estimated by UV/vis spectrophotometry. Solutions of **36**, **38**, **39** and methyl mannose were added to

the Con A solutions. Absorbance values at 500 nm were read after 0.5, 1, and 2 h and at regular intervals afterwards for 24 h. For Con A concentrations of 18 μg/mL (concentration at which hemagglutination assays were performed), absorbances were read for the serial dilutions of **36**, **38, 39** and methyl mannose that were used in the hemagglutination assays. Absorbances were always ~0.01, indicating that precipitation of the Con A-dendrimer complex is not occurring under the conditions at which the hemagglutination assays are performed. For Con A concentrations of 0.2 mg/mL, absorbances were ~0.03 for methyl mannose and ~0.4-0.5 for **36**, **38** and **39** (0.25 mg/mL). Precipitate remained clearly visible for 24 h. Upon addition of methyl mannose after 24 h the precipitate dissolved and the absorbance reduced back to ~0.03.

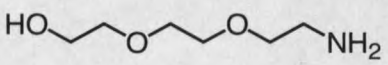
Additional synthetic procedures (unoptimized)

The following experimental procedures are typically unoptimized and the products are typically not fully characterized. This is because, while the molecules described below are important to this project, their development was abandoned when the development of **12** was abandoned.

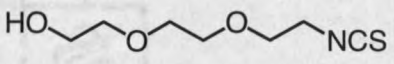


2-[2-(2-Azidoethoxy)ethoxy]ethanol (**18**).[159] A mixture of 2-[2-(2-chloroethoxy)ethoxy]ethanol (10.2 g, 60 mmol) and sodium azide (7.86 g, 120 mmol) was heated to 85 °C in DMF (60 mL) overnight. The DMF was *removed in*

vacuo. The oily residue was extracted with CH_2Cl_2 (100 mL) and filtered. The CH_2Cl_2 was removed *in vacuo* to leave 10.2 g (96%) of **18** as a yellow oil. The product was used with no further purification. ^{1}H NMR (300 MHz, $CDCl_3$) δ 3.64-3.74 (m, 8H), 3.59 (t, 2H, J = 4.1 Hz), 3.37 (t, 2H, J = 4.9 Hz), 2.29 (t, 1H, J = 6.2 Hz) ppm.

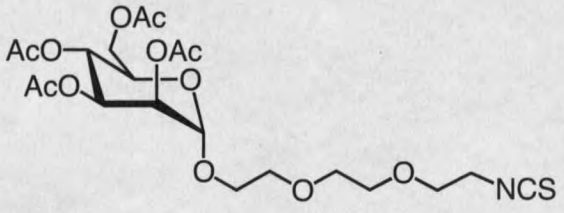


2-[2-(2-Aminoethoxy)ethoxy]ethanol (**20**).[159] At r.t., **18** (10.2 g, 58 mmol), PPh_3 (17.5 g, 66 mmol) and water (1.6 g, 1.6 mL, 90 mmol) in THF (100 mL) were stirred for 4 h. The solvent was removed *in vacuo*. A majority of the PPh_3 was removed by using a plug of silica gel ($CHCl_3$:MeOH:Et_3N 3:3:1). The product was purified by Kugelrohr distillation (b.p. 100 °C at 0.1 torr) to give 8.4 g (96%) of **20** as a clear oil.[183] ^{1}H NMR (500 MHz, $CDCl_3$) δ 3.62 (t, 2H, J = 4.5 Hz, HOCH_2), 3.54- 3.59 (m, 4H, $CH_2OCH_2CH_2OCH_2$), 3.51 (t, 2H, J = 4.5, $HOCH_2CH_2O$), 3.45 (t, 2H, J = 5.1 Hz, $OCH_2CH_2NH_2$), 2.78 (t, 2H, J = 5.1 Hz, CH_2NH_2), 2.23 (s, 3H, NH_2, OH) ppm; ^{13}C NMR (125 MHz, $CDCl_3$) δ 72.9, 72.7, 70.3, 70.2, 61.3, 41.4 ppm.



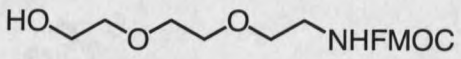
2-[2-(2-Isothiocyanatoethoxy)ethoxy]ethanol (**15**). A solution of **20** (3.58 g, 24 mmol) and triethylamine (5.33 g, 7.4 mL, 53 mmol) in CH_3Cl (50 mL) was added via syringe over the course of an hour to a stirred solution of thiophosgene

(3.04 g, 2.0 mL, 27 mmol) in CH_3Cl (150 mL). The solvent was removed *in vacuo*. The residue was dissolved in water (50 mL) and extracted with CH_2Cl_2 (2 x 50 mL). The organic layers were combined and washed with water (2 x 50 mL), dried over $MgSO_4$, and removed *in vacuo*. Column chromatography on silica gel (1:1 ethyl acetate:hexanes) yielded 2.66 g (58%) of **15** as a yellowish oil. ^{1}H NMR (300 MHz, $CDCl_3$) δ 3.74 (t, 2H, J = 4.5 Hz, $HOCH_2$), 3.64-3.70 (m, 8H), 3.60 (t, 2H, J = 4.5 Hz, CH_2NCS), 2.07 (s, 1H, OH) ppm; ^{13}C NMR (125 MHz, $CDCl_3$) δ 132.2, 72.6, 70.5, 70.3, 69.2, 61.5, 45.2 ppm.

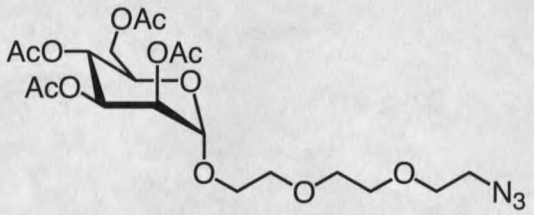


1-*O*-(8-isothiocyanato-3,6-dioxaoctyl)-2,3,4,6-tetra -*O*-acetyl-α–D-mannopyranoside (**24**). The trichloroacetimidate **13** (5.75 g, 11.7 mmol) was dissolved in CH_2Cl_2 (150 mL) with **15** (2.24 g, 11.7 mmol) and 4 Å molecular sieves (0.3 g). Under an N_2 atmosphere, $BF_3{\cdot}Et_2O$ (1.66 g, 1.5 mL, 11.7 mmol) was added slowly. The reaction was stirred at room temperature for 7 h. After which, the mixture was filtered over Celite, concentrated *in vacuo*, and purified by silica gel chromatography (1:1 hexanes:ethyl acetate) to yield **24** (3.72 g, 60%) as a yellow oil. ^{1}H NMR (500 MHz, $CDCl_3$) δ 5.25 (ap. dd, 1H, J = 10.0, 3.4, H-1), 5.19 (m, 2H), 4.79 (s, 1H), 4.19 (ap. dd, 1H, J = 12.1, 4.9),4.00 (m, 2H), 3.74 (m, 1H), 3.61 (m, 11H), 2.07 (s, 3H), 2.01 (s, 3H), 1.96 (s, 3H), 1.90 (s, 3H) ppm; ^{13}C

NMR (125 MHz, $CDCl_3$) δ 107.6, 169.9, 169.8, 169.6, 132.4, 97.6, 70.8, 70.7, 70.0, 69.5, 69.3, 69.0, 68.4, 67.3, 66.1, 62.4, 45.3, 20.8, 20.7, 20.6, 20.6 ppm.

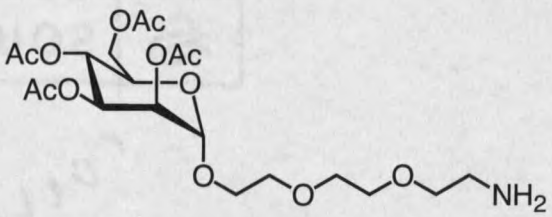


{2-[2-(2-Hydroxy-ethoxy)-ethoxy]ethyl}-carbamic acid 9*H*-fluoren-9-ylmethyl ester (**21**). A solution of **20** (1.0 g, 6.7 mmol) in 30 mL of a 1:1 dioxane: 10% K_2CO_3 solution was stirred while a solution of FMOC-Cl (1.72 g, 6.7 mmol) in 10 mL of dioxane was added dropwise. After the addition, the reaction was stirred for 4 hours, during which a white precipitate formed. The product was extracted with ether (3 x 20 mL). The organic layers were combined and washed with water (3 x 30 mL), dried over $MgSO_4$, and removed *in vacuo* to leave a clear oil. The product was purified on silica gel using ethyl acetate to give 2.17 g (87%) of **21** as a clear oil. ^{1}H NMR (300 MHz, $CDCl_3$) δ 7.74 (d, 2H, J = 7.5 Hz), 7.59 (d, 2H, J = 7.4 Hz), 7.38 (t, 2H, J = 7.2), 7.29 (td, 2H, J = 7.4, 1.2 Hz), 5.42 (bs, 1H, NH), 4.41 (d, 2H, J = 6.8 Hz), 4.21 (t, 1H, J = 6.6 Hz), 3.5—3.8 (m, 10H), 3.38 (bs, 2H), 2.33 (bs, 1H, OH).



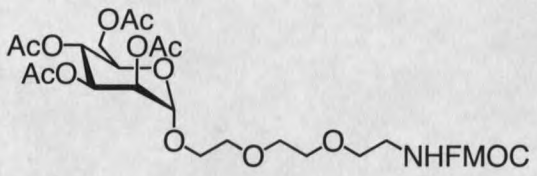
1-*O*-(8-azido-3,6-dioxaoctyl)-2,3,4,6-tetra-*O*-acetyl-α-D-mannopyranoside (**22**). Freshly distilled BF_3•Et_2O (2.24 g, 2.0 mL 15 mmol) was added slowly to a stirring solution of **13** (9.7 g, 19.7 mmol) and **18** (10.4 g, 59 mmol) in CH_2Cl_2 (100

mL) containing crushed 4Å molecular sieves (1.2 g). The reaction was followed by TLC using 1:1 EtOAc:petroleum ether. The reaction was stirred under Ar for 12 hours. After which, about 2 g of solid $NaHCO_3$ was added slowly to the mixture. The mixture was filtered over celite and the solvents were removed *in vacuo*. The oily product was purified by column chromatography on SiO_2 using 1:1 EtOAc:petroleum ether as eluent to give 6.68 g (65%) of **22** as a very thick oil. ^1H NMR (300 MHz, $CDCl_3$) δ 5.15—5.40 (m, 3H), 4.83 (d, 1H, J = 1.5 Hz) 4.25 (ap. dd, 1H, J = 12.4, 5.2 Hz), 4.08 (d, 1H, J = 2.3), 3.95—4.05 (m, 1H), 3.7—3.8 (m, 2H), 3.60—3.68 (m, 8H), 3.36 (t, 2H, J = 5.2 Hz), 2.11 (s, 3H), 2.06 (s, 3H), 2.00 (s, 3H), 1.95 (s, 3H).



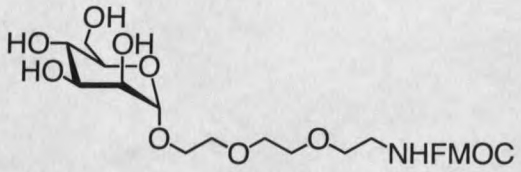
1-*O*-(8-amino-3,6-dioxaoctyl)-2,3,4,6-tetra-*O*-acetyl-α-D-mannopyranoside (**23**). A solution of **22** (1.2 g, 2.3 mmol), Ph_3P (0.66 g, 2.5 mmol), and water (62 mg, .06 mL, 3.4 mmol) in THF (10 mL) were stirred overnight. The solvents were removed *in vacuo* and the product purified by column chromatography on SiO_2 using 8:2 $CHCl_3$:MeOH as eluent. An analytical sample was purified by column chromatography on SiO_2 using the same eluent containing 5% Et_3N. ^1H NMR (300 MHz, $CDCl_3$) δ 5.10—5.25 (m, 3H), 4.79 (s, 1H), 4.17 (ap. dd, 1H, J = 12.2,

4.9 Hz), 3.90—4.05 (m, 2H), 3.71 (bt, 2H), 3.58 (s, 10H), 3.12 (bt, 2H), 2.05 (s, 3H), 1.99 (s, 3H), 1.95 (s, 3H), 1.89 (s, 3H).



(2-{2-[2-*O*-(2,3,4,6-tetra-*O*-acetyl-α-D-mannopyranosyl)-ethoxy]-ethoxy}ethyl)-carbamic acid 9*H*-fluoren-9-ylmethyl ester (**25**). Freshly distilled $BF_3 \cdot Et_2O$ (3.97 g, 3.6 mL 28.0 mmol) was added slowly to a stirring solution of **13** (14.0 g, 28.0 mmol) and **21** (10.6 g, 28.0 mmol) in CH_2Cl_2 (100 mL) containing crushed 4Å molecular sieves (1.4 g). The reaction was followed by TLC using 1:1 EtOAc-hexanes. The reaction was stirred under Ar for 4 hours. After which, about 2 g of solid $NaHCO_3$ was added slowly to the mixture. The mixture was filtered over celite and the solvents were removed *in vacuo*. The product was purified by column chromatography on SiO_2 using 1:1 EtOAc-petroleum ether as eluent to give 11.5 g (59%) of **25** as a fluffy white solid. ^1H NMR (300 MHz, $CDCl_3$) δ 7.70 (d, 2H, J = 7.4 Hz), 7.55 (d, 2H, J = 7.3 Hz), 7.34 (t, 2H, J = 7.3 Hz), 7.25 (t, 2H, J = 7.3 Hz), 5.42 (bt, 1H), 5.20—5.35 (m, 3H), 4.82 (s, 1H), 4.35 (d, 2H, J = 6.8 Hz), 4.10—4.30 (m, 2H), 3.95—4.10 (m, 2H), 3.70—3.80 (m, 1H), 3.45—3.65 (m, 9H), 3.30—3.40 (m, 2H), 2.10 (s, 3H), 2.04 (s, 3H), 1.98 (s, 3H), 1.94 (s, 3H). ^{13}C NMR (75 MHz, $CDCl_3$) δ 170.5, 169.8, 169,7, 169.5, 156.3, 143.9, 141.1, 127.5, 126.8, 124.9, 119.8, 97.5, 70.5, 70.2, 69.9, 69.8, 69.4, 68.9, 68.3, 67.2, 66.4,

66.0, 62.3, 47.1, 40.8, 20.7, 20.6, 20.5 ppm; HRMS (MALDI-TOF) *m/z* 724.2585 (M + Na, calcd 724.2581 for $C_{35}H_{43}NO_{14}$).



(2-{2-[2-*O*-(α-D-mannopyranosyl)-ethoxy]-ethoxy}ethyl)-carbamic acid 9*H*-fluoren-9-ylmethyl ester (**25b**). A solution of **25** (3.14g, 4.48 mmol) in methanol was stirred while 0.7 M NaOMe (0.6 mL, 0.5 mmol) was added. The reaction was stirred for 1 h, after which acidic Amberlite IR-120(plus) ion-exchange resin was added until the reaction was neutral. The mixture was filtered and concentrated to give a crude oil. The oil was absorbed onto a plug of silica gel and most impurities were washed away using warm EtOAc. The product was extracted from the silica gel using 1:2:1 EtOAc-IPA-H_2O. A final purification was done using column chromatography on silica gel and 10:3:1 EtOAc:IPA:H_2O to give 1.3 g (55%) of **25b**. ^{1}H NMR (500 MHz, $CDCl_3$) δ 7.71 (d, 2H, J = 7.5 Hz), 7.56 (d, 2H, J = 7.5 Hz), 7.35 (t, 2H, J = 7.4 Hz), 7.26 (dd, 2H, J = 13, 7.4 Hz), 4.81 (s, 1H), 4.66 (bs, 4H) 4.35 (d, 2H, J = 6.6 Hz), 4.17 (t, 1H, J = 6.6 Hz), 3.92 (bs, 3H), 3.83 (bs, 1H), 3.71 (bt, 2H), 3.51 (bs, 10H), 3.32 (bs, 2H); ^{13}C NMR (75 MHz, $CDCl_3$) δ 156.6, 143.9, 141.2, 127.6, 127.0, 125.0, 119.9, 100.0, 72.3, 71.5, 70.8, 70.4, 70.1, 70.0, 66.5, 66.4, 61.0, 47.1, 40.8 ppm; HRMS (MALDI-TOF) *m/z* 556.2173 (M + Na, calcd 556.2159 for $C_{27}H_{35}NO_{10}$).

CHAPTER 4

HETEROGENEOUS PAMAM FUNCTIONALIZATION

Introduction

While the full functionalization of a dendrimer or of any other scaffold provides valuable information about the mechanism of multivalent binding, varying the number of sugars or binding epitopes in general on the surface could provide even more information. A number of systems have been reported that vary the density of binding epitopes presented by the ligand.[14, 16, 32, 64, 66, 71, 72, 184-189] In general, the best activity of the partially functionalized ligands does not come from the most functionalized case. It is very often that a less functionalized ligand exhibits the greatest activity.

A couple of examples that illustrate this phenomenon are shown in Figure 4.1. In 1999, Houseman and Mrksich used a self-assembled monolayer of alkanethiolates on gold to demonstrate that the enzymatic activity of bovine β-1,4-galactosyltransferase (GalTase) depended on the density of N-acetylglucosamine (GlcNAc) on the gold surface (Figure 4.1a).[185] The highest enzymatic activity was achieved when 0.7 mole percent of GlcNAc was placed on the surface. At higher densities of GlcNAc, the activity dropped off rapidly.

Kiessling and co-workers demonstrated in 1997 that the interaction of mannose-functionalized polymers synthesized by ROMP with Con A depended on the number of sugars present (Figure 4.1b).[72] They found that when the repeating unit contained only one mannose residue, the polymer was eight times more active than the polymer that contained two mannose residues per repeating unit (see Figure 1.8).

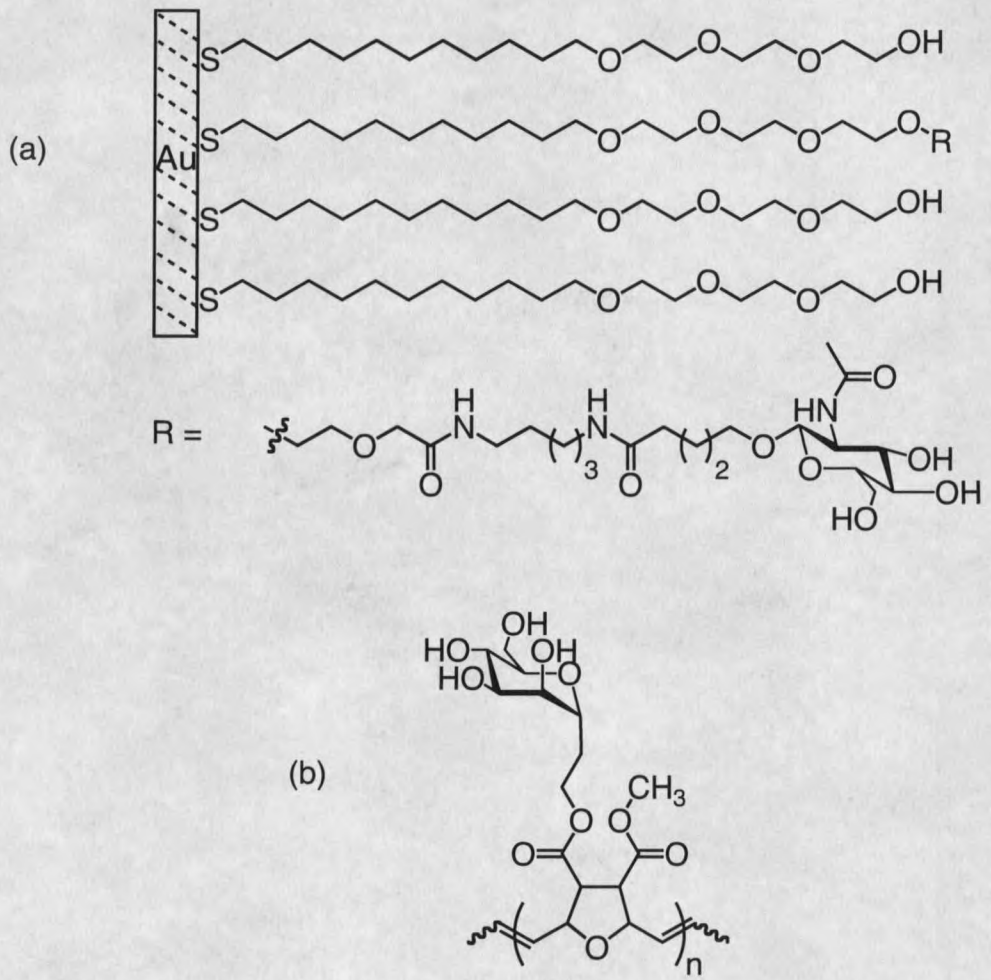


Figure 4.1 Systems that demonstrate the effect of epitope density; (a) self-assembled monolayer presenting varying amounts of N-acetylglucosamine; (b) ROMP synthesized glycopolymer that contains 50% mannose units.

In both cases, the rationale for the decrease in activity as the number of epitopes increased is due to steric crowding. This and the results of other similar investigations suggest that the best multivalent ligand would be one in which the scaffold is only partially functionalized. However, the optimal epitope density cannot be predicted and must be determined experimentally.

Heterogeneous Dendrimer Functionalization

In order to systematically study the effect of changing epitope density on the surface of the dendrimer as well the size of the dendrimer, the next phase of this project dealt with synthesizing a series of heterogeneously mannose-functionalized PAMAM dendrimers. By the controlled heterogeneous functionalization of dendrimers, it should be possible to vary the number of sugars on the surface of the dendrimer, thus controlling the epitope density on the surface. Controlling the epitope density has the advantage of changing the number of sugars present without drastically changing the size of the dendrimer. On the other hand, by using different generations of PAMAM dendrimers, we will be able to control the size of the molecule.

The heterogeneous functionalization of dendrimers is not new. Recently, brilliant researchers in our lab published a review on heterogeneous dendrimer functionalization.[190] A few points are briefly given here to put this work in context with the field.

Just as there are two main ways to synthesize dendrimers (convergently and divergently, see Figure 1.10 and Figure 1.11), there are also two main ways to heterogeneously functionalize dendrimers. Both are closely related to the divergent and convergent methods of dendrimer synthesis. The first is to include the various epitopes into the dendrons that are being pieced together (Figure 4.2). This method is labor intensive, but it provides control over where the epitopes are on the dendrimer.

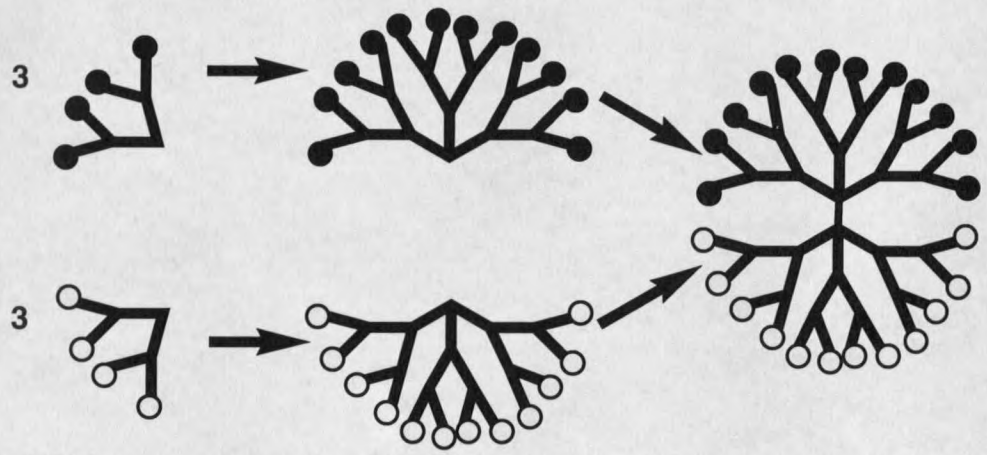


Figure 4.2 Heterogeneous dendrimer functionalization by including the various epitopes with each dendron.

A more straightforward method is the functionalization of an existing dendrimer. By stoichiometric control, the degree of functionalization can be controlled. While this method is a more direct route to heterogeneously functionalized dendrimers, there is no control over the location of the epitopes. Ideally the addition is random, but this may not always be the case.

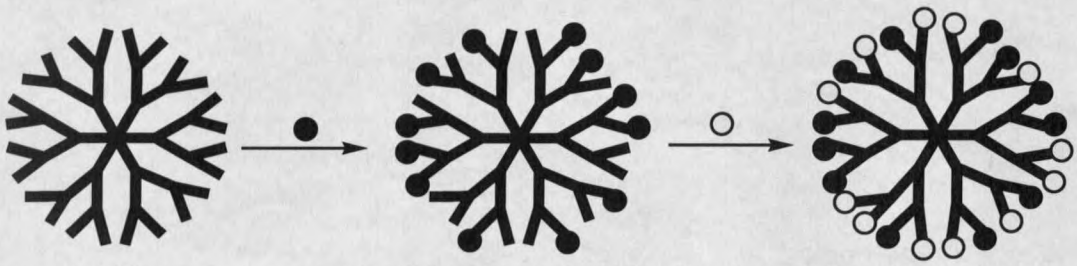
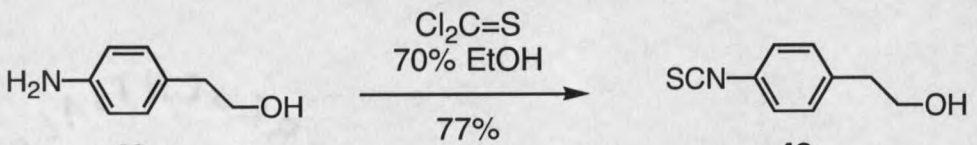


Figure 4.3 Heterogeneous dendrimer functionalization by adding the epitopes directly to an existing dendrimer.

Initial Attempt to Heterogeneously Functionalize a PAMAM Dendrimer

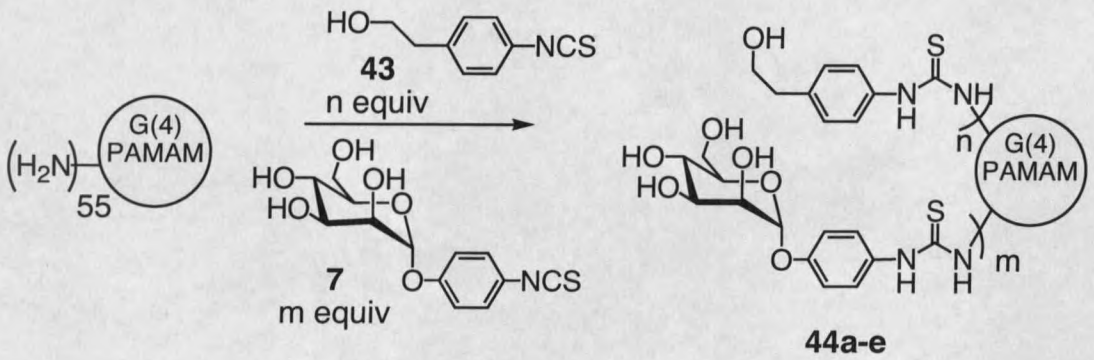
Before the successful synthesis of water-soluble mannose-functionalized PAMAM dendrimer had been achieved (as described in Chapter 3), heterogeneous functionalization was done using **7** and **43**. The synthesis of **43**[191] is shown in Scheme 4.1. The reaction of the amino alcohol **42** with thiophosgene in 70% aqueous ethanol produced **43** in 77% yield.



42 **43**

Scheme 4.1 Synthesis of **43** to be used as a spacer in heterogeneous dendrimer functionalization.

The phenyl isothiocyanate **43** was chosen as the second surface residue because of its obvious similarity to the aglycon portion of **7**. The similarity was expected to make the reactivity of the two similar. In addition, the ethyl alcohol portion is relatively similar in length compared to the mannose portion of **7**.



44a-e

Scheme 4.2 Initial effort for heterogeneous functionalization of G(4)-PAMAM using **7** and **43**.

The general reaction for the heterogeneous functionalization of a G(4)-PAMAM dendrimer is shown in Scheme 4.2. Solutions in DMSO of the alcohol **43** and carbohydrate **7** were made and aliquots of varying stoichiometry were added to a stirred DMSO solution of the G(4)-PAMAM dendrimer. The product was purified by dialysis against 2:1 DMSO:water.

Characterization of Heterogeneously Functionalized Generation 4.0 PAMAM-Based Thiourea-Linked Phenyl Ethanol and Phenyl-α-D-mannopyranoside Dendrimers

Data for the heterogeneously functionalized PAMAM dendrimers shown in Scheme 4.2 is shown in Table 4.1. The theoretical ratio of **7**:**43** was determined by the stoichiometry of reagents. As can be seen, the actual values as determined by ^{1}H NMR (vide infra) are very close to the desired ratios, indicating that it should be possible to control the number of carbohydrates on the surface by simply control of the stoichiometry of reagents.

Table 4.1 Data for heterogeneously functionalized PAMAM dendrimers shown in Scheme 4.2.

Compound	**7**:**43** Theory	**7**:**43** Actual by NMR	M_W from MALDI-TOF	Theoretical M_W[a]
44a	2:1	2:1	25800	28300
44b	1:1	1.2:1	25400	27280
44c	1:2	1:2.3	22400	25760
44d	1:5	1:4.5	21900	24550
44e	1:7	1:7.2	21500	24283

[a] Theoretical M_W values based on theoretical ratio of **7**:**43** shown in column two.

The ^{1}H NMR (500 MHz) spectrum of **44c** is shown in Figure 4.4. As expected, there are a number of similarities and differences between this spectrum and the spectrum for **8** (fully phenyl mannose-functionalized) seen in Figure 2.1. First, both have broad singlets for the amide protons on the interior of the dendrimers at around δ 7.8 and δ 7.6. The peak at δ 8.0 corresponds to the thiourea NH signal (ArNHCSN*H*R). This proton is far enough removed from the aromatic ring that the difference between the chemical shifts arising from **43** and **7** should be small and both signals should and do appear together. The difference in peaks for the thiourea NH signals (ArN*H*CSNHR) adjacent to the aromatic ring is evident from the peaks at δ 9.5 and δ 9.4. The peak at δ 9.5 corresponds to the thiourea NH peak from the addition of **43**, while the peak at δ 9.4 corresponds to the thiourea NH peak from the addition of **7**. Because the thiourea NH peaks are broad and overlapping, using integration values to determine the ratio of **7**:**43** is not possible with the thiourea NH peaks.

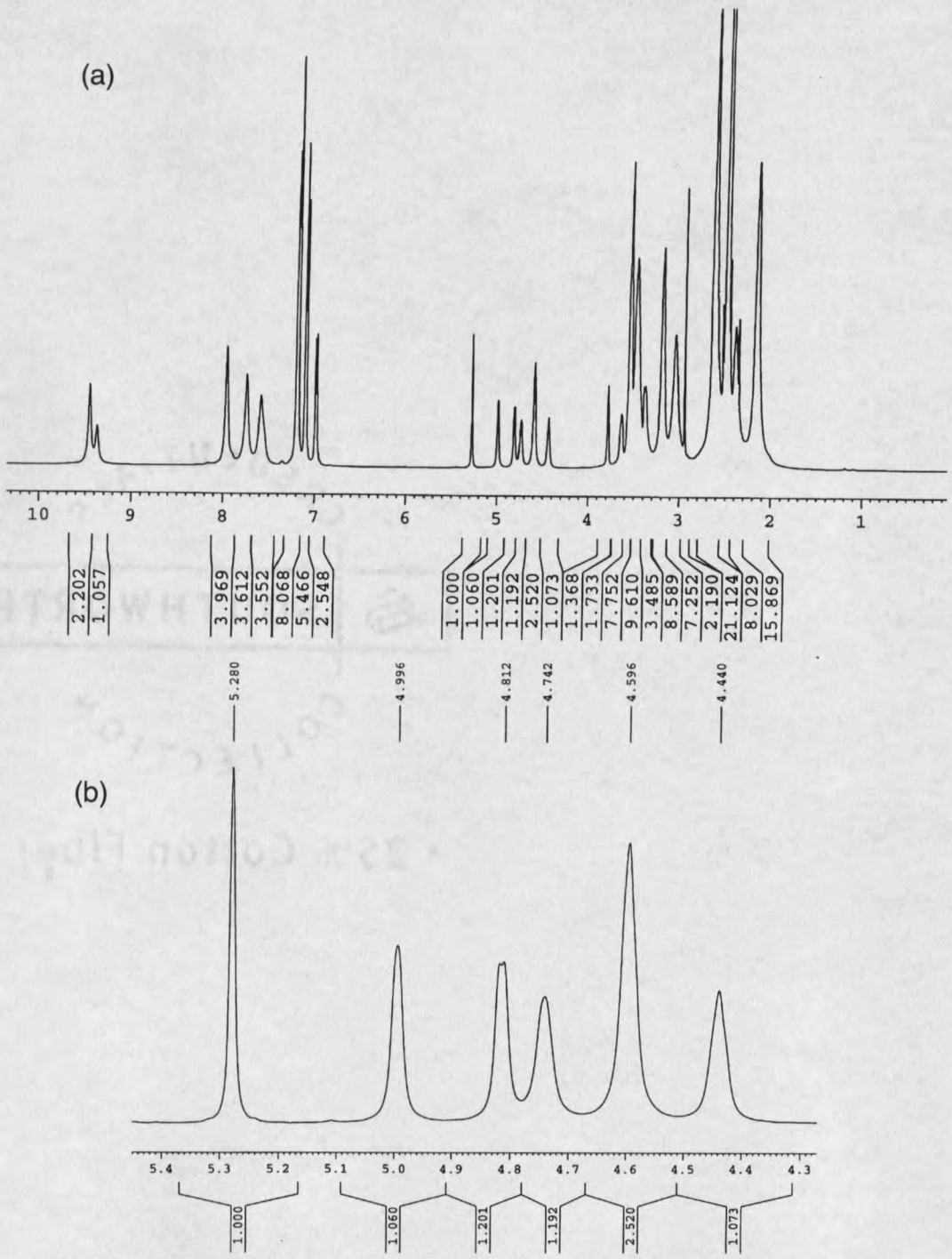


Figure 4.4 ^{1}H NMR spectrum of **44c**, (a) the full spectrum, (b) the region from which the ratios of **7**:**43** are derived.

In the aromatic region of the spectrum, the peaks of **7** changed in the same way as seen before in the formation of **8**. Both aromatic peaks shifted upfield by about 0.2 ppm. In contrast, only one of the aromatic peaks from **43** changed from δ 7.2. One peak shifted upfield by 0.1 ppm. The result is that half of the aromatic signals for **43** and **7** overlap at δ 7.2, which corresponds to the protons in the *meta* position relative to the thiourea group. The other aromatic peak from addition of **43** is at δ 7.1 and the peak from addition of **7** is at δ 7.0. Since there is enough separation between the peaks at δ 7.1 and δ 7.0, the integration can be used to get a ratio of **7**:**43**. In the case of **44c**, the ratio is 1:2.2.

Another very diagnostic region of the ^{1}H NMR spectrum is shown in Figure 4.4b. This region from δ 4.3—5.4 contains the signals from the anomeric proton and the mannose hydroxyl protons. The anomeric peak is at δ 5.28, and the hydroxyl protons are at δ 4.99, 4.81, 4.74, 4.44. A satisfying observation was made concerning the alcohol proton of **43**. It is located at δ 4.59, between two mannose peaks, and it does not overlap with anything. Because of this, the ratio of the integration of peaks from the anomeric and hydroxyl signals gives an accurate ratio of **7**:**43**. For **44c**, the ratio derived from this region is 1:2.3, which is in very close agreement with the ratio derived from the aromatic region. All values shown in Table 4.1 are derived using integration data taken from this region.

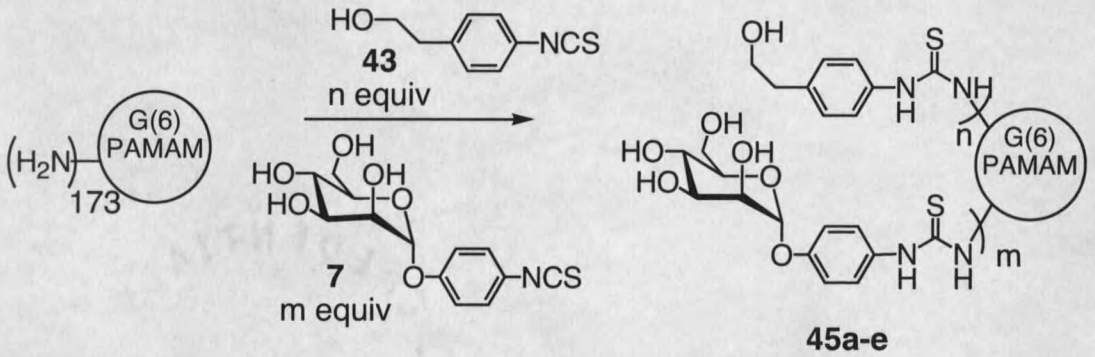
The MALDI-TOF MS data was collected for dendrimers **44a-e**. That data is also reported in Table 4.1. In all cases the polydispersities were quite low. None were higher than 1.02, which indicates that mixing both **7** and **43** resulted in an equal distribution of the molecules and thus a specific degree of functionalization. In other words, there were few molecules that were functionalized with just **7** or just **43** or anywhere in between. Most molecules were functionalized with the ratio as given by NMR.

Heterogeneous Functionalization of G(6)-PAMAM Using *p*-Isothiocyanatophenyl-α-D-mannopyranoside (**7**) and 2-(4-Isothiocyanatophenyl) Ethanol (**43**)

The heterogeneous functionalization was also done using G(6)-PAMAM dendrimers using the same technique as mentioned for the G(4)-PAMAM case. The reaction is shown in Scheme 4.3. As in the G(4)-PAMAM case (see Scheme 4.2) the components **7** and **43** were mixed and added together directly to the reaction mixture. In this case, a dendrimer functionalized only with **43** was also synthesized. The results and data are shown in Table 4.2. The compound **45e** containing only **43** was synthesized in order to identify the peaks in the ^{1}H NMR that are due to the addition of **43**.

The ^{1}H NMR spectrum of **45a** is shown in Figure 4.5. Figure 4.5a shows the complete spectrum and Figure 4.5b shows the region that is used to determine the ratio of **7**:**43**. In the case of G(6)-PAMAM functionalization, **45a-e**,

due to the symmetric nature of the dendrimers, the NMR spectra look almost identical to the G(4)-PAMAM case, **44a-e**. In the larger dendrimers the peaks tend to be broader, but the peak locations are often very similar. Therefore the determination of the **7**:**43** ratio is done as previously described for **44a-e**. While the peaks are broader for the G(6) dendrimer, the peak at δ 4.6, which corresponds to the alcohol peak of **43,** is still distinct from the surrounding peaks such that accurate integration values can be calculated.



45a-e

Scheme 4.3 Heterogeneous functionalization of G(6)-PAMAM using **7** and **43**.

Table 4.2 Data for heterogeneously functionalized PAMAM dendrimers shown in Scheme 4.3

Compound	**7:43** Theory	**7:43** Actual by NMR	M_W by MALDI-TOF	Polydispersity	Theoretical M_W[a]
45a	3:1	2.5:1	83900	1.09	99190
45b	1:1	1:1.3	88950	1.02	93600
45c	1:3	1:4.3	73160	1.06	87530
45d	1:8	1:13.5	72950	1.06	84310
45e	Just **43**	NA[b]	ND[c]	ND	81770

[a] Theoretical M_W based on theoretical value of **7**:**43** in column two.
[b] NA = Not Applicable
[c] ND = Not Determined

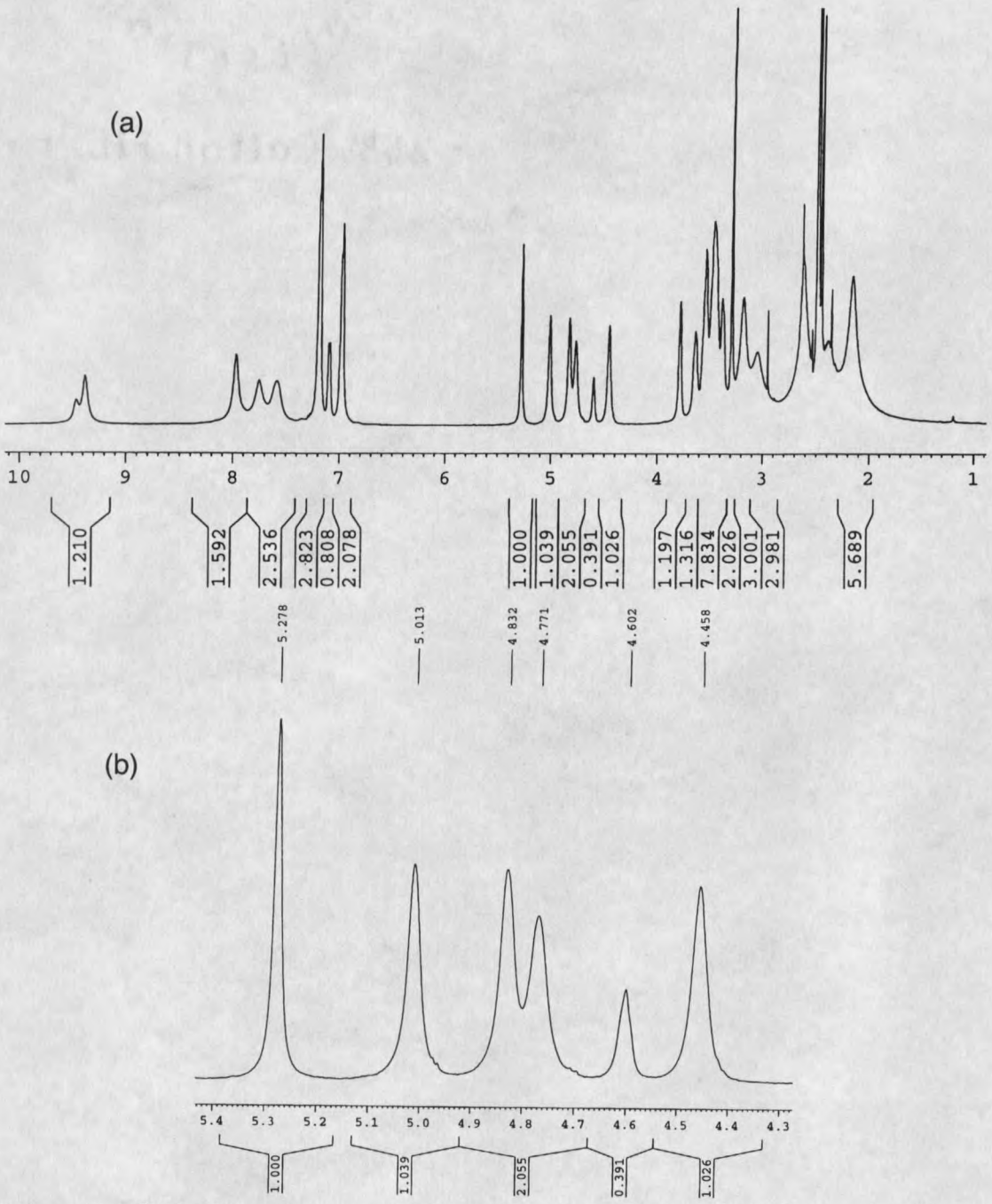


Figure 4.5 ^{1}H NMR spectrum of **45a**, (a) the full spectrum, (b) the region from which the ratios of **7**:**43** are derived.

From the data in Table 4.2, the ratio of **7**:**43** determined by NMR is close to the theoretical value as determined by stoichiometry. However, as one component (in this case **43**) increases to a large excess, it seems the desired ratio is more difficult to achieve.

Table 4.2 also shows the molecular mass data obtained from MALDI-TOF MS. Inspection of the mass data reveals a discrepancy; the mass of **45b** should be lower than **45a** since it contains less **7** than **45b** does. This may be a result of experimental error, but it may also be a result of the system. The polydispersities of the molecules are higher than in the G(4)-PAMAM case (which were all less than 1.02). When measured by MALDI-TOF, it is known that polymers with high polydispersities tend to give lower mass data than the actual value (the theoretical M_W values based on the theoretical ratios of **7**:**43** are given in Table 4.2 for comparison).[147, 148] Whether that is the case here is not clear, but the discrepancy emphasizes that collecting data for high weight polymers is often difficult.

Summary of Heterogeneous PAMAM Functionalization Using *p*-Isothiocyanatophenyl-α-D-mannopyranoside (**7**) and 2-(4-Isothiocyanatophenyl) Ethanol (**43**)

As was mentioned in Chapter 2, the solubility of the phenyl mannose functionalized dendrimers in water is poor. The addition of **43** certainly did nothing to improve that. Therefore, **44** and **45** could not be tested for biological

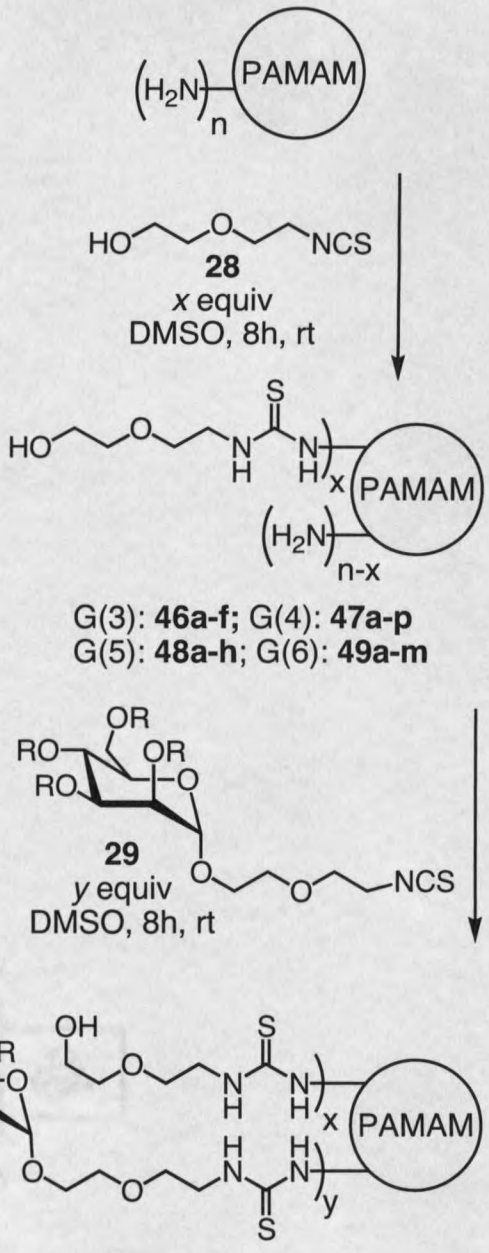
activity. Despite this, a good deal was learned about the heterogeneous functionalization of PAMAM dendrimers using isothiocyanates.

First, NMR provides a useful tool for the determination of the ratio of components on the surface of dendrimer. This does, however, rely on having surface residues that have at least one proton chemical shift that is unique from all signals from other surface groups. If the peaks overlap, the accuracy of the NMR determined ratio will be compromised.

A second lesson learned was that sequential addition of the various isothiocyanates should be explored. Sequential addition might eliminate the discrepancy between the ratios of reagents added and the ratios of surface groups in **45c** and **45d**. Sequential addition might also decrease the polydispersities of **45a-d**.

Heterogeneous PAMAM Functionalization Using 2-(2-isothiocyanatoethoxy)ethanol (**28**) and 1-*O*-(5-isothiocyanato-3-oxapentyl)-2,3,4,6-tetra-*O*-acetyl-α-D-mannopyranoside (**29**)

After having developed a method for the formation of water-soluble mannose-functionalized PAMAM dendrimers (see Chapter 3), it became clear that the same method could be applied to the synthesis of water-soluble heterogeneously functionalized PAMAM dendrimers. The main approach relied on the use of **28** and **29**.



Scheme 4.4 Heterogeneous functionalization of PAMAM dendrimers using **28** and **29**.

The general procedure for the heterogeneous functionalization of PAMAM dendrimers is shown in Scheme 4.4. The method employed is similar to that used in Scheme 4.2 and Scheme 4.3. However, in this case, the spacer isothiocyanate (**28**) and mannose unit (**29**) were added sequentially.

Briefly, an aqueous solution of commercially prepared PAMAM dendrimer was lyophilized to leave a foamy residue. This residue was dissolved in DMSO and an appropriate volume of a DMSO solution of **28** corresponding to *x* equivalents was added to the reaction and stirred overnight to form **46-49** for G(3) through G(6), respectively. Without isolating this product, an appropriate volume of a DMSO solution of **29** corresponding to *y* equivalents was added to the reaction and stirred overnight to form acetyl protected dendrimers **50-53** for G(3) through G(6), respectively.

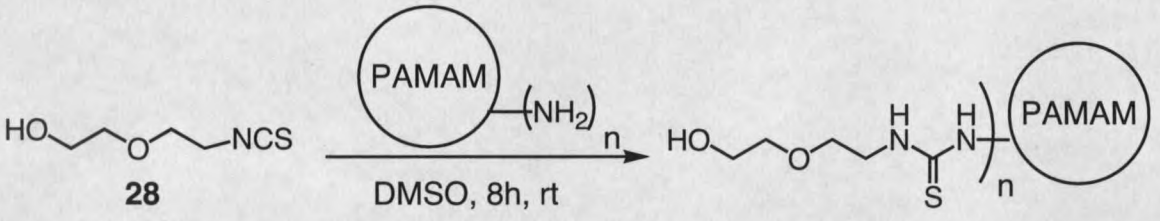
The acetylated products were purified by dialysis in DMSO (cellulose, MW cutoff 1000 g/mol). After lyophilization to remove the DMSO, global deprotection was achieved using Zemplén conditions in 1:1 H_2O:MeOH. The products were purified by dialysis against water (cellulose, MW cutoff 1000 g/mol) and then lyophilized to leave a foam of products **54-57** for G(3) to G(6), respectively.

The acetylated products, **50-53**, were not appreciably soluble in water or methanol, while the deacetylated products, **54-57**, were water-soluble unless the ratio of **28:29** was above 9:1. If the ratio became higher, the solubility of the

product in water decreased significantly. In fact, dendrimers that contained only **28** (i.e. **58-61**) were nearly insoluble in water.

While protection of the mannose hydroxyl groups is not necessary during thiourea formation, it proved advantageous to form the thiourea with the acetyl groups on the sugars. This is because the acetyl groups provide sharper NMR signals than the deprotected dendrimer and allow for the ratio of **28:29** on the surface of the dendrimer to be determined by integration of appropriate peaks.

In addition to heterogeneously functionalizing the dendrimers using **28** and **29**, G(3)- to G(6)-PAMAM were also completely functionalized using **28** to be used as a controls (Scheme 4.5). The procedure was the same as for the formation of the mannose-functionalized dendrimers **38-41**.



58 G(3); **59** G(4)
60 G(5); **61** G(6)

Scheme 4.5 Complete functionalization of G(3)- to G(6)-PAMAM dendrimer with just **28**.

Characterization of Heterogeneous Functionalized Dendrimers

All heterogeneously functionalized dendrimers and intermediates were characterized by NMR and MALDI-TOF MS. Both techniques provided

complimentary data that could be used to determine the number of sugars on the surface of each dendrimer.

Figure 4.6 shows the ^{1}H NMR spectra of peracetylated **51l** (G(4)-PAMAM with 35 sugars) and the same dendrimer after deacetylation, **55l**. The spectra of the acetylated dendrimer in Figure 4.6a provides a significant amount of information.

Since **28** and **29** have similar methylenes adjacent to the isothiocyanate functionality, the thioureas that form upon reaction with the dendrimer of **28** and **29** are also expected to be quite similar. Indeed, the ^{1}H NMR signals for the thiourea protons are indistinguishable in the spectrum. The thiourea protons signals are seen at around 7.5 ppm. The two broad peaks further downfield are from the amide protons on the interior of the dendrimer.

The broad peak at 4.56 ppm in Figure 4.6a is from the OH group of **28**. The peaks at ∂ 5.07 (3H), 4.88 (1H), 4.11 (1H), 4.00 (1H) and 3.95 (1H) ppm correspond to the seven protons on the carbon chain of the sugar in **29** (see inset in Figure 4.6a for blow up of the region from 3.0 to 5.1 ppm). As in the case of dendrimers **44** and **45**, some of the peaks from **28** and from **29** do not overlap. As a result, the NMR spectra of the peracetylated dendrimers are very useful for the determination of the ratio of **28**:**29** on the surface of the dendrimer.

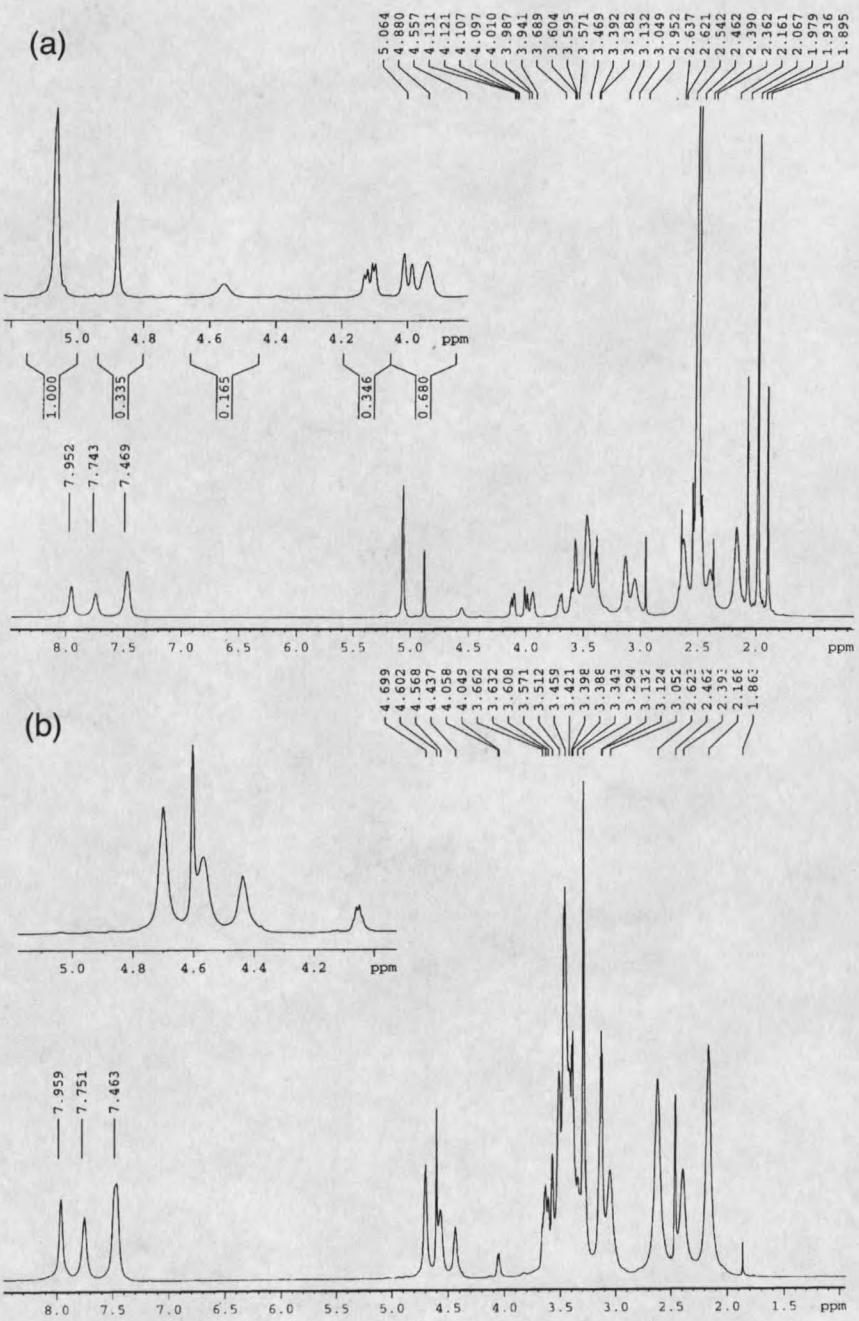


Figure 4.6 ^{1}H NMR (500 MHz) spectra of (a) peracetylated **51l** and (b) deprotected **55l**.

For the example shown in Figure 4.6a, the ratio of **28**:**29** is 1:2 which corresponds to 67% mannose. In general, the experimentally determined ratio of endgroups from **28**:**29** on the dendrimers was typically very close to the expected values. This indicates that the degree of functionalization can be easily controlled by stoichiometric control of reagents. Figure 4.6b shows deacetylated **55I**. After deprotection, the overlap of peaks makes quantitative analysis by NMR much more difficult.

While ^{1}H NMR integrations provide an excellent measure of the ratio of functional groups (see Figure 4.6a for an example), the MALDI-TOF MS spectra give a much more accurate quantitative indication of how many mannose residues are present on the dendrimers. During the reaction sequences (see Scheme 4.4), small samples of **47-49** and **50-53** were removed and, along with the final products **54-57** and the starting material PAMAMs, were analyzed by MALDI-TOF MS. Representative mass spectra are shown in Figure 4.7 and Figure 4.8.

Tomalia *et. al.* have reported that the average molecular weights of PAMAM dendrimers are smaller than the theoretical weights; our MALDI results are consistent with Tomalia's electrospray results.[155] That the shape of the product peaks is nearly identical to the shape of the starting material peak (see Figure 3.7 and Figure 3.8) suggests that most (if not all) of the peak broadening in the MALDI spectra is caused by defects in the dendrimers.

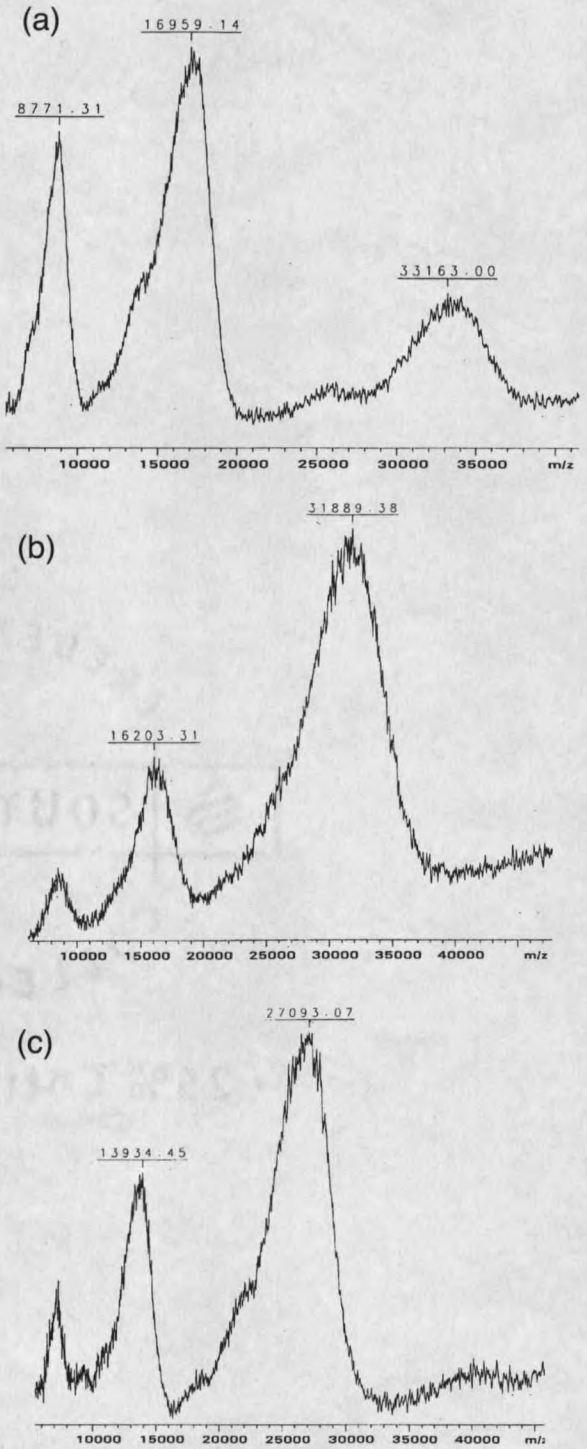


Figure 4.7 MALDI-TOF MS spectra of: (a) **47j**, (b) **51j**, (c) **55j** (from G(4)-PAMAM series).

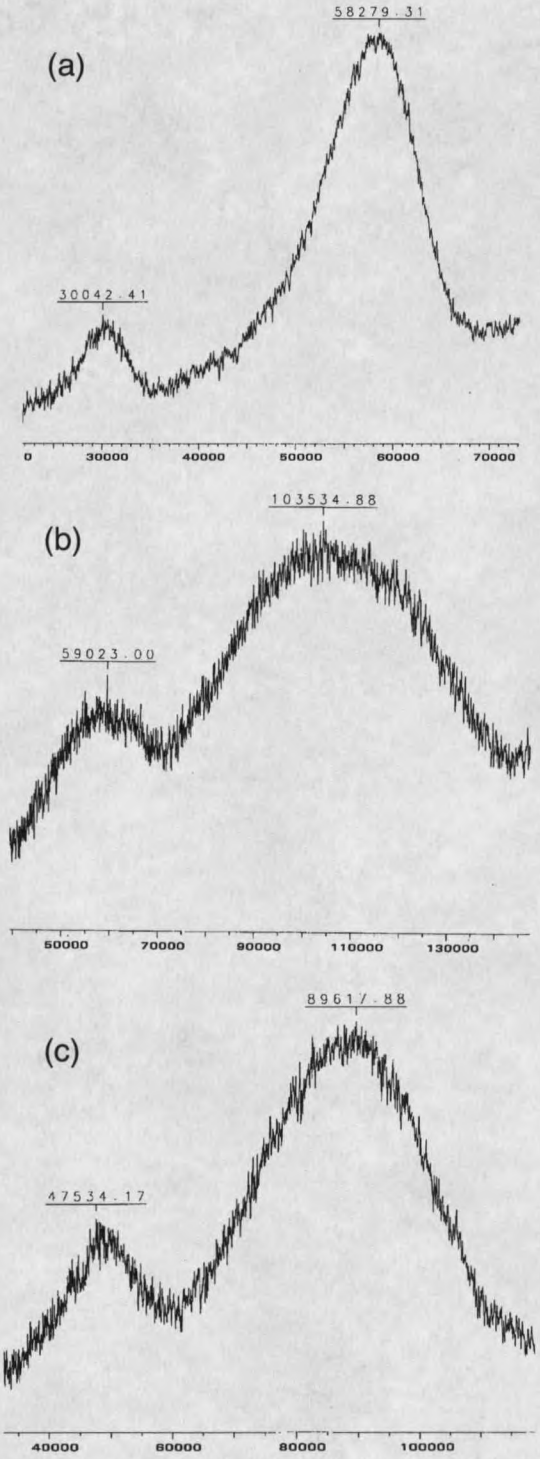


Figure 4.8 MALDI-TOF MS spectra of: (a) **49i,** (b) **53i**, (c) **57i** (from G(6)-PAMAM series).

Table 4.3 shows molecular mass data for many of the products formed for each generation of dendrimer (see Scheme 4.4 and Scheme 4.5) as determined by MALDI-TOF MS. Table 4.3 also shows the number of sugars per molecule and percent functionalization, which was derived from the mass data.

Comparison of the molecular mass data of the products (in addition to the NMR data) provided significant information on the number of sugars on the surface of the dendrimer. For example, the mass (M_W) of **47j** is 16,900 g/mol, **51j** is 31,950 g/mol, and **55j** is 26,600 g/mol. The difference between **51j** and **47j** is the number of molecules of **29** added (MW = 477), so: (31,950 – 16,900)/477 = 31.6 sugars. Likewise, the difference between **47j** and **55j** is the number of deprotected carbohydrates (MW = 306), so: (26,600 – 16,900)/ 306 = 31.7 sugars. The difference between **51j** and **55j** is the result of the loss of four acetyl protecting groups per sugar (MW = 172), so: (31,950 – 26,600)/172 = 31.1 sugars. The average number of sugars is 31.5, which is rounded up to 32 sugars. This procedure was repeated for all dendrimers synthesized, and the calculated values are shown in Table 4.3.

In some cases, the molecular weights of the dendrimers after the addition of **28** (i.e. the dendrimers that contained only polyethylene glycol, see **46a-f**) were not determined. Despite this, by using the mass values for **50a-f**, **54a-f**, and the G(3)-PAMAM reliable calculations to determine the number of sugar residues per dendrimer could be performed.

Table 4.3 Molecular weight data from MALDI-TOF MS. Number of sugars and percent functionalization. Molecule numbers are in parenthesis.

Generation	M_w (g/mol) (just **28**)	M_w (g/mol) (**28** + **29**)	M_w (g/mol) Deacetylated	Sugars[c]	% funct.[d]
3	11200 (**58**)	NA[a]	NA	0	0
3	ND[b] (**46a**)	11590 (**50a**)	10900 (**54a**)	4	14
3	ND (**46b**)	12700 (**50b**)	11800 (**54b**)	6	21
3	ND (**46c**)	14100 (**50c**)	12050 (**54c**)	12	42
3	ND (**46d**)	15100 (**50d**)	12600 (**54d**)	15	52
3	ND (**46e**)	17080 (**50e**)	13600 (**54e**)	21	72
3	ND (**46f**)	18370 (**50f**)	14300 (**54f**)	25	86
3	NA	21000 (**32**)	15930 (**38**)	29	100
4	21100 (**59**)	NA	NA	0	0
4	ND (**47a**)	22300 (**51a**)	21220 (**55a**)	7	13
4	20000 (**47b**)	23700 (**51b**)	22340 (**55b**)	8	15
4	19700 (**47c**)	24100 (**51c**)	22500 (**55c**)	9	16
4	ND (**47d**)	24800 (**51d**)	22500 (**55d**)	13	24
4	18800 (**47e**)	25800 (**51e**)	23300 (**55e**)	15	27
4	ND (**47f**)	26200 (**51f**)	23100 (**55f**)	18	33
4	17900 (**47g**)	27900 (**51g**)	24500 (**55g**)	21	38
4	ND (**47h**)	28500 (**51h**)	23800 (**55h**)	27	49
4	ND (**47i**)	31600 (**51i**)	26600 (**55i**)	30	55
4	16900 (**47j**)	31950 (**51j**)	26600 (**55j**)	31	56
4	ND (**47k**)	30500 (**51k**)	25000 (**55k**)	32	58
4	16300 (**47l**)	32900 (**51l**)	27100 (**55l**)	35	64
4	ND (**47m**)	32000 (**51m**)	25200 (**55m**)	37	67
4	15800 (**47n**)	35000 (**51n**)	28100 (**55n**)	40	73
4	14800 (**47o**)	37000 (**51o**)	29100 (**55o**)	46	84
4	14100 (**47p**)	38400 (**51p**)	30000 (**55p**)	51	93
4	NA	39000 (**33**)	30600 (**39**)	55	100
5	40150 (**60**)	NA	NA	0	0
5	41300 (**48a**)	42800 (**52a**)	42750 (**56a**)	4	4
5	ND (**48b**)	41500 (**52b**)	40100 (**56b**)	8	8
5	39000 (**48c**)	47300 (**52c**)	45000 (**56c**)	17	18
5	36700 (**48d**)	51800 (**52d**)	47400 (**56d**)	33	35
5	34400 (**48e**)	58100 (**52e**)	50600 (**56e**)	51	54
5	ND (**48f**)	59700 (**52f**)	48100 (**56f**)	67	71
5	30500 (**48g**)	64500 (**52g**)	54200 (**56g**)	74	78
5	28900 (**48h**)	69400 (**52h**)	55600 (**56h**)	86	91
5	NA	73600 (**34**)	58500 (**40**)	95	100
6	81550 (**61**)	NA	NA	0	0

Generation	M_W (g/mol) (just **28**)	M_W (g/mol) (**28** + **29**)	M_W (g/mol) Deacetylated	Sugars[c]	% funct.[d]
6	73800 (**49a**)	79200 (**53a**)	77400 (**57a**)	11	6
6	72100 (**49b**)	81000 (**53b**)	78000 (**57b**)	18	10
6	72100 (**49c**)	84400 (**53c**)	80100 (**57c**)	26	15
6	70400 (**49d**)	86400 (**53d**)	80100 (**57d**)	33	19
6	68400 (**49e**)	87900 (**53e**)	81000 (**57e**)	40	22
6	67700 (**49f**)	93200 (**53f**)	83100 (**57f**)	52	29
6	64800 (**49g**)	99200 (**53g**)	87100 (**57g**)	73	41
6	60600 (**49h**)	106500 (**53h**)	91000 (**57h**)	95	53
6	58100 (**49i**)	106300 (**53i**)	89500 (**57i**)	100	56
6	ND (**49j**)	111000 (**53j**)	93900 (**57j**)	102	57
6	54900 (**49k**)	114000 (**53k**)	96000 (**57k**)	122	69
6	53100 (**49l**)	122900 (**53l**)	97700 (**57l**)	146	82
6	ND(**49m**)	126000 (**53m**)	99900 (**57m**)	151	85
6	NA	132000 (**35**)	101200 (**41**)	178	100

[a] NA = Not Applicable
[b] ND = Not Determined
[c] See text preceding table for the method used to determine the number of sugars.
[d] Percent functionalization based on the maximum possible number of sugars for each generation.

We find that, although the theoretical number of endgroups for G(3), G(4), G(5), and G(6)-PAMAMs are 32, 64, 128, and 246 respectively, we are only able to add a maximum of 29, 55, 95, and 178 mannose groups to the dendrimer. Since we calculate that on average G(4), G(5), and G(6)-PAMAMs are missing 9, 26, and 44 terminal groups respectively (see Chapter 2), the mannose functionalization proceeds in 84% yield or higher.

To determine the percent mannose functionalization listed in Table 4.3, the calculated number of sugars was compared to the maximum number of sugars that can be added to the PAMAM dendrimer (see Chapter 2 for a discussion on the actual number of terminal amines on each generation of

dendrimer). For example, G(4)-PAMAM theoretically has 64 terminal amines. Analysis of MALDI MS data of the G(4)-PAMAM indicates that there are only 55 terminal amines present on the surface. This value of 55 is used as the maximum number of sites available for functionalization. Analysis of the mass data for compound **39** indicates that there are 55 carbohydrate residues on the surface, which means the percent functionalization of **39** is 100%. The percent functionalization of all generation four carbohydrate-functionalized PAMAM dendrimers are determined relative to 55 sites available for thiourea formation.

It should be noted that reversing the order of the addition of **28** and **29** showed no change in the ratio of **28**:**29** in the product (i.e. both **28** and **29** seemed to react similarly and predictably). However, stoichiometric control does not guarantee an exact ratio. In a typical procedure, the reagents are added in stoichiometric amounts that would result in a given ratio, but this actual ratio must be determined experimentally using NMR and MALD-TOF MS.

For the dendrimers listed in Table 4.3, the polydispersities were all less than 1.02, indicating a narrow range of molecular weights, which means, on the average, all of the dendrimers in a given sample were functionalized uniformly

It is important to point out the NMR data provides a ratio of **28**:**29**. This does not necessarily tell how many sugars are on the dendrimer. If one assumes that every amine is functionalized with either **28** or **29** than indeed the ratio will tell how many sugars are present. However, this assumption cannot always be

made. A dendrimer may not be fully functionalized, even though by all appearances (i.e. NMR data) it seems to be. The most reliable determination of the number of sugars on the surface is the MALDI data. The MALDI data will identify the number of carbohydrates on the surface regardless of whether the dendrimer has been fully functionalized or not, or whether the commercially prepared dendrimer being used from a given lot has as many amines as a dendrimer from a different lot.

Hemagglutination Assay of Heterogeneously Functionalized Dendrimers

As a means to determine the activity of the newly synthesized heterogeneously functionalized glycodendrimers, we chose to perform a hemagglutination assay. While this assay does not provide information regarding binding affinity, it does provide data that is useful in making a general comparison of the effect heterogeneous functionalization has on the activity of heterogeneously functionalized glycodendrimers for Con A. In a recent review article discussing the various assays that have been used to study protein-carbohydrate interactions, Lundquist and Toone note that "the inhibition of hemagglutination assay is a quick, simple assay that orders soluble ligands in a rough order of binding affinity."[22]

To perform the hemagglutination, erythrocytes (rabbit) were added to preincubated solutions of Con A and varying concentrations of dendrimer. The

concentration of Con A was kept around 1 μM for all assays. At this concentration, no deleterious precipitation of ligand and lectin was observed. The lowest amount of dendrimer that caused inhibition of hemagglutination was determined. The results are shown in Table 4.4. The large standard deviations occur because, while the overall trends are consistent, different blood sources (i.e. different blood from different rabbits on different days) give different numbers. Each value represents the average of at least three assays.

The hemagglutination assay data as shown in Table 4.4 reveals that there is a significant increase in activity for the fourth, fifth, and sixth generation dendrimer **55-57** as the number of mannose residues on the dendrimer is increased. As shown in Table 4.4, maximum activity occurs at just over 50% sugar loading for all generations (56% or 31 sugars on **55j**, 54% or 51 sugars on **56e**, and 53% or 95 sugars on **57h**).

The G(3) functionalized dendrimers **54a-f** and **38** do not show a sharp increase in activity with increasing sugar functionalization, nor would such an increase be expected since dendrimers **54a-f** and **38** are not large enough to span the multiple binding sites of Con A. In all cases, dendrimers that did not contain any mannose (**58-60**) showed no activity in the hemagglutination assay. Compound **61**, which was the G(6)-PAMAM functionalized with only **28** (i.e. **61** does not contain any mannose) was not soluble enough in the aqueous buffers to obtain reliable data.

Table 4.4 Summary of results for hemagglutination inhibition assay and precipitation assay.

Gen.	Cmpd.	Sugars	Rel. activity per mannose	Rel. activity per molecule[a]	Con A Stoich.[b]	Sugars per Con A[c]
3	**58**	0	0	0	0	0
3	**54a**	4	6 ± 2	24	ND	
3	**54b**	6	8 ± 4	48	4	1.5
3	**54c**	12	13 ± 11	156	7	1.7
3	**54d**	15	26 ±13	390	10	1.5
3	**54e**	21	20 ± 9	420	10	2.1
3	**54f**	25	18 ± 8	450	11	2.3
3	**38**	29	21 ±5	609	10	2.9
4	**59**	0	0	0	0	0
4	**55a**	7	31 ± 27	217	ND	
4	**55b**	8	49 ± 29	392	5	1.6
4	**55c**	9	94 ± 13	846	6	1.5
4	**55d**	13	120 ± 44	1560	ND	
4	**55e**	15	124 ± 8	1860	7	2.1
4	**55f**	18	157 ± 53	2826	ND	
4	**55g**	21	163 ± 28	3423	8	2.6
4	**55h**	27	174 ± 44	4698	9	3.0
4	**55i**	30	256 ± 51	7680	10	3.0
4	**55j**	31	273 ± 13	8463	ND	
4	**55k**	32	245 ± 6	7840	10	3.2
4	**55l**	35	242 ± 28	8575	10	3.5
4	**55m**	37	213 ± 55	7881	ND	
4	**55n**	40	222 ± 13	8880	10	4.0
4	**55o**	46	203 ± 8	9338	12	3.8
4	**55p**	51	184 ± 12	9384	11	4.6
4	**39**	55	204 ± 90	11220	12	4.6
5	**60**	0	0	0	0	0
5	**56a**	4	48 ± 3	192	ND	
5	**56b**	8	65 ± 46	520	ND	
5	**56c**	17	188 ± 21	3196	11	1.5
5	**56d**	33	324 ± 104	10692	15	2.2
5	**56e**	51	447 ± 133	22848	17	3.0
5	**56f**	67	366 ± 120	24522	ND	

Gen.	Cmpd.	Sugars	Rel. activity per mannose	Rel. activity per molecule[a]	Con A Stoich.[b]	Sugars per Con A[c]
5	**56g**	74	388 ± 17	28712	16	4.6
5	**56h**	86	247 ± 18	21242	16	5.4
5	**40**	95	305 ± 209	28975	16	5.9
6	**61**	0	Insoluble	Insoluble	ND	
6	**57a**	11	Insoluble	Insoluble	ND	
6	**57b**	18	Insoluble	Insoluble	ND	
6	**57c**	26	Insoluble	Insoluble	ND	
6	**57d**	33	148 ± 100	4884	ND	
6	**57e**	40	350 ± 319	14000	17	2.3
6	**57f**	52	390 ± 380	20280	22	2.4
6	**57g**	73	492 ± 259	35916	21[d]	3.5
6	**57h**	95	595 ± 62	56525	22	4.3
6	**57i**	100	570 ± 29	57000	21	4.8
6	**57j**	102	516 ± 145	52626	ND	
6	**57k**	122	407 ± 202	49654	25	4.9
6	**57l**	146	397 ± 74	57962	24	6.1
6	**57m**	151	350 ± 106	52850	ND	
6	**41**	178	354 ± 89	63012	25	7.1

[a] Number of sugars x relative activity per mannose.
[b] Determined from precipitation assay (see page 164 and following). Expressed as Con A molecules per dendrimer.
[c] Number of sugars ÷ Con A molecules per dendrimer.
[d] Value determined using only two assay trials.

The hemagglutination assay data is summarized in Figure 4.9. Figure 4.9a shows the relationship between activity of the dendrimer relative to methyl mannose and density of the sugars on the surface of the dendrimer. The relative activity was adjusted to a per mannose basis for direct comparison to α-D-methyl mannoside.

The density of the sugars was based on the number of sugars per molecule as determined by the MALDI-TOF MS and NMR data and the surface

area of the dendrimer based on measured dendrimer diameters. To determine the sizes of the mannose-functionalized dendrimers in solution, other workers in our group synthesized spin-labeled dendrimers and compared the linebroadening effects in the EPR spectra of the spin-labeled dendrimers to linebroadening effects for solutions of known concentrations of spin label. Because the spin label (4-iosothiocyanato-2,2,6,6-tetramethylpiperidine *N*-oxide or 4-NCS TEMPO) is six atoms shorter that the mannose tether **29**, a length of 5 Å was added per surface group or 10 Å total was added to the measured diameters. Thus, the approximate diameters of **54-57** are 60, 78, 95, and 130 Å, respectively.[192]

The experimentally determined values are not in agreement with the PAMAM data shown in Table 1.1. However, it has been previously reported that dendrimers can exhibit significant deformation.[172, 173] In fact, dendrimers deposited on mica surfaces are dome-shaped; a G(5)-PAMAM dendrimer was reported from an AFM study to have a height of approximately 10 Å and a diameter of more than 150 Å![172]

Figure 4.9a shows that, while the area available per sugar at maximum activity varies slightly for the different generation, the trend is similar in each case. What is most striking is that the maximum activity does not correlate to maximum sugar loading of the dendrimer. The decrease in activity as the number of sugars increases above about 50% loading is most likely a result of

accumulating unfavorable steric interactions between Con A and the dendrimer. Similar loading effects have been observed in a number of systems in which the binding epitope was varied.[16, 32, 64, 72, 185]

Another salient point that is illustrated in Figure 4.9a is that the maximum activity occurs at slightly closer packing of the sugars as the generation increases. The G(3) series (**54a-f**, and **38**) reaches a maximum at approximately 750 $Å^2$ per sugar, the G(4) series (**55a-p,** and **39**) reaches a maximum at approximately 620 $Å^2$ per sugar, and the G(5) series (**56a-h,** and **40**) and the G(6) series (**57d-m**, and **41**) both reach a maximum at approximately 550 $Å^2$ per sugar. A reasonable explanation is that the larger dendrimers are more dynamic and flexible and are thus better able to avoid unfavorable steric interactions that smaller, less flexible dendrimers cannot avoid as readily.

Figure 4.9b shows the relationship between the concentration of sugars on the surface of the dendrimer and activity on a per dendrimer basis (compared to methyl mannose). A similar trend to that observed in Figure 4.9a is evident, however, in this case as the epitope density increases (i.e. as the number of sugars increase) the activity continues to increase beyond what was the maximum activity on a per sugar basis (Figure 4.9a).

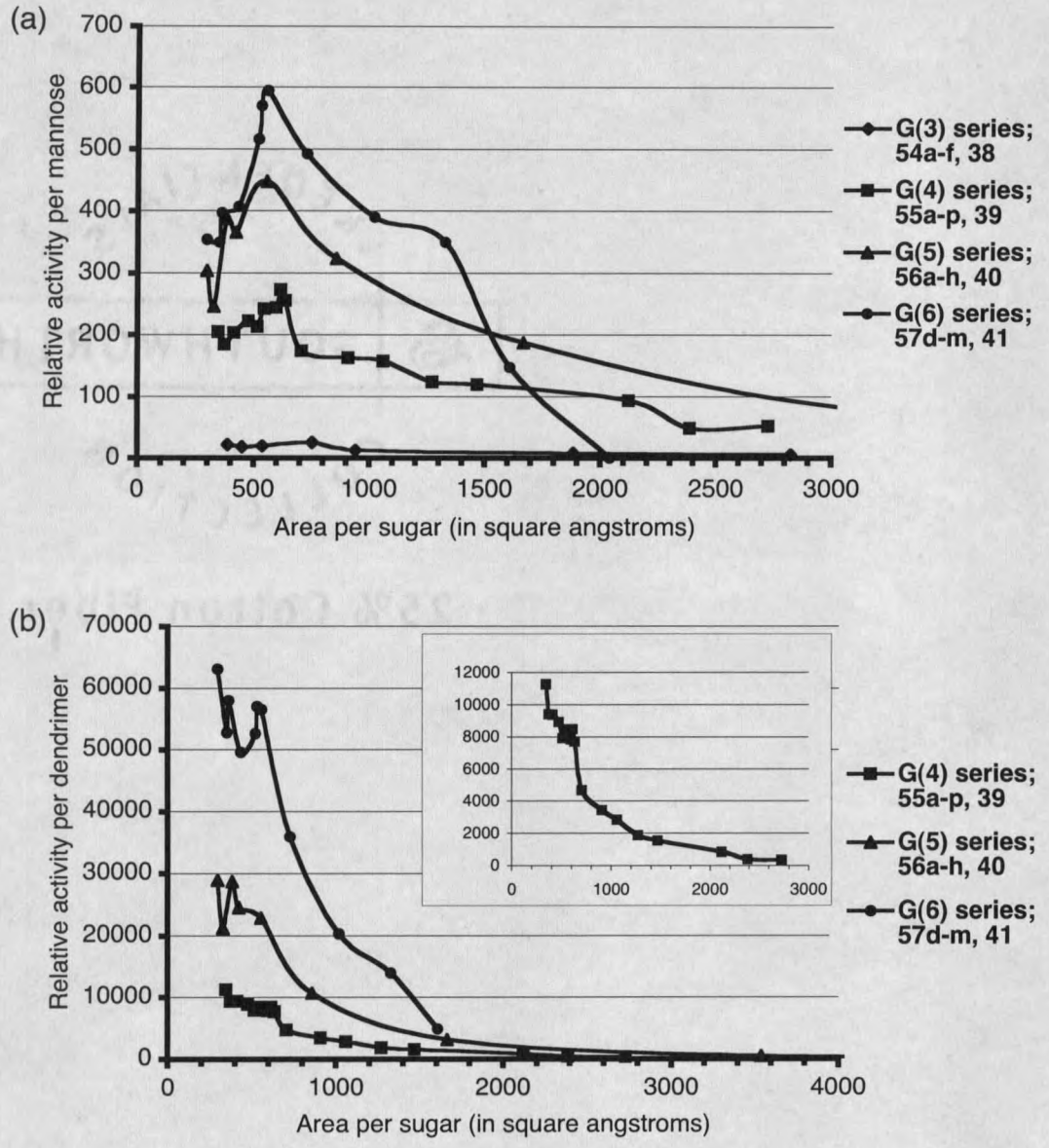


Figure 4.9 Graphs of (a) activity toward Con A relative to mannose vs. area per sugar for G(3) to G(6) series of heterogeneously functionalized dendrimers (see Table 4.4), (b) activity towards Con A per dendrimer vs. area per sugar for G(4) to G(6) series of heterogeneously functionalized dendrimers (see Table 4.4). (N.B. lines shown are shown for clarity and are not curve fits).

Since the graph compares number of molecules of dendrimer relative to molecules of methyl mannose, this continuing increase in activity can be attributed to the statistical glycoside clustering effect. As the number of sugars available to a given binding site increases, the activity toward Con A increases. This modest increase in activity is not as dramatic as the increase gained when the molecule is capable of multivalent binding (G(3) vs. G(4), G(5), and G(6) in Figure 4.9), but its effect is evident.

Precipitation Assay

To gain insight into the stoichiometry between the dendrimers and Con A, a precipitation assay was performed. In this procedure as described by Kahn *et. al.*[193] the ligand in varying concentrations is incubated with a constant Con A concentration. If the Con A concentration is high enough (in this case 33 μM), the mannose-functionalized dendrimer will precipitate Con A. After washing the precipitate with cold buffer to remove any unprecipitated Con A, the precipitate is redissolved by addition of monomeric methyl mannose and the concentration of Con A is determined by UV absorbance at 280 nm. The graph of the data collected is shown in Figure 4.10 (G(3) series), Figure 4.11 (G(4) series), Figure 4.12 (G(6) series), Figure 4.13 (G(5) series). The ratio of dendrimer to Con A at the point that maximum precipitation of Con A is observed is considered to be the

maximum stoichiometry of Con A to dendrimer. The results are shown in Table 4.4.

From the data listed in Table 4.4, the most obvious result is that, for each generation **54-57**, the number of Con A molecules binding to a dendrimer reaches a maximum and levels off. This maximum is 10-11 Con A lectins for **54** (G(3) series), 11-12 Con A lectins for **55** (G(4) series), 16 Con A lectins for **56** (G(5) series), and 24-25 Con A lectins for **57** (G(6) series).

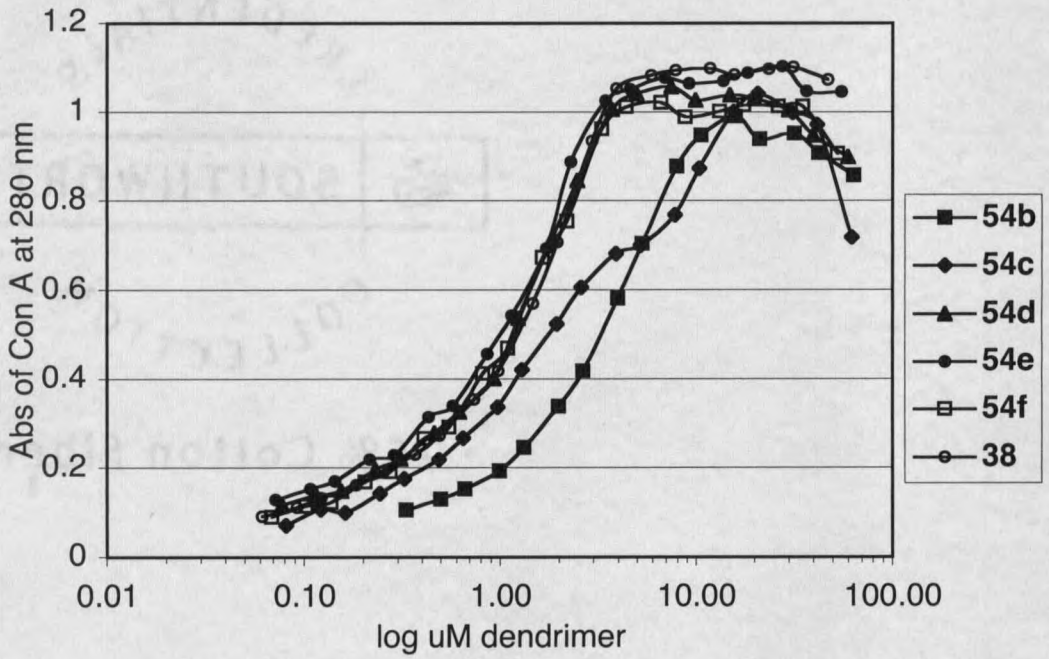


Figure 4.10 Precipitation assay data for G(3) series.

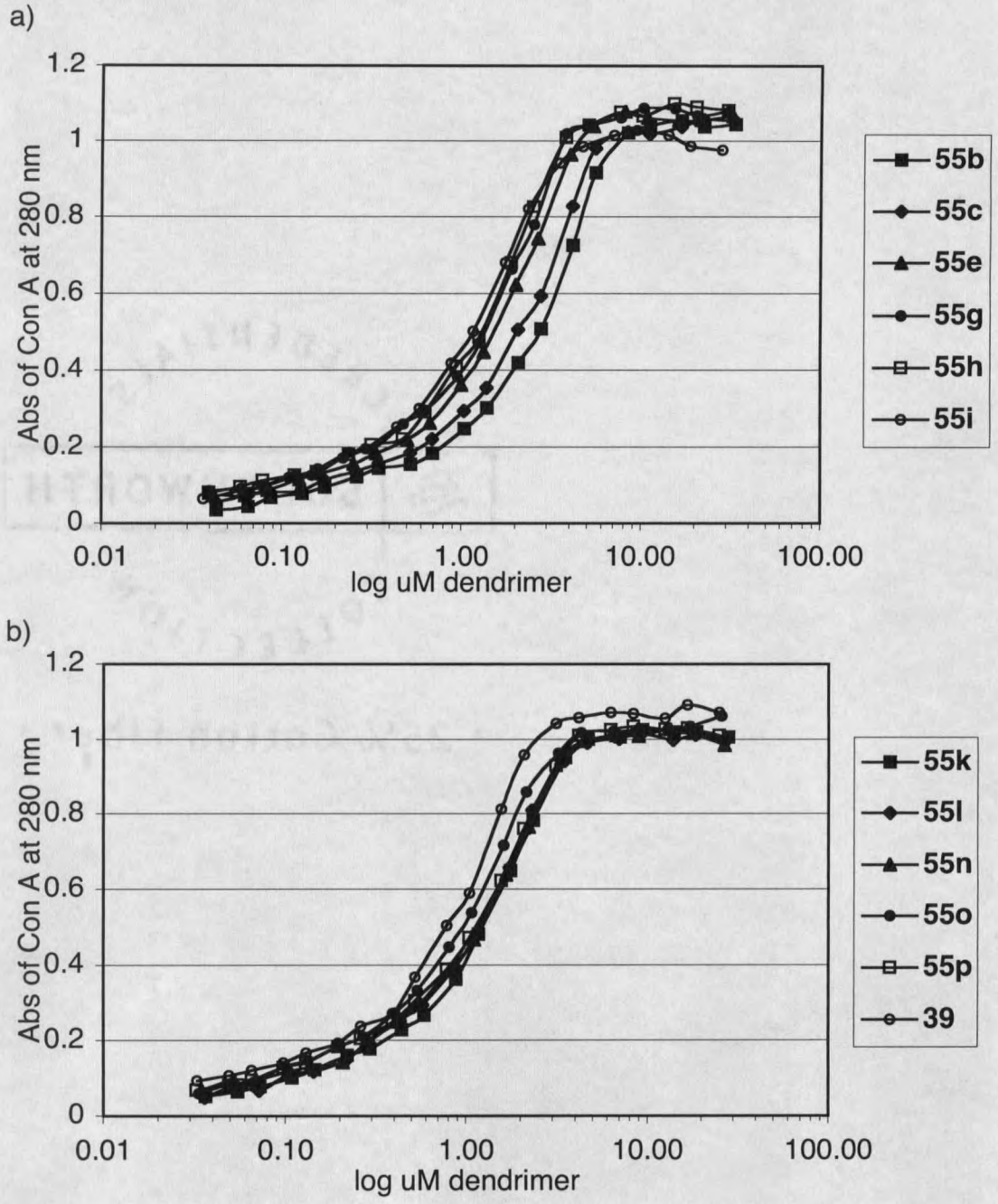


Figure 4.11 Precipitation assay data for G(4) series. Data is divided into two graphs for clarity.

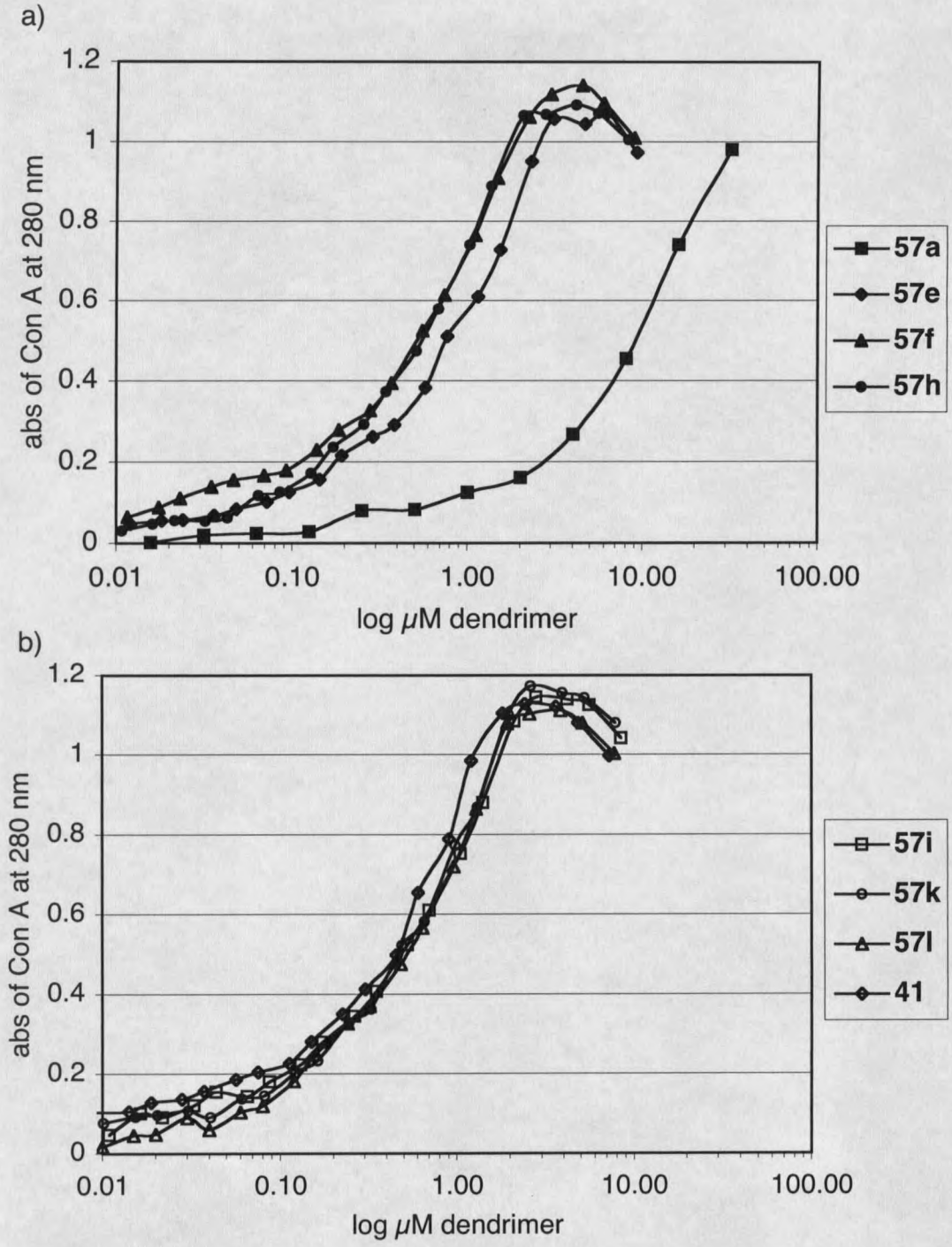


Figure 4.12 Precipitation assay data for G(6) series. Data is divided into two graphs for clarity.

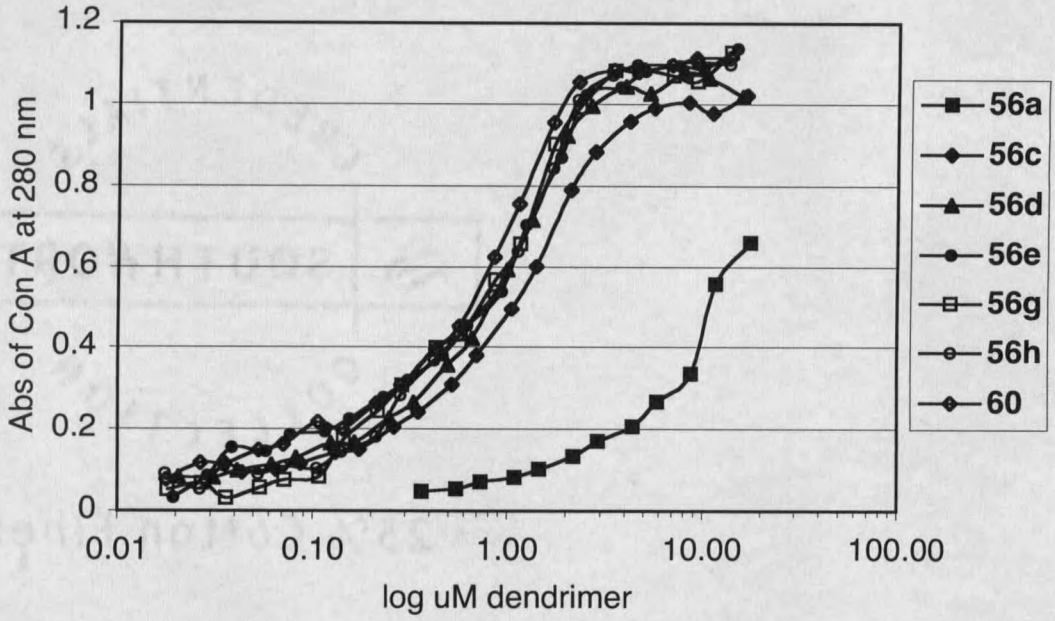


Figure 4.13 Precipitation assay data for G(5) series.

The theoretical maximum number of Con A molecules that would fit around **54-57** was determined using a computer program.[194] The dendrimer was modeled as a central sphere with a diameter from 10 to 240 Å, with spherical Con A molecules (65 or 70 Å sphere to mimic Con A) placed on the dendrimer surface. As the size of the dendrimer was varied, the maximum number of Con A molecules that could fit around the dendrimer at each size was calculated. As a check of the simulation, the results were compared to those obtained by placing the outer (Con A) spheres at the vertices of a polyhedra with the inner (dendrimer) sphere at the center. The computed and experimental results are shown in Figure 4.14.

Using the dendrimer diameters of 60, 78, 95, and 130 Å for **54**, **55**, **56**, and **57** respectively, the calculated number of Con A lectins that should fit around each dendrimer is in excellent agreement with the maximum number of Con A lectins obtained in the precipitation assay. The simulation predicts 9-10 Con A lectins for **54**, 12-13 Con A lectins for **55**, 15-16 Con A lectins for **56**, and 22-23 Con A lectins for **57**.

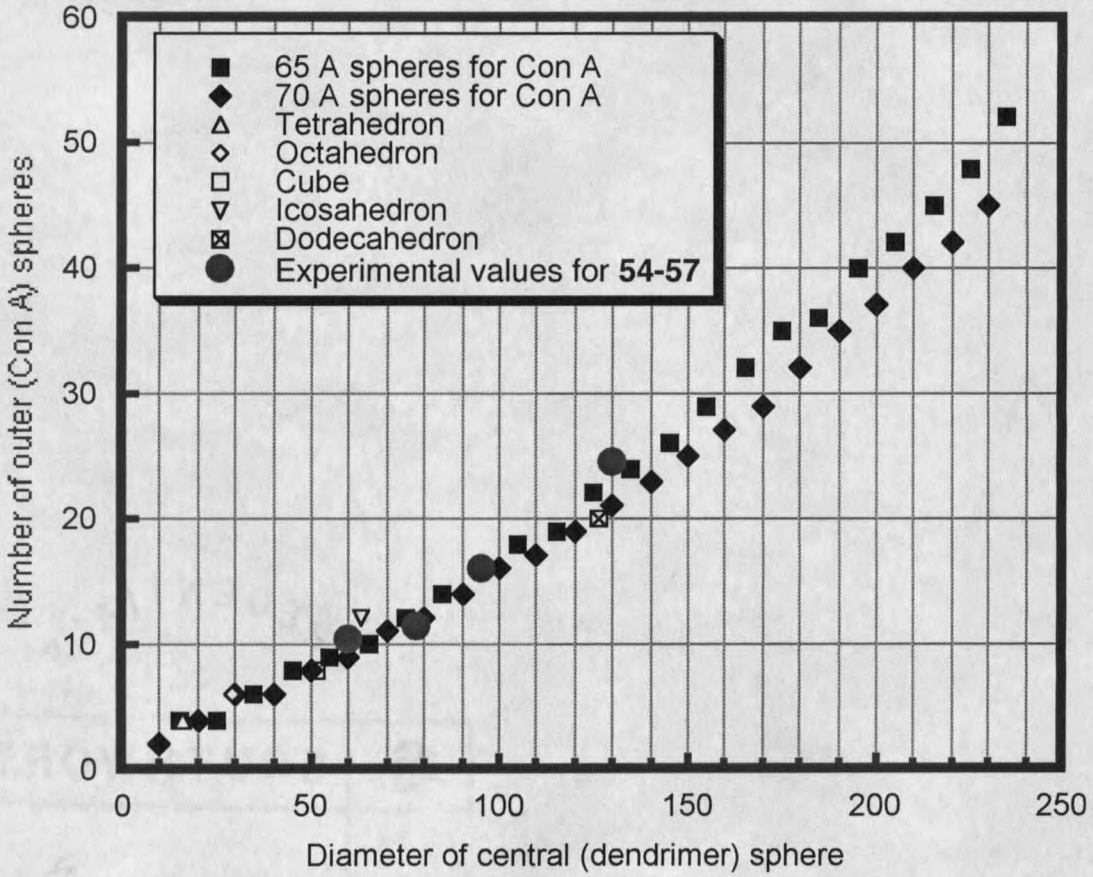


Figure 4.14 Graph showing the calculated and the experimentally determined maximum number of Con A lectins that can be complexed by the dendrimers.

The only experimental value that varies significantly from the computational value is that for the sixth generation dendrimers **57**. The

calculated maximum number of Con A lectins per dendrimer is smaller (22-23) than the observed value (24-25). This can be attributed to the increasingly dynamic nature of the dendrimers. Highest generation dendrimers are expected to be most dynamic, and **57** likely stretches to complex with a few extra Con A molecules. That the calculated maximum number of complexed Con A lectins is obtained in all cases qualitatively suggests a reasonably high affinity of Con A for mannose-functionalized dendrimers.

Another interesting observation is that, after a certain percent loading, the dendrimers for a given generation interact with nearly the same number of Con A molecules, regardless of how many sugars are present on the surface. For example, **55i-55p** and **39** all bind with the same number of Con A molecules within experimental error (of those that were analyzed). While the number of Con A molecules binding to a dendrimer reaches a maximum, activity still increases, as seen in Figure 4.9b. The results shown in Figure 4.9b and the results of the precipitation assay support the conclusion that after a certain degree of functionalization, the increased activity can be attributed to the statistical glycoside clustering effect. In this case, due to the fact that there is an increase in the number of sugars available to a given binding site, the reassociation of the ligand to the binding site is much more probable.

Although assay conditions such as Con A concentration are quite different for the hemagglutination assay and the precipitation assay, it is illuminating to

evaluate the results of the two assays together. For dendrimers with per mannose activities of >100 (relative to methyl mannose) in the hemagglutination assay, the number of Con A molecules attracted to each dendrimer in the precipitation assay was less than or equal to half the number of sugars on the dendrimer surface (21 of 22 such dendrimers for which data was collected with **56c** being the only exception). Another way this can be stated is that there were at least two sugars available to each Con A molecule. The last column in Table 4.4 shows the number of sugars available to each Con A molecule bound.

This indicates that each dendrimer with a hemagglutination activity of >100 probably binds Con A in a bidentate fashion. For the dendrimer with the highest activity in the hemagglutination assay in the fourth and fifth generational series (**55j** and **56e**), three sugars per Con A are stoichiometrically available. The value is higher (4.3 sugars per Con A) for **57h** in the G(6) series. Moreover, after the maximum possible number of Con A molecules have been bound to the dendrimer, adding more sugars reduces the dendrimer's activity in the hemagglutination assay on a per mannose basis but does not lower the activity so much that fewer Con A molecules are recruited.

Summary

We have shown that the heterogeneous functionalization of PAMAM dendrimers is easily achieved by the stoichiometric control of reactants. MALDI-

TOF-MS and NMR are useful techniques for the determination of surface functionalization. The degree of functionalization has a significant effect on the activity towards Con A. By controlling the number of sugars present on the surface of the dendrimer, the different modes of increased binding can be observed. For example, when the number of sugars is low enough, multivalent binding can be avoided. In this case the increased binding is most likely due to glycoside cluster effect. At some point, evident by an obvious significant increase in activity, multivalent binding becomes possible and becomes the significant contributor. As the number of sugars on the surface continues to increase, when compared per molecule with methyl mannose, a less dramatic increase in activity (on a per dendrimer basis) is again a result of a statistical glycoside cluster effect.

In addition, by controlling the number of sugars present on the surface of the dendrimer, both the binding activity of the dendrimer with lectin (as measured in the hemagglutination assay) and the number of lectins clustered around the dendrimer (as measured in the precipitation assay) can be controlled.

Taken together, the results from the hemagglutination assay and the precipitation assay suggest that we can independently attenuate lectin binding affinity and lectin clustering. Considering the huge number of lectins presented on cell surfaces,[3, 7, 103, 195] it is probable that recruitment of far more than 25 lectins occurs in many cellular processes. However, one could imagine using the

results reported here to construct dendrimer/polymer superstructures with a high degree of control over both lectin binding affinity and the number of lectins clustered into a specific area of the cell.

Experimental Procedures

General methods

General reagents were purchased from Aldrich, Sigma, and Acros. Generation 3.0 PAMAM dendrimers in methanol were purchased from Aldrich. Generations 4.0, 5.0 and 6.0 PAMAM dendrimers as aqueous solutions were purchased from Dendritech. Concanavalin A was purchased from Calbiochem. All solvents and reagents were used as supplied.

MALDI-TOF MS

Matrix assisted laser desorption ionization mass spectra data obtained as described in the experimental procedures in Chapter 3 (page 106).

Hemagglutination assay

HIA was performed as described in the experimental procedures in Chapter 3 (page 106).

Computer Modeling

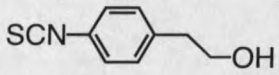
A C program [196] was used to model the packing of Con A around a dendrimer. The dendrimer was modeled as a sphere, with spherical Con A lectins tangent and not overlapping. The coordinates for the outer spheres (65 or

70 Å spheres to mimic Con A) were chosen randomly on the surface of the interior (dendrimer) sphere and then were tested for overlap. The program would try for a non-overlapping spot on the dendrimer surface up to 100,000 times. Upon reaching 100,000 unsuccessful tries, the program would record the number of successfully placed outer spheres. This sequence was repeated 10,000 times for each inner-sphere diameter, which was incremented in 10 Å steps. As a check of our random method, the results were compared to placing the outer (Con A) spheres at the vertices of polyhedra, with the inner (dendrimer) sphere at the center.

General quantitative precipitation assay procedure

The assay was performed at 22° C in 0.1 M Tris/HCl buffer, pH 7.2, containing 0.15 M NaCl, 1 mM $CaCl_2$ and 1 mM $MnCl_2$. Con A (500 μL, 66 μM) was added to 500 μL of a two-fold serial dilution of a mannose-functionalized dendrimer (refer to Table 4.4 for dendrimers that were tested). The mixtures were allowed to sit for 20 h. The solutions were centrifuged (5000 rpm for 5 minutes) to pellet the precipitate. The pellets were washed with 500 μL of cold buffer three times. The precipitates were dissolved in 500 μL of 0.1 M methyl mannoside solution and diluted with 1000 μL of buffer. The concentration of Con A in each solution was determined by UV at 280 nm using an extinction coefficient at 280 nm of 1.37 for a 1 mg/mL solution. The values given in Table 4.4 are the average of three independent measurements.

Synthetic procedures



2-(4-Isothiocyanatophenyl) ethanol (**43**). 2-(4-Aminophenyl) ethanol (5.04 g, 36.7 mmol) was dissolved in 70% aqueous EtOH (300 mL). Thiophosgene (6.33g, 4.2 mL, 55.1 mmol) was added via syringe while the reaction was stirred. After the addition of the thiophosgene, a solution of 11 M KOH (10 mL, 110 mmol) was added. Saturated $NaHCO_3$ was added until the solution was no longer acidic. The EtOH was removed *in vacuo*, and the product was extracted into Et_2O (3 x 80 mL). The organic layers were combined and washed with water (3 x 100 mL) and brine (2 x 100 mL) and dried over $MgSO_4$ The ether was removed *in vacuo* and the product was purified using column chromatography on SiO_2 using 1:1: EtOAc:hexanes. The resulting oil crystallized upon standing and was washed with hexanes and water to yield 5.08 g (77%) of **43** as a yellowish solid. ^{1}H NMR (250 MHz, $CDCl_3$) δ 7.14—7.24 (m, 4H), 3.84 (t, 2H, J = 6.5 Hz), 2.86 (t, 2H, J = 6.5 Hz), 1.61 (s, 1H) ppm; ^{13}C NMR (125 MHz, $CDCl_3$) 138.3, 135.1, 130.1, 129.5, 125.8, 63.2, 38.7 ppm; IR (KBr) 3342, 2942, 2860, 2108 cm^{-1}.

General procedure for the synthesis of heterogeneously functionalized generation 4.0 PAMAM-based thiourea-linked phenyl ethanol and phenyl-α-D-mannopyranoside dendrimers (**44a-e**) (see Table 4.5 for quantities of each component used in the series). A methanolic solution of amine-terminated G(4)-

PAMAM dendrimer (1.18 g of a 10 % (w/w) solution in MeOH, 118 mg of dendrimer, 8.4 μmol based on the M_W of 13,500 g/mol as determined by MALDI-TOF) was evaporated *in vacuo*. The resulting residue was dissolved in DMSO (15 mL). A solution was made by dissolving **7** (116 mg, 371 μmol) and **43** (33.2 mg, 185 μmol) in DMSO (4 mL). This solution was added to the dendrimer solution and the reaction was stirred for 8 h. The product was dialyzed against 2:1 DMSO-H_2O (MW cutoff 1 kDa). The solution was lyophilized to give **44a** as an off white solid. Accurate yields were not determined as the dendrimers **44a-e** were unavoidably contaminated with DMSO, which could not be removed.

Table 4.5 Quantities of reactants used to synthesize **44a-e**. See general procedure above for specific details.

Compound	Quantity of G(4)-PAMAM mg (μmol)	Quantity of **7** mg (μmol)	Quantity of **43** mg (μmol)
44a	118 (8.4)	116 (370)	33.2 (185)
44b	191 (13.6)	171 (545)	97.6 (545)
44c	118 (8.4)	58 (186)	66.5 (371)
44d	113 (8.5)	26.7 (85.4)	82.5 (462)
44e	108 (8.2)	20.5 (65.5)	82.2 (459)

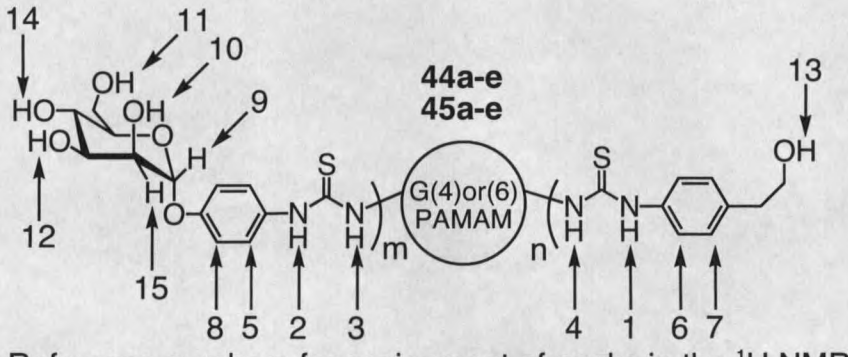


Figure 4.15 Reference numbers for assignment of peaks in the ^1H NMR of **44a-e** and **45a-e**. Protons are numbered in order from low to high field.

For the following ^{1}H NMR characterization data for 44a-e, see Figure 4.15 for proton designations. Integration values for H-13 (the hydroxyl proton of **43**) is given as a decimal in order to make a comparison to the sugar protons and thus a determination of the ratio of **7**:**43** straightforward:

44a: Ratio of m:n is 2:1; ^{1}H NMR (500 MHz, CD_3SOCD_3) δ 9.46 (bs, H-1), 9.38 (bs, H-2), 7.98 (bs, H-3 and H-4), 7.75 (bs, amide NH's), 7.56 (bs, NH's), 7.20 (d, H-5 and H-6), 7.11 (d, H-7), 7.00 (d, H-8), 5.28 (s, 1H, H-9), 4.99 (s, 1H, H-10), 4.81 (s, 1H, H-11), 4.74 (s, 1H, H-12), 4.59 (s, 0.5H, H-13), 4.44 (s, 1H, H-14), 3.79 (s, 1H, H-15), 3.30—3.70 (m), 2.90—3.25 (m), 2.30—2.70 (m), 2.17 (bs) ppm.; MALDI-TOF-MS (pos) found 25,800.

44b: Ratio of m:n is 1.2:1; ^{1}H NMR (500 MHz, CD_3SOCD_3) δ 9.51 (bs, H-1), 9.43 (bs, H-2), 8.03 (bs, H-3 and H-4), 7.80 (bs, amide NH's), 7.65 (bs, NH's), 7.26 (d, H-5 and H-6), 7.17 (d, H-7), 7.05 (d, H-8), 5.33 (s, 1H, H-9), 5.04 (s, 1H H-10), 4.86 (s, 1H, H-11), 4.80 (s, 1H, H-12), 4.65 (s, 0.89H, H-13), 4.49 (s, 1H, H-14), 3.84 (s, 1H, H-15), 3.32—3.75 (m), 3.00—3.28 (m), 2.30—2.80 (m), 2.23 (bs) ppm.; MALDI-TOF-MS (pos) found 25,400.

44c: Ratio of m:n is 1:2.3; ^{1}H NMR (500 MHz, CD_3SOCD_3) δ 9.46 (bs, H-1), 9.38 (bs, H-2), 7.97 (bs, H-3 and H-4), 7.75 (bs, amide NH's), 7.60 (bs, NH's), 7.20 (d, H-5 and H-6), 7.11 (d, H-7), 7.00 (d, H-8), 5.28 (s, 1H, H-9), 5.00 (s, 1H, H-10), 4.81 (s, 1H, H-11), 4.74 (s, 1H, H-12), 4.60 (s, 2.52H, H-13), 4.44 (s, 1H,

H-14), 3.79 (s, 1H, H-15), 3.30—3.70 (m), 2.90—3.25 (m), 2.30—2.70 (m), 2.17 (bs) ppm.; MALDI-TOF-MS (pos) found 22,400.

44d: Ratio of m:n is 1:4.5; ^{1}H NMR (500 MHz, CD_3SOCD_3) δ 9.47 (bs, H-1), 9.38 (bs, H-2), 7.98 (bs, H-3 and H-4), 7.75 (bs, amide NH's), 7.60 (bs, NH's), 7.20 (d, H-5 and H-6), 7.11 (d, H-7), 6.99 (d, H-8), 5.27 (s, 1H, H-9), 4.99 (s, 1H, H-10), 4.81 (s, 1H, H-11), 4.74 (s, 1H, H-12), 4.60 (s, 4.50H, H-13), 4.44 (s, 1H, H-14), 3.77 (s, 1H, H-15), 3.30—3.70 (m), 2.90—3.25 (m), 2.30—2.70 (m), 2.16 (bs) ppm.; MALDI-TOF-MS (pos) found 21,900.

44e: Ratio of m:n is 1:7.2; ^{1}H NMR (500 MHz, CD_3SOCD_3) δ 9.46 (bs, H-1), 9.38 (bs, H-2), 7.97 (bs, H-3 and H-4), 7.75 (bs, amide NH's), 7.59 (bs, NH's), 7.20 (d, H-5 and H-6), 7.11 (d, H-7), 7.00 (d, H-8), 5.28 (s, 1H, H-9), 5.00 (s, 1H, H-10), 4.81 (s, 1H, H-11), 4.74 (s, 1H, H-12), 4.60 (s, 7.20H, H-13), 4.45 (s, 1H, H-14), 3.79 (s, 1H, H-15), 3.30—3.70 (m), 2.90—3.25 (m), 2.30—2.70 (m), 2.17 (bs) ppm.; MALDI-TOF-MS (pos) found 21,500.

General procedure for the synthesis of heterogeneously functionalized generation 6.0 PAMAM-based thiourea-linked phenyl ethanol and phenyl-α-D-mannopyranoside dendrimers (**45a-e**) (see Table 4.6 for quantities of each component used in the series). A methanolic solution of amine-terminated G(6)-PAMAM dendrimer (1.0 g of a 10 % (w/w) solution in MeOH, 100 mg of dendrimer, 1.7 μmol based on the M_W of 58,000 g/mol as determined by MALDI-TOF) was evaporated *in vacuo*. The resulting residue was dissolved in DMSO

(15 mL). A solution was made by dissolving **7** (64.7 mg, 207 μmol) and **43** (37.1 mg, 207 μmol) in DMSO (4 mL). This solution was added to the dendrimer solution and the reaction was stirred for 8 h. The product was dialyzed against 2:1 DMSO:H_2O (MW cutoff 1 kDa). The solution was lyophilized to give **45b** as an off white solid. Accurate yields were not determined as the dendrimers **45a-e** were unavoidably contaminated with DMSO, which could not be removed.

Table 4.6 Quantities of reactants used to synthesize **45a-e**. See general procedure above for specific details.

Compound	Quantity of G(6)-PAMAM mg (μmol)	Quantity of **7** mg (μmol)	Quantity of **43** mg (μmol)
45a	162 (3.1)	183 (584)	34.9 (195)
45b	100 (1.7)	64.7 (207)	37.1 (207)
45c	191 (3.6)	72.2 (230)	124 (691)
45d	152 (2.9)	25.1 (80.0)	117 (651)
45e	140 (2.4)	0 (0)	113 (628)

For the following ^{1}H NMR characterization data for 45a-e, see Figure 4.15 for proton designations. Integration values for H-13 (the hydroxyl proton of **43**) is given as a decimal in order to make a comparison to the sugar protons and thus a determination of the ratio of **7**:**43** straightforward:

45a: Ratio of m:n is 2.5:1; ^{1}H NMR (500 MHz, CD_3SOCD_3) δ 9.47 (bs, H-1), 9.38 (bs, H-2), 7.98 (bs, H-3 and H-4), 7.76 (bs, amide NH's), 7.59 (bs, NH's), 7.19 (d, H-5 and H-6), 7.10 (d, H-7), 6.98 (d, H-8), 5.28 (s, 1H, H-9), 5.01 (s, 1H, H-10), 4.83 (s, 1H, H-11), 4.77 (s, 1H, H-12), 4.60 (s, 0.39H, H-13), 4.46 (s, 1H,

H-14), 3.79 (s, 1H, H-15), 3.30—3.70 (m), 2.90—3.25 (m), 2.30—2.70 (m), 2.16 (bs) ppm.; MALDI-TOF-MS (pos) found 83,900.

45b: Ratio of m:n is 1:1.3; ^{1}H NMR (500 MHz, CD_3SOCD_3) δ 9.47 (bs, H-1), 9.39 (bs, H-2), 7.98 (bs, H-3 and H-4), 7.76 (bs, amide NH's), 7.60 (bs, NH's), 7.19 (d, H-5 and H-6), 7.10 (d, H-7), 6.98 (d, H-8), 5.27 (s, 1H, H-9), 5.02 (s, 1H, H-10), 4.83 (s, 1H, H-11), 4.78 (s, 1H, H-12), 4.61 (s, 1.3H, H-13), 4.46 (s, 1H, H-14), 3.78 (s, 1H, H-15), 3.30—3.70 (m), 2.90—3.25 (m), 2.30—2.70 (m), 2.16 (bs) ppm.; MALDI-TOF-MS (pos) found 88,950.

45c: Ratio of m:n is 1:4.3; ^{1}H NMR (500 MHz, CD_3SOCD_3) δ 9.47 (bs, H-1), 9.38 (bs, H-2), 7.98 (bs, H-3 and H-4), 7.75 (bs, amide NH's), 7.60 (bs, NH's), 7.19 (d, H-5 and H-6), 7.10 (d, H-7), 6.98 (d, H-8), 5.28 (s, 1H, H-9), 5.01 (s, 1H, H-10), 4.83 (s, 1H, H-11), 4.77 (s, 1H, H-12), 4.60 (s, 4.3H, H-13), 4.45 (s, 1H, H-14), 3.78 (s, 1H, H-15), 3.30—3.70 (m), 2.90—3.25 (m), 2.30—2.70 (m), 2.16 (bs) ppm.; MALDI-TOF-MS (pos) found 73,158.

45d: Ratio of m:n is 1:13.5; ^{1}H NMR (500 MHz, CD_3SOCD_3) δ 9.47 (bs, H-1), 9.38 (bs, H-2), 7.97 (bs, H-3 and H-4), 7.75 (bs, amide NH's), 7.60 (bs, NH's), 7.19 (d, H-5 and H-6), 7.10 (d, H-7), 6.98 (d, H-8), 5.28 (s, 1H, H-9), 5.01 (s, 1H, H-10), 4.83 (s, 1H, H-11), 4.77 (s, 1H, H-12), 4.60 (s, 13.5H, H-13), 4.46 (s, 1H, H-14), 3.79 (s, 1H, h-15), 3.30—3.70 (m), 2.90—3.25 (m), 2.30—2.70 (m), 2.16 (bs) ppm.; MALDI-TOF-MS (pos) found 72,952.

45e: ^{1}H NMR (500 MHz, CD_3SOCD_3) δ 9.47(bs, H-1), 7.98 (bs, H-4), 7.76 (bs, amide NH's), 7.60 (bs, NH's), 7.19 (d, H-6, J = 7.2 Hz), 7.10 (d, H-7, J = 7.2 Hz), 4.61 (bs, H-13), 3.40—3.60 (m), 2.90—3.25 (m), 2.30—2.80 (m), 2.16 (bs).

Representative procedure for the synthesis of heterogeneously functionalized generation 3.0 PAMAM-based thiourea-linked ethoxy ethanol and 1-*O*-(5-thiourea-3-oxapentyl)-2,3,4,6-tetra-*O*-acetyl-α-D-mannopyranoside dendrimers (**50a-f**) (the following procedure is for **50a**. See Table 4.7 for quantities of reactants for **50b-f**). An aqueous solution of amine-terminated Starburst G(3)-PAMAM dendrimer (2.07 g of a 10% (w/w) solution in water, 207 mg, 30.0 μmol of dendrimer based on the M_W of 6909 g/mol as determined by MALDI-TOF for G(3)-PAMAM) was lyophilized to leave a foam. The resulting residue was dissolved in DMSO (10 mL) followed by the addition of a 0.1 g/mL DMSO solution of **28** (1320 μL, 132 mg, 899 μmol). The reaction was stirred for 8 hours. At this point, an aliquot (approx. 250 μL) containing **46a** was removed for MALDI-TOF MS analysis. A solution of a 0.1 g/mL DMSO solution of **29** (289 μL, 28.9 mg, 59.9 μmol) was added to the reaction. The reaction was stirred for 8 hours. The reaction mixture was added to a dialysis membrane (cellulose, MW cutoff 1 kDa) and the solution was dialyzed against DMSO for 12 hours. The solution was lyophilized nearly to dryness to give **50a** as a thick syrupy product (some DMSO remained) that was used without further purification.

Approximately, 20-40 mg of the acetylated product was removed for MALDI-TOF MS analysis.

Representative deacetylation procedure to form generation 3.0 PAMAM-based thiourea-linked ethoxy ethanol and 1-*O*-(5-thiourea-3-oxapentyl)-α-D-mannopyranoside dendrimers (**54a-f**) (the following procedure is for **54a**. See Table 4.7 for quantities of reactants for the formation of **54b-f**). A suspension of acetylated mannose functionalized dendrimer **50a** in MeOH:H_2O (1:1, 20 mL) and 0.3 M methanolic NaOMe (180 μL, based on 0.9 moles of NaOMe for every mole of **29** on **50a**) was stirred overnight until all of the solid had dissolved. The solution was neutralized with Amberlite IR-120 (acidic). The reaction mixture was subjected to dialysis against 1:1 MeOH-H_2O, which was gradually changed to pure water. The aqueous solution was lyophilized to give **54a** as a fluffy, white solid.

Table 4.7 Quantities of reactants used to synthesize **54a-f**. See general procedure above for specific details.

#	Quantity of G(3)-PAMAM mg (μmol)	Quantity of **28** mg (μmol)	Quantity of **29** mg (μmol)	μL of 0.3M NaOMe	Yield of **54**[a] mg (%)
54a	207 (30.0)	132 (899)	28.6 (59.9)	180	218 (66)
54b	260 (37.6)	143 (977)	108 (226)	680	300 (68)
54c	257 (37.1)	115 (779)	195 (409)	1230	391 (87)
54d	252 (36.5)	85.8 (583)	278 (584)	1750	378 (82)
54e	255 (36.9)	59.7 (405)	370 (775)	2330	359 (72)
54f	257 (37.2)	32.8 (223)	461 (967)	2900	447 (84)

[a] Reported yields are of isolated products and are lower than the actual yields because of removal of aliquots for MALDI-TOF MS. Percent yields are for three steps (addition of **28**, addition of **29** and deprotection).

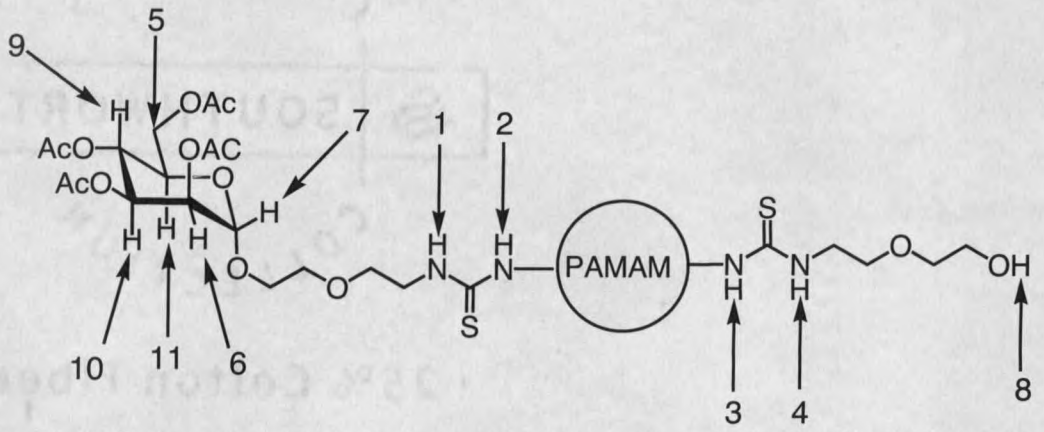


Figure 4.16 Reference numbers for assignment of peaks in the ^{1}H NMR of **50a-f**. Protons are numbered in order from low to high field.

Heterogeneously functionalized generation 3.0 PAMAM-based thiourea-linked ethoxy ethanol and 1-*O*-(5-thiourea-3-oxapentyl)-2,3,4,6-tetra-*O*-acetyl-α-D-mannopyranoside dendrimers (**50a-f**). Refer to Figure 4.16 for peak assignments. Integration values for H-8 (the hydroxyl proton of **28**) is given as a decimal in order to make a comparison to sugar protons straightforward:

50a: ^{1}H NMR (500 MHz, CD_3SOCD_3) δ 8.02 (bs, amide NH's), 7.75 (bs, amide NH's), 7.48 (bs, 4H, H-1, H-2, H-3, and H-4), 5.06 (bs, 3H, H-5, H-6), 4.88 (bs, 1H, H-7) 4.57 (bs, 7.6H, H-8), 4.11 (m, 1H, H-9), 3.90—4.05 (m, 2H, H-10 and H-11), 2.80—3.80 (m), 2.10—2.70 (m), 2.07 (s, 3H), 1.98 (s, 6H), 1.89 (s, 3H); MALDI-TOF MS (pos) found 11,590.

50b: ^{1}H NMR (500 MHz, CD_3SOCD_3) δ 7.96 (bs, amide NH's), 7.76 (bs, amide NH's), 7.48 (bs, 4H, H-1, H-2, H-3, and H-4), 5.07 (bs, 3H, H-5, H-6), 4.89 (bs, 1H, H-7) 4.57 (bs, 3.1H, H-8), 4.11 (m, 1H, H-9), 3.90—4.05 (m, 2H, H-10

and H-11), 2.80—3.80 (m), 2.10—2.70 (m), 2.07 (s, 3H), 1.98 (s, 6H), 1.90 (s, 3H); MALDI-TOF MS (pos) found 12,700.

50c: ^{1}H NMR (500 MHz, CD_3SOCD_3) δ 7.98 (bs, amide NH's), 7.76 (bs, amide NH's), 7.48 (bs, 4H, H-1, H-2, H-3, and H-4), 5.07 (bs, 3H, H-5, H-6), 4.88 (bs, 1H, H-7) 4.57 (bs, 1.4H, H-8), 4.11 (m, 1H, H-9), 3.90—4.05 (m, 2H, H-10 and H-11), 2.80—3.80 (m), 2.10—2.70 (m), 2.16 (s, 3H), 1.98 (s, 6H), 1.89 (s, 3H); MALDI-TOF MS (pos) found 14,100.

50d: ^{1}H NMR (500 MHz, CD_3SOCD_3) δ 7.96 (bs, amide NH's), 7.75 (bs, amide NH's), 7.48 (bs, 4H, H-1, H-2, H-3, and H-4), 5.07 (bs, 3H, H-5, H-6), 4.88 (bs, 1H, H-7) 4.57 (bs, 0.76H, H-8), 4.11 (m, 1H, H-9), 3.90—4.05 (m, 2H, H-10 and H-11), 2.80—3.80 (m), 2.10—2.70 (m), 2.16 (s, 3H), 1.98 (s, 6H), 1.89 (s, 3H); MALDI-TOF MS (pos) found 15,100.

50e: ^{1}H NMR (500 MHz, CD_3SOCD_3) δ 7.96 (bs, amide NH's), 7.75 (bs, amide NH's), 7.47 (bs, 4H, H-1, H-2, H-3, and H-4), 5.07 (bs, 3H, H-5, H-6), 4.88 (bs, 1H, H-7) 4.57 (bs, 0.35H, H-8), 4.11 (m, 1H, H-9), 3.90—4.05 (m, 2H, H-10 and H-11), 2.80—3.80 (m), 2.10—2.70 (m), 2.16 (s, 3H), 1.98 (s, 6H), 1.89 (s, 3H); MALDI-TOF MS (pos) found 17,080.

50f: ^{1}H NMR (500 MHz, CD_3SOCD_3) δ 7.95 (bs, amide NH's), 7.75 (bs, amide NH's), 7.48 (bs, 4H, H-1, H-2, H-3, and H-4), 5.07 (bs, 3H, H-5, H-6), 4.88 (bs, 1H, H-7) 4.57 (bs, 0.13H, H-8), 4.11 (m, 1H, H-9), 3.90—4.05 (m, 2H, H-10

and H-11), 2.80—3.80 (m), 2.10—2.70 (m), 2.16 (s, 3H), 1.98 (s, 6H), 1.89 (s, 3H); MALDI-TOF MS (pos) found 18,370.

Deacetylated generation 3.0 PAMAM-based thiourea-linked ethoxy ethanol and 1-*O*-(5-thiourea-3-oxapentyl)-α-D-mannopyranoside dendrimers (**54a-f**):

54a: ^{1}H NMR (500 MHz, CD_3SOCD_3) δ 7.98 (bs, amide NH's), 7.77 (bs, amide NH's), 7.48 (bs, all thiourea protons), 4.59 (bs), 2.80—3.60 (m), 2.63 (bs), 2.40 (bs), 2.17 (bs); MALDI-TOF MS (pos) found 10,900.

54b: ^{1}H NMR (500 MHz, CD_3SOCD_3) δ 7.97 (bs, amide NH's), 7.76 (bs, amide NH's), 7.47 (bs, all thiourea protons), 4.40—4.80 (m), 2.80—3.60 (m), 2.62 (bs), 2.40 (bs), 2.18 (bs); MALDI-TOF MS (pos) found 11,800.

54c: ^{1}H NMR (500 MHz, CD_3SOCD_3) δ 7.97 (bs, amide NH's), 7.76 (bs, amide NH's), 7.47 (bs, all thiourea protons), 4.40—4.80 (m), 2.80—3.60 (m), 2.63 (bs), 2.40 (bs), 2.17 (bs); MALDI-TOF MS (pos) found 12,050.

54d: ^{1}H NMR (500 MHz, CD_3SOCD_3) δ 7.97 (bs, amide NH's), 7.76 (bs, amide NH's), 7.47 (bs, all thiourea protons), 4.40—4.80 (m), 2.80—3.60 (m), 2.62 (bs), 2.40 (bs), 2.17 (bs); MALDI-TOF MS (pos) found 12,600.

54e: ^{1}H NMR (500 MHz, CD_3SOCD_3) δ 7.96 (bs, amide NH's), 7.76 (bs, amide NH's), 7.47 (bs, all thiourea protons), 4.40—4.80 (m), 2.80—3.60 (m), 2.62 (bs), 2.40 (bs), 2.18 (bs); MALDI-TOF MS (pos) found 13,600.

54f: ^{1}H NMR (500 MHz, CD_3SOCD_3) δ 7.97 (bs, amide NH's), 7.76 (bs, amide NH's), 7.47 (bs, all thiourea protons), 4.40—4.80 (m), 2.80—3.60 (m), 2.62 (bs), 2.40 (bs), 2.18 (bs); MALDI-TOF MS (pos) found 14,300.

Representative procedure for the synthesis of heterogeneously functionalized generation 4.0 PAMAM-based thiourea-linked ethoxy ethanol and 1-*O*-(5-thiourea-3-oxapentyl)-2,3,4,6-tetra-*O*-acetyl-α-D-mannopyranoside dendrimers (**51a-p**) (the following procedure is for **51a**. See Table 4.8 for quantities of reactants for **51b-p**). An aqueous solution of amine-terminated Starburst G(4)-PAMAM dendrimer (0.618 g of a 10% (w/w) solution in water, 61.8 mg, 4.57 μmol of dendrimer based on the M_W of 13,500 g/mol as determined by MALDI-TOF for G(4)-PAMAM) was lyophilized to leave a foam. The resulting residue was dissolved in DMSO (10 mL) followed by the addition of a 0.1 g/mL DMSO solution of **28** (350 μL, 35.0 mg, 238 μmol). The reaction was stirred for 8 hours. At this point, an aliquot (approx. 250 μL) containing **48a** was removed for MALDI-TOF MS analysis. A solution of a 0.1 g/mL DMSO solution of **29** (65 μL, 6.5 mg, 13.7 μmol) was added to the reaction. The reaction was stirred for 8 hours. The reaction mixture was added to a dialysis membrane (cellulose, MW cutoff 1 kDa) and the solution was dialyzed against DMSO for 12 hours. The solution was lyophilized to give **51a** as a thick syrupy product that was used without further purification. Approximately, 20-40 mg of the acetylated product was removed for MALDI-TOF MS analysis.

Representative deacetylation procedure to form generation 4.0 PAMAM-based thiourea-linked ethoxy ethanol and 1-*O*-(5-thiourea-3-oxapentyl)-α-D-mannopyranoside dendrimers (**55a-p**) (the following procedure is for **55a**. See Table 4.8 for quantities of reactants for the formation of **55b-h**). A suspension of acetylated mannose functionalized dendrimer **51a** in MeOH:H_2O (1:1, 20 mL) and 0.3 M methanolic NaOMe (41 μL, based on 0.9 moles of NaOMe for every mole of **29** on **51a**) was stirred overnight until all of the solid had dissolved. The solution was neutralized with Amberlite IR-120 (acidic). The reaction mixture was subjected to dialysis against 1:1 MeOH-H_2O, which was gradually changed to pure water. The aqueous solution was lyophilized to give **55a** as a fluffy, white solid.

Table 4.8 Quantities of reactants used to synthesize **55a-p**. See general procedure above for specific details.

#	Quantity of G(4)-PAMAM mg (μmol)	Quantity of **28** mg (μmol)	Quantity of **29** mg (μmol)	μL of 0.3M NaOMe	Yield of **55**[a] mg (%)
55a	61.8 (4.57)	35.0 (238)	6.54 (13.7)	41	67 (69)
55b	115 (8.51)	65.1 (443)	12.2 (25.5)	77	69 (36)
55c	145 (10.7)	77.3 (526)	30.7 (64.4)	193	71 (29)
55d	77.1 (5.71)	37.1 (252)	30.0 (62.8)	188	68 (53)
55e	136 (10.0)	64.9 (442)	52.7 (110)	330	124 (53)
55f	58.8 (4.35)	23.7 (161)	37.3 (78.3)	235	29 (29)
55g	137 (10.2)	56.7 (386)	82.3 (173)	519	100 (40)
55h	62.2 (4.61)	18.3 (125)	61.6 (129)	387	47 (43)
55i	113 (8.40)	27.2 (185)	133 (272)	816	179 (80)
55j	156 (11.5)	45.7 (311)	154 (323)	969	149 (49)
55k	67.5 (5.00)	14.0 (95.2)	85.9 (180)	540	44 (35)
55l	203 (15.1)	48.7 (331)	237 (497)	1490	167 (41)
55m	59.2 (4.38)	4.5 (31)	100 (210)	630	49 (41)
55n	149 (11.0)	27.5 (187)	199 (418)	1250	62 (20)

#	Quantity of G(4)-PAMAM mg (μmol)	Quantity of **28** mg (μmol)	Quantity of **29** mg (μmol)	μL of 0.3M NaOMe	Yield of **55**[a] mg (%)
55o	145 (10.7)	17.4 (118)	225 (471)	1410	200 (64)
55p	146 (10.7)	7.9 (53.1)	255 (535)	1600	117 (37)

[a] Reported yields are of isolated products and are lower than the actual yields because of removal of aliquots for MALDI-TOF MS. Percent yields are for three steps (addition of **28**, addition of **29** and deprotection).

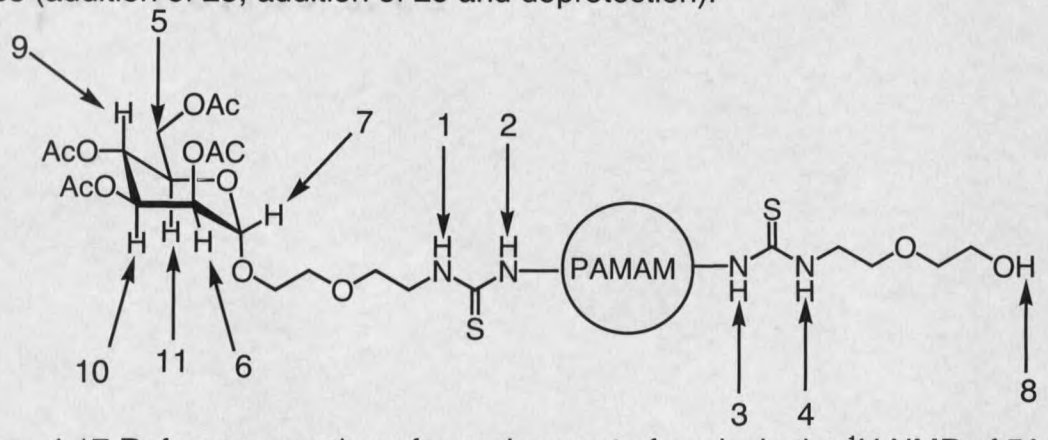


Figure 4.17 Reference numbers for assignment of peaks in the ^{1}H NMR of **51a-p**. Protons are numbered in order from low to high field.

Heterogeneously functionalized generation 4.0 PAMAM-based thiourea-linked ethoxy ethanol and 1-*O*-(5-thiourea-3-oxapentyl)-2,3,4,6-tetra-*O*-acetyl-α-D-mannopyranoside dendrimers (**51a-f**). Refer to Figure 4.17 for peak assignments. Integration values for H-8 (the hydroxyl proton of 28) is given as a decimal in order to make a comparison to sugar protons straightforward:

51a: ^{1}H NMR (500 MHz, CD_3SOCD_3) δ 7.97 (bs, amide NH's), 7.75 (bs, amide NH's), 7.47 (bs, 4H, H-1, H-2, H-3, and H-4), 5.07 (bs, 3H, H-5, H-6), 4.88 (bs, 1H, H-7) 4.57 (bs, 6.65H, H-8), 4.11 (m, 1H, H-9), 3.90—4.05 (m, 2H, H-10 and H-11), 2.80—3.80 (m), 2.10—2.70 (m), 2.09 (s, 3H), 1.98 (s, 6H), 1.89 (s, 3H); MALDI-TOF MS (pos) found 22,300.

51b: ^{1}H NMR (500 MHz, CD_3SOCD_3) δ 7.97 (bs, amide NH's), 7.76 (bs, amide NH's), 7.49 (bs, 4H, H-1, H-2, H-3, and H-4), 5.07 (bs, 3H, H-5, H-6), 4.88 (bs, 1H, H-7) 4.57 (bs, 4.10H, H-8), 4.11 (m, 1H, H-9), 3.90—4.05 (m, 2H, H-10 and H-11), 2.80—3.80 (m), 2.10—2.70 (m), 2.08 (s, 3H), 1.98 (s, 6H), 1.90 (s, 3H); MALDI-TOF MS (pos) found 23,700

51c: ^{1}H NMR (500 MHz, CD_3SOCD_3) δ 7.97 (bs, amide NH's), 7.76 (bs, amide NH's), 7.48 (bs, 4H, H-1, H-2, H-3, and H-4), 5.07 (bs, 3H, H-5, H-6), 4.88 (bs, 1H, H-7) 4.57 (bs, 3.73H, H-8), 4.11 (m, 1H, H-9), 3.90—4.05 (m, 2H, H-10 and H-11), 2.80—3.80 (m), 2.10—2.70 (m), 2.07 (s, 3H), 1.98 (s, 6H), 1.90 (s, 3H); MALDI-TOF MS (pos) found 24,100.

51d: ^{1}H NMR (500 MHz, CD_3SOCD_3) δ 7.97 (bs, amide NH's), 7.75 (bs, amide NH's), 7.47 (bs, 4H, H-1, H-2, H-3, and H-4), 5.06 (bs, 3H, H-5, H-6), 4.88 (bs, 1H, H-7) 4.57 (bs, 2.75H, H-8), 4.11 (m, 1H, H-9), 3.90—4.05 (m, 2H, H-10 and H-11), 2.80—3.80 (m), 2.10—2.70 (m), 2.07 (s, 3H), 1.98 (s, 6H), 1.89 (s, 3H); MALDI-TOF MS (pos) found 24,800.

51e: ^{1}H NMR (500 MHz, CD_3SOCD_3) δ 7.97 (bs, amide NH's), 7.75 (bs, amide NH's), 7.48 (bs, 4H, H-1, H-2, H-3, and H-4), 5.07 (bs, 3H, H-5, H-6), 4.88 (bs, 1H, H-7) 4.57 (bs, 1.83H, H-8), 4.11 (m, 1H, H-9), 3.90—4.05 (m, 2H, H-10 and H-11), 2.80—3.80 (m), 2.10—2.70 (m), 2.07 (s, 3H), 1.98 (s, 6H), 1.89 (s, 3H); MALDI-TOF MS (pos) found 25,800.

51f: ^{1}H NMR (500 MHz, CD_3SOCD_3) δ 7.97 (bs, amide NH's), 7.75 (bs, amide NH's), 7.47 (bs, 4H, H-1, H-2, H-3, and H-4), 5.07 (bs, 3H, H-5, H-6), 4.88 (bs, 1H, H-7) 4.57 (bs, 1.61H, H-8), 4.11 (m, 1H, H-9), 3.90—4.05 (m, 2H, H-10 and H-11), 2.80—3.80 (m), 2.10—2.70 (m), 2.06 (s, 3H), 1.98 (s, 6H), 1.89 (s, 3H); MALDI-TOF MS (pos) found 26,200.

51g: ^{1}H NMR (500 MHz, CD_3SOCD_3) δ 7.97 (bs, amide NH's), 7.75 (bs, amide NH's), 7.48 (bs, 4H, H-1, H-2, H-3, and H-4), 5.06 (bs, 3H, H-5, H-6), 4.88 (bs, 1H, H-7) 4.56 (bs, 1.09H, H-8), 4.11 (m, 1H, H-9), 3.90—4.05 (m, 2H, H-10 and H-11), 2.80—3.80 (m), 2.10—2.70 (m), 2.06 (s, 3H), 1.98 (s, 6H), 1.89 (s, 3H); MALDI-TOF MS (pos) found 27,900.

51h: ^{1}H NMR (500 MHz, CD_3SOCD_3) δ 7.96 (bs, amide NH's), 7.75 (bs, amide NH's), 7.47 (bs, 4H, H-1, H-2, H-3, and H-4), 5.06 (bs, 3H, H-5, H-6), 4.88 (bs, 1H, H-7) 4.57 (bs, 0.79H, H-8), 4.11 (m, 1H, H-9), 3.90—4.05 (m, 2H, H-10 and H-11), 2.80—3.80 (m), 2.10—2.70 (m), 2.06 (s, 3H), 1.98 (s, 6H), 1.89 (s, 3H); MALDI-TOF MS (pos) found 28,500.

51i: ^{1}H NMR (500 MHz, CD_3SOCD_3) δ 7.96 (bs, amide NH's), 7.75 (bs, amide NH's), 7.47 (bs, 4H, H-1, H-2, H-3, and H-4), 5.06 (bs, 3H, H-5, H-6), 4.88 (bs, 1H, H-7) 4.56 (bs, 0.37H, H-8), 4.11 (m, 1H, H-9), 3.90—4.05 (m, 2H, H-10 and H-11), 2.80—3.80 (m), 2.10—2.70 (m), 2.07 (s, 3H), 1.98 (s, 6H), 1.89 (s, 3H); MALDI-TOF MS (pos) found 31,600.

51j: ^{1}H NMR (500 MHz, CD_3SOCD_3) δ 7.95 (bs, amide NH's), 7.74 (bs, amide NH's), 7.47 (bs, 4H, H-1, H-2, H-3, and H-4), 5.06 (bs, 3H, H-5, H-6), 4.88 (bs, 1H, H-7) 4.56 (bs, 0.66H, H-8), 4.11 (m, 1H, H-9), 3.90—4.05 (m, 2H, H-10 and H-11), 2.80—3.80 (m), 2.10—2.70 (m), 2.07 (s, 3H), 1.98 (s, 6H), 1.89 (s, 3H); MALDI-TOF MS (pos) found 31,950.

51k: ^{1}H NMR (500 MHz, CD_3SOCD_3) δ 7.95 (bs, amide NH's), 7.74 (bs, amide NH's), 7.47 (bs, 4H, H-1, H-2, H-3, and H-4), 5.06 (bs, 3H, H-5, H-6), 4.88 (bs, 1H, H-7) 4.56 (bs, 0.44H, H-8), 4.11 (m, 1H, H-9), 3.90—4.05 (m, 2H, H-10 and H-11), 2.80—3.80 (m), 2.10—2.70 (m), 2.07 (s, 3H), 1.98 (s, 6H), 1.89 (s, 3H); MALDI-TOF MS (pos) found 30,500.

51l: ^{1}H NMR (500 MHz, CD_3SOCD_3) δ 7.95 (bs, amide NH's), 7.74 (bs, amide NH's), 7.47 (bs, 4H, H-1, H-2, H-3, and H-4), 5.06 (bs, 3H, H-5, H-6), 4.88 (bs, 1H, H-7) 4.56 (bs, 0.49H, H-8), 4.11 (m, 1H, H-9), 3.90—4.05 (m, 2H, H-10 and H-11), 2.80—3.80 (m), 2.10—2.70 (m), 2.07 (s, 3H), 1.98 (s, 6H), 1.90 (s, 3H); MALDI-TOF MS (pos) found 32,900.

51m: ^{1}H NMR (500 MHz, CD_3SOCD_3) δ 7.96 (bs, amide NH's), 7.75 (bs, amide NH's), 7.47 (bs, 4H, H-1, H-2, H-3, and H-4), 5.06 (bs, 3H, H-5, H-6), 4.88 (bs, 1H, H-7) 4.56 (bs, 0.40H, H-8), 4.11 (m, 1H, H-9), 3.90—4.05 (m, 2H, H-10 and H-11), 2.80—3.80 (m), 2.10—2.70 (m), 2.07 (s, 3H), 1.98 (s, 6H), 1.89 (s, 3H); MALDI-TOF MS (pos) found 32,000.

51n: ^{1}H NMR (500 MHz, CD_3SOCD_3) δ 7.95 (bs, amide NH's), 7.74 (bs, amide NH's), 7.47 (bs, 4H, H-1, H-2, H-3, and H-4), 5.06 (bs, 3H, H-5, H-6), 4.88 (bs, 1H, H-7) 4.56 (bs, 0.31H, H-8), 4.11 (m, 1H, H-9), 3.90—4.05 (m, 2H, H-10 and H-11), 2.80—3.80 (m), 2.10—2.70 (m), 2.07 (s, 3H), 1.98 (s, 6H), 1.90 (s, 3H); MALDI-TOF MS (pos) found 35,000.

51o: ^{1}H NMR (500 MHz, CD_3SOCD_3) δ 7.95 (bs, amide NH's), 7.74 (bs, amide NH's), 7.47 (bs, 4H, H-1, H-2, H-3, and H-4), 5.06 (bs, 3H, H-5, H-6), 4.88 (bs, 1H, H-7) 4.56 (bs, 0.05H, H-8), 4.11 (m, 1H, H-9), 3.90—4.05 (m, 2H, H-10 and H-11), 2.80—3.80 (m), 2.10—2.70 (m), 2.07 (s, 3H), 1.98 (s, 6H), 1.90 (s, 3H); MALDI-TOF MS (pos) found 37,000.

51p: ^{1}H NMR (500 MHz, CD_3SOCD_3) δ 7.95 (bs, amide NH's), 7.74 (bs, amide NH's), 7.47 (bs, 4H, H-1, H-2, H-3, and H-4), 5.06 (bs, 3H, H-5, H-6), 4.88 (bs, 1H, H-7) 4.56 (bs, 0.05H, H-8), 4.11 (m, 1H, H-9), 3.90—4.05 (m, 2H, H-10 and H-11), 2.80—3.80 (m), 2.10—2.70 (m), 2.07 (s, 3H), 1.98 (s, 6H), 1.90 (s, 3H); MALDI-TOF MS (pos) found 38,400.

Deacetylated generation 4.0 PAMAM-based thiourea-linked ethoxy ethanol and 1-*O*-(5-thiourea-3-oxapentyl)-α-D-mannopyranoside dendrimers (**55a-p**):

55a: ^{1}H NMR (500 MHz, CD_3SOCD_3) δ 7.97 (bs, amide NH's), 7.76 (bs, amide NH's), 7.47 (bs, all thiourea protons), 4.40—4.80 (m), 2.80—3.60 (m), 2.63 (bs), 2.40 (bs), 2.17 (bs); MALDI-TOF MS (pos) found 21,220.

55b: ^{1}H NMR (500 MHz, CD_3SOCD_3) δ 7.97 (bs, amide NH's), 7.76 (bs, amide NH's), 7.47 (bs, all thiourea protons), 4.40—4.80 (m), 2.80—3.60 (m), 2.63 (bs), 2.40 (bs), 2.17 (bs); MALDI-TOF MS (pos) found 22,340.

55c: ^{1}H NMR (500 MHz, CD_3SOCD_3) δ 7.97 (bs, amide NH's), 7.76 (bs, amide NH's), 7.47 (bs, all thiourea protons), 4.40—4.80 (m), 2.80—3.60 (m), 2.63 (bs), 2.40 (bs), 2.17 (bs); MALDI-TOF MS (pos) found 22,500.

55d: ^{1}H NMR (500 MHz, CD_3SOCD_3) δ 7.97 (bs, amide NH's), 7.76 (bs, amide NH's), 7.47 (bs, all thiourea protons), 4.40—4.80 (m), 2.80—3.60 (m), 2.63 (bs), 2.40 (bs), 2.17 (bs); MALDI-TOF MS (pos) found 22,500.

55e: ^{1}H NMR (500 MHz, CD_3SOCD_3) δ 7.97 (bs, amide NH's), 7.76 (bs, amide NH's), 7.47 (bs, all thiourea protons), 4.40—4.80 (m), 2.80—3.60 (m), 2.63 (bs), 2.40 (bs), 2.17 (bs); MALDI-TOF MS (pos) found 23,300.

55f: ^{1}H NMR (500 MHz, CD_3SOCD_3) δ 7.97 (bs, amide NH's), 7.76 (bs, amide NH's), 7.47 (bs, all thiourea protons), 4.40—4.80 (m), 2.80—3.60 (m), 2.63 (bs), 2.40 (bs), 2.17 (bs); MALDI-TOF MS (pos) found 23,100.

55g: ^{1}H NMR (500 MHz, CD_3SOCD_3) δ 7.96 (bs, amide NH's), 7.76 (bs, amide NH's), 7.48 (bs, all thiourea protons), 4.40—4.80 (m), 2.80—3.60 (m), 2.63 (bs), 2.40 (bs), 2.17 (bs); MALDI-TOF MS (pos) found 24,500.

55h: ^{1}H NMR (500 MHz, CD_3SOCD_3) δ 7.97 (bs, amide NH's), 7.76 (bs, amide NH's), 7.47 (bs, all thiourea protons), 4.40—4.80 (m), 2.80—3.60 (m), 2.63 (bs), 2.40 (bs), 2.17 (bs); MALDI-TOF MS (pos) found 23,800.

55i: ^{1}H NMR (500 MHz, CD_3SOCD_3) δ 7.97 (bs, amide NH's), 7.76 (bs, amide NH's), 7.47 (bs, all thiourea protons), 4.40—4.80 (m), 2.80—3.60 (m), 2.63 (bs), 2.40 (bs), 2.17 (bs); MALDI-TOF MS (pos) found 26,600.

55j: ^{1}H NMR (500 MHz, CD_3SOCD_3) δ 7.97 (bs, amide NH's), 7.77 (bs, amide NH's), 7.47 (bs, all thiourea protons), 4.40—4.80 (m), 2.80—3.60 (m), 2.63 (bs), 2.40 (bs), 2.17 (bs); MALDI-TOF MS (pos) found 26,600.

55k: ^{1}H NMR (500 MHz, CD_3SOCD_3) δ 7.97 (bs, amide NH's), 7.76 (bs, amide NH's), 7.47 (bs, all thiourea protons), 4.40—4.80 (m), 2.80—3.60 (m), 2.63 (bs), 2.40 (bs), 2.17 (bs); MALDI-TOF MS (pos) found 25,000.

55l: ^{1}H NMR (500 MHz, CD_3SOCD_3) δ 7.96 (bs, amide NH's), 7.75 (bs, amide NH's), 7.47 (bs, all thiourea protons), 4.40—4.80 (m), 2.80—3.60 (m), 2.63 (bs), 2.40 (bs), 2.17 (bs); MALDI-TOF MS (pos) found 27,100.

55m: ^{1}H NMR (500 MHz, CD_3SOCD_3) δ 7.97 (bs, amide NH's), 7.76 (bs, amide NH's), 7.47 (bs, all thiourea protons), 4.40—4.80 (m), 2.80—3.60 (m), 2.63 (bs), 2.40 (bs), 2.17 (bs); MALDI-TOF MS (pos) found 25,200.

55n: ^{1}H NMR (500 MHz, CD_3SOCD_3) δ 7.97 (bs, amide NH's), 7.76 (bs, amide NH's), 7.47 (bs, all thiourea protons), 4.40—4.80 (m), 2.80—3.60 (m), 2.63 (bs), 2.40 (bs), 2.17 (bs); MALDI-TOF MS (pos) found 28,100.

55o: ^{1}H NMR (500 MHz, CD_3SOCD_3) δ 7.96 (bs, amide NH's), 7.76 (bs, amide NH's), 7.47 (bs, all thiourea protons), 4.40—4.80 (m), 2.80—3.60 (m), 2.63 (bs), 2.40 (bs), 2.17 (bs); MALDI-TOF MS (pos) found 29,100.

55p: ^{1}H NMR (500 MHz, CD_3SOCD_3) δ 7.97 (bs, amide NH's), 7.76 (bs, amide NH's), 7.47 (bs, all thiourea protons), 4.40—4.80 (m), 2.80—3.60 (m), 2.63 (bs), 2.40 (bs), 2.17 (bs); MALDI-TOF MS (pos) found 30,000.

Representative procedure for the synthesis of heterogeneously functionalized generation 5.0 PAMAM-based thiourea-linked ethoxy ethanol and 1-*O*-(5-thiourea-3-oxapentyl)-2,3,4,6-tetra-*O*-acetyl-α-D-mannopyranoside dendrimers (**52a-h**) (the following procedure is for **52a**. See Table 4.10 for quantities of reactants for **52b-h**). An aqueous solution of amine-terminated Starburst G(5)-PAMAM dendrimer (0.338 g of a 23% (w/w) solution in water, 77.7 mg, 3.05 μmol of dendrimer based on the M_W of 25,500 g/mol as determined by MALDI-TOF for G(5)-PAMAM) was lyophilized to leave a foam. The resulting residue was dissolved in DMSO (10 mL) followed by the addition of a 0.1 g/mL DMSO solution of **28** (421 μL, 42.1 mg, 286 μmol). The reaction was stirred for 8 hours. At this point, an aliquot (approx. 250 μL) containing **48a** was removed for MALDI-TOF MS analysis. A solution of a 0.1 g/mL DMSO solution of **29** (87 μL, 8.7 mg, 18.3 μmol) was added to the reaction. The reaction was stirred for 8 hours. The reaction mixture was added to a dialysis membrane (cellulose, MW cutoff 1 kDa) and the solution was dialyzed against DMSO for 12 hours. The solution was lyophilized to give **52a** as a thick syrupy product that was used without further purification. Approximately, 20-40 mg of the acetylated product was removed for MALDI-TOF MS analysis.

Representative deacetylation procedure to form generation 5.0 PAMAM-based thiourea-linked ethoxy ethanol and 1-*O*-(5-thiourea-3-oxapentyl)-α-D-mannopyranoside dendrimers (**56a-h**) (the following procedure is for **56a**. See Table 4.10 for quantities of reactants for the formation of **56b-h**). A suspension of acetylated mannose functionalized dendrimer **52a** in MeOH:H_2O (1:1, 20 mL) and 0.3 M methanolic NaOMe (55 μL, based on 0.9 moles of NaOMe for every mole of **29** on **52a**) was stirred overnight until all of the solid had dissolved. The solution was neutralized with Amberlite IR-120 (acidic). The reaction mixture was subjected to dialysis against 1:1 MeOH-H_2O, which was gradually changed to pure water. The aqueous solution was lyophilized to give **56a** as a fluffy, white solid.

Table 4.9 Quantities of reactants used to synthesize **56a-h**. See general procedure above for specific details.

#	Quantity of G(5)-PAMAM mg (μmol)	Quantity of **28** mg (μmol)	Quantity of **29** mg (μmol)	μL of 0.3M NaOMe	Yield of **56**[a] mg (%)
56a	77.7 (3.05)	42.1 (286)	8.72 (18.3)	55	84 (64)
56b	39.9 (1.56)	21.5 (146)	4.48 (9.38)	28	18 (29)
56c	62.2 (2.43)	28.7 (195)	23.3 (48.8)	146	41 (38)
56d	62.4 (2.44)	24.0 (163)	38.5 (80.7)	242	51 (44)
56e	61.1 (2.40)	17.6 (120)	57.1 (120)	360	93 (77)
56f	37.0 (1.45)	7.24 (49.3)	45.7 (95.7)	287	22 (32)
56g	64.7 (2.53)	8.95 (60.9)	79.8 (168)	505	122 (89)
56h	68.1 (2.69)	4.7 (32.0)	112 (235)	705	134 (90)

[a] Reported yields are of isolated products and are lower than the actual yields because of removal of aliquots for MALDI-TOF MS. Percent yields are for three steps (addition of **28**, addition of **29** and deprotection).

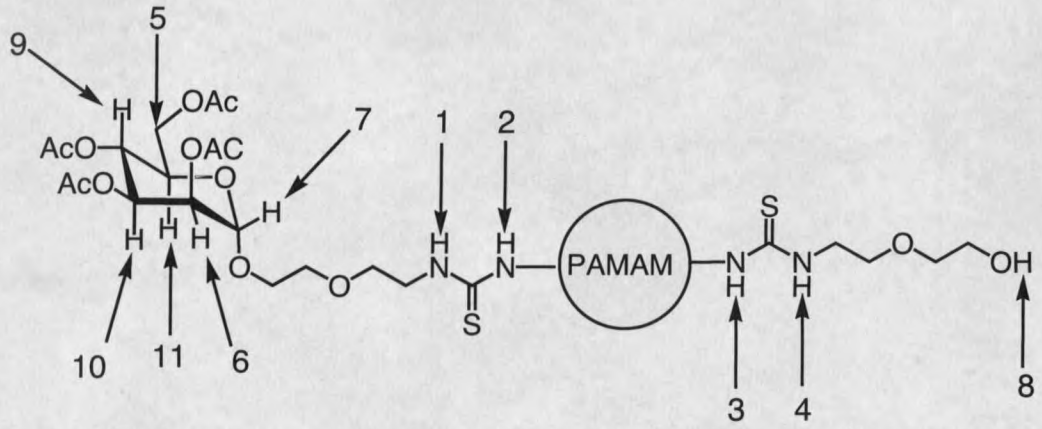


Figure 4.18 Reference numbers for assignment of peaks in the ^{1}H NMR of **52a-h**. Protons are numbered in order from low to high field.

Heterogeneously functionalized generation 5.0 PAMAM-based thiourea-linked ethoxy ethanol and 1-*O*-(5-thiourea-3-oxapentyl)-2,3,4,6-tetra-*O*-acetyl-α-D-mannopyranoside dendrimers (**52a-h**). Refer to Figure 4.18 for peak assignments. Integration values for H-8 (the hydroxyl proton of 28) is given as a decimal in order to make a comparison to sugar protons straightforward:

52a: ^{1}H NMR (500 MHz, CD_3SOCD_3) δ 7.97 (bs, amide NH's), 7.76 (bs, amide NH's), 7.47 (bs, 4H, H-1, H-2, H-3, and H-4), 5.07 (bs, 3H, H-5, H-6), 4.89 (bs, 1H, H-7) 4.58 (bs, 9.80H, H-8), 4.11 (m, 1H, H-9), 3.90—4.05 (m, 2H, H-10 and H-11), 2.80—3.80 (m), 2.10—2.70 (m), 2.07 (s, 3H), 1.98 (s, 6H), 1.89 (s, 3H); MALDI-TOF MS (pos) found 42,800.

52b: ^{1}H NMR (500 MHz, CD_3SOCD_3) δ 7.97 (bs, amide NH's), 7.76 (bs, amide NH's), 7.47 (bs, 4H, H-1, H-2, H-3, and H-4), 5.07 (bs, 3H, H-5, H-6), 4.88 (bs, 1H, H-7) 4.58 (bs, 11.2H, H-8), 4.11 (m, 1H, H-9), 3.90—4.05 (m, 2H, H-10

and H-11), 2.80—3.80 (m), 2.10—2.70 (m), 2.07 (s, 3H), 1.98 (s, 6H), 1.89 (s, 3H); MALDI-TOF MS (pos) found 41,500.

52c: ^{1}H NMR (500 MHz, CD_3SOCD_3) δ 7.97 (bs, amide NH's), 7.76 (bs, amide NH's), 7.47 (bs, 4H, H-1, H-2, H-3, and H-4), 5.07 (bs, 3H, H-5, H-6), 4.89 (bs, 1H, H-7) 4.58 (bs, 3.50H, H-8), 4.11 (m, 1H, H-9), 3.90—4.05 (m, 2H, H-10 and H-11), 2.80—3.80 (m), 2.10—2.70 (m), 2.07 (s, 3H), 1.98 (s, 6H), 1.89 (s, 3H); MALDI-TOF MS (pos) found 47,300.

52d: ^{1}H NMR (500 MHz, CD_3SOCD_3) δ 7.97 (bs, amide NH's), 7.75 (bs, amide NH's), 7.47 (bs, 4H, H-1, H-2, H-3, and H-4), 5.07 (bs, 3H, H-5, H-6), 4.89 (bs, 1H, H-7) 4.58 (bs, 1.52H, H-8), 4.11 (m, 1H, H-9), 3.90—4.05 (m, 2H, H-10 and H-11), 2.80—3.80 (m), 2.10—2.70 (m), 2.07 (s, 3H), 1.98 (s, 6H), 1.89 (s, 3H); MALDI-TOF MS (pos) found 51,800.

52e: ^{1}H NMR (500 MHz, CD_3SOCD_3) δ 7.96 (bs, amide NH's), 7.75 (bs, amide NH's), 7.47 (bs, 4H, H-1, H-2, H-3, and H-4), 5.07 (bs, 3H, H-5, H-6), 4.89 (bs, 1H, H-7) 4.57 (bs, 0.74H, H-8), 4.11 (m, 1H, H-9), 3.90—4.05 (m, 2H, H-10 and H-11), 2.80—3.80 (m), 2.10—2.70 (m), 2.07 (s, 3H), 1.98 (s, 6H), 1.89 (s, 3H); MALDI-TOF MS (pos) found 58,100.

52f: ^{1}H NMR (500 MHz, CD_3SOCD_3) δ 7.95 (bs, amide NH's), 7.74 (bs, amide NH's), 7.47 (bs, 4H, H-1, H-2, H-3, and H-4), 5.06 (bs, 3H, H-5, H-6), 4.88 (bs, 1H, H-7) 4.56 (bs, 0.42H, H-8), 4.11 (m, 1H, H-9), 3.90—4.05 (m, 2H, H-10

and H-11), 2.80—3.80 (m), 2.10—2.70 (m), 2.07 (s, 3H), 1.98 (s, 6H), 1.89 (s, 3H); MALDI-TOF MS (pos) found 59,700.

52g: ^{1}H NMR (500 MHz, CD_3SOCD_3) δ 7.95 (bs, amide NH's), 7.74 (bs, amide NH's), 7.47 (bs, 4H, H-1, H-2, H-3, and H-4), 5.07 (bs, 3H, H-5, H-6), 4.89 (bs, 1H, H-7) 4.56 (bs, 0.21H, H-8), 4.11 (m, 1H, H-9), 3.90—4.05 (m, 2H, H-10 and H-11), 2.80—3.80 (m), 2.10—2.70 (m), 2.07 (s, 3H), 1.98 (s, 6H), 1.89 (s, 3H); MALDI-TOF MS (pos) found 64,500.

52h: ^{1}H NMR (500 MHz, CD_3SOCD_3) δ 7.95 (bs, amide NH's), 7.74 (bs, amide NH's), 7.47 (bs, 4H, H-1, H-2, H-3, and H-4), 5.08 (bs, 3H, H-5, H-6), 4.89 (bs, 1H, H-7) 4.56 (bs, 0.08H, H-8), 4.11 (m, 1H, H-9), 3.90—4.05 (m, 2H, H-10 and H-11), 2.80—3.80 (m), 2.10—2.70 (m), 2.07 (s, 3H), 1.98 (s, 6H), 1.89 (s, 3H); MALDI-TOF MS (pos) found 69,400.

Deacetylated generation 5.0 PAMAM-based thiourea-linked ethoxy ethanol and 1-*O*-(5-thiourea-3-oxapentyl)-α-D-mannopyranoside dendrimers (**56a-h**):

56a: ^{1}H NMR (500 MHz, CD_3SOCD_3) δ 7.98 (bs, amide NH's), 7.78 (bs, amide NH's), 7.47 (bs, all thiourea protons), 4.30—4.80 (m), 2.90—3.70 (m), 2.64 (bs), 2.41 (bs), 2.18 (bs); MALDI-TOF MS (pos) found 42,750.

56b: ^{1}H NMR (500 MHz, CD_3SOCD_3) δ 7.98 (bs, amide NH's), 7.76 (bs, amide NH's), 7.48 (bs, all thiourea protons), 4.30—4.80 (m), 2.90—3.70 (m), 2.63 (bs), 2.40 (bs), 2.17 (bs); MALDI-TOF MS (pos) found 40,100.

56c: ^{1}H NMR (500 MHz, CD_3SOCD_3) δ 7.98 (bs, amide NH's), 7.78 (bs, amide NH's), 7.47 (bs, all thiourea protons), 4.30—4.80 (m), 2.90—3.70 (m), 2.65 (bs), 2.41 (bs), 2.18 (bs); MALDI-TOF MS (pos) found 45,000.

56d: ^{1}H NMR (500 MHz, CD_3SOCD_3) δ 7.98 (bs, amide NH's), 7.80 (bs, amide NH's), 7.47 (bs, all thiourea protons), 4.30—4.80 (m), 2.90—3.70 (m), 2.64 (bs), 2.41 (bs), 2.19 (bs); MALDI-TOF MS (pos) found 47,400.

56e: ^{1}H NMR (500 MHz, CD_3SOCD_3) δ 7.98 (bs, amide NH's), 7.79 (bs, amide NH's), 7.47 (bs, all thiourea protons), 4.30—4.80 (m), 2.90—3.70 (m), 2.64 (bs), 2.41 (bs), 2.18 (bs); MALDI-TOF MS (pos) found 50,600.

56f: ^{1}H NMR (500 MHz, CD_3SOCD_3) δ 7.98 (bs, amide NH's), 7.79 (bs, amide NH's), 7.47 (bs, all thiourea protons), 4.30—4.80 (m), 2.90—3.70 (m), 2.65 (bs), 2.41 (bs), 2.19 (bs); MALDI-TOF MS (pos) found 48,100.

56g: ^{1}H NMR (500 MHz, CD_3SOCD_3) δ 7.99 (bs, amide NH's), 7.82 (bs, amide NH's), 7.48 (bs, all thiourea protons), 4.30—4.80 (m), 2.90—3.70 (m), 2.67 (bs), 2.41 (bs), 2.19 (bs); MALDI-TOF MS (pos) found 54,200.

56h: ^{1}H NMR (500 MHz, CD_3SOCD_3) δ 7.99 (bs, amide NH's), 7.81 (bs, amide NH's), 7.47 (bs, all thiourea protons), 4.30—4.80 (m), 2.90—3.70 (m), 2.67 (bs), 2.41 (bs), 2.20 (bs); MALDI-TOF MS (pos) found 55,600.

Representative procedure for the synthesis of heterogeneously functionalized generation 6.0 PAMAM-based thiourea-linked ethoxy ethanol and 1-*O*-(5-thiourea-3-oxapentyl)-2,3,4,6-tetra-*O*-acetyl-α-D-mannopyranoside

dendrimers (**53a-m**) (the following procedure is for **53a**. See Table 4.10 for quantities of reactants for **53b-m**). An aqueous solution of amine-terminated Starburst G(6)-PAMAM dendrimer (0.578 g of a 17.3% (w/w) solution in water, 100 mg, 1.96 μmol of dendrimer based on the M_W of 50,800 g/mol as determined by MALDI-TOF for G(6)-PAMAM) was lyophilized to leave a foam. The resulting residue was dissolved in DMSO (10 mL) followed by the addition of a 0.1 g/mL DMSO solution of **28** (555 μL, 55.5 mg, 378 μmol). The reaction was stirred for 8 hours. At this point, an aliquot (approx. 250 μL) containing **49a** was removed for MALDI-TOF MS analysis. A solution of a 0.1 g/mL DMSO solution of **29** (187 μL, 18.7 mg, 39.4 μmol) was added to the reaction. The reaction was stirred for 8 hours. The reaction mixture was added to a dialysis membrane (cellulose, MW cutoff 1 kDa) and the solution was dialyzed against DMSO for 12 hours. The solution was lyophilized to give **53a** as a thick syrupy product that was used without further purification. Approximately, 20-40 mg of the acetylated product was removed for MALDI-TOF MS analysis.

Representative deacetylation procedure to form generation 6.0 PAMAM-based thiourea-linked ethoxy ethanol and 1-*O*-(5-thiourea-3-oxapentyl)-α-D-mannopyranoside dendrimers (**57a-m**) (the following procedure is for **57a**. See Table 4.10 for quantities of reactants for the formation of **57b-m**). A suspension of acetylated mannose functionalized dendrimer **53a** in MeOH:H_2O (1:1, 20 mL) and 0.3 M methanolic NaOMe (65 μL, based on 0.9 moles of NaOMe for every

mole of **29** on **53a**) was stirred overnight until all of the solid had dissolved. The solution was neutralized with Amberlite IR-120 (acidic). The reaction mixture was subjected to dialysis against 1:1 MeOH-H_2O, which was gradually changed to pure water. The aqueous solution was lyophilized to give **57a** as a fluffy, white solid.

Table 4.10 Quantities of reactants used to synthesize **57a-m**. See general procedure above for specific details.

#	Quantity of G(6)-PAMAM mg (μmol)	Quantity of **28** mg (μmol)	Quantity of **29** mg (μmol)	μL of 0.3M NaOMe	Yield of **57**[a] mg (%)
57a	100 (1.96)	55.5 (378)	18.7 (39.4)	118	87 (57)
57b	100 (1.96)	49.2 (335)	39.4 (82.6)	247	75 (49)
57c	70.8 (1.38)	29.4 (200)	45 (94.3)	283	78 (70)
57d	77.7 (1.53)	36.0 (245)	7.3 (15.3)	100	91 (74)
57e	100 (1.96)	42.8 (291)	60.1 (126)	378	124 (78)
57f	80.6 (1.59)	31.7 (215)	25.7 (53.9)	162	75 (57)
57g	78.1 (1.53)	25.8 (175)	41.1 (86.0)	258	48 (36)
57h	100 (1.96)	30.7 (209)	99.5 (208)	624	81 (46)
57i	100 (1.96)	18.5 (126)	139 (291)	873	125 (71)
57j	84.1 (1.66)	14.1 (95.9)	88.4 (185)	555	125 (80)
57k	100 (1.96)	12.1 (82.6)	160 (335)	1005	68 (36)
57l	100 (1.96)	6.07 (41.3)	179 (376)	1128	149 (78)
57m	85.7 (1.69)	4.96 (33.7)	120 (253)	759	137 (81)

[a] Reported yields are of isolated products and are lower than the actual yields because of removal of aliquots for MALDI-TOF MS. Percent yields are for three steps (addition of **28**, addition of **29** and deprotection).

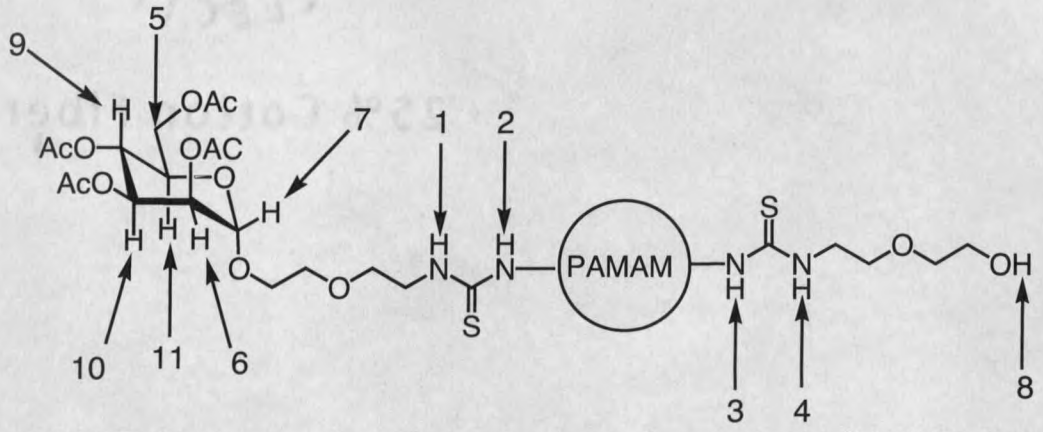


Figure 4.19 Reference numbers for assignment of peaks in the ^{1}H NMR of **53a-m**. Protons are numbered in order from low to high field.

Heterogeneously functionalized generation 6.0 PAMAM-based thiourea-linked ethoxy ethanol and 1-*O*-(5-thiourea-3-oxapentyl)-2,3,4,6-tetra-*O*-acetyl-α-D-mannopyranoside dendrimers (**53a-m**). Refer to Figure 4.19 for peak assignments. Integration values for H-8 (the hydroxyl proton of 28) is given as a decimal in order to make a comparison to sugar protons straightforward:

53a: ^{1}H NMR (500 MHz, CD_3SOCD_3) δ 7.98 (bs, amide NH's), 7.76 (bs, amide NH's), 7.48 (bs, 4H, H-1, H-2, H-3, and H-4), 5.07 (bs, 3H, H-5, H-6), 4.88 (bs, 1H, H-7) 4.58 (bs, 15.11H, H-8), 4.11 (m, 1H, H-9), 3.90—4.05 (m, 2H, H-10 and H-11), 2.80—3.80 (m), 2.10—2.70 (m), 2.07 (s, 3H), 1.98 (s, 6H), 1.90 (s, 3H); MALDI-TOF MS (pos) found 79,200.

53b: ^{1}H NMR (500 MHz, CD_3SOCD_3) δ 7.98 (bs, amide NH's), 7.77 (bs, amide NH's), 7.48 (bs, 4H, H-1, H-2, H-3, and H-4), 5.07 (bs, 3H, H-5, H-6), 4.88 (bs, 1H, H-7) 4.58 (bs, 8.52H, H-8), 4.11 (m, 1H, H-9), 3.90—4.05 (m, 2H, H-10

and H-11), 2.80—3.80 (m), 2.10—2.70 (m), 2.07 (s, 3H), 1.98 (s, 6H), 1.90 (s, 3H); MALDI-TOF MS (pos) found 81,000.

53c: ^{1}H NMR (500 MHz, CD_3SOCD_3) δ 7.97 (bs, amide NH's), 7.75 (bs, amide NH's), 7.46 (bs, 4H, H-1, H-2, H-3, and H-4), 5.07 (bs, 3H, H-5, H-6), 4.88 (bs, 1H, H-7) 4.58 (bs, 5.77H, H-8), 4.11 (m, 1H, H-9), 3.90—4.05 (m, 2H, H-10 and H-11), 2.80—3.80 (m), 2.10—2.70 (m), 2.07 (s, 3H), 1.98 (s, 6H), 1.90 (s, 3H); MALDI-TOF MS (pos) found 84,400.

53d: ^{1}H NMR (500 MHz, CD_3SOCD_3) δ 7.97 (bs, amide NH's), 7.75 (bs, amide NH's), 7.46 (bs, 4H, H-1, H-2, H-3, and H-4), 5.07 (bs, 3H, H-5, H-6), 4.88 (bs, 1H, H-7) 4.57 (bs, 4.15H, H-8), 4.11 (m, 1H, H-9), 3.90—4.05 (m, 2H, H-10 and H-11), 2.80—3.80 (m), 2.10—2.70 (m), 2.07 (s, 3H), 1.98 (s, 6H), 1.90 (s, 3H); MALDI-TOF MS (pos) found 86,400.

53e: ^{1}H NMR (500 MHz, CD_3SOCD_3) δ 7.97 (bs, amide NH's), 7.75 (bs, amide NH's), 7.47 (bs, 4H, H-1, H-2, H-3, and H-4), 5.07 (bs, 3H, H-5, H-6), 4.88 (bs, 1H, H-7) 4.57 (bs, 3.14H, H-8), 4.11 (m, 1H, H-9), 3.90—4.05 (m, 2H, H-10 and H-11), 2.80—3.80 (m), 2.10—2.70 (m), 2.07 (s, 3H), 1.98 (s, 6H), 1.90 (s, 3H); MALDI-TOF MS (pos) found 87,900.

53f: ^{1}H NMR (500 MHz, CD_3SOCD_3) δ 7.96 (bs, amide NH's), 7.75 (bs, amide NH's), 7.46 (bs, 4H, H-1, H-2, H-3, and H-4), 5.07 (bs, 3H, H-5, H-6), 4.88 (bs, 1H, H-7) 4.57 (bs, 2.16H, H-8), 4.11 (m, 1H, H-9), 3.90—4.05 (m, 2H, H-10

and H-11), 2.80—3.80 (m), 2.10—2.70 (m), 2.07 (s, 3H), 1.98 (s, 6H), 1.90 (s, 3H); MALDI-TOF MS (pos) found 93,200.

53g: ^{1}H NMR (500 MHz, CD_3SOCD_3) δ 7.96 (bs, amide NH's), 7.74 (bs, amide NH's), 7.46 (bs, 4H, H-1, H-2, H-3, and H-4), 5.07 (bs, 3H, H-5, H-6), 4.88 (bs, 1H, H-7) 4.57 (bs, 1.38H, H-8), 4.11 (m, 1H, H-9), 3.90—4.05 (m, 2H, H-10 and H-11), 2.80—3.80 (m), 2.10—2.70 (m), 2.07 (s, 3H), 1.98 (s, 6H), 1.90 (s, 3H); MALDI-TOF MS (pos) found 99,200.

53h: ^{1}H NMR (500 MHz, CD_3SOCD_3) δ 7.96 (bs, amide NH's), 7.75 (bs, amide NH's), 7.47 (bs, 4H, H-1, H-2, H-3, and H-4), 5.07 (bs, 3H, H-5, H-6), 4.88 (bs, 1H, H-7) 4.57 (bs, 0.87H, H-8), 4.11 (m, 1H, H-9), 3.90—4.05 (m, 2H, H-10 and H-11), 2.80—3.80 (m), 2.10—2.70 (m), 2.07 (s, 3H), 1.98 (s, 6H), 1.90 (s, 3H); MALDI-TOF MS (pos) found 106,500.

53i: ^{1}H NMR (500 MHz, CD_3SOCD_3) δ 7.95 (bs, amide NH's), 7.74 (bs, amide NH's), 7.47 (bs, 4H, H-1, H-2, H-3, and H-4), 5.07 (bs, 3H, H-5, H-6), 4.88 (bs, 1H, H-7) 4.57 (bs, 0.47H, H-8), 4.11 (m, 1H, H-9), 3.90—4.05 (m, 2H, H-10 and H-11), 2.80—3.80 (m), 2.10—2.70 (m), 2.07 (s, 3H), 1.98 (s, 6H), 1.90 (s, 3H); MALDI-TOF MS (pos) found 106,300.

53j: ^{1}H NMR (500 MHz, CD_3SOCD_3) δ 7.95 (bs, amide NH's), 7.74 (bs, amide NH's), 7.46 (bs, 4H, H-1, H-2, H-3, and H-4), 5.07 (bs, 3H, H-5, H-6), 4.88 (bs, 1H, H-7) 4.56 (bs, 0.32H, H-8), 4.11 (m, 1H, H-9), 3.90—4.05 (m, 2H, H-10

and H-11), 2.80—3.80 (m), 2.10—2.70 (m), 2.07 (s, 3H), 1.98 (s, 6H), 1.90 (s, 3H); MALDI-TOF MS (pos) found 111,000.

53k: ^{1}H NMR (500 MHz, CD_3SOCD_3) δ 7.95 (bs, amide NH's), 7.74 (bs, amide NH's), 7.47 (bs, 4H, H-1, H-2, H-3, and H-4), 5.07 (bs, 3H, H-5, H-6), 4.88 (bs, 1H, H-7) 4.55 (bs, 0.28H, H-8), 4.11 (m, 1H, H-9), 3.90—4.05 (m, 2H, H-10 and H-11), 2.80—3.80 (m), 2.10—2.70 (m), 2.07 (s, 3H), 1.98 (s, 6H), 1.90 (s, 3H); MALDI-TOF MS (pos) found 114,000.

53l: ^{1}H NMR (500 MHz, CD_3SOCD_3) δ 7.95 (bs, amide NH's), 7.74 (bs, amide NH's), 7.46 (bs, 4H, H-1, H-2, H-3, and H-4), 5.07 (bs, 3H, H-5, H-6), 4.88 (bs, 1H, H-7) 4.55 (bs, 0.14H, H-8), 4.11 (m, 1H, H-9), 3.90—4.05 (m, 2H, H-10 and H-11), 2.80—3.80 (m), 2.10—2.70 (m), 2.07 (s, 3H), 1.98 (s, 6H), 1.89 (s, 3H); MALDI-TOF MS (pos) found 122,900.

53m: ^{1}H NMR (500 MHz, CD_3SOCD_3) δ 7.94 (bs, amide NH's), 7.73 (bs, amide NH's), 7.46 (bs, 4H, H-1, H-2, H-3, and H-4), 5.06 (bs, 3H, H-5, H-6), 4.88 (bs, 1H, H-7) 4.55 (bs, 0.10H, H-8), 4.11 (m, 1H, H-9), 3.90—4.05 (m, 2H, H-10 and H-11), 2.80—3.80 (m), 2.10—2.70 (m), 2.07 (s, 3H), 1.98 (s, 6H), 1.90 (s, 3H); MALDI-TOF MS (pos) found 126,000.

Deacetylated generation 3.0 PAMAM-based thiourea-linked ethoxy ethanol and 1-*O*-(5-thiourea-3-oxapentyl)-α-D-mannopyranoside dendrimers (**57a-m**):

57a: ^{1}H NMR (500 MHz, CD_3SOCD_3) δ 7.97 (bs, amide NH's), 7.75 (bs, amide NH's), 7.46 (bs, all thiourea protons), 4.35—4.90 (m), 2.90—3.80 (m), 2.00—3.80 (m); MALDI-TOF MS (pos) found 77,400.

57b: ^{1}H NMR (500 MHz, CD_3SOCD_3) δ 7.97 (bs, amide NH's), 7.75 (bs, amide NH's), 7.46 (bs, all thiourea protons), 4.35—4.90 (m), 2.90—3.80 (m), 2.00—3.80 (m); MALDI-TOF MS (pos) found 78,000.

57c: ^{1}H NMR (500 MHz, CD_3SOCD_3) δ 7.97 (bs, amide NH's), 7.75 (bs, amide NH's), 7.46 (bs, all thiourea protons), 4.35—4.90 (m), 2.90—3.80 (m), 2.00—3.80 (m); MALDI-TOF MS (pos) found 80,100.

57d: ^{1}H NMR (500 MHz, CD_3SOCD_3) δ 7.97 (bs, amide NH's), 7.75 (bs, amide NH's), 7.46 (bs, all thiourea protons), 4.35—4.90 (m), 2.90—3.80 (m), 2.00—3.80 (m); MALDI-TOF MS (pos) found 80,100.

57e: ^{1}H NMR (500 MHz, CD_3SOCD_3) δ 7.97 (bs, amide NH's), 7.75 (bs, amide NH's), 7.46 (bs, all thiourea protons), 4.35—4.90 (m), 2.90—3.80 (m), 2.00—3.80 (m); MALDI-TOF MS (pos) found 81,000.

57f: ^{1}H NMR (500 MHz, CD_3SOCD_3) δ 7.97 (bs, amide NH's), 7.75 (bs, amide NH's), 7.46 (bs, all thiourea protons), 4.35—4.90 (m), 2.90—3.80 (m), 2.00—3.80 (m); MALDI-TOF MS (pos) found 83,100.

57g: ^{1}H NMR (500 MHz, CD_3SOCD_3) δ 7.97 (bs, amide NH's), 7.75 (bs, amide NH's), 7.46 (bs, all thiourea protons), 4.35—4.90 (m), 2.90—3.80 (m), 2.00—3.80 (m); MALDI-TOF MS (pos) found 87,100.

57h: ^{1}H NMR (500 MHz, CD_3SOCD_3) δ 7.97 (bs, amide NH's), 7.75 (bs, amide NH's), 7.46 (bs, all thiourea protons), 4.35—4.90 (m), 2.90—3.80 (m), 2.00—3.80 (m); MALDI-TOF MS (pos) found 91,000.

57i: ^{1}H NMR (500 MHz, CD_3SOCD_3) δ 7.97 (bs, amide NH's), 7.75 (bs, amide NH's), 7.46 (bs, all thiourea protons), 4.35—4.90 (m), 2.90—3.80 (m), 2.00—3.80 (m); MALDI-TOF MS (pos) found 89,500.

57j: ^{1}H NMR (500 MHz, CD_3SOCD_3) δ 7.97 (bs, amide NH's), 7.75 (bs, amide NH's), 7.46 (bs, all thiourea protons), 4.35—4.90 (m), 2.90—3.80 (m), 2.00—3.80 (m); MALDI-TOF MS (pos) found 93,900.

57k: ^{1}H NMR (500 MHz, CD_3SOCD_3) δ 7.97 (bs, amide NH's), 7.75 (bs, amide NH's), 7.46 (bs, all thiourea protons), 4.35—4.90 (m), 2.90—3.80 (m), 2.00—3.80 (m); MALDI-TOF MS (pos) found 96,000.

57l: ^{1}H NMR (500 MHz, CD_3SOCD_3) δ 7.97 (bs, amide NH's), 7.75 (bs, amide NH's), 7.46 (bs, all thiourea protons), 4.35—4.90 (m), 2.90—3.80 (m), 2.00—3.80 (m); MALDI-TOF MS (pos) found 97,700.

57m: ^{1}H NMR (500 MHz, CD_3SOCD_3) δ 7.97 (bs, amide NH's), 7.75 (bs, amide NH's), 7.46 (bs, all thiourea protons), 4.35—4.90 (m), 2.90—3.80 (m), 2.00—3.80 (m); MALDI-TOF MS (pos) found 99,900.

Generation 3.0 PAMAM-based thiourea-linked ethoxy ethanol dendrimer (**58**). An aqueous solution of amine-terminated Starburst PAMAM dendrimer (generation 3.0) (1000 mg of a 10% (w/w) solution in water, 100 mg, 14.5 μmol of

dendrimer based on the M_W of 6909 g/mol as determined by MALDI-TOF for G(3)-PAMAM) was lyophilized to leave a foam. The resulting residue was dissolved in DMSO (10 mL) followed by the addition of a 0.1 g/mL DMSO solution of **28** (684 μL, 68.4 mg, 465 μmol). The reaction was stirred for 8 hours. The reaction mixture was added to a dialysis membrane (cellulose, MW cutoff 1 kDa) and the solution was dialyzed against DMSO for 12 hours. The solution was lyophilized to give **58** as a sticky product: ^{1}H NMR (500 MHz, CD_3SOCD_3) δ 7.97 (bs, amide NH's), 7.76 (bs, amide NH's), 7.47 (bs, thiourea protons), 4.58 (bs, OH), 3.45 (bs), 3.39 (bs), 3.31 (bs), 3.13 (bs), 3.05 (bs), 2.62 (bs), 2.46 (bs), 2.39 (bs), 2.16 (bs); MALDI-TOF MS (pos) found 11,200.

Generation 4.0 PAMAM-based thiourea-linked ethoxy ethanol dendrimer (**59**). An aqueous solution of amine-terminated Starburst PAMAM dendrimer (generation 4.0) (284 mg of a 20% (w/w) solution in water, 56.9 mg, 4.2 μmol of dendrimer based on the M_W of 13,500 g/mol as determined by MALDI-TOF for G(4)-PAMAM) was lyophilized to leave a foam. The resulting residue was dissolved in DMSO (10 mL) followed by the addition of a 0.1 g/mL DMSO solution of **28** (397 μL, 39.7 mg, 270 μmol). The reaction was stirred for 8 hours. The reaction mixture was added to a dialysis membrane (cellulose, MW cutoff 1 kDa) and the solution was dialyzed against DMSO for 12 hours. The solution was lyophilized to give **59** as a sticky product: ^{1}H NMR (500 MHz, CD_3SOCD_3) δ 7.97 (bs, amide NH's), 7.76 (bs, amide NH's), 7.47 (bs, thiourea protons), 4.58 (bs,

OH), 3.45 (bs), 3.38 (bs), 3.31 (bs), 3.13 (bs), 3.05 (bs), 2.62 (bs), 2.46 (bs), 2.39 (bs), 2.16 (bs); MALDI-TOF MS (pos) found 21,100.

Generation 5.0 PAMAM-based thiourea-linked ethoxy ethanol dendrimer (**60**). An aqueous solution of amine-terminated Starburst PAMAM dendrimer (generation 5.0) (284 mg of a 22.5% (w/w) solution in water, 63.9 mg, 2.5 μmol of dendrimer based on the M_W of 25,500 g/mol as determined by MALDI-TOF for G(5)-PAMAM) was lyophilized to leave a foam. The resulting residue was dissolved in DMSO (10 mL) followed by the addition of a 0.1 g/mL DMSO solution of **28** (368 μL, 36.8 mg, 251 μmol). The reaction was stirred for 8 hours. The reaction mixture was added to a dialysis membrane (cellulose, MW cutoff 1 kDa) and the solution was dialyzed against DMSO for 12 hours. The solution was lyophilized to give **60** as a sticky product: ^{1}H NMR (500 MHz, CD_3SOCD_3) δ 7.97 (bs, amide NH's), 7.76 (bs, amide NH's), 7.47 (bs, thiourea protons), 4.58 (bs, OH), 3.45 (bs), 3.39 (bs), 3.30 (bs), 3.14 (bs), 3.05 (bs), 2.62 (bs), 2.46 (bs), 2.39 (bs), 2.16 (bs); MALDI-TOF MS (pos) found 40,850.

Generation 6.0 PAMAM-based thiourea-linked ethoxy ethanol dendrimer (**61**). An aqueous solution of amine-terminated Starburst PAMAM dendrimer (generation 6.0) (262 mg of a 20% (w/w) solution in water, 52.4 mg, 1.0 μmol of dendrimer based on the M_W of 50,800 g/mol as determined by MALDI-TOF for G(4)-PAMAM) was lyophilized to leave a foam. The resulting residue was dissolved in DMSO (10 mL) followed by the addition of a 0.1 g/mL DMSO

solution of **28** (367 μL, 36.7 mg, 250 μmol). The reaction was stirred for 8 hours. The reaction mixture was added to a dialysis membrane (cellulose, MW cutoff 1 kDa) and the solution was dialyzed against DMSO for 12 hours. The solution was lyophilized to give **61** as a sticky product: ^{1}H NMR (500 MHz, CD_3SOCD_3) δ 7.98 (bs, amide NH's), 7.76 (bs, amide NH's), 7.47 (bs, thiourea protons), 4.59 (bs, OH), 3.46 (bs), 3.39 (bs), 3.30 (bs), 3.14 (bs), 3.05 (bs), 2.64 (bs), 2.46 (bs), 2.36 (bs), 2.17 (bs); MALDI-TOF MS (pos) found 81,550.

CHAPTER 5

SUMMARY AND CONCLUSIONS

The Benefits of Using Isothiocyanates

A number of conclusions can be made based on the results described in this work. First, we have shown that PAMAM dendrimers up to generation six are easily functionalized using isothiocyanates. The use of a variety of isothiocyanates has been described indicating that the use of isothiocyanates may be a general method for the functionalization of amine-terminated dendrimers, such as PAMAMs. In addition, isothiocyanates are useful for the heterogeneous functionalization of PAMAM dendrimers. The degree of surface functionalization is conveniently controlled by the stoichiometry of the various isothiocyanates.

Of all of the methods described in Scheme 1.2, the use of an isothiocyanate to form a thiourea linkage may be the most attractive and useful. The reaction proceeds very cleanly and efficiently without the need for activators or high temperature. Thiourea formation does not create any byproducts that must be removed. Typically, the only impurity after reaction is excess reagent. The isothiocyanate is also tolerant of a variety of functional groups, indicated by its selective reactivity with amines.

The result of the synthetic portion of this project was the successful synthesis of water-soluble mannose-functionalized PAMAM dendrimers. The use of a polyethylene glycol linker proved beneficial for achieving water solubility.

Characterization

Of critical importance to the success of this project was the development of characterization methods for mannose-functionalized dendrimers. Specifically, the development and application of MALDI-TOF MS to the analysis of functionalized dendrimers was paramount. Previous to this work, reports of a general method for MALDI-TOF MS analysis of glycodendrimers were lacking in the literature.

MALDI-TOF MS was used to determine the number of sugars on the dendrimers and thus the degree of functionalization. Not only was MALDI applied to characterization of the functionalized dendrimers, but also to the characterization of the starting material PAMAMs.

NMR characterization was also valuable for the analysis of mannose-functionalized dendrimers. NMR has been extensively used for macromolecule characterization. We were fortunate, thanks to the isolation of peaks, to be able to use the integration of peaks to determine ratios of surface residues on the dendrimers. This data combined with the MALDI data provided a complete picture of the degree of dendrimer functionalization.

Activity Determination

A number of assays were used to determine the activity of mannose-functionalized PAMAM dendrimers toward Concanavalin A. The three main assays used were a hemagglutination inhibition assay (HIA), a precipitation assay and turbidity assay. HIA proved to be of significant importance.

From the assays, a few general conclusions can be made. First, the size of the ligand matters. The most dramatic increase in activity was observed when the dendrimers were large enough to bind with multiple sites on the Con A. The largest dendrimers were not only able to multivalently bind, but due to the increased number of sugars on their surface, they showed enhanced activity relative to the smaller dendrimers.

A second conclusion is that the density of sugars on the surface of the dendrimers has a profound effect on the activity towards Con A. In all cases, the highest activity was observed when the dendrimers were only partially functionalized with carbohydrates. This general observation is not new, but it provides specific and valuable information for the design of effective dendrimer-based ligands.

During the course of this work, a third conclusion has been made that deals with the true nature of dendrimer molecules. PAMAM dendrimers (and probably most dendrimers with similar structures) are much more dynamic than was first thought. This results in greater flexibility of the scaffold. In addition,

dendrimers synthesized by an iterative process will almost always have omissions in their structure that results in a heterogeneous mixture of molecules. Claims in the literature that all PAMAM dendrimers of a given generation have identical structures are misleading. While these conclusions are not surprising, these points are not always explicitly stated in the literature.

Finally, the assays have shown that mannose-functionalized PAMAM dendrimers are effective at clustering lectins. In a practical application, similar ligands may be able to cluster the lectins in the surface of various animal cells. While the clustering of lectins may or may not provide a therapeutic benefit (since the function of many lectins is unknown), the basic results described here may find application in other biologically more important systems.

APPENDICES

APPENDIX A

METHODS OF MALDI-TOF MS DATA ANALYSIS

General Formulas

The following formulas have been used to calculate all molecular mass values from MALDI-TOF data.

Number-Average Molecular Weight

$$M_N = \frac{\Sigma N_i M_i}{\Sigma N_i}$$

Equation A.1

M_N is the number-average molecular weight, N_i is the number of counts and M_i is the mass.

Weight-Average Molecular Weight

$$M_W = \frac{\Sigma N_i M_i^2}{\Sigma N_i M_i}$$

Equation A.2

M_W is the weight-average molecular weight.

Polydispersity

$$PD = \frac{M_W}{M_N}$$

Equation A.3

Data Transfer and Analysis Using the PerSeptive System

As was mentioned in the main text, during the course of this project two different MALDI-TOF MS instruments were used. The new Bruker Biflex included

software that could perform the calculations given above on the data collected (more details are given below). However, the older PerSeptive Biosystems Voyager system did not have adequate data analysis capabilities. In fact, the computer used to run the data collections software was inadequate for the detailed data analysis necessary for the determination of M_N and M_W.

Therefore, data collected on this system had to be transported and analyzed using a different computer. To do so, the data collection during the MALDI-TOF experiment was saved to the Gateway PC interfaced with the mass spectrometer. Using the Grams data analysis program, the data was calibrated and smoothed. This saved file was then exported using the "ASCIIXYS (ASCII X,Y data pair format (non-even X spacing)" option. Other options would unavoidably modify the data.

The exported data was written to a floppy disk, which was then transferred to an iMac computer. All of the collected data was imported into an Excel spreadsheet and analyzed. Using Equation A.1, Equation A.2, and Equation A.3, the values of M_N, M_w, and polydispersity were obtained by selecting the theoretical molecular weight of the compound as one endpoint and a point of comparable intensity on the other side of the peak as the second endpoint (to account for a slightly uneven baseline). Although values are not accurate to a single amu, full values are reported and carried through calculations of sugar

incorporation (or amino acid residue deletion) and the final value is rounded to the nearest whole number of sugars (or amine residue).

Data Analysis Using the Bruker System

The laborious and time-consuming process of transferring and analyzing the data was avoided when the Chemistry department purchased the new MALDI-TOF MS instrument. The XTOF software used to analyze data collected by the Bruker Biflex III instrument included a preprogrammed polymer module. This module can be used to analyze continuous polymers in which the peaks are continuous over a broad range of mass values, which is exactly the case here.

Figure A.1 shows how the XTOF software analyzes a continuous polymer peak. This figure is taken directly from the XTOF users manual.

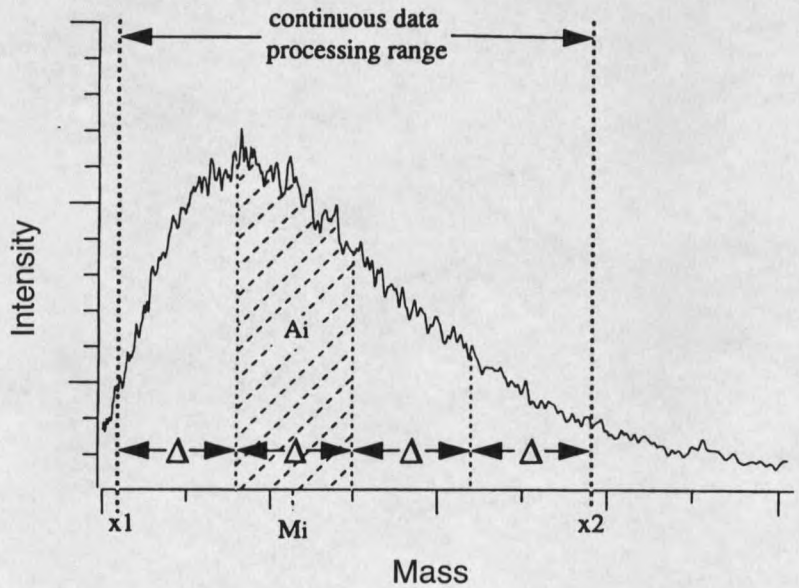


Figure A.1 Method for continuous polymer data processing.

The formulas used by the software are very similar to Equation A.1, Equation A.2, and Equation A.3. The software calculates the molecular mass values by an integration by parts method. Equation A.4 shows the formula for the calculation of the number-average molecular weight.

$$M_N = \frac{\sum_{i=1}^{N} A_i M_i}{\sum_{i=1}^{N} A_i}$$

Equation A.4

Equation A.5 shows the formula for the calculation of the weight-average molecular weight.

$$M_W = \frac{\sum_{i=1}^{N} A_i M_i^2}{\sum_{i=1}^{N} A_i M_i}$$

Equation A.5

In this formula, A_i is the area as shown in Figure A.1. It is calculated using the formula in Equation A.6.

$$A_i = \Delta \circ I(x_1 + i \bullet \Delta);\ i = 0, N - 1$$

Equation A.6

In this formula, I is the intensity and Δ is the user definable range of the area calculation. In all calculations, Δ was set to the minimum value allowed at the various mass ranges.

The average mass for each area, M_i, was determined by the formula in Equation A.7.

$$M_i = x_1 + \frac{2 \circ i + 1}{2} \bullet \Delta; i = 0, N - 1$$

Equation A.7

APPENDIX B

APPLICATION OF MALDI-TOF MS TO ADDITIONAL DENDRIMER EXAMPLES

Background

During the National American Chemical Society meeting in Washington, D.C. in fall 2000, an opportunity arose to establish a collaboration with the research group of Martin Brechbiel at the National Institutes of Health. The Brechbiel group had been doing research on the functionalization of PAMAM dendrimers with TEMPO groups. However, they had not had good success obtaining mass spectrometry data for their products.

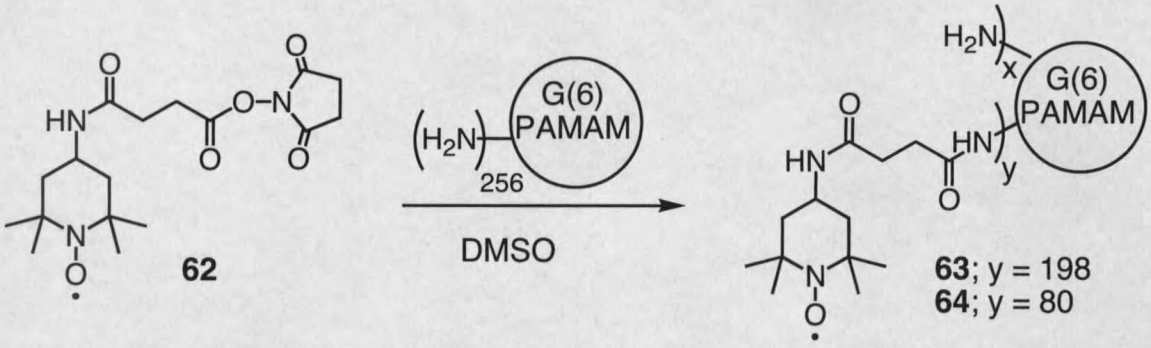
Using the techniques described in this work, attempts were made to obtain MALDI-TOF MS data for compounds from the Brechbiel labs. Co-authorship of two papers was the result. A brief description of our contributions to these papers is given below.

Spin-Labeled PAMAM Dendrimers

[The following is a brief description of the work described in Yordanov, A. T., Yamada, K.-i., Krishna, M. C., Mitchell, J. B., Woller, E. K., Cloninger, M. J., and Brechbiel, M. W. (2001). Spin-Labeled Dendrimers in EPR Imaging with Low Molecular Weight Nitroxides. Angew. Chem., Int. Ed. Engl., *40*, 2690-2692. Specifically, the MALDI-TOF MS analysis is described.]

The use of electron paramagnetic resonance (EPR) imaging as a method for the analysis of free radical distribution, metabolism and extent of oxygenation in tumors, organs and tissues is limited by the short lives of the stable nitroxyl radicals that are necessary for success of the technique. In an attempt to synthesize biologically safe macromolecules capable of reoxidizing EPR-silent

hydroxylamine to EPR-active nitroxide, workers in the NIH labs of Martin Brechbiel functionalized generation six PAMAM dendrimers using the *N*-succinimidyl activated ester method. The reaction is shown in Scheme B.1. By controlling the amount of **62**, the amount of TEMPO on the surface could be controlled, albeit unpredictably.

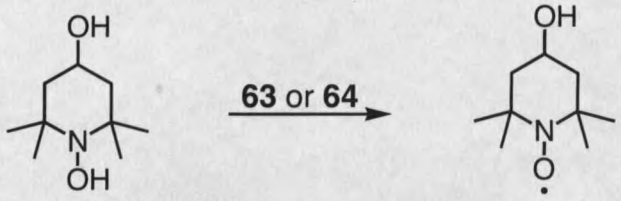


Scheme B.1 Functionalization of a G(6)-PAMAM dendrimer with TEMPO.

In order to characterize the macromolecules and to determine the number of TEMPO groups on the dendrimer, MALDI-TOF MS was used. The number-average molecular weight of **63** was found to be 101,000 g/mol, and the weight-average molecular weight was found to be 102,000 g/mol. Comparison of this value to the experimentally determined molecular weight of the starting material G(6)-PAMAM (50,900 g/mol) indicated that there were 198 TEMPO molecules on the surface of dendrimer **63** on average.

A similar analysis of **64** was done. The weight-average and number-average molecular weights were 71,000 g/mol and 72,000 g/mol respectively. Comparison to the weight of the starting material indicated that on average, there were 80 TEMPO residues per dendrimer.

Additional studies showed that when TEMPOL-H (an EPR-silent molecule) and **63** or **64** were mixed together, the dendrimer nitroxyl conjugates reoxidized the hydroxylamine back to TEMPOL, the EPR active analogue (see Scheme B.2), indicating that spin-labeled G(6)-PAMAM dendrimers are potential candidates for TEMPO free radical life supporters in EPR imaging.



TEMPOL-H TEMPOL

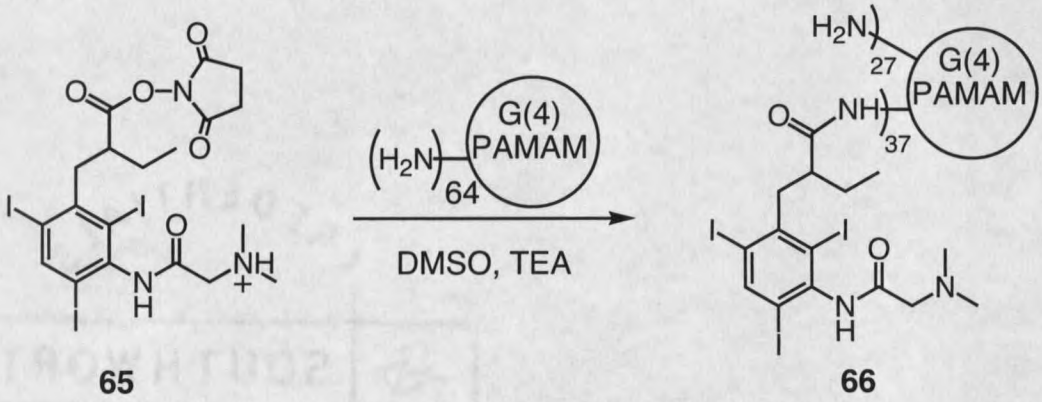
Scheme B.2 The reoxidation of TEMPOL-H to TEMPOL by the use of **63** or **64**.

Novel Iodinated Dendritic Nanoparticles

[The following is a brief description of the work described in Yordanov, A. T., Lodder, A., Woller, E. K., Cloninger, M. J., Patronas, N., Milenic, D., and Brechbiel, M. W. (2002). Novel Iodinated Dendritic Nanoparticles for Computed Tomography (CT) Imaging. Nano Letters, *2*, 595-599. Specifically, the MALDI-TOF MS analysis is described.]

Computed tomography (CT) is a reliable and widely available imaging method with high spatial resolution. CT relies on the use of imaging agents that are typically iodinated ionic or nonionic small molecules. A limitation is the short lifetime of existing contrast agents in the vascular regions of the human body. The objective of extensive research efforts has therefore been the development of macromolecular CT agents, which would result in higher and in longer-lived vascular concentrations. One potential solution would be the use of water-soluble iodinated macromolecules.

To that end, a G(4)-PAMAM dendrimer was partially functionalized with 3-*N*-[(*N',N'*-dimethylaminoacetyl)amino]-α-ethyl-2,4,6-triiodobenzenepropanoic acid (**65**) by the Brechbiel group at NIH using the *N*-succinimidyl activated ester method to form **66** (Scheme B.3). This synthesis and subsequent full characterization was the first for a water-soluble iodinated dendritic nanoparticles.



Scheme B.3 Synthesis of iodinated nanoparticle **66**, by the partial functionalization of a G(4)-PAMAM with **65**.

To determine the number of 3-*N*-[(*N',N'*-dimethylaminoacetyl)amino]-α-ethyl-2,4,6-triiodobenzenepropanoic acid molecules (DMAA-IPA) on **66**, MALDI-TOF MS was used. The method used was similar to the method described earlier. The parent G(4)-PAMAM dendrimer has a M_W of 13,450 g/mol. The MALDI-TOF is shown in Figure B.1. The iodinated dendritic nanoparticles have a weight-average molar mass (M_W) of 37,000 g/mol, the number-average (M_N) was 36,657, and the polydispersity was 1.0121. The molecular weight increase when

compared to the starting material indicates that there are 37 DMAA-IPA residues on the surface of **66**.

Although there are in theory 64 primary amino groups on the surface of the G(4) dendrimer, it was not possible to conjugate more than 37 residues to the surface even under forcing conditions. The most likely reason for low loading is the accumulated steric hindrance of the bulky DMAA-IPA molecules on the surface which prevents access to the unreacted primary amine groups.

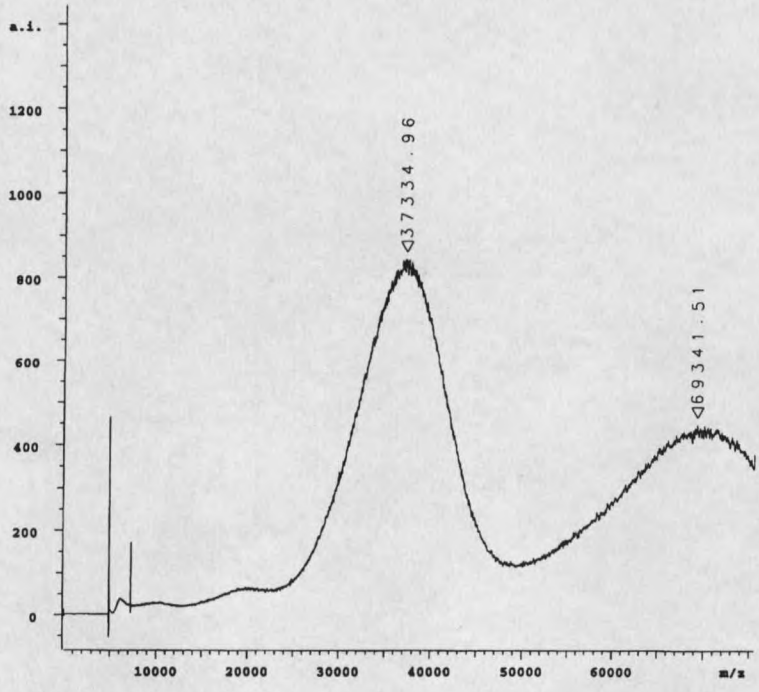


Figure B.1 MALDI spectrum of **66**.

The MALDI-TOF spectrum in Figure B.1 shows an apparently large amount of dimer formation. While noncovalent di-, tri- and polymerization is generally common under the conditions of MALDI-TOF spectroscopy, this particular sample showed more dimer than is typically seen. Increased dimer

formation was not surprising when considering the lipophilic nature of **66,** and it was concluded that the dimeric polymers were probably not a result of the synthetic method employed. Other characterization techniques confirmed this conclusion.

In summary, the synthesis and characterization of novel water-soluble iodinated dendritic nanoparticles was achieved. The uniformity of the dendritic nanoparticles was established by MALDI-TOF (in addition to elemental analysis and multi-angle light scattering). Further studies have indicated that **66** is a potential candidate for use as a CT imaging agent.

APPENDIX C

ATTEMPTS USING ISOTHERMAL MICROCALORIMETRY

Background

Calorimetry has been used for decades to study various chemical and biological systems. With the significant improvements in electronics and computing power during the 1980's, the area of microcalorimetry (i.e. the use of calorimetry to study small volumes and weak interactions) was developed. In 1989, a new titration calorimeter was introduced that featured very high sensitivity, rapid calorimetric response, and fast thermal equilibration.[197] This signaled a significant development in the field, upon which even more improvements have been made.

One of the main versions of microcalorimetry is isothermal microcalorimetry (ITC). The use of ITC to study protein-carbohydrate interactions has increased dramatically in recent years. This is due primarily to the fact that in one experiment the association constant (K_a), free energy (ΔG), enthalpy (ΔH), entropy (ΔS) and stoichiometry (*n*) can all be determined.

A number of excellent reviews have appeared that describe in greater detail the theory and applications of ITC and microcalorimetry in general.[198-201] The review by Brewer and Dam is an excellent report on the use of ITC to study lectin-carbohydrate interactions.[200] ITC has been used in a number of examples to study protein-carbohydrate interactions.[42, 116, 202-204] In many of the ITC

studies described, not only was thermodynamic data determined, but structural information of the receptor was determined as well.

Recently, microcalorimetry has been used to study multivalent interactions.[70, 118, 205-207] What many of the ITC studies have found is that the "multivalency effect" (the increase in K_a value of the multivalent carbohydrate display relative to the carbohydrate monomer) is due to increased positive entropy ($T\Delta S$) contributions.[118, 200] In addition, in some cases the value of *n* determined by ITC shows that the functional valency of a multivalent ligand may differ from its structural valency.[118, 200]

General ITC Experiment Considerations

Briefly, a typical ITC experiment involves the computer-controlled titration of a ligand solution into a receptor solution while stirring. The heat that is generated by the binding event is used to calculate the thermodynamic data. Current instrumentation is such that very small temperature changes (<0.1° C) can be detected and measured. Here, an ITC microcalorimeter manufactured by MicroCal, LLC of Northampton, Massachusetts, was used.

One requirement when performing an ITC experiment is that the reactants and complexes remain soluble during the duration of the experiment (~1-2 h). One significant problem of studying the interaction between Con A and high valency or large ligands is the potential for the formation of precipitates. In fact,

as seen previously in the precipitation assay and turbidity assay, when it is desired, the formation of a Con A-ligand precipitate can be used to provide important information regarding multivalent interactions.

The dimer-tetramer equilibrium for Con A is pH sensitive. Con A is a tetramer at pH > 7.0. However, at pH 5.0 the dimer is the predominate species.[208, 209] Previous reports indicate that the formation of a Con A-ligand precipitate can be avoided by using Con A as a dimer at low ionic strength.[42, 116, 118, 204] Under conditions that favor Con A dimers, a variety of multivalent ligands have been successfully studied. However, none of the ligands described contained more than six carbohydrates.[47] With this in mind, a study of mannose-functionalized PAMAM dendrimers (in which the smallest ligand contained eight carbohydrate) was attempted with a bit of trepidation.

Attempted ITC Measurements

In an attempt to learn the technique necessary to obtain useful data and to verify the accuracy of the ITC instrument, the interaction between methyl mannose and Con A was measured.

Following a procedure by Dam *et. al.*[118], using a 3,3-dimethylglutaric acid (DMG) buffer at pH 5.2 containing 1 mM $CaCl_2$ and 1mM $MnCl_2$ and without NaCl, a methyl mannose solution was titrated into a stirred Con A solution at 25°

C. The resulting isotherm is shown in Figure C.1a. The resulting thermodynamic data was in good agreement with the literature values.

As another way to check the operator's technique and the accuracy of the instrument, a titration of ribonuclease A with cytidine 2'-monophosphate was performed. This was done per the instrument manufacturers protocol. The isotherm is shown in Figure C.1b. Again, the results were within acceptable limits.

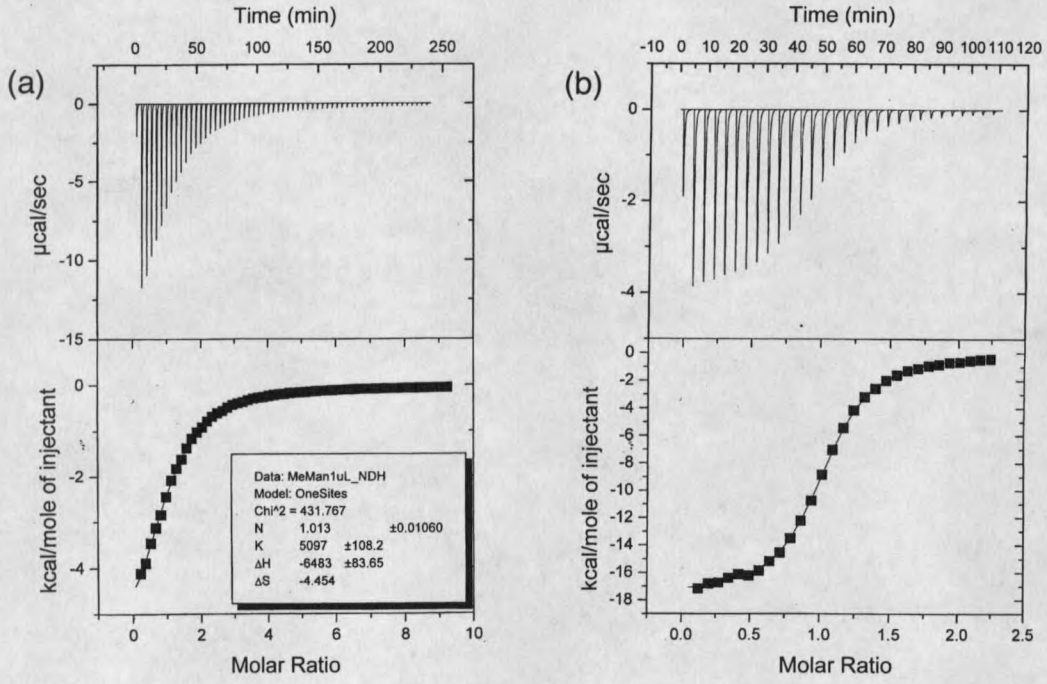


Figure C.1 (a) ITC profile for the titration of Con A with methyl mannose, (b) ITC profile for the titration of RNase A with 2'-CMP.

Having learned the technique and calibrated the instrument, attempts were made to test the mannose-functionalized dendrimers. In order to develop conditions suitable to study mannose-functionalized PAMAM dendrimers, **36** and **38** were first studied. Dendrimer **36** was a generation one dendrimer containing

eight carbohydrates and dendrimer **38** was a generation three dendrimer containing 30 carbohydrates.

As was the case in the methyl mannose experiment, all experiments were performed in DMG buffer at pH 5.2 containing 1 mM $CaCl_2$ and 1mM $MnCl_2$ and without NaCl present. A wide range of dendrimer and Con A concentrations were used at a variety of temperatures. However, the final result was that precipitation was too prevalent to make any meaningful data acquisition possible.

The data for a specific example is shown in Figure C.2. The graph shown in Figure C.2a shows the data for the heat of dilution of **38** (open circles) into DMG buffer and the heat evolved when **38** was added to a buffer solution containing Con A. As can be seen, the data look similar. Figure C.2b shows the result after the heat of dilution is subtracted from the interaction with Con A. What is obvious is the lack of a sigmoidal curve that was evident with methyl mannose (Figure C.2). As a result, performing a least squares analysis of the data is unproductive.

In the isotherm shown in Figure C.2b, the uneven baseline is evidence of precipitation. This was observed for nearly all samples tested. Thus, we had to conclude that, while ITC is an incredible technique for the determination of the thermodynamics of binding events, it may not be appropriate for the study of large ligands such as dendrimers.

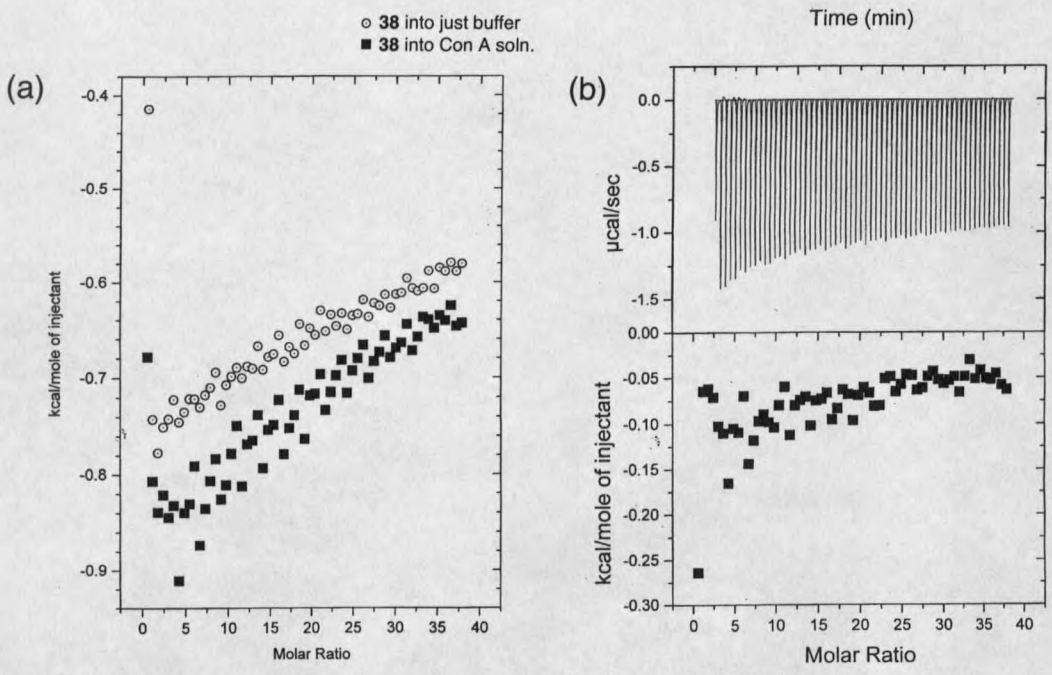


Figure C.2 (a) open circles show the heat of dilution of **38** into DMG buffer; black squares show the interaction of **38** with Con A, (b) resulting ITC profile after the subtraction of the heat of dilution of **38** into DMG from the interaction of **38** with Con A.

Experimental Procedures

General procedures

Concanavalin A was purchased from Calbiochem. The concentration of Con A was determined spectrophotometrically at 280 nm using $A^{1\%}_{1\ cm} = 12.4$ at pH 5.2 and expressed in terms of monomer (MW = 25,600). Manganese (II) chloride, calcium chloride, methyl mannose and 3,3-dimethylglutaric acid (DMG) were purchased from Sigma-Aldrich and used as supplied.

Buffer preparation

The DMG buffer was prepared by titrating a 0.050 M DMG solution with NaOH until the pH was 5.2. Addition of $MnCl_2$ and $CaCl_2$ was done to make the

concentration of each metal 1 mM. No NaCl was added to the buffer. Enough buffer was made to ensure that all ITC experiments and solutions were made in the same buffer.

Isothermal Titration Microcalorimetry (ITC)

ITC experiments were performed using a VP model ITC instrument from MicroCal, LLC (Northampton, MA). Injections (40—60) of carbohydrate solutions ranged from 1—4 μL using a computer controlled 250-μL syringe at 4 min intervals. The cell temperature was 30° C, the reference power was 30 μCal/sec, and the initial delay was 60 sec. The concentration range of Con A was 20—350 μM and the mannose concentration range was 2—20 mM (concentration was in terms of sugars and not dendrimers).

The instrument calibration was verified by using the calibration protocol for the interaction between ribonuclease A (RNase A) and cytidine 2'-monophosphate as described by the instrument manufacturer. Ribonuclease A and cytidine 2'-monophosphate were purchased from Sigma and used as supplied.

During titrations using dendrimers **36** and **38**, precipitation was observed and could be identified by the significant noise of the baseline.

APPENDIX D

STUDIES TOWARD ALPHA-D-GALACTOSE FUNCTIONALIZED DENDRIMERS

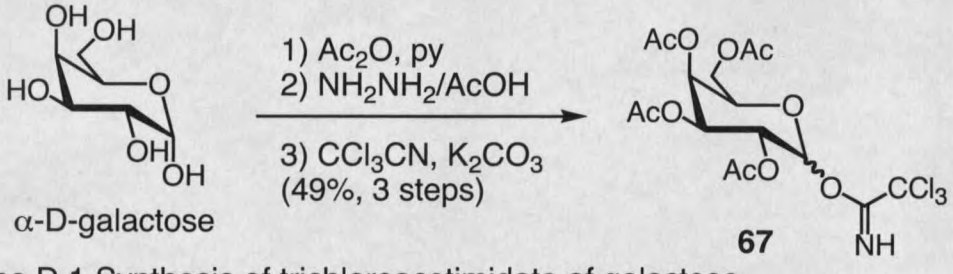
Introduction

After having fully and heterogeneously functionalized PAMAM dendrimers with mannose residues, the use of galactose was briefly explored. Since Con A does not bind with galactose, full functionalization with galactose will provide a good non-binding control. Use of galactose-functionalized dendrimers in the hemagglutination and precipitation assay would further confirm that the interaction seen between the mannose-functionalized PAMAM dendrimers and Con A is indeed a specific interaction. (Recall that precipitates formed by mannose-functionalized PAMAM dendrimers were redissolved by the addition of methyl mannose monomer, which indicates a specific interaction. The use of galactose-functionalized PAMAM dendrimers would support this conclusion.)

A second use of the galactose is to synthesize dendrimers bearing mannose and galactose surface residues. In this case, the galactose will present a steric bulk nearly identical to mannose. While it has been critical in working out the methods of heterogeneous functionalization, the use of **28** as a nonbinding surface residue is limited by the fact that it is not a sugar. With galactose as a nonbinding surface residue that is the same size as mannose, a very interesting picture of the effects of sugar density on the surface of the dendrimer should emerge.

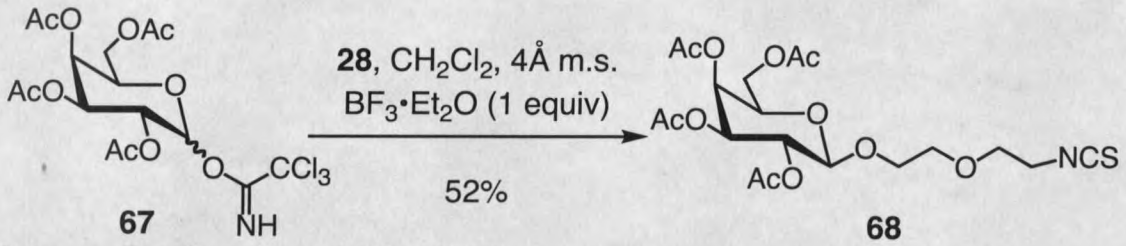
Approaches to an Isothiocyanato Galactose

It seemed logical at this point to apply the same method used to form **29** to form an analogous version of galactose. Therefore, α-D-galactose was acylated using acetic anhydride in pyridine (Scheme D.1), the anomeric position was deprotected using hydrazine acetate, and the trichloroacetimidate **67**[162] was formed using trichloroacetonitrile in the presence of potassium carbonate. The α:β ratio at this point favored the β anomer by a 1:4 ratio. This was not a concern, as the coupling of the alcohol does not depend on which anomer of **67** is used.



Scheme D.1 Synthesis of trichloroacetimidate of galactose.

The coupling of **28** to **67** is shown in Scheme D.2. The reaction was done in an analogous manner to the reaction used to form **29**, however, in this case the β anomer was formed predominantly. Although a small amount of α was formed, it quickly became evident that this would not be a feasible route for the formation of α-substituted galactose on a gram scale.



Scheme D.2 Coupling of **28** with **67**.

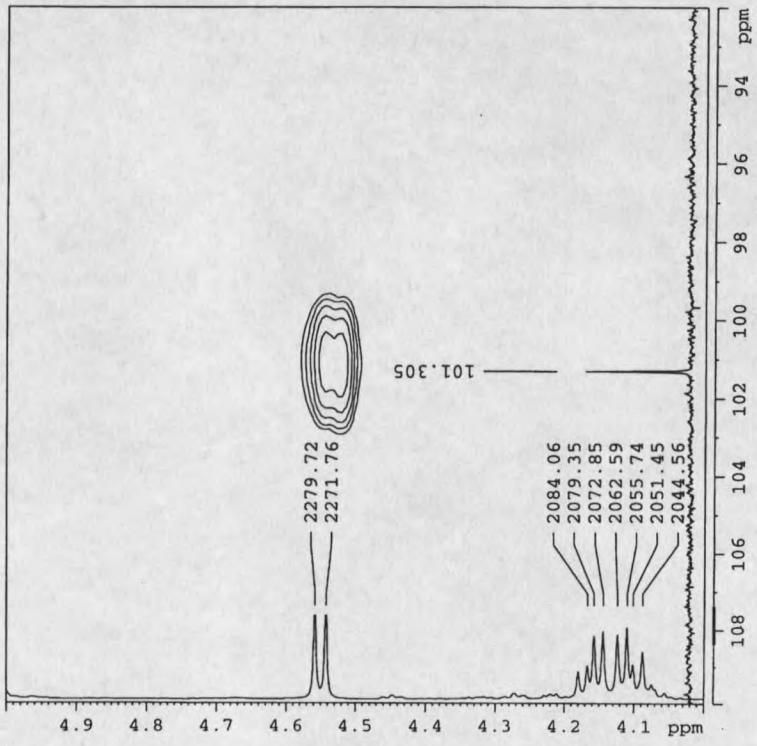


Figure D.1 Inverse HETCOR NMR spectra used to identify which peak corresponds to the anomeric proton of **68**.

The formation of the β anomer of **68** was confirmed by ^{1}H NMR. The first step was to identify the signal that corresponded to the anomeric proton. To do so, an inverse HETCOR NMR experiment was performed. The region of interest is shown in Figure D.1. In the ^{13}C, the anomeric carbon was easily identified at δ 101.3 ppm. This peak showed a strong correlation with the proton at δ 4.55 ppm

thus confirming the assignment of this peak to the anomeric proton. The coupling constant of this proton with the proton at C-2 in the galactose ring is 8.0 Hz. This strong coupling indicates a trans orientation and thus the β anomer.

The cause of the formation of β over α is neighboring group participation (as is the case of α anomer formation with **29**). As seen in Figure D.2, the carbonyl of the acetyl protecting group can interact with the anomeric position to form the oxocarbenium ion shown. This results in making the bottom face of galactose even less accessible than normal.

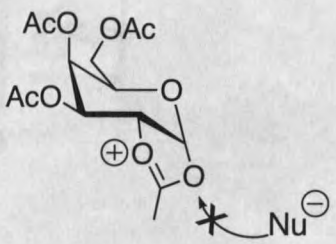
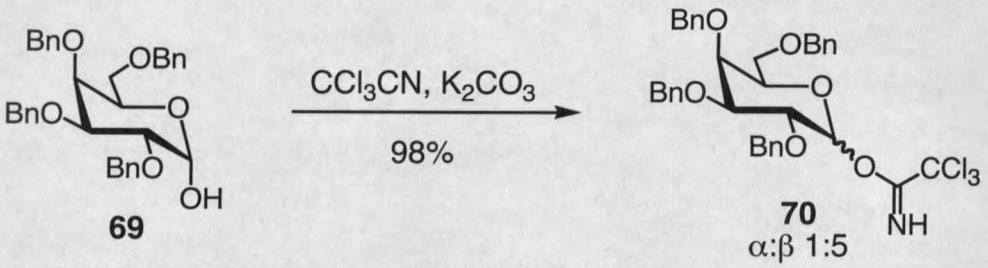


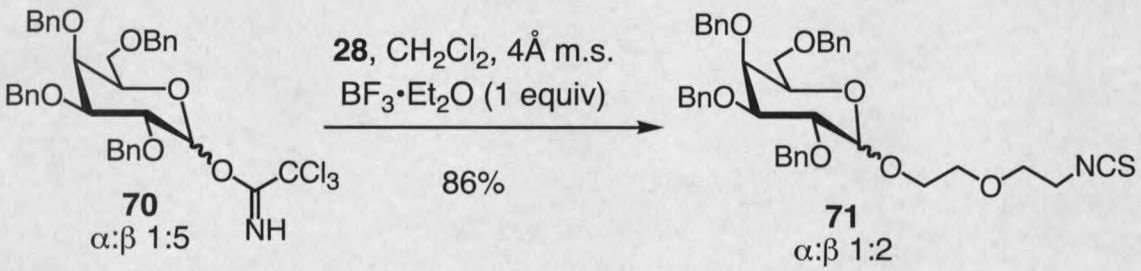
Figure D.2 Neighboring group participation by the ester protecting group prevents the nucleophile from attacking from the bottom.

It is clear that any ester protecting group has the same potential pitfalls. To avoid this problem, the hydroxyl groups were protected using benzyl ethers. Commercially available tetrabenzylated galactose **69** was converted to the trichloroacetimidate **70**[210] using standard conditions (Scheme D.3). While the reaction proceeded in high yield, the alpha selectivity was poor. The β anomer was favored 5:1. However, this selectivity is of little consequence since the subsequent coupling reaction does not rely on which anomer of the trichloroacetimidate is used.



Scheme D.3 Synthesis of benzyl protected trichloroacetimidate.

The coupling of the activated galactose **70** with **28** was done following the standard procedure as shown in Scheme D.4. The reactants were dissolved in dry CH_2Cl_2 under Ar in the presence of 4Å molecular sieves. The $BF_3 \cdot Et_2O$ was added via syringe. The yield was 86%, but the selectivity favored the β anomer (1:2 α:β).



Scheme D.4 Coupling of **28** with activated galactose residue.

Upon separation of the two products by column chromatography, IR analysis showed an absorbance at 2110 cm^{-1} for both products, which indicates the SCN group was present in both compounds. To identify which product was the α anomer and which was the β anomer, an inverse HETCOR NMR experiment was performed.

The portion of the inverse HETCOR NMR spectra that is of interest is shown in Figure D.3. As in the case of **71**, the anomeric carbon is easily distinguished. The ^{13}C shows the anomeric carbon at δ 97.8 ppm. There is an obvious correlation between the anomeric carbon and the ^{1}H peak centered at δ 4.87 ppm. The coupling constant for this peak is 3.4 Hz. Weak coupling between the anomeric proton and the proton at H-2 in the galactose ring identifies the minor reaction product as the α anomer.

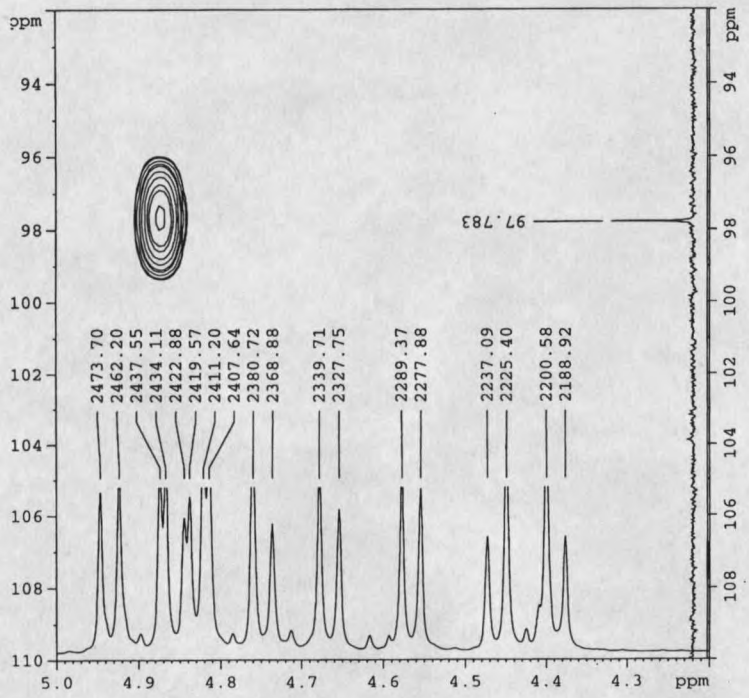


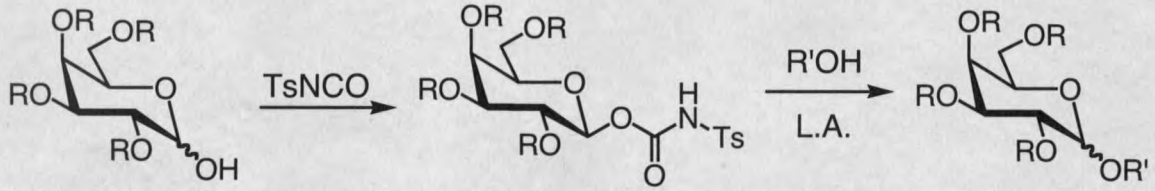
Figure D.3 Inverse HETCOR NMR spectra used to identify which peak corresponds to the anomeric proton of **71**.

While glycosylation of benzylated galactose produced the desired product, the fact that the anomeric selectivity was poor required that another method be

explored. The following section describes an alternative route to the desired α-galactose monomer.

Sulfonylcarbamate Method of Activating Galactose

A recent report by Hinklin and Kiessling described the use of glycosyl sulfonylcarbamates as glycosyl donors for the coupling of galactose (among other sugars) with a variety of alcohols.[211] The general reaction is shown in Scheme D.5. The reaction of a protected carbohydrate with *p*-toluenesulfonyl isocyanate forms the activated carbohydrate, which in the presence of a Lewis acid promoter reacts smoothly with an alcohol. The reaction is proposed to proceed through the oxonium ion via the mechanism shown in Figure D.4.



Scheme D.5 General reaction for the formation and reaction of a sulfonylcarbamate of galactose.

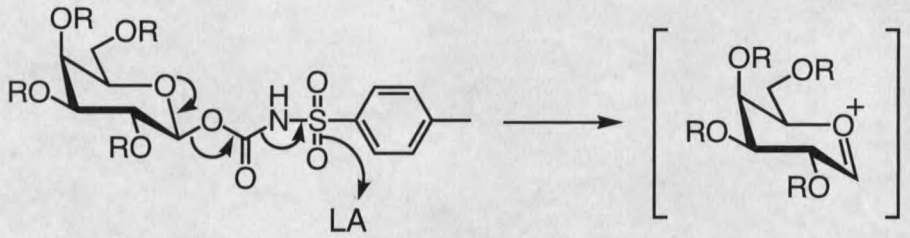
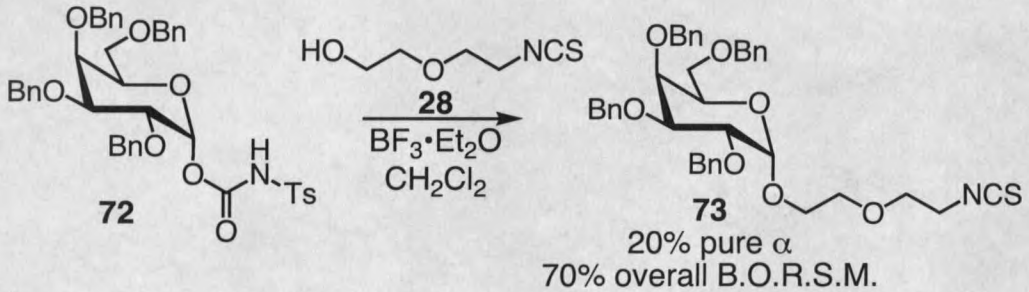


Figure D.4 Proposed reaction of the glycosyl sulfonylcarbamate with a Lewis acid to form an oxonium ion.

The use of sulfonylcarbamates is particularly attractive due to the ease of handling of the sulfonylcarbamate. Sulfonylcarbamates can be purified on silica

gel and possess long shelf lives. More importantly, they have been shown to have high α selectivity when coupled to a variety of alcohols under the appropriate conditions.

Sulfonylcarbamate **72** was synthesized using the method described by Hinklin and Kiessling.[211] The coupling of isothiocyanate **28** to **72** using $BF_3 \cdot Et_2O$ proceeded smoothly (see Scheme D.6). The reaction proceeded in 70% yield based on recovered starting material. Of the 70%, 20% was pure α anomer and 22% was a mixture of α and β anomers. The result of this reaction was 0.5 g of **73** as the α anomer, demonstrating that this method may be more economical for the multi-gram formation of α polyethylene glycol galactose derivatives such as **73**.



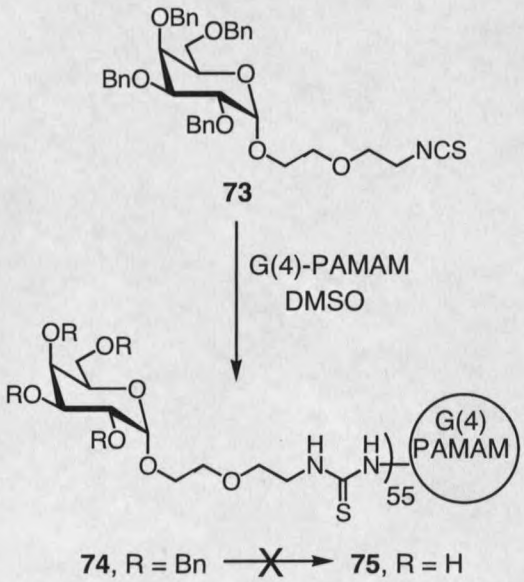
Scheme D.6 Coupling of isothiocyanate **28** with sulfonylcarbamate **72**. The overall yield is based on recovered starting material and product isolated.

Single Attempt to Functionalize a PAMAM Dendrimer with Benzylated Galactose

In an effort to provide proof of principle, a single attempt was made to functionalize a PAMAM dendrimer with **73**. The reaction was performed following the standard procedure (Scheme D.7). The G(4)-PAMAM dendrimer was

dissolved in DMSO and a DMSO solution containing **73** was added. The reaction immediately turned yellow. After stirring for 8 hours, the reaction mixture was dialyzed against DMSO (MW cutoff 1000). Lyophilization resulted in a yellowish solid. Interestingly, in contrast to the acetyl-protected mannose-functionalized dendrimers, **74** was soluble in a number of organic solvents, including CH_2Cl_2 and $CHCl_3$.

A couple of attempts to perform a global deprotection of **74** to form **75** failed. In both attempts, catalytic hydrogenation was used. Both Pd on carbon and $Pd(OH)_2$ on carbon were used but failed. During the course of the reaction, the catalyst clumped together, resulting in the loss of the suspension. This may be a result of the palladium interacting with the sulfur in the dendrimer. Other methods were not tried.



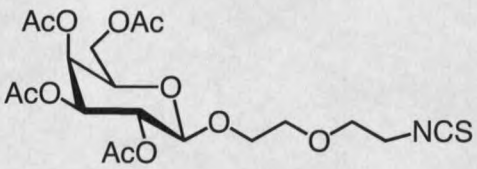
Scheme D.7 Functionalization of a G(4)-PAMAM dendrimer with benzylated galactose and unsuccessful attempts to perform a global deprotection.

Experimental Procedures

General methods

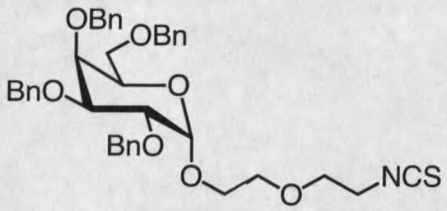
General reagents were purchased from Aldrich, Sigma, and Acros. Methylene chloride and diethyl ether were purified on basic alumina. Benzene and toluene were distilled from CaH_2. The distillation of $BF_3 \cdot Et_2O$ was done from CaH_2 immediately before use (62° C at 33 mm Hg). All other solvents and reagents were used as supplied.

Synthetic Procedures



1-*O*-(5-isothiocyanato-3-oxapentyl)-2,3,4,6-tetra-*O*-acetyl-β-D-galactopyranoside (**68**). The trichloroacetimidate **67**[162] (12.2 g, 24.8 mmol) was dissolved in CH_2Cl_2 (125 mL) with **28** (3.65 g, 24.8 mmol) and 4 Å molecular sieves (1.2 g) under an N_2 atmosphere. $BF_3 \cdot Et_2O$ (3,52 g, 3.1 mL, 24.8 mmol) was added slowly and the reaction was stirred at room temperature for 7 h. Solid $NaHCO_3$ (~2 g) was added to the reaction. The mixture was filtered over Celite, concentrated *in vacuo*, and purified by silica gel chromatography (1:1 hexanes:ethyl acetate) to give **68** as a thick yellow oil (6.2 g, 52%). ^{1}H NMR (500 MHz, $CDCl_3$) δ 5.37 (d, 1H, J = 3.2 Hz, H-4), 5.18 (t, 1H, J = 8.0 Hz, H-2), 5.01 (dd, 1H, J = 10.5, 3.2 Hz, H-3), 4.55 (d, 1H, 8.0 Hz, H-1), 4.05—4.20 (m, 3H), 3.85—4.00 (m, 2H), 3.70—3.80 (m, 1H), 3.60—3.65 (m, 7H), 2.14 (s, 3H), 2.05

(s, 3H), 2.03 (s, 3H), 1.96 (s, 3H) ppm; ^{13}C NMR (125 MHz, $CDCl_3$) δ 169.9, 169.9, 169.6, 169.1, 132.0, 100.9, 70.6, 70.5, 70.1, 69.0, 68.8, 68.7, 67.1, 61.2, 45.2, 20.4, 20.3, 20.3, 20.2 ppm; IR (film) 2108 cm^{-1}.



1-*O*-(5-isothiocyanato-3-oxapentyl)-2,3,4,6-tetra-*O*-benzyl-α-D-galactopyranoside (**73**). The trichloroacetimidate **72**[210] (2.89 g, 3.92 mmol) and isothiocyanate **28** (0.864 g, 5.88 mmol) were azeotroped three times with dry benzene and the resulting residue was dissolved in dry CH_2C1_2 (25 mL). Under an N_2 atmosphere, $BF_3{\cdot}Et_2O$ (.056 g, 0.5 mL, 3.9 mmol) was added slowly and the reaction was stirred at room temperature for 3 h. Solid $NaHCO_3$ (~2 g) was added to the reaction. The mixture was filtered over Celite, concentrated *in vacuo*, and purified by silica gel chromatography (7:3 hexanes:ethyl acetate) to give 0.52 g of **73** as a white solid (20% yield). An additional 0.59 g of α and β mixture was collected, and 0.80 g of **728** was recovered (70% yield based on recovered starting material). ^1H NMR (500 MHz, $CDCl_3$) δ 7.20—7.40 (m, 20H), 4.93 (d, 1H, J = 11.5 Hz), 4.87 (d, 1H, J = 3.4), 4.83 (dd, 2H, J = 11.8, 3.4 Hz), 4.75 (d, 1H, J = 11.8 Hz), 4.66 (d, 1H, J = 11.9 Hz), 4,56 (d, 1H, J = 11.5 Hz), 4.46 (d, 1H, J = 11.7 Hz), 4.39 (d, 1H, J = 11.5 Hz), 3.93—4.08 (m, 4H), 3.79 (t, 1H, J = 6.5 Hz), 3.58—3.71 (m, 4H), 3.40—3.57 (m, 5H) ppm; ^{13}C NMR (125

MHz, $CDCl_3$) δ 139.1, 138.9, 138.3, 128.5, 128.5, 128.5, 128.4, 128.3, 128.1, 128.0, 127.9, 127.8, 127.7, 127.6, 98.2, 79.1, 76.7, 75.3, 74.9, 73.6, 73.5, 73.2, 70.5, 69.7, 69.5, 69.2, 67.6, 45.3 ppm; IR (film) 2916, 2862, 2196, 2110 cm^{-1}; MS (MALDI-TOF) *m/z* 692.20 (M + Na, calcd 692.26 for $C_{39}H_{43}NO_7S$).

Generation 4.0 PAMAM-based thiourea polyethylene glycol-2,3,4,6-tetra-*O*-benzyl–α-D-galactopyranoside dendrimer (**74**): A aqueous solution of amine-terminated Starburst PAMAM dendrimer (generation 4.0) (940 mg of a 20% (w/w) solution, 8.7 μmol of dendrimer based on the M_W of 13,500 g/mol as determined by MALDI-TOF) was lyophilized to leave a white solid. The resulting residue was dissolved in DMSO (5 mL) followed by the addition of **73** (359 mg, 0.53 mmol). After 8 hours, the reaction mixture was dialysed against DMSO (MW cutoff 1 kDa). The solution was lyophilized to give **74** as an off white solid. ^1H NMR (500 MHz) δ 7.97 (bs, amide NH's), 7.76 (bs, amide NH's), 7.20 (m, benzyl, thiourea NH's), 4.83 (bs), 4.55—4.75 (m), 4.47 (d), 4.41 (d), 4.32 (d), 3.91 (bt), 3.10—3.75 (bm), 2.20—2.80 (bm) ppm; ^{13}C NMR (125 MHz) δ 173.6, 172.9, 138.9, 138.8, 138.6, 138.0, 128.6, 128.5, 128.3, 128.3, 128.2, 128.1, 128.0, 127.9, 127.8, 127.7, 127.6, 127.5, 97.9, 79.0, 76.5, 75.2, 74.9, 73.6, 73.3, 73.0, 70.0, 69.6, 69.3, 67.2, 52.5, 50.3, 44.4, 41.1, 39.8, 37.7, 34.1 ppm.

REFERENCES CITED

1. Kiessling, L. L. (1998). The Molecular Recognition of Saccharides and Glycoprotein-Inspired Materials. In *Recent Trends on Molecular Recognition*, Diederich, F. and Künzer, H., eds. (Berlin: Springer-Verlag Berlin Heidelberg), pp. 183-212.

2. Mammen, M., Choi, S.-K., and Whitesides, G. M. (1998). Polyvalent Interactions in Biological Systems: Implications for Design and Use of Multivalent Ligands and Inhibitors. Angew. Chem., Int. Ed. Engl., *37*, 2754-2794.

3. Lis, H., and Sharon, N. (1998). Lectins: Carbohydrate-Specific Proteins That Mediate Cellular Recognition. Chem. Rev., *98*, 637-674.

4. Sharon, N., and Lis, H. (1993). Carbohydrates in Cell Recognition. Sci. Am., 82-89.

5. Williams, S. J., and Davies, G. J. (2001). Protein-carbohydrate interactions: learning lessons from nature. Trends in Biotech, *19*, 356-362.

6. Feizi, T., Stoll, M. S., Yuen, C. T., Chai, W. G., and Lawson, A. M. (1994). Neoglycolipids - Probes of Oligosaccharide Structure, Antigenicity, and Function. Methods Enzymol., *230*, 484-519.

7. Gabius, H. J. (1997). Animal lectins. Eur. J. Biochem., *243*, 543-576.

8. Dwek, R. A. (1996). Glycobiology: Toward understanding the function of sugars. Chem. Rev., *96*, 683-720.

9. Kamitakahara, H., Suzuki, T., Nishigori, N., Suzuki, Y., Kanie, O., and Wong, C.-H. (1998). A Lysoganglioside/Poly-L-glutamic Acid Conjugate as a Picomolar Inhibitor of Influenza Hemagglutinin. Angew. Chem., Int. Ed. Engl., *37*, 1524-1528.

10. Kingery-Wood, J. E., Williams, K. W., Sigal, G. B., and Whitesides, G. M. (1992). The Agglutination of Erythrocytes by Influenza Virus is Strongly Inhibited by Liposomes Incorporating an Analog of Sialyl Gangliosides. J. Am. Chem. Soc., *114*, 7303-7305.

11. Spaltenstein, A., and Whitesides, G. M. (1991). Polyacrylamides Bearing Pendant alpha-Sialoside Groups Strongly Inhibit Agglutination of Erythrocytes by Influenza Virus. J. Am. Chem. Soc., *113*, 686-687.

12. Gamian, A., Chomik, M., Laferrière, C. A., and Roy, R. (1991). Inhibition of Influenza A Virus Hemagglutinin and Induction of Interferon by Synthetic Sialylated Glycoconjugates. Can. J. Microbiol., *37*, 233-237.

13. Sigal, G. B., Mammen, M., Dahmann, G., and Whitesides, G. M. (1996). Polyacrylamides Bearing Pendant alpha-Sialoside Groups Strongly Inhibit Agglutination of Erythrocytes by Influenza Virus: The Stong Inhibition Reflects Enhanced Binding through Cooperative Polyvalent Interactions. J. Am. Chem. Soc., *118*, 3789-3800.

14. Matrosovich, M. N., Mochalova, L. V., Marinina, V. P., Byramova, N. E., and Bovin, N. V. (1990). Synthetic polymeric sialoside inhibitors of influenza virus receptor-binding activity. FEBS Lett., *272*, 209-212.

15. Lees, W. J., Spaltenstein, A., Kingery-Wood, J. E., and Whitesides, G. M. (1994). Polyacrylamides Bearing Pendant alpha-Sialoside Groups Strongly Inhibit Agglutination of Erythrocytes by Influenza A Virus: Multivalency and Steric Stabilization of Particulate Biological Systems. J. Med. Chem., *37*, 3419-3433.

16. Mammen, M., Dahmann, G., and Whitesides, G. M. (1995). Effective Inhibitors of Hemagglutination by Influenza Virus Synthesized from Polymers having Active Ester Groups: Insights into Mechanism of Inhibition. J. Med. Chem., *38*, 4179-4190.

17. Sauter, N. K., Bednarski, M. D., Wurzburg, B. A., Hanson, J. E., Whitesides, G. M., Skehel, J. J., and Wiley, D. C. (1989). Hemagglutinins from Two Influenza Virus Variants Bind to Sialic Acid Derivatives with millimolar Dissociation Constants: A 500 MHz Proton Nuclear Magnetic Resonance Study. Biochemistry, *28*, 8388-8396.

18. Glick, G. D., Toogood, P. L., Wiley, D. C., Skehel, J. J., and Knowles, J. R. (1991). Ligand Recognition by Influenza Virus. J. Biol. Chem., *266*, 23660-23669.

19. Glick, G. D., and Knowles, J. R. (1991). Molecular Recognition of Bivalent Sialosides by Influenza Virus. J. Am. Chem. Soc., *113*, 4701-4703.

20. Roy, R., Zanini, D., Meunier, S. J., and Romanowska, A. (1993). Solid-phase Synthesis of Dendritic Sialoside Inhibitors of Influenza A Virus Hemagluttinin. J. Chem. Soc., Chem. Commun., 1869-1872.

21. Gestwicki, J. E., Strong, L. E., and Kiessling, L. L. (2000). Tuning chemotactic responses with synthetic multivalent ligands. Chem. Biol., *7*, 583-591.

22. Lundquist, J. J., and Toone, E. J. (2002). The cluster glycoside effect. Chem. Rev., *102*, 555-578.

23. Toone, E. J. (1994). Structure and Energetics of Protein Carbohydrate Complexes. Curr. Opin. Struct. Biol., *4*, 719-728.

24. Lee, Y. C., Townsend, R. R., Hardy, M. R., Lönngren, J., Arnarp, J., Haraldsson, M., and Lönn, H. (1983). Binding of Synthetic Oligosaccharides to the Hepatic Gal/GalNAc Lectin. J. Biol. Chem., *258*, 199-202.

25. Quesenberry, M. S., Lee, R. T., and Lee, Y. C. (1997). Difference in the binding mode of two mannose-binding proteins: Demonstration of a selective minicluster effect. Biochemistry, *36*, 2724-2732.

26. Borman, S. (2000). Multivalency: Strength in Numbers. C&EN, *78*, 48-53.

27. Roy, R. (2001). Designing Novel Multivalent Glycotools for Biochemical Investigations Related to Sialic Acid. In *Glycochemistry: Principles, Synthesis, and Applications*, Wang, P. G. and Bertozzi, C. R., eds. (New York, New York: Marcel Dekker, Inc.), pp. 277-305.

28. Fan, E. K., Merritt, E. A., Verlinde, C., and Hol, W. G. J. (2000). AB(5) toxins: structures and inhibitor design. Curr. Opin. Struct. Biol., *10*, 680-686.

29. Kiessling, L. L., and Pohl, N. L. (1996). Strength in numbers: Non-natural polyvalent carbohydrate derivatives. Chemistry & Biology, *3*, 71-77.

30. Sucheck, S. J., Wong, A. L., Koeller, K. M., Boehr, D. D., Draker, K.-a., Sears, P., Wright, G. D., and Wong, C.-H. (2000). Design of Bifunctional Antibiotics that Target Bacterial rRNA and Inhibit Resistance-Causing Enzymes. J. Am. Chem. Soc., *122*, 5230-5231.

31. DeFrees, S. A., Phillips, L., Guo, L., and Zalipsky, S. (1996). Sialyl Lewis X Liposomes as a Multivalent Ligand and Inhibitor of E-Selectin Mediated Cellular Adhesion. J. Am. Chem. Soc., *118*, 6101-6104.

32. Thoma, G., Duthaler, R. O., Magnani, J. L., and Patton, J. T. (2001). Nanomolar E-Selectin INhibitors: 700-Fold Potentiation of Affinity by Multivalent Ligand Presentation. J. Am. Chem. Soc., *123*, 10113-10114.

33. Roy, R., Page, D., Perez, S. F., and Bencomo, V. V. (1998). Effect of shape, size, and valency of multivalent mannosides on their binding properties to phytohemagglutinins. Glycoconjugate J., *15*, 251-263.

34. Heldin, C. H. (1995). Dimerization of Cell-Surface Receptors in Signal-Transduction. Cell, *80*, 213-223.

35. Klemm, J. D., Schreiber, S. L., and Crabtree, G. R. (1998). Dimerization as a regulatory mechanism in signal transduction. Annu. Rev. Immunol., *16*, 569-592.

36. Metzger, H. (1992). Transmembrane Signaling: The Joy of Aggregation. J. Immunol., *149*, 1477-1487.

37. Schlessinger, J. (1988). Signal Transduction by Allosteric Receptor Oligomerization. Trends Biochem.Sci., *13*, 443-447.

38. Weiss, A., and Schlessinger, J. (1998). Switching signals on or off by receptor dimerization. Cell, *94*, 277-280.

39. Kiessling, L. L., Gestwicki, J. E., and Strong, L. E. (2000). Synthetic multivalent ligands in the exploration of cell- surface interactions. Current Opinion in Chemical Biology, *4*, 696-703.

40. Mann, D. A., and Kiessling, L. L. (2001). The Chemistry and Biology of Multivalent Saccharide Displays. In *Glycochemistry: Principles, Synthesis, and Applications*, Wang, P. G. and Bertozzi, C. R., eds. (New York, New York: Marcel Dekker, Inc.), pp. 221-275.

41. Page, M. I., and Jencks, W. P. (1971). Entropic Contributions to Rate Accelerations in Enzymic and Intramolecular Reactions and the Chelate Effect. Proc. Natl. Acad. Sci. USA, *68*, 1678-1683.

42. Mandal, D. K., Kishore, N., and Brewer, C. F. (1994). Thermodynamics of Lectin-Carbohydrate Interactions. Titration Microcalorimetry, Measurements of the Binding of N-Linked Carbohydrates and Ovalbumin to Concanavalin A. Biochemistry, *33*, 1149-1156.

43. Kitov, P. I., Sadowska, J. M., Mulvey, G., Armstrong, G. D., Ling, H., Pannu, N. S., Read, R. J., and Bundle, D. R. (2000). Shiga-like Toxins are Neutralized by Tailored Multivalent Carbohydrate Ligands. Nature, *403*, 669-672.

44. Jencks, W. P. (1981). On the attribution and additivity of binding energies. Proc. Natl. Acad. Sci. USA, *78*, 4046-4050.

45. Dunitz, J. D. (1995). Win Some, Lose Some - Enthalpy-Entropy Compensation in Weak Intermolecular Interactions. Chemistry & Biology, *2*, 709-712.

46. Lindhorst, T. K. (2002). Artificial multivalent sugar ligands to understand and manipulate carbohydrate-protein interactions. In *Host-Guest Chemistry*, Volume 218. pp. 201-235.

47. Dimick, S. M., Powell, S. C., McMahon, S. A., Moothoo, D. N., Naismith, J. H., and Toone, E. J. (1999). On the Meaning of Affinity: Cluster Glycoside Effects and Concanavalin A. J. Am. Chem. Soc., *121*, 10286-10296.

48. Lee, Y. C., and Lee, R. T. (1995). Carbohydrate-Protein Interactions - Basis of Glycobiology. Acc. Chem. Res., *28*, 321-327.

49. Lee, R. T., and Lee, Y. C. (2000). Affinity enhancement by multivalent lectin-carbohydrate interaction. Glycoconjugate J., *17*, 543-551.

50. Olsen, L. R., Dessen, A., Gupta, D., Sabesan, S., Sacchettini, J. C., and Brewer, C. F. (1997). X-ray crystallographic studies of unique cross-linked lattices between four isomeric biantennary oligosaccharides and soybean agglutinin. Biochemistry, *36*, 15073-15080.

51. Kiessling, L. L., Strong, L. E., and Gestwicki, J. E. (2000). Principles for multivalent ligand design. In *Annual Reports in Medicinal Chemistry, Vol 35*, Volume 35. pp. 321-330.

52. Burke, S. D., Zhao, Q., Schuster, M. C., and Kiessling, L. L. (2000). Synergistic formation of soluble lectin clusters by a templated multivalent saccharide ligand. J. Am. Chem. Soc., *122*, 4518-4519.

53. Kretzschmar, G., Sprengard, U., Kunz, H., Bartnik, E., Schmidt, W., Toepfer, A., Hörsch, B., Krause, M., and Seiffge, D. (1995). Oligosaccharide Recognition by Selectins: Synthesis and Biological Activity of Multivalent Sialyl Lewis-X Ligands. Tetrahedron, *51*, 13015-13030.

54. Lehmann, J., and Weitzel, U. P. (1996). Synthesis and application of alpha-D-mannosyl clusters as photoaffinity ligands for mannose-binding proteins: Concanavalin A as a model receptor. Carbohydr. Res., *294*, 65-94.

55. Hansen, H. C., Haataja, S., Finne, J., and Magnusson, G. (1997). Di-, Tri-, and Tetravalent Dendritic Galabiosides That inhibit Hemagglutination by *Streptococcus suis* at Nanomolar Concentration. J. Am. Chem. Soc., *119*, 6974-6979.

56. Fujimoto, K., Miyata, T., and Aoyama, Y. (2000). Saccharide-Directed Cell Recognition and Molecular Delivery Using Macrocyclic Saccharide Clusters: Masking of Hydrophobicity to Enhance the Saccharide Specificity. J. Am. Chem. Soc., *122*, 3558-3559.

57. Page, D., and Roy, R. (1997). Optimizing lectin-carbohydrate interactions: Improved binding of divalent alpha-mannosylated ligands towards Concanavalin A. Glycoconjugate J., *14*, 345-356.

58. Page, D., Aravind, S., and Roy, R. (1996). Synthesis and lectin binding properties of dendritic mannopyranoside. J. Chem. Soc., Chem. Commun., 1913-1914.

59. Okada, M. (2001). Molecular design and syntheses of glycopolymers. Prog. Polym. Sci., *26*, 67-104.

60. Nagahori, N., and Nishimura, S.-I. (2001). Tailored Glycopolymers: Controlling the Carbohydrate-Protein Interaction Based on Template Effect. Biomacromolecules, *2*, 22-24.

61. Bovin, N. V., and Gabius, H.-J. (1995). Polymer-immobilized Carbohydrate Ligands: Versatile Chemical Tools for Biochemistry and Medicinal Sciences. Chem. Soc. Rev., *24*, 413-421.

62. Kiessling, L. L., and Strong, L. E. (1998). Bioactive Polymers. Top. Organomet. Chem., 199-231.

63. Matsuoka, K., and Nishimura, S.-I. (1995). Synthetic Glycoconjugates. 5. Polymeric Sugar Ligands Available for Determining the Binding Specificity of Lectins. Macromolecules, *28*, 2961-2968.

64. Bovin, N. V. (1998). Polyacrylamide-based glycoconjugates as tools in glycobiology. Glycoconjugate J., *15*, 431-446.

65. Fraser, C., and Grubbs, R. H. (1995). Synthesis of Glycopolymers of Controlled Molecular-Weight by Ring-Opening Metathesis Polymerization Using Well-Defined Functional-Group Tolerant Ruthenium Carbene Catalysts. Macromolecules, *28*, 7248-7255.

66. Maynard, H. D., Okada, S. Y., and Grubbs, R. H. (2001). Inhibition of cell adhesion to fibronectin by oligopeptide- substituted polynorbornenes. J. Am. Chem. Soc., *123*, 1275-1279.

67. Lynn, D. M., Kanaoka, S., and Grubbs, R. H. (1996). Living ring-opening metathesis polymerization in aqueous media catalyzed by well-defined ruthenium carbene complexes. J. Am. Chem. Soc., *118*, 784-790.

68. Lynn, D. M., Mohr, B., and Grubbs, R. H. (1998). Living ring-opening metathesis polymerization in water. J. Am. Chem. Soc., *120*, 1627-1628.

69. Kanai, M., Mortell, K. H., and Kiessling, L. L. (1997). Varying the Size of Multivalent Ligands: The Dependence of Concanavalin A Binding on Neoglycopolymer Length. J. Am. Chem. Soc., *119*, 9931-9932.

70. Mann, D. A., Kanai, M., Maly, D. J., and Kiessling, L. L. (1998). Probing low affinity and multivalent interactions with surface plasmon resonance: Ligands for concanavalin A. J. Am. Chem. Soc., *120*, 10575-10582.

71. Cairo, C. W., Gestwicki, J. E., Kanai, M., and Kiessling, L. L. (2002). Control of multivalent interactions by binding epitope density. J. Am. Chem. Soc., *124*, 1615-1619.

72. Schuster, M. C., Mortell, K. H., Hegeman, A. D., and Kiessling, E. L. (1997). Neoglycopolymers produced by aqueous ring-opening metathesis polymerization: Decreasing saccharide density increases activity. J. Mol. Catal. A-Chem., *116*, 209-216.

73. Gestwicki, J. E., Strong, L. E., Cairo, C. W., Boehm, F. J., and Kiessling, L. L. (2002). Cell aggregation by scaffolded receptor clusters. Chem. Biol., *9*, 163-169.

74. Owen, R. M., Gestwicki, J. E., Young, T., and Kiessling, L. L. (2002). Synthesis and applications of end-labeled neoglycopolymers. Organic Letters, *4*, 2293-2296.

75. Mortell, K. H., Weatherman, R. V., and Kiessling, L. L. (1996). Recognition specificity of neoglycopolymers prepared by ring- opening metathesis polymerization. J. Am. Chem. Soc., *118*, 2297-2298.

76. Matthews, O. A., Shipway, A. N., and Stoddart, J. F. (1998). Dendrimers-Branching Out From Curiosities into New Technologies. Prog. Polym. Sci., *23*, 1-56.

77. Bosman, A. W., Jansenn, H. M., and Meijer, E. W. (1999). About Dendrimers: Structure, Physical Properties, and Applications. Chem. Rev., *99*, 1665-1688.

78. Freemantle, M. (1999). Blossoming of Dendrimers. In *C&EN*. pp. 27-35.

79. Esfand, R., and Tomalia, D. A. (2001). Poly(amidoamine) (PAMAM) dendrimers: from biomimicry to drug delivery and biomedical applications. Drug Discov. Today, *6*, 427-436.

80. Astruc, D., and Chardac, F. (2001). Dendritic Catalysts and Dendrimers in Catalysis. Chem. Rev., *101*, 2991-3023.

81. Zeng, F. W., and Zimmerman, S. C. (1997). Dendrimers in supramolecular chemistry: From molecular recognition to self-assembly. Chem. Rev., *97*, 1681-1712.

82. Dykes, G. M. (2001). Dendrimers: a review of their appeal and applications. J. Chem. Technol. Biotechnol., *76*, 903-918.

83. Zimmerman, S. C., and Lawless, L. J. (2001). Supramolecular chemistry of dendrimers. In *Dendrimers IV*, Volume 217. pp. 95-120.

84. Florence, A. T., and Hussain, N. (2001). Transcytosis of nanoparticle and dendrimer delivery systems: evolving vistas. Adv. Drug Deliv. Rev., *50*, S69-S89.

85. Vogtle, F., Gestermann, S., Hesse, R., Schwierz, H., and Windisch, B. (2000). Functional dendrimers. Prog. Polym. Sci., *25*, 987-1041.

86. Newkome, G. R., Moorefield, C. N., and Vögtle, F. (2001). Dendrimers and Dendrons: Concepts, Syntheses, Applications (Weinheim: Wiley-VCH).

87. Cloninger, M. J. (2002). Biological applications of dendrimers. Current Opinion in Chemical Biology, *6*, 742-748.

88. Tomalia, D. A., Baker, H., Dewald, J., Hall, M., Kallos, G., Martin, S., Roeck, J., Ryder, J., and Smith, P. (1985). A New Class of Polymers - Starburst-Dendritic Macromolecules. Polym. J., *17*, 117-132.

89. Naylor, A. M., Goddard III, W. A., Kiefer, G. E., and Tomalia, D. A. (1989). Starburst Dendrimers. 5. Molecular Shape Control. J. Am. Chem. Soc., *111*, 2339-2341.

90. Tomalia, D. A., Naylor, A. M., and Goddard II, W. A. (1990). Starburst Dendrimers: Molecular-Level Control of Size, Shape, Surface Chemistry, Topology, and Flexibility from Atoms to Macroscopic Matter. Angew. Chem., Int. Ed. Engl., *29*, 138-175.

91. Tomalia, D. A., and Hurst, H. D. (1993). Genealogically Directed Synthesis: Starburst/Cascade Dendrimers and Hyperbranched Structures. In *Topics in Current Chemistry*, Volume 165. (Berlin: Springer-Verlag), pp. 193-313.

92. Ottaviani, M. F., Sacchi, B., Turro, N. J., Chen, W., Jockusch, S., and Tomalia, D. A. (1999). An EPR Study of the Interactions between Starburst Dendrimers and Polynucleotides. Macromolecules, *32*, 2275-2282.

93. Topp, A., Bauer, B. J., Klimash, J. W., Spindler, R., Tomalia, D. A., and Amis, E. J. (1999). Probing the Location of the Terminal Groups of Dendrimers in Dilute Solution. Macromolecules, *32*, 7226-7231.

94. Topp, A., Bauer, B. J., Tomalia, D. A., and Amis, E. J. (1999). Effect of Solvent Quality on the Molecular Dimensions of PAMAM Dendrimers. Macromolecules, *32*, 7232-7237.

95. Chen, W., Tomalia, D. A., and Thomas, J. L. (2000). Unusual pHG-Dependent Polarity Changes in PAMAM Dendrimers: Evidence for pH-Reponsive Conformational Changes. Macromolecules, *33*, 9169-9172.

96. Bhalgat, M. K., and Roberts, J. C. (2000). Molecular modeling of polyamidoamine (PAMAM) Starburst (TM) dendrimers. Eur. Polym. J., *36*, 647-651.

97. Polydispersity is defined as Mw/Mn

98. Data taken from Dendritech Inc. website at www.dendritech.com/pamam.html

99. Roberts, J. C., Bhalgat, M. K., and Zera, R. T. (1996). Preliminary biological evaluation of polyamidoamine (PAMAM) Starburst(TM) dendrimers. J. Biomed. Mater. Res., *30*, 53-65.

100. Bittiger, H., and Schnebli, H. P. (1976). Concanavalin A as a Tool (New York: John Wiley & Sons).

101. Derewenda, Z., Yariv, J., Helliwell, J. R., Kald, A. J., Dodson, E. J., Papiz, M. Z., Wan, T., and Campbell, J. (1989). The Structure of the Saccharide-Binding Site of Concanavalin A. EMBO J., *8*, 2189-2193.

102. Sharon, N., and Lis, H. (1990). Legume Lectins- A Large Family of Homologous Proteins. FASEB Journal, *4*, 3198-3208.

103. Singh, R. S., Tiwary, A. K., and Kennedy, J. F. (1999). Lectins: Sources, activities, and applications. Crit. Rev. Biotechnol., *19*, 145-178.

104. Simanek, E. E., McGarvey, G. J., Jablonowski, J. A., and Wong, C.-H. (1998). Selectin-Carbohydrate Interactions: From Natural Ligands to Designed Mimics. Chem. Rev., *98*, 833-862.

105. Koenig, S. H., Brown III, R. D., and Brewer, C. F. (1983). Binding of Saccharide to Demetalized Concanavalin A. Biochemistry, *22*, 6221-6226.

106. Brown III, R. D., Brewer, C. F., and Koenig, S. H. (1977). Conformation States of Concanavalin A: Kinetics of Transitions Induced by Interactions with Mn2+ and Ca2+ Ions. Biochemistry, *16*, 3883-3896.

107. Brown, R. D., Koenig, S. H., and Brewer, C. F. (1982). Conformational Equilibrium of Demetallized Concanavalin-A. Biochemistry, *21*, 465-469.

108. Emmerich, C., Helliwell, J. R., Redshaw, M., Naismith, J. H., Harrop, S. J., Raftery, J., Kalb, A. J., Yariv, J., Dauter, Z., and Wilson, K. S. (1994). High-Resolution Structures of Single-Metal-Substituted Concanavalin-a - the Co,Ca-Protein at 1.6-Angstrom and the Ni,Ca-Protein at 2.0-Angstrom. Acta Crystallogr. Sect. D-Biol. Crystallogr., *50*, 749-756.

109. Brewer, C. F., Brown, R. D., and Koenig, S. H. (1983). Stoichiometry of Manganese and Calcium-Ion Binding to Concanavalin-A. Biochemistry, *22*, 3691-3702.

110. Sadhu, A., and Magnuson, J. A. (1989). Role of 2nd Metal-Ion in Establishing Active Conformations of Concanavalin-A. Biochemistry, *28*, 3197-3204.

111. Harrop, S. J., Naismith, J. H., Emmerich, C., Habash, J., Weisgerber, S., Kalb, A. J., Yariv, J., and Helliwell, J. R. (1993). Acta Crystallogr., *A49*, C-94.

112. Moothoo, D. N., and Naismith, J. H. (1998). Glycobiology, *8*, 173.

113. Naismith, J. H., and Field, R. A. (1996). Structural Basis of Trimannoside Recognition by Concanavalin A. J. Biol. Chem., *271*, 972.

114. Parkin, S., Rupp, B., and Hope, H. (1996). Atomic resolution structure of concanavalin A at 120 K. Acta Crystallogr. Sect. D-Biol. Crystallogr., *52*, 1161-1168.

115. Weisgerber, S., and Helliwell, J. R. (1993). High-resolution Crystallographic Studies of Native Concanavalin A using Rapid Laue Data Collection Methods and the Introduction of a Monochromatic Large-angle Oscillation Technique (LOT). J. Chem. Soc. Faraday Trans., *89*, 2667.

116. Schwarz, F., Puri, K. D., Bhat, R. G., and Surolia, A. (1993). Thermodynamics of Monosaccharide Binding to Concanavalin A, Pea (*Pisum sativum*) Lectin, and Lentil (*Lens culinaris*) Lectin. J. Biol. Chem., *268*, 7668-7677.

117. Williams, B. A., Chervenak, M. C., and Toone, E. J. (1992). Energetics of Lectin-Carbohydrate Binding. J. Biol. Chem., *267*, 22907-22911.

118. Dam, T. K., Roy, R., Das, S. K., Oscarson, S., and Brewer, C. F. (2000). Binding of multivalent carbohydrates to concanavalin A and Dioclea grandiflora lectin - Thermodynamic analysis of the "multivalency effect". J. Biol. Chem., *275*, 14223-14230.

119. Naismith, J. H., Emmerich, C., Habash, J., Harrop, S. J., Helliwell, J. R., Hunter, W. N., Raftery, J., Kalb, A. J., and Yariv, J. (1994). Refined Structure of Concanavalin-a Complexed with Methyl Alpha-D-Mannopyranoside at 2.0 Angstrom Resolution and Comparison with the Saccharide-Free Structure. Acta Crystallogr. Sect. D-Biol. Crystallogr., *50*, 847-858.

120. Turnbull, W. B., and Stoddart, J. F. (2002). Design and synthesis of glycodendrimers. Reviews in Molecular Biotechnology, *90*, 231-255.

121. Peerlings, H. W. I., Nepogodiev, S. A., Stoddart, J. F., and Meijer, E. W. (1998). Synthesis of spacer-armed glucodendrimers based on the modification of poly(propylene imine) dendrimers. Eur. J. Org. Chem., 1879-1886.

122. Baek, M.-G., and Roy, R. (2002). Synthesis and protein binding properties of T-antigen containing glycoPAMAM dendrimers. Bioorg. Med. Chem., *10*, 11-17.

123. Page, D., and Roy, R. (1997). Synthesis and Biological Properties of Mannosylated Starburst Poly(amidoamine) Dendrimers. Bioconjugate Chem., *8*, 714-723.

124. Sashiwa, H., Shigemasa, Y., and Roy, R. (2000). Chemical Modification of Chitosan. 3. Hyperbranched Chitosan–Sialic Acid Dendrimer Hybrid with Tetraethylene Glycol Spacer. Macromolecules, *33*, 6913-6915.

125. Sashiwa, H., Shigemasa, Y., and Roy, R. (2002). Chemical modification of chitosan 11: chitosan-dendrimer hybrid as a tree like molecule. Carbohydr. Polym., *49*, 195-205.

126. Aoi, K., Tsutsumiuchi, K., Yamamoto, A., and Okada, M. (1998). Globular carbohydrate macromolecule "sugar balls", 2 - Synthesis of mono(glycopeptide)-persubstituted dendrimers by polymer reaction with sugar-substituted alpha-amino acid N- carboxyanhydrides (glycoNCAs). Macromol. Rapid Commun., *19*, 5-9.

127. Andre, S., Ortega, P. J. C., Perez, M. A., Roy, R., and Gabius, H. J. (1999). Lactose-containing starburst dendrimers: influence of dendrimer generation and binding-site orientation of receptors (plant/animal lectins and immunoglobulins) on binding properties. Glycobiology, *9*, 1253-1261.

128. Tsutsumiuchi, K., Aoi, K., and Okada, M. (1999). Globular carbohydrate macromolecule "sugar balls" IV. Synthesis of dendritic nanocapsules with molecular recognition sites on periphery. Polym. J., *31*, 935-941.

129. Woller, E. K., and Cloninger, M. J. (2001). Mannose Functionalization of a Sixth Generation Dendrimer. Biomacromolecules, *2*, 1052-1054.

130. Woller, E. K., and Cloninger, M. J. (2002). The Lectin Binding Properties of Six Generations of Mannose-Functionalized Dendrimers. Organic Letters, *4*, 7-10.

131. Lindhorst, T. K., and Kieburg, C. (1996). Glycocoating of oligovalent amines: Synthesis of thiourea- bridged cluster glycosides from glycosyl isothiocyanates. Angew. Chem., Int. Ed. Engl., *35*, 1953-1956.

132. Kieburg, C., and Lindhorst, T. K. (1997). Glycodendrimer Synthesis Without Using a Protecting Group. Tetrahedron Lett., *38*, 3885-3888.

133. Dubber, M., and Lindhorst, T. K. (2001). Trehalose-based octapus glycosides for the synthesis of carbohydrate-centered PAMAM dendrimers and thiourea-bridged glycoclusters. Organic Letters, *3*, 4019-4022.

134. Maya, I., Lopez, O., Fernandez-Bolanos, J. G., Robina, I., and Fuentes, J. (2001). A practical one-pot synthesis of O-unprotected glycosyl thioureas. Tetrahedron Lett., *42*, 5413-5416.

135. Pavlov, G. M., Errington, N., Harding, S. E., Korneeva, E. V., and Roy, R. (2001). Dilute solution properties of lactosylated polyamidoamine dendrimers and their structural characteristics. Polymer, *42*, 3671-3678.

136. Poretz, R. D., and Goldstein, I. J. (1971). Protein-Carbohydrate Interaction: On the Mode of Binding of Aromatic Moieties to Concanavalin A, the Phytohemagglutinin of the Jack Bean. Biochemical Pharmacology, *20*, 2727-2739.

137. Iyer, R. N., and Goldstein, I. J. (1973). Quantitative Studies on the Interaction of Concanavalin A, the Carbohydrate-Binidng Protein of the Jack Bean, with Model Carbohydrate-Protein Conjugates. Immunochemistry, *10*, 313-322.

138. Loontiens, F. G., Van Wauwe, J. P., De Gussem, R., and De Bruyne, C. K. (1973). Binding of Para-Substituted Phenyl Glycosides to Concanavalin A. Carbohydr. Res., *30*, 51-62.

139. Van Wauwe, J. P., Loontiens, F. G., Carchon, H. A., and De Bruyne, C. K. (1973). Binding of *p*-Substituted-Phenyl Glycosides to the Lectins from the Pea and the Lentil. Carbohydr. Res., *30*, 249-256.

140. Van Wauwe, J. P., Loontiens, F. G., and De Bruyne, C. K. (1975). Carbohydrate Binding Specificity of the Lectin from the Pea (*Pisum Sativum*). Biochim. Biophys. Acta, *379*, 456-461.

141. Westphal, O., and Feier, H. (1956). Dartstellung künstlicher Antigene mit determinanten Zuckergruppen, II. Mitteil.: Synthese der *p*-Aminophenyl-*O*-alpha- glykoside von L-Fucose, L-Rhamnose, D-Galaktose, und D-Mannose. Chem. Ber., *89*, 582-588.

142. McBroom, C. R., Samanen, C. H., and Goldstein, I. J. (1972). Carbohydrates Antigens: Coupling of Carbohydrates to Proteins by Diazonium and Phenylisothiocyanate Reactions. In *Complex Carbohydrates*, Volume 28, Ginsburg, V., ed. (New York and London: Academic Press), pp. 212-219.

143. Sanders, J. K. M., and Hunter, B. K. (1993). Modern NMR Spectroscopy: a guide for chemists, Second Edition (Oxford: Oxford University Press).

144. Aoi, K., Itoh, K., and Okada, M. (1995). Globular Carbohydrate Macromolecule "Sugar Balls." 1. Synthesis of Novel Sugar-Persubstituted Poly(amido amine) Dendrimers. Macromolecules, *28*, 5391-5393.

145. Karas, M., and Hillenkamp, F. (1988). Laser Desorption Ionization of Proteins with Molecular Masses Exceeding 10000 Daltons. Anal. Chem., *60*, 2299-2301.

146. Bahr, U., Deppe, A., Karas, M., Hillenkamp, F., and Giessmann, U. (1992). Mass-Spectrometry of Synthetic-Polymers by Uv Matrix-Assisted Laser Desorption Ionization. Anal. Chem., *64*, 2866-2869.

147. Macha, S. F., and Limbach, P. A. (2002). Matrix-assisted laser desorption/ionization (MALDI) mass spectrometry of polymers. Curr. Opin. Solid State Mat. Sci., *6*, 213-220.

148. McEwen, C. N., and Peacock, P. M. (2002). Mass spectrometry of chemical polymers. Anal. Chem., *74*, 2743-2748.

149. Timpin, S., Rouhanipour, A., Az, R., Rader, H. J., and Mullen, K. (2001). New aspects in matrix-assisted laser desorption/ionization time-of-flight mass spectrometry: a universal solvent-free sample preparation. Rapid Commun. Mass Spectrom., *15*, 1364-1373.

150. Skelton, R., Dubois, F., and Zenobi, R. (2000). A MALDI sample preparation method suitable for insoluble polymers. Anal. Chem., *72*, 1707-1710.

151. Stump, M. J., Fleming, R. C., Gong, W. H., Jaber, A. J., Jones, J. J., Surber, C. W., and Wilkins, C. L. (2002). Matrix-assisted laser desorption mass spectrometry. Appl. Spectrosc. Rev., *37*, 275-303.

152. Rader, H. J., and Schrepp, W. (1998). MALDI-TOF mass spectrometry in the analysis of synthetic polymers. Acta Polym., *49*, 272-293.

153. Nielen, M. W. F. (1999). Maldi time-of-flight mass spectrometry of synthetic polymers. Mass Spectrom. Rev., *18*, 309-344.

154. Limbach, P. A. (1998). Matrix-assisted laser desorption ionization mass spectrometry: An overview. Spectroscopy, *13*, 16-+.

155. Tolic, L. P., Anderson, G. A., Smith, R. D., Brothers II, H. M., Spindler, R., and Tomalia, D. D. (1997). Electrospray ionization Fourier transform ion cyclotron resonance mass spectrometric characterization of high molecular mass Starburst dendrimers. Int. J. Mass Spec. and Ion Processes, *165*, 405-418.

156. Aoi, K., Tsutsumiuchi, K., Yamamoto, A., and Okada, M. (1997). Globular Carbohydrate Macromolecule "Sugar Balls" 3. "Radial-Growth Polymerization" of Sugar Substitued alpha-Amino Acid N-Carboxyanhydrides (GlycoNCAs) with a Dendritic Initiator. Tetrahedron, *53*, 15415-15427.

157. Page, D., Zanini, D., and Roy, R. (1996). Macromolecular recognition: Effect of multivalency in the inhibition of binding of yeast mannan to concanavalin A and pea lectins by mannosylated dendrimers. Bioorg. Med. Chem., *4*, 1949-1961.

158. Pan, Y., and Ford, W. T. (1999). Dendrimers with Both Hydrophilic and Hydrophobic Chains at Every End. Macromolecules, *32*, 5468-5470.

159. Lebeau, L., Oudet, P., and Mioskowski, C. (1991). Synthesis of New Phospholipids LInked to Steroid-Hormone Derivatives Designed for Two-Dimensional Crystallization of Proteins. Helv. Chim. Acta, *74*, 1697-1706.

160. Corbell, J. B., Lundquist, J. J., and Toone, E. J. (2000). A comparison of biological and calorimetric analyses of multivalent glycodendrimer ligands for concanavalin A. Tet. Asym., *11*, 95-111.

161. Haag, R., Sunder, A., and Stumbé, J.-F. (2000). An Approach to Glycerol Dendrimers and Pseudo-Dendritic Polyglycerols. J. Am. Chem. Soc., *122*, 2954-2955.

162. Ren, T., and Liu, D. (1999). Synthesis of targetable cationic amphiphiles. Tetrahedron Lett., *40*, 7621-7625.

163. Schmidt, R. R. (1986). New Methods for the Synthesis of Glycosides and Oligosaccharides- Are There Alternatives to the Koenigs-Knorr Method? Angew. Chem., Int. Ed. Engl., *25*, 212-235.

164. Schmidt, R. R., and Michel, J. (1980). Facile Synthesis of alpha- and beta-O-Glycosyl Imidates; Preparation of Glycosides and Disaccharides. Angew. Chem., Int. Ed. Engl., *19*, 731-732.

165. Carpino, L., and Han, G. Y. (1972). The 9-Fluorenylmethoxycarbonyl Amino-Protecting Group. J. Org. Chem., *37*, 3404-3409.

166. Matsuo, I., Isomura, M., Miyazaki, T., Sakakibara, T., and Ajisaka, K. (1998). Chemoenzymatic synthesis of the branched oligosaccharides which correspond to the core structures of N-linked sugar chains. Carbohydr. Res., *305*, 401-413.

167. Mori, M., Ito, Y., and Ogawa, T. (1990). Total Synthesis of the Mollu-Series Glycosyl Ceramides - Alpha-D-Manp-(1-->3)-Beta-D-Manp-(1-->4)-Beta-D-Glcp-(1-->1)-Cer and Alpha-D-Manp-(1-->3)-[Beta-D-Xylp-(1-->2)]-Beta-D-Manp-(1->4)- Beta-D-Glcp-(1-->1)-Cer. Carbohydr. Res., *195*, 199-224.

168. Upreti, M., Ruhela, D., and Vishwakarma, R. A. (2000). Synthesis of the tetrasaccharide cap domain of the antigenic lipophosphoglycan of Leishmania donovani parasite. Tetrahedron, *56*, 6577-6584.

169. Zanini, D., and Roy, R. (1998). Practical Synthesis of Starburst PAMAM alpha-Thiosialodendrimers for Probing Multivalent Carbohydrate-Lectin Binding Properties. J. Org. Chem., *63*, 3486-3491.

170. Ashton, P. R., Hounsell, E. F., Jayaraman, N., Nilsen, T. M., Spencer, N., Stoddart, J. F., and Young, M. (1998). Synthesis and Biological Evaluation of alpha-D-Mannopyranoside-Containing Dendrimers. J. Org. Chem., *63*, 3429-3437.

171. Osawa, T., and Matsumoto, I. (1972). Gorse (*Ulex europeus)* Phytohemagglutinins. Meth. Enzymol., *28*, 323-327.

172. Li, J., Piehler, L. T., Qin, D., Baker, J. R., Tomalia, D. A., and Meier, D. J. (2000). Visualization and characterization of poly(amidoamine) dendrimers by atomic force microscopy. Langmuir, *16*, 5613-5616.

173. Uppuluri, S., Keinath, S. E., Tomalia, D. A., and Dvornic, P. R. (1998). Rheology of dendrimers. I. Newtonian flow behavior of medium and highly concentrated solutions of polyamidoamine (PAMAM) dendrimers in ethylenediamine (EDA) solvent. Macromolecules, *31*, 4498-4510.

174. Bhattacharyya, L., and Brewer, C. F. (1992). Formation of Homogeneous Carbohydrate Lectin Cross-Linked Precipitates from Mixtures of D-

Galactose/N-Acetyl-D- Galactosamine-Specific Lectins and Multiantennary Galactosyl Carbohydrates. Eur. J. Biochem., *208*, 179-185.

175. Bhattacharyya, L., Khan, M. I., and Brewer, C. F. (1988). Interactions of Concanavalin-a with Asparagine-Linked Glycopeptides - Formation of Homogeneous Cross-Linked Lattices in Mixed Precipitation Systems. Biochemistry, *27*, 8762-8767.

176. Bhattacharyya, L., Khan, M. I., Fant, J., and Brewer, C. F. (1989). Formation of Highly Ordered Cross-Linked Lattices between Asparagine-Linked Oligosaccharides and Lectins Observed by Electron-Microscopy. J. Biol. Chem., *264*, 11543-11545.

177. Brewer, C. F. (1996). Multivalent Lectin-Carbohydrate Cross-Linking Interactions. Chemtract- Biochemistry and Molecular Biology, *6*, 165-179.

178. Brewer, C. F. (2001). Lectin cross-linking interactions with multivalent carbohydrates. In *Molecular Immunology of Complex Carbohydrates-2*, Volume 491. pp. 17-25.

179. Kooijman, R., Dewildt, P., Beumer, S., Vandervliet, G., Homan, W., Kalshoven, H., Musgrave, A., and Vandenende, H. (1989). Wheat-Germ Agglutinin Induces Mating Reactions in Chlamydomonas-Eugametos by Cross-Linking Agglutinin-Associated Glycoproteins in the Flagellar Membrane. J. Cell Biol., *109*, 1677-1687.

180. Perillo, N. L., Pace, K. E., Seilhamer, J. J., and Baum, L. G. (1995). Apoptosis of T-Cells Mediated by Galectin-1. Nature, *378*, 736-739.

181. Sacchettini, J. C., Baum, L. G., and Brewer, C. F. (2001). Multivalent Protein-Carbohydrate Interactions. A New Paradigm for Supermolecular Assembly and Signal Transduction. Biochemistry, *40*, 3009-3015.

182. Aoi, K., Itoh, K., and Okada, M. (1997). Divergent/Convergent Joint Approach with a Half-Protected Initiator Core To Synthesize Surface-Block Dendrimers. Macromolecules, *30*, 8072-8074.

183. Maeda, H., Furuyoshi, S., Nakatsuji, Y., and Mitsuo, O. (1982). Intramolecular Cyclization of N,N-Di(oligooxyethylene)amines: A New Synthesis of Monoaza Crown Ethers. Tetrahedron, *38*, 3359-3362.

184. Allen, J. R., Harris, C. R., and Danishefsky, S. J. (2001). Pursuit of optimal carbohydrate-based anticancer vaccines: Preparation of a multiantigenic unimolecular glycopeptide containing the Tn, MBr1, and Lewis(y) antigens. J. Am. Chem. Soc., *123*, 1890-1897.

185. Houseman, B. T., and Mrksich, M. (1999). The role of ligand density in the enzymatic glycosylation of carbohydrates presented on self-assembled monolayers of alkanethiolates on gold. Angew. Chem., Int. Ed. Engl., *38*, 782-785.

186. Krantz, M. J., Holtzman, N. A., Stowell, C. P., and Lee, Y. C. (1976). Attachment of Thioglycosides to Proteins: Enhancement of Liver Membrane Binding. Biochemistry, *15*, 3963-3968.

187. Maheshwari, G., Brown, G., Lauffenburger, D. A., Wells, A., and Griffith, L. G. (2000). Cell adhesion and motility depend on nanoscale RGD clustering. J. Cell Sci., *113*, 1677-1686.

188. Kudryashov, V., Glunz, P. W., Williams, L. J., Hintermann, S., Danishefsky, S. J., and Lloyd, K. O. (2001). Toward optimized carbohydrate-based anticancer vaccines: Epitope clustering, carrier structure, and adjuvant all influence antibody responses to Lewis(y) conjugates in mice. Proc. Natl. Acad. Sci. U. S. A., *98*, 3264-3269.

189. Spevak, W., Nagy, J. O., Charych, D. H., Schaefer, M. E., Gilbert, J. H., and Bednarski, M. D. (1993). Polymerized Liposomes Containing C-Glycosides of Sialic-Acid - Potent Inhibitors of Influenza-Virus Invitro Infectivity. J. Am. Chem. Soc., *115*, 1146-1147.

190. Morgan, J. R., and Cloninger, M. J. (2002). Heterogeneously functionalized dendrimers. Current Opinion in Drug Discovery and Development, *5*, 966-973.

191. Zhang, X. C., Lee, Y. K., Kelley, J. A., and Burke, T. R. (2000). Preparation of aryl isothiocyanates via protected phenylthiocarbamates and application to the synthesis of caffeic acid (4-isothiocyanato)phenyl ester. J. Org. Chem., *65*, 6237-6240.

192. Walter, E. D.; Sebby, K. B.; Singel, D. J.; Cloninger, M. J.: unpublished results at time of writing.

193. Khan, M. I., Mandal, D. K., and Brewer, C. F. (1991). Interactions of Concanavalin-a with Glycoproteins - a Quantitative Precipitation Study of Concanavalin-a with the Soybean Agglutinin. Carbohydr. Res., *213*, 69-77.

194. This computer programming work was performed by Eric D. Walter of the Singel research group at Montana State University. It is included here to help explain the results of the precipitation assay.

195. Kilpatrick, D. C. (2000). Handbook of Animal Lectins: Properties and Biomedical Applications (New York: John Wiley and Sons).

196. This computer programming work was performed by Eric D. Walter of the Singel research group at Montana State University. It is included here to help explain the results of the precipitation assay.

197. Wiseman, T., Williston, S., Brandts, J. F., and Lin, L. N. (1989). Rapid Measurement of Binding Constants and Heats of Binding Using a New Titration Calorimeter. Anal. Biochem., *179*, 131-137.

198. Wadso, I., and Goldberg, R. N. (2001). Standards in isothermal microcalorimetry (IUPAC technical report). Pure Appl. Chem., *73*, 1625-1639.

199. Cooper, A., and Johnson, C. M. (1994). Isothermal Titration Microcalorimetry. In *Microscopy, Optical Microscopy, and Macroscopic Techniques*, Jones, C., Mulloy, B. and Thomas, A. H., eds. (Totowa, New Jersey: Humana Press), pp. 137-150.

200. Dam, T. K., and Brewer, C. F. (2002). Thermodynamic studies of lectin-carbohydrate interactions by isothermal titration calorimetry. Chem. Rev., *102*, 387-429.

201. Holdgate, G. (2001). Making cool drugs hot: Isothermal titration calorimetry as a tool to study binding energetics. Biotechniques, *31*, 164-184.

202. Gupta, D., Dam, T. K., Oscarson, S., and Brewer, C. F. (1997). Thermodynamics of Lectin-Carbohydrate Interactions. J. Biol. Chem., *272*, 6388-6392.

203. Clarke, C., Woods, R. J., Gluska, J., Cooper, A., Nutley, M. A., and Boons, G. J. (2001). Involvement of water in carbohydrate-protein binding. J. Am. Chem. Soc., *123*, 12238-12247.

204. Weatherman, R. V., Mortell, K. I., Chervenak, M., Kiessling, L. L., and Toone, E. J. (1996). Specificity of C-glycoside complexation by mannose glucose specific lectins. Biochemistry, *35*, 3619-3624.

205. Lundquist, J. J., Debenham, S. D., and Toone, E. J. (2000). Multivalency Effects in Protein-Carbohydrate Interaction: The Binding of the Shiga-like Toxin 1 Binding Subunit to Multivalent *C*-Linked Glycopeptides. J. Org. Chem., *65*, 8245-8250.

206. Dam, T. K., Roy, R., Page, D., and Brewer, C. F. (2002). Thermodynamic binding parameters of individual epitopes of multivalent carbohydrates to concanavalin a as determined by "reverse" isothermal titration microcalorimetry. Biochemistry, *41*, 1359-1363.

207. Dam, T. K., Roy, R., Page, D., and Brewer, C. F. (2002). Negative cooperativity associated with binding of multivalent carbohydrates to lectins. thermodynamic analysis of the "multivalency effect". Biochemistry, *41*, 1351-1358.

208. McKenzie, G. H., Sawyer, W. H., and Nichol, L. W. (1972). The Molecular Weight and Stability of Concanavalin A. Biochim. Biophys. Acta, *263*, 283-293.

209. Huet, M. (1975). Factors Affecting the Molecular Structure and the Agglutinating Ability of Concanavalin A and Other Lectins. Eur. J. Biochem., *59*, 627-632.

210. Wegmann, B., and Schmidt, R. R. (1987). Glycosylimidates .27. The Application of the Trichloroacetimidate Method to the Synthesis of Alpha-D- Glucopyranosides and Alpha-D-Galactopyranosides. J. Carbohydr. Chem., *6*, 357-375.

211. Hinklin, R. J., and Kiessling, L. L. (2001). Glycosyl sulfonylcarbamates: New glycosyl donors with tunable reactivity. J. Am. Chem. Soc., *123*, 3379-3380.

THE END

MONTANA STATE UNIVERSITY - BOZEMAN
3 1762 10385593 6